ADVANCES IN NASOPHARYNGEAL CANCER:

NEW TARGETS, BIOMARKERS AND THERAPIES

Hui, Pun

A Thesis Submitted in Fulfilment

of the Requirements for the Degree of

Doctor of Medicine

The Chinese University of Hong Kong

September 2010

This thesis is dedicated to

My wife Adeliné and our daughters Ruby and Iris

Our parents Mr. and Mrs. Hui and Mr. and Mrs. Poon

For their unreserved support and everlasting love

This thesis is also dedicated to my patients

Who have taught me how to be a good doctor

And have always reminded me to be a better medical oncologist

ABSTRACT

Nasopharyngeal cancer (NPC) is endemic in Southern China and Hong Kong. It has traditionally been treated by local radiotherapy with great success especially for early stage disease. However the treatment outcome in advanced stage disease is unsatisfactory.

To investigate potential new therapeutic targets and biomarkers in NPC, we first confirmed from the Hong Kong NPC study group of 2915 patients' database that distant metastasis was the leading cause of NPC failure after primary radiotherapy. We further showed that hypoxia induced broad changes of both up- and down-regulated gene expressions involved in diverse biological processes in NPC cells. Over-expression of biomarkers of hypoxia and angiogenesis (including HIF-1α, CA IX and VEGF) is common in NPC and is associated with poor prognosis. Elevated plasma osteopontin is a biomarker of distant metastasis, and pre-treatment plasma osteopontin level may be a useful biomarker of response to radiotherapy in NPC.

To develop new therapies in NPC, we demonstrated in a randomized controlled phase 2 clinical trial that sequential therapy of neoadjuvant chemotherapy followed by chemoradiotherapy was well tolerated with a manageable toxicity profile that allowed subsequent delivery of full dose chemoradiotherapy. This strategy reduced distant metastasis which translated into improved patient survival. In preclinical studies, the antiangiogenesis agent sunitinib demonstrated potent *in vitro* and *in vivo* growth inhibition in NPC. In a phase 2 clinical trial, sunitinib demonstrated modest clinical activity in heavily pretreated NPC patients. However, the unexpected high incidence of severe hemorrhage from upper aero-digestive tract in NPC patients who received prior high dose RT to the region is of concern. We propose to exclude NPC patients with disease recurrence within previous radiation field and/or with vascular invasion from future antiangiogenesis therapy.

Results from this series of combined clinical, translational and laboratory studies have redefined the role of hypoxia, angiogenesis and metastasis as new therapeutic targets in NPC. Novel biomarkers and new therapeutic approaches were developed based on these targets.

TABLE OF CONTENTS

STATEMENT OF ORIGINALITY

I hereby declare that this thesis was written by myself and represents my own work, except where due acknowledgement is made, and that it has not been submitted to a University or any other institution for a degree or diploma.

Part of the work in this thesis (study 3) was performed during my overseas training from Jan to June 2001 at the Weatherall Institute of Molecular Medicine, John Radcliffe Hospital, University of Oxford, UK. I was responsible for the study design, laboratory work, data analysis and preparation of the manuscript under the guidance of Prof Adrian Harris and Dr Francesco Pezzella (Cancer Research UK, University of Oxford), and Prof Anthony Chan and Prof KF To (Chinese University of Hong Kong).

All the other laboratory and clinical studies were conducted at Sir YK Pao Center for Cancer, Department of Clinical Oncology, Prince of Wales Hospital, Chinese University of Hong Kong. I was principally responsible for the study design, monitoring of experiments and studies, recruitment of patients, data analysis and preparation of the manuscript under the mentorship of Prof Anthony Chan, Chairman and Professor of Clinical Oncology, Chinese University of Hong Kong. The microarray experiment described in study 2 was performed by Dr Nancy Tsui at Prof Dennis Lo's laboratory at Chinese University of Hong Kong, of which I was responsible for the experimental design and data analysis. I received technical assistance from Dr Fion Sung, Wai-lap Wong and Xiaorong Lin for the experiments in studies 2 and 4, and from the staff of the Cancer Drug Testing Unit (Dr Vivian Lui, Cecilia Lau, Crystal Cheung and Kakiu Ho) for the drug testing and xenograft experiments in study 6. The clinical trials reported in study 5 and 7 were assisted by research staff of the Comprehensive Cancer Trials Unit (CCTU) of Department of Clinical Oncology, of which I was the Deputy Director.

PRÉCIS TO THE THESIS

INTRODUCTION

Nasopharyngeal carcinoma (NPC) is endemic in Southern China and Southeast Asia. It is the fifth commonest cancer in men and the eighth leading cause of cancer death in Hong Kong (Hong Kong Cancer Registry 2007). The current standard therapy for NPC without distant metastasis is radical radiotherapy for early stage disease and concurrent chemoradiotherapy in advanced disease. With the recent advances in tumor localization and high precision radiotherapy delivery, the local control rate in NPC has been improved and distant metastasis has emerged as the predominant mode of treatment failures. For patients who presented or relapsed with distant metastasis, the prognosis is poor with reported median survival times ranging from only 5 to 11 months. Hence, new therapeutic strategies are urgently needed to further improve the treatment outcome.

Although early stage NPC is highly curable by radiotherapy, the cure rate for those with locoregionally advanced NPC remains unsatisfactory. Because NPC is also highly sensitive to chemotherapy, the addition of chemotherapy to radiotherapy in various combinations has been explored to improve the cure rate. From the results of randomized clinical trials conducted in the past two decades, the addition of chemotherapy to radiotherapy has been proven to improve the treatment outcome. However, the optimal timing of chemotherapy when combined with radiotherapy remains to be defined.

Tumor hypoxia has long been known to be associated with resistance to

chemotherapy and radiotherapy as well as a more malignant tumor phenotype with increased invasiveness, metastasis, and poorer survival. Recently it is shown that hypoxia induces the expression of hypoxia-inducible factor-1α and 2α (HIF-1α and HIF-2α), which then up-regulate the expression of downstream genes carbonic anhydrase IX (CA IX) and vascular endothelial growth factor (VEGF). Detection of these intrinsic markers of hypoxia would be of clinical importance for the identification of subgroups of patients that could benefit from hypoxia targeting therapies.

Angiogenesis is another key pathway involved in tumor growth and metastasis. Hypoxia is a key signal for the induction of angiogenesis, and one of the key angiogenic factors regulated by hypoxia is VEGF. In NPC, the expression of VEGF was demonstrated to have significant association with angiogenesis and lymph node metastasis. Therefore targeting angiogenesis and VEGF represent a potential new therapeutic approach in NPC.

The central theme of this thesis is to define the new therapeutic targets in the malignant progression pathways of NPC (namely hypoxia, angiogenesis and metastasis, Figure 1.1), and to evaluate the corresponding novel biomarkers, and finally based on the knowledge gained to develop new therapeutic approaches in NPC, with the ultimate aim to further improve the treatment outcome in NPC.

Figure 1.1

The proposed pathway of malignant tumor progression in nasopharyngeal cancer. The corresponding study number described in this thesis is shown on the right panel.

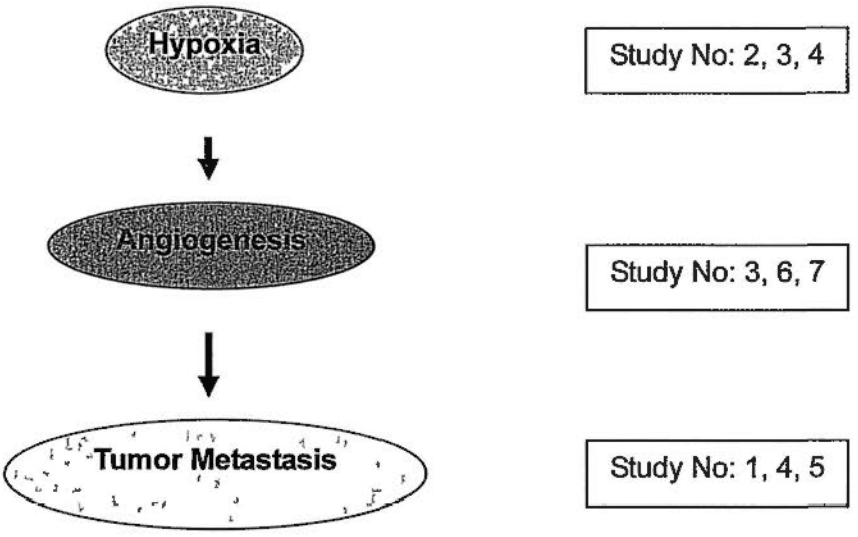

OBJECTIVES

Part 1: New targets and biomarkers (study No 1, 2, 3 and 4)

1) To study the pattern of treatment failure and metastasis in NPC.

2) To study hypoxia regulated gene expression profile in NPC.

3) To study the expression of hypoxia regulated proteins and their clinical significance in NPC.

4) To investigate the relationship of plasma osteopontin, hypoxia and response to radiotherapy in NPC.

Part 2: New therapeutic approaches (study No 5, 6 and 7)

5) To investigate sequential strategy of neoadjuvant chemotherapy followed by concurrent chemoradiotherapy in NPC.

6) To evaluate the preclinical activities of sunitinib, a novel VEGF receptor tyrosine kinase inhibitor and antiangiogenesis agent, in NPC cell lines and xenograft model.

7) To evaluate the clinical activities of sunitinib in a phase 2 clinical trial in NPC patients.

RESEARCH HYPOTHESES

Part 1: New targets and biomarkers

1) Distant metastasis is the major cause of treatment failure after successful local control in NPC, and patients with different sites of metastases have different survival.

2) Hypoxia induces global changes in gene expression patterns in NPC that contributes to the clinical hypoxic tumor phenotype.

3) Hypoxia regulated proteins are detectable in NPC tumor biopsies and their expressions correlate with clinical outcome.

4) Plasma osteopontin is associated with distant metastasis, and is predictive of response to radiotherapy in NPC.

Part 2: New therapeutic approaches

5) The sequential therapy of neoadjuvant chemotherapy followed by concurrent chemoradiotherapy is a tolerable new therapeutic approach in advanced NPC, which can reduce distant metastasis and improve patient survival, when compared with chemoradiotherapy alone.

6) Sunitinib, a novel multi-targeted receptor kinase inhibitor of VEGF, is an active agent in preclinical models of NPC.

7) Sunitinib is an active anti-angiogenesis agent in NPC patients in the clinic.

SUMMARY OF RESEARCH METHODS AND RESULTS

Part 1: New targets and biomarkers

Study 1: Pattern of failure and metastasis in NPC

Methods. Clinical data from all five oncology centers in Hong Kong was retrospectively collected from medical records and pooled for this study coordinated by the Hong Kong NPC Study Group. The sample consisted of all the 2915 NPC patients without distant metastasis at presentation treated by radiotherapy in the five cancer centers during the period from January 1996 to December 2000.

Results. Distant metastasis was the leading cause of NPC failure, with 5-year actuarial rate of 14.9% in this cohort. Despite the poor overall survival (OS) of these patients, those with lung metastasis alone represented a distinctive group associated with a significantly better OS. UICC N-stage, T-stage, advanced age and male sex were the significant and independent determinants for distant metastases.

Interpretations: Long term survival is possible in patients with distant metastatic NPC confined to the lung. An aggressive approach to treatment for this group of patients should be considered.

Study 2: Hypoxia regulated gene expression profile in NPC

Methods: We studied hypoxic induction of hypoxia-inducible factor (HIF)-1α, HIF-2α, carbonic anhydrase IX (CA IX) and vascular endothelial growth factor (VEGF) in NPC cell lines, investigated hypoxia-modulated gene expression in NPC cell lines by Affymetrix GeneChip Array expression profiling, and identified pathways influenced by hypoxia and novel genes not previously recognized as hypoxia-inducible. Differentially regulated genes under hypoxia were identified genome-widely and selected genes validated by RT-PCR.

Results: We found that hypoxia induced HIF-1α, CA IX and VEGF expression but not HIF-2α in NPC cells. Microarray expression analysis showed that 222 genes were commonly up-regulated and 137 genes down-regulated in hypoxic-treated CNE-2 and HONE-1 cells.

Interpretations: Hypoxia induced broad changes of both up- and down-regulated gene expressions involved in diverse biological processes in NPC cells. Elucidation of the coordinated functions modulated by hypoxia could lead to a better understanding of the clinical significance of the hypoxic tumor phenotype.

Study 3: Biomarkers of hypoxia and angiogenesis in NPC

Methods: We examined the expression of HIF-1α, HIF-2α, CA IX and VEGF by immunohistochemistry in NPC biopsies from 90 consecutive patients recruited between 1994 and 1997 in a randomized controlled trial of chemoradiotherapy in locally advanced NPC, and investigated their relationship with survival.

Results: HIF-1α was expressed in 52/90 (58%), HIF-2α in 6/89 (7%), CA IX in 51/90 (57%) and VEGF in 54/90 (60%) of tumors. High tumor HIF-1α expression was associated with a trend for poor overall survival ($p = 0.06$). Tumors with a positive hypoxic profile (defined as high expression of both HIF-1α and CA IX) were associated with worse progression free survival ($p = 0.04$). Tumors with both hypoxic and angiogenic profile (defined as high VEGF expression) were associated with a worse progression free survival ($p = 0.0095$).

Interpretations: Over-expression of HIF-1α, CA IX and VEGF is common in NPC, which is probably related to hypoxia up-regulated expression involving a HIF dependent pathway, and is associated with poor prognosis. Targeting the hypoxia pathway may be useful in the treatment of NPC.

Study 4: Plasma osteopontin, hypoxia and response to radiotherapy in NPC

Methods: We investigated the response of osteopontin (OPN) to in-vitro hypoxia in NPC cell lines, and determined plasma OPN levels in NPC, non-NPC head and neck cancer (HNC) patients and healthy controls. We explored the relationship of plasma OPN and response to radiotherapy in NPC. NPC cell lines (HK1, HONE-1, C666-1 and CNE-2) were treated with 0-48 hours of hypoxia or normoxia, +/- reoxygenation. OPN secretion in the supernatant was measured by ELISA assay. Cellular OPN protein and mRNA were detected by Western blotting and RT-PCR respectively. Plasma OPN levels in patients (n=66; 44 NPC, 22 HNC) and controls (n=29) were measured by ELISA.

Results: Hypoxia has no effect on OPN protein and mRNA level in NPC cells. Only CNE-2 secreted OPN and there was no significant induction by hypoxia. Plasma OPN levels in patients of metastatic NPC and HNC, but not in loco-regional NPC, were significantly higher than controls. In patients with loco-regional NPC receiving curative radiotherapy (n=31), a high (> median) pre-treatment plasma OPN level was a significant predictor of poor response to radiotherapy (complete response rate, 40% vs 88%; p=0.009), which remained significant in multivariate analysis.

Interpretations: Elevated plasma OPN is a biomarker of distant metastasis, and pre-treatment plasma OPN level may be a useful biomarker of response to radiotherapy in NPC.

Part 2: New therapeutic approaches

Study 5: Targeting distant metastasis in NPC - neoadjuvant chemotherapy

Methods: We aimed to compare the toxicities, tumor control, survival and quality of

life of NPC patients treated with sequential neoadjuvant chemotherapy followed by concurrent cisplatin-radiotherapy (CRT) or CRT alone. Previously untreated stage III to IVB NPC were randomized to (1) neoadjuvant chemotherapy of docetaxel 75 mg/m^2 and cisplatin 75 mg/m^2 every 3 weeks for two cycles, followed by cisplatin 40mg/m^2/week concurrent with radiotherapy (CRT), or (2) CRT alone. Planned accrual was 30 patients per arm to detect 20% difference of toxicities based on 95% confidence intervals (C.I.).

Results: From November 2002 to November 2004, 65 eligible patients were randomly assigned to neoadjuvant chemotherapy followed by CRT (n=34) or CRT alone (n=31). There was a high rate of grade 3/4 neutropenia (97%) but not neutropenic fever (12%) during neoadjuvant chemotherapy. No significant differences in rates of acute toxicities were observed between the two arms during CRT. Dose intensities of concurrent cisplatin, late RT toxicities and quality of life scores were comparable in both arms. The 3-year progression free survival for neoadjuvant versus control arm was 88.2% and 59.5% (hazard ratio 0.49; 95% C.I.=0.20 to 1.19; p=0.12). The 3-year overall survival for neoadjuvant versus control arm was 94.1% and 67.7% (hazard ratio 0.24; 95% C.I.=0.078 to 0.73; p=0.012). The preliminary results on pattern of failures suggest that the potential benefit of neoadjuvant chemotherapy is in the reduction of distant metastases (11.8% in the neoadjuvant arm versus 23.1-29.0% in the control arm).

Interpretations: Neoadjuvant chemotherapy followed by CRT was well tolerated with a manageable toxicity profile that allowed subsequent delivery of full dose CRT. Preliminary results suggested a positive impact on survival. A phase 3 study to definitively test this neoadjuvant-concurrent strategy is warranted.

Study 6: Targeting tumor angiogenesis in NPC - Preclinical study

Methods: Sunitinib is a multi-target receptor tyrosine kinase (RTK) inhibitor against vascular endothelial growth factor receptors (VEGFR), platelet-derived growth factor receptors (PDGFR), c-kit and RET. Several of these RTKs are known to be involved in the progression of NPC. We evaluated the preclinical activities of sunitinib in NPC. We determined the basal level of total and phosphorylated PDGFR, c-kit and RET by immunoblotting in a panel of five NPC cell lines. The effect of sunitinib on NPC cell proliferation was evaluated by MTT assay. We further studied the effect of sunitinib on NPC cell cycle progression and apoptosis. We investigated the *in vitro* and *in vivo* activities of sunitinib as single agent and in combination with cisplatin or docetaxel in NPC cell lines and tumor xenografts.

Results: Sunitinib exhibited dose-dependent growth inhibition in all NPC cell lines tested with IC_{50} between 2-7.5 μM and maximum inhibition of over 97%. Sunitinib induced apoptosis and cell cycle arrest at G_0/G_1 phase. *In vitro*, sunitinib moderately enhanced the growth inhibition of cisplatin or docetaxel. Single agent sunitinib demonstrated significant growth inhibition, reduced microvessel density and caused extensive tumor necrosis in a NPC xenograft model. However, concurrent administration of sunitinib and docetaxel induced severe toxicity in mice without enhanced antitumor effect.

Interpretations: Single agent sunitinib demonstrated potent *in vitro* and *in vivo* growth inhibition in NPC. When combined with chemotherapy, sequential instead of concurrent administration schedule should be further explored.

Study 7: Targeting tumor angiogenesis in NPC - Clinical study

Methods: We aimed to evaluate the efficacy and safety of single agent sunitinib in

recurrent or metastatic NPC patients whose disease progressed after prior platinum-based chemotherapy. Patients received continuous daily dosing of Sunitinib at 37.5 mg once-daily in 4-week cycles until progression. Primary endpoint was clinical benefit rate (CBR, % of pts with RECIST defined CR, PR or SD >12 wks). Secondary endpoints included progression free survival (PFS), overall survival (OS), and adverse events (AEs).

Results: Thirteen patients were enrolled. Recruitment was stopped after two patients died of hemorrhagic events. All patients had history of radiotherapy (RT) to nasopharynx/neck (including 9 had chemoradiotherapy). Two, 5, 4 and 3 patients had received 1, 2, 3 and 4 lines of prior chemotherapy respectively after recurrence. Patients received a median of 3 cycles of sunitinib. One patient was still on sunitinib with stable disease after 24 cycles. Most common treatment-related AEs included fatigue (71%), dermatological (71%), hemorrhage (64%), neutropenia (50%), pain (50%), odynophagia/glossitis (50%), hypertension (43%), mucositis (29%) and hypothyroidism (29%). Hemorrhagic events occurred in nine patients (64%), including epistaxis in six, hemoptyses in three and hemetemesis in two patients. Prior RT to thorax was significantly associated with hemoptyses (p=0.03). Two patients with local tumor invasion into the carotid sheath developed fatal epistaxis/hemetemesis within the first cycle of sunitinib, likely due to internal carotid blowout after tumor shrinkage. Clinical benefit rate was 29% (1 partial response and 3 stable diseases lasting for at least 12 weeks). The median time-to-progression was 4.4 months (95% CI 2.8 – 9.4) and the median overall survival was 10.5 months (95% CI 7.2 – 20.7).

Interpretations: Sunitinib demonstrated modest clinical activity in heavily pretreated NPC patients. However, the high incidence of hemorrhage from upper aero-digestive tract in NPC patients who received prior high dose RT to the region is

of concern. Recurrence within previously RT field and direct vascular invasion by tumors appeared to increase the risk of serious bleeding and such patients should be excluded from future antiangiogenesis therapy.

CONCLUSIONS

To investigate potential new therapeutic targets and biomarkers, we first confirmed in the Hong Kong NPC study group of 2915 patient database that distant metastasis was the leading cause of NPC failure after primary radiotherapy. We further showed that hypoxia induced broad changes of both up- and down-regulated gene expressions involved in diverse biological processes in NPC cells. Over-expression of biomarkers of hypoxia and angiogenesis (including HIF-1α, CA IX and VEGF) is common in NPC and is associated with poor prognosis. Elevated plasma osteopontin (OPN) is a biomarker of distant metastasis, and pre-treatment plasma OPN level may be a useful biomarker of response to radiotherapy in NPC.

To develop new therapies in NPC, we demonstrated in a randomized controlled phase 2 clinical trial that sequential therapy of neoadjuvant chemotherapy followed by chemoradiotherapy was well tolerated with a manageable toxicity profile that allowed subsequent delivery of full dose chemoradiotherapy. This strategy reduced distant metastasis which translated into improved patient survival. In preclinical studies, single agent sunitinib demonstrated potent *in vitro* and *in vivo* growth inhibition in NPC. In a phase 2 clinical trial, sunitinib demonstrated modest clinical activity in heavily pretreated NPC patients. However, the unexpected high incidence of severe hemorrhage from upper aero-digestive tract in NPC patients who received prior high dose RT to the region is of concern. We propose to exclude NPC patients with

disease recurrence within previous radiation field and/or with vascular invasion from future antiangiogenesis therapy. Our results highlighted the importance of careful patient selection for future antiangiogenesis therapy.

Results from this series of combined clinical, translational and laboratory studies (study 1 to 7) have redefined the role of hypoxia, angiogenesis and metastasis as new therapeutic targets in NPC. Novel biomarkers and new therapeutic approaches were developed based on these targets. It is concluded that the research hypotheses of this thesis have been confirmed.

CAPTIONS FOR TABLES

CAPTIONS FOR FIGURES

List of Abbreviations used in this Thesis

5-FU	fluorouracil
AE	adverse event
AJCC	American Joint Committee on Cancer
C666-1	nasopharygneal carcinoma cell line
CA IX	carbonic anhydrase IX
CBR	clinical benefit rate
cDNA	complementary DNA
CI	confidence interval
c-kit	stem cell factor receptor
CNE-1/CNE-2	nasopharygneal carcinoma cell line
CO2	carbon dioxide
CR	complete response
CRT	cisplatin-radiotherapy
CT	computed tomography
CT	chemotherapy
CTCAE	Common Terminology Criteria for Adverse Event
DFS	disease free survival
DM	distant metastasis
DNA	deoxyribonucleic acid
EBV	Epstein-Barr virus
ECOG	Eastern Cooperative Oncology Group
ELISA	enzyme-linked immunosorbent assay
EORTC	European Organisation for Research and Treatment of Cancer
FBS	fetal bovine serum
FIH	factor inhibiting HIF-1
GIST	gastrointestinal stromal tumour
GO	Gene Ontology
Gy	gray
H&E	Haematoxylin and Eosin
HER2/neu	Human epidermal growth factor receptor 2
HIF-1a	hypoxia-inducible factor-1a
HIF-2a	hypoxia-inducible factor-2a
HK1	nasopharygneal carcinoma cell line
HLA	human leukocyte antigen
HNC	head and neck cancer
HNSCC	head and neck squamous cell carcinoma
HONE-1	nasopharygneal carcinoma cell line
IC50	inhibitory concentration 50%
IMRT	intensity modulated radiotherapy
ITT	intention-to-treat
IV	intravenous
LF	local failure
LN	lymph node

mNPC	metastatic nasopharyngeal carcinoma
MRI	magnetic resonance imaging
mRNA	messenger RNA
MTT	3-(4,5-Dimethylthiazol-2-yl)-2,5-diphenyltetrazolium bromide (a standard colorimetric assay)
MVD	microvessel density
NCI	National Cancer Institute
NCI-CTC	National Cancer Institute Common Toxicity Criteria
NP	nasopharynx
NPC	nasopharyngeal cancer/carcinoma
O2	oxygen
OPN	osteopontin
ORR	overall response rate
OS	overall survival
PCR	polymerase chain reaction
PD	progressive disease
PDGFR	platelet-derived growth factor receptor
PET	positron emission tomography
PFS	progression free survival
PR	partial response
RCC	renal cell carcinoma
RECIST	Response Evaluation Criteria in Solid Tumors
RET	glial cell-line derived neurotrophic factor receptor (REarranged during Transfection)
RF	regional faliure
RNA	ribonucleic acid
rNPC	recurrent nasopharyngeal carcinoma
RT	radiotherapy
RTK	receptor tyrosine kinase
RTOG	Radiation Therapy Oncology Group
RT-PCR	reverse transcription polymerase chain reaction
S.D.	standard deviation
SD	stable disease
SEM	standard error of mean
SPECT	single photon emission computed tomography
TBS	Tris buffered saline
TNM	tumor, nodal, metastasis
TSG	tumor suppressor gene
TTP	time-to-progression
UICC	International Union Against Cancer
UK	United Kingdom
VEGF	vascular endothelial growth factor
VEGFR	vascular endothelial growth factor receptor
WHO	World Health Organization

Chapter 1

Introduction

Epidemiology

Nasopharyngeal carcinoma (NPC) has a remarkable geographical variation in incidence. In the United States and Western Europe, NPC is a rare tumor with an incidence of 0.5 to 2 per 100,000. In sharp contrast, NPC is endemic in southern China including Hong Kong, where incidence rates as high as 25 to 50/100,000 per year have been reported. There is an intermediate incidence in populations in the Mediterranean basin, and in Alaskan Eskimos. The incidence rate rises from the age of 20 and decreases after 60 years and males are more often affected with a male-female ratio of 3:1. The median age at presentation is 40-50 years, significantly younger than that of other head and neck cancers (Wei and Sham 2005; Chan, Hui, and Leung 2007).

Etiology and molecular pathogenesis

The dramatic difference in the incidence among populations and geographical areas suggest a strong association of NPC with genetic and environmental factors. Previous epidemiological studies strongly suggest three major etiological factors for NPC: genetic susceptibility, early-age exposure to chemical carcinogens (e.g. Cantonese salted fish), and latent Epstein-Barr virus (EBV) infection.

Recent studies have disclosed critical genetic and epigenetic events in NPC. Copy number losses on chromosomes 1p, 3p, 9p, 9q, 11q, 13q, 14q and 16q and recurrent gains on chromosome 1q, 3q, 8q, 12p and 12q were frequently observed in NPC. The roles of several important tumor suppressors (e.g., *p16, RASSF1A*) and oncogenes

(e.g., *CCND1*) have been described (Lo, To, and Huang 2004). Although alterations of the well-established tumor suppressor genes (TSGs, such as TP53 and RB1) are relatively rare in NPC tumors, multiple genetic and epigenetic alterations in other TSGs and oncogenes have been detected (Tao and Chan 2007).

Although the molecular basis of NPC pathogenesis is still poorly understood, it has been proposed that the pathogenesis and development of NPC follows a multistep process. In individuals from endemic regions, the NPC associated genotypes for various alleles (such as HLA and the polymorphic genes for carcinogen metabolism, detoxification and DNA repair) may predispose the nasopharyngeal epithelial cells to DNA damage. As a consequence of chronic exposure to specific carcinogens (e.g., nitrosamines), increased DNA damage may lead to the formation of multiple lesions with clonal genetic changes in nasopharynx. Genetic and epigenetic changes collaborate with EBV latent infection in disrupting major cellular mechanisms and contribute to the initiation and progression of NPC (Lo, To, and Huang 2004).

Principles of therapy

NPC is distinct from other head and neck squamous cell carcinoma (HNSCC) in its epidemiology, pathology, clinical behavior and response to treatment (Chan, Teo, and Huang 2004). The WHO histology type in most (>95%) of the NPC in Hong Kong is undifferentiated carcinoma, which is uniformly associated with Epstein Barr virus infection. Because of its deep anatomical location, surgery is not an option as first line treatment. Therefore, all patients of newly diagnosed NPC whose disease is confined locally (nasopharynx) and regionally (neck lymph nodes), but has not spread to other parts of body (distant metastases, DM), have traditionally been treated with

radiotherapy alone.

Early stage NPC is highly curable (>90%) by radiotherapy (RT) alone, but the cure rate for those with locoregionally advanced NPC (advanced T stage and/or N stage) remains unsatisfactory. Because NPC is also highly sensitive to chemotherapy, the addition of chemotherapy to radiotherapy in various combinations (delivered before, during, and after radiotherapy) has been explored to improve the cure rate. From the results of randomized clinical trials conducted in the past two decades, the addition of chemotherapy to radiotherapy has been proven to improve the treatment outcome. However, the optimal timing, dosing, duration, and regimens of chemotherapy drugs to be combined with radiotherapy remain to be defined. Despite a high response rate of NPC to systemic chemotherapy, the prognosis for patients with distant metastatic disease remains poor (Hui et al. 2004). Moreover, NPC survivors often suffered from moderate to severe late complications, many of which result from the effect of radiation on the organs adjacent to nasopharynx and lymph neck nodes. The use of chemotherapy in advanced cases further adds to these side effects. Therefore novel and more targeted therapies with reduced side effect need to be explored.

The role of chemotherapy

At the time of initial diagnosis, less than 5% of patients with NPC were found to have distant metastasis (DM) in modern series. Control of primary tumor (local control) and prevention of DM has been the major treatment goals in NPC, whereas regional control (neck lymph nodes) is of less a problem, owing to the high success rate of radical neck dissection as a salvage strategy after RT. With the prospect of high local control rate achievable by the application of high-precision RT, DM is expected to

become the predominant cause of treatment failure from NPC.

Chemotherapy is the use of cytotoxic drugs to target cancer cells. Chemotherapy can be combined with RT in order to enhance the effect RT on local control or to eradicate occult DM. Theoretically combination chemotherapy regimen is probably more effective in eradicating micro-metastases, although it may be practically impossible to deliver at full doses concurrently or sequentially with radiotherapy. Optimal timing of the two treatment modalities will be crucial for the success of this strategy. Although treatment strategies other than the addition of chemotherapy (three-dimensional conformal or intensity modulated RT, accelerated fractionation schedule, intracavitary boost) are currently being pursued to enhance locoregional control, systemic chemotherapy is the only available option to directly target occult DM. Nevertheless, it cannot be excluded that optimal locoregional control can translate into a better DM control (the chicken-and-egg hypothesis, where the seeds of DM may come from uncontrolled locoregional disease), and that a treatment modality primarily addressed to attack DM may also be beneficial on control of locoregional disease (Sanguineti et al. 2003).

The sequence and timing of chemotherapy and radiotherapy

The best timing of chemotherapy to be delivered in relation to RT has been an ongoing controversy for some years. Chemotherapy may be given before RT (neoadjuvant or induction chemotherapy), parallel to RT (concurrent or concomitant chemoradiation), or after RT (adjuvant chemotherapy). Figure 1.2 illustrated the possible schemes to deliver chemotherapy (CT) in relation to RT.

Figure 1.2

Scheme of integration of chemotherapy and radiotherapy

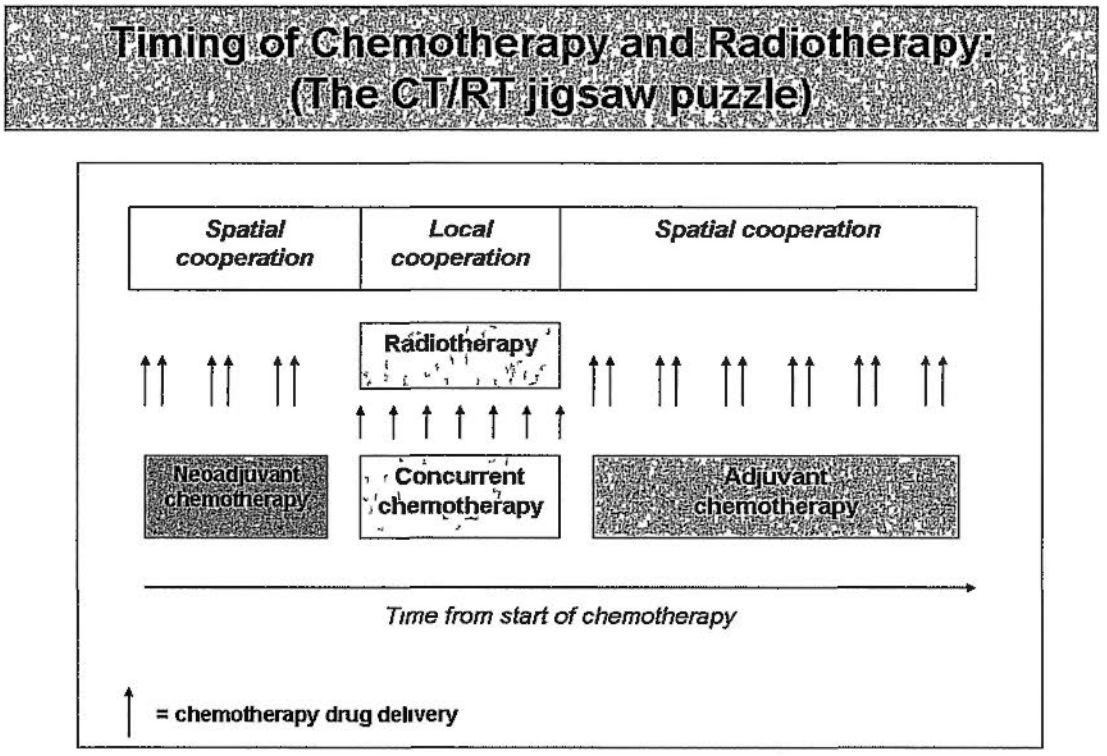

When two treatment modalities are expected to work independently at two different targets (radiotherapy at local and regional sites, and chemotherapy on distant micro-metastases), the best therapeutic index is usually obtained when the two treatments are given at different times (i.e. neoadjuvant chemotherapy followed by RT, or RT first followed by adjuvant chemotherapy), because of the concern that any interaction between the two modalities may prohibitively increase the risk of acute side effect. This strategy is called "spatial cooperation" (Sanguineti et al. 2003). However, if local tumor control is the primary aim, then concurrent administration of both modalities is usually preferred. This strategy of "local cooperation" aims to produce an additive or synergistic interaction between radiation and chemotherapy (radiosensitizer). Results from studies in head and neck squamous cell carcinomas confirm that the concurrent administration of chemoradiation is superior to sequential use in obtaining a local effect. However, acute and sometimes late reactions become the limiting factor. Drugs with non-overlapping toxicity with that of radiation are preferred.

In the past two decades, fourteen randomized controlled trials have been reported on the use of neoadjuvant, concurrent, and adjuvant chemotherapy, or a combination of these approaches in the treatment of advanced NPC (summarized in Table 1.1 and 1.2). The available clinical data has supported the role of neoadjuvant chemotherapy in reducing DM and concurrent chemoradiation in enhancing local control. Interestingly, some locoregional effect of sequential chemotherapy and some distant effect of concurrent chemoradiation have also been observed.

Table 1.1
Randomized clinical trials of neoadjuvant/adjuvant chemotherapy with radiotherapy vs radiotherapy alone in locally advanced nasopharyngeal carcinoma.

Institution	Year of publication	Patient number	Timing of chemotherapy	DFS		OS		Benefit	Reference
				RT	CT/RT	RT	CT/RT		
Adjuvant trials									
Institute Nationale Tumori, Italy	1988	229	Adjuvant VCA x 6 cycles	4-yr: 56%	58%	4-yr: 67%	59%		(Rossi et al. 1988)
TCOG (Taiwan Cooepative Oncology Group)	2002	157	Adjuvant PFL x 9 cycles	5-yr: 50%	54%	5-yr: 61%	55%	DM	(Chi et al. 2002)
Neoadjuvant trials									
PWH (Prince of Wales Hospital, Hong Kong))	1995	82	Neoadjuvant PF x 2 cycles and adjuvant PF x 4 cycles	2-yr: 72%	68%	2-yr: 81%	80%		(Chan et al. 1995)
VUMCA I (International NPC Study Group)	1996	339	Neoadjuvant BEC x 3 cycles	5-year: 30% (P<0.01)	39%	5-yr: 46%	40%		(VUMCA-I 1996)
AOCOA (Asian Oceanian Clinical Oncology Association)	1998	334	Neoadjuvant PE x 2-3 cycles	3-yr: 42%	48%	3-yr: 71%	78%	Local control in subgroup	(Chua et al. 1998)
Sun Yat-Sen University, China	2001	456	Neoadjuvant PFB x 2-3 cycles	5-yr: 49% (p=0.05)	59%	5-yr: 56%	63%	Local control	(Ma et al. 2001)
AOCOA + Sun Yat-Sen (Pooled update)	2004	784	(As above)	5-yr: 58% (p<0.05)	64%	5-yr: 58%	62%	Local control and DM	(Chua et al. 2005)
Sapporo Medical University, Japan	2002	80	Neoadjuvant PF x 2	5-yr: 43%	55%	5-yr: 48%	60%	DM	(Hareyama et al. 2002)

DFS, Disease free survival; OS, overall survival; RT, radiotherapy arm; CT/RT, combined chemotherapy and radiotherapy arm; VCA, vincristine + cyclophosphamide + doxorubicin,; PFL, cisplatin + 5-FU + leucovorin; PF, cisplatin + 5-FU; BEC, bleomycin + epirubicin + cisplatin; PE, cisplatin + epirubicin; PFB, cisplatin + 5-FU + bleomycin; (p-value) indicate significant difference

Table 1.2
Randomized clinical trials of concurrent chemoradiation (with or without adjuvant chemotherapy) vs radiotherapy alone in locally advanced nasopharyngeal carcinoma.

Institution	Year of publication	Patient number	Timing of chemotherapy	DFS		OS		Benefit	Reference
				RT	CRT	RT	CRT		
Intergroup 0099	1998, 2001	147	Concurrent cisplatin every 3 week x 3 cycles then adjuvant cisplatin + 5-FU x 3 cycles	5-yr: 29% (p<0.001)	58%	5-yr: 37% (p<0.001)	67%	Local control and DM	(Al-Sarraf et al. 1998, 2001)
PWH-QEH (Prince of Wales Hospital and Queen Elizabeth Hospital, Hong Kong)	2002, 2005	350	Concurrent cisplatin weekly x 8 cycles	5-yr: 52%	60%	5-yr: 59% (p<0.05)	70%		(Chan, Teo et al. 2002; Chan, Leung et al. 2005)
Taichung Veterans General Hospital, Taiwan	2003	284	Concurrent cisplatin + 5-FU x 2 cycles	5-yr: 53% (p<0.01)	72%	5-yr: 54% (p<0.01)	72%	Local control	(Lin et al. 2003)
QMH (Queen Mary Hospital, Hong Kong)	2004	219	Concurrent uracil And adjuvant cisplatin + 5-FU alternating with vincristine + bleomycin + methotrexate x 6 cycles	3-yr: 58%	69%	3-yr: 77% (p=0.06)	87%	DM	(Kwong et al. 2004)
National Cancer Center, Singapore	2004, 2008	221	Concurrent cisplatin every 3 week x 3 cycles then adjuvant cisplatin + 5-FU x 3 cycles	5-yr: 46% (p=0.0318)	59%	5-yr: 49% (p=0.0077)	67%	DM	(Wee et al. 2005; Wee 2008)
Hong Kong NPC Study Group 9901	2004, 2010	348	Concurrent cisplatin every 3 week x 3 cycles Then adjuvant cisplatin + 5-FU x 3 cycles	5-yr 55% (p=0.014)	67%	5-yr: 64%	68%	Local control	(Lee, Lau et al. 2005; Lee et al. 2010)
Sun Yat-Sen University, China	2005	115	Concurrent oxaliplatin weekly x 6 cycles	2-yr: 83% (p<0.05)	96%	2-yr: 77% (p=0.01)	100%	DM	(Zhang et al. 2005)

RT, radiotherapy alone arm; CRT, concurrent chemoradiation arm; Yr, year; DM, distant metastases; (p-value) indicate significant difference

Neoadjuvant chemotherapy

The theoretical advantages of neoadjuvant (induction) chemotherapy include: (1) a lower tumor load of distant micro-metastatic deposits and thus a higher chance of eradication; (2) a higher tolerance and compliance to chemotherapy in untreated patients; (3) in vivo testing of chemotherapy sensitivity by evaluating clinical response of measurable disease. The disadvantages include: (1) delay in giving definitive local treatment, favouring the outgrowth of resistant cells and selection of partial resistance to radiotherapy; (2) accelerated tumor repopulation. These may theoretically reduce the efficacy of subsequent RT.

However, neoadjuvant chemotherapy may provide a "local cooperation" effect in the primary tumor bed by killing a few logs of cells before RT. This effect will be greater at the tumor periphery where cells are better vascularised and accessible to drug killing. Primary tumor volume reduction after neoadjuvant chemotherapy may be crucial for optimal RT delivery.

Although no significant improvement in overall survival was seen in all the published neoadjuvant chemotherapy trials (Chan et al. 1995; VUMCA-I 1996; Chua et al. 1998; Ma et al. 2001; Chua et al. 2005; Hareyama et al. 2002), the clinical data confirmed the theoretical expectation of neoadjuvant chemotherapy in the endpoints of progression free survival. Benefit has been seen in both local control and DM (Table 1.1). The probability of tumor progression before RT is shown to be remote. However, the selection and dosage of drugs is crucial, as an over-toxic schedule has been shown to impair the delivery of subsequent RT. As the VUMCA I experience strongly suggest, any possible benefit on survival may be offset by increased treatment

related mortality (VUMCA-I 1996).

Adjuvant chemotherapy

Adjuvant chemotherapy does not delay or interfere with local treatment, but is often poorly tolerated after an intensive course of radical RT. Seven randomized trials have tested the role of adjuvant chemotherapy (Chan et al. 1995; Kwong et al. 2004; Wee et al. 2005; Lee, Lau et al. 2005; Rossi et al. 1988; Chi et al. 2002; Al-Sarraf et al. 1998). However, only two studies addressed solely the use of adjuvant chemotherapy alone (Rossi et al. 1988; Chi et al. 2002). In summary, no evident benefit appears to be derived from adjuvant chemotherapy when this approach is analyzed separately. Moreover, adjuvant chemotherapy is less well tolerated, especially when concurrent chemotherapy is also given. In all the clinical trials, the compliance to adjuvant chemotherapy remains a major problem. In the neoadjuvant setting, 87-100% of patients received the planned cycles of chemotherapy, while 44-93% of patients scheduled for concurrent chemotherapy received their planned cycles, and only 14-55% of patients completed their planned adjuvant chemotherapy. Chemotherapy dose intensity is most optimally maintained in the neoadjuvant setting. This disparity in dose intensities may partially explain the lack of treatment benefit associated with the administration of adjuvant chemotherapy alone.

Concurrent chemoradiation

There are two potential mechanisms by which chemotherapy given concurrently with RT might affects DM. The first is a direct effect on distant micro-metastases. The second is through improved locoregional control. Clinical evidence suggested that improved local control contributes to survival including prevention of DM arising from

uncontrolled locoregional disease (Kwong, Sham, and Choy 1994).

A major breakthrough in the management of locally advanced NPC came about in 1998 with the publication of the pivotal phase III randomized Intergroup 0099 trial (Al-Sarraf et al. 1998). This study used both concurrent and adjuvant chemotherapy combined with RT. At 3 years, the disease free survival (DFS) was 69% in the chemotherapy arm and 24% in the RT alone arm. The 3-year overall survival (OS) was 78% vs 47%, favoring chemotherapy. Updated analysis at five years confirms the benefit of chemotherapy (Al-Sarraf et al. 2001) (shown in Table 2). This dramatic improvement of both DFS and OS has led to the adoption of combined modality treatment as standard care for advanced stage NPC in the United States.

However, the RT control arm of the intergroup study has been criticized for its poor results in a heterogeneous histology mix of World Health Organization (WHO) type I, II and III NPC patients, raising questions regarding the applicability of the results for NPC patients with mostly WHO type II and III histology in endemic areas. Subsequently, several confirmatory studies from Asia (Hong Kong, Taiwan and Singapore) all supported the survival benefit of concurrent chemoradiation (with or without adjuvant chemotherapy) in advanced NPC in endemic areas (Chan, Teo et al. 2002; Chan, Leung et al. 2005; Lin et al. 2003; Kwong et al. 2004; Wee et al. 2005; Lee, Lau et al. 2005; Zhang et al. 2005). Interestingly, three of the studies (Hong Kong (Chan, Leung et al. 2005), Taiwan (Lin et al. 2003), and China (Zhang et al. 2005) employed a purely concurrent chemotherapy regimen without the intergroup adjuvant component, and all confirmed a positive survival benefit from the use of concurrent chemotherapy.

A metaanalysis of 1753 individual patient data from eight randomized trials has further confirmed that the addition of chemotherapy to radiotherapy provides significant benefit in OS and DFS. The pooled hazard ratio of death was 0.82 (95% confidence interval (CI) 0.71 to 0.95; P = 0.006) corresponding to an absolute survival benefit of 6% at five years from chemotherapy (from 56% to 62%). A significant interaction was observed between the timing of chemotherapy and overall survival, with the highest benefit observed when chemotherapy was administered concurrently with RT (Baujat et al. 2006).

The sequential strategy: neoadjuvant chemotherapy followed by concurrent chemoradiation

Since the use of both neoadjuvant chemotherapy and concurrent chemoradiation has been shown consistently to improve progression free and/or overall survival in advanced NPC, the development of sequential neoadjuvant chemotherapy followed by concurrent chemo-radiation ("neoadjuvant-concurrent" chemotherapy) would seem a logical strategy in an attempt to maximize the benefit from both approaches. In fact, this "neoadjuvant-concurrent" strategy has been pursued by several groups in phase 2 studies and reported excellent outcome (Benasso et al. 2000; Rischin et al. 2002; Oh et al. 2003; Chan et al. 2004; Lee, Yau et al. 2005).

Is there a standard chemoradiotherapy regimen?

With all the available evidence, one can firmly conclude that concurrent chemoradiation (with or without adjuvant chemotherapy) is the standard of care in advanced NPC. However, due to the heterogeneity of chemotherapy protocols used

in clinical trials, one cannot conclude about the superiority of one chemotherapy regimen to be combined with RT. The addition of further chemotherapy to concurrent chemoradiation, delivered in a neoadjuvant or adjuvant sequence, may further augment disease control. As evident from the metanalysis, the treatment effect could be dependent on the timing of chemotherapy. No evidence of overall survival benefit was observed with neoadjuvant and adjuvant chemotherapy. A benefit for event free survival was, however, demonstrated in the subset of trials using neoadjuvant chemotherapy. In this group, there was an excess of treatment-related deaths in the chemotherapy group. This may suggest that if toxicity was better managed, which is the case in the more recent trials, neoadjuvant chemotherapy may improve OS (Baujat et al. 2006).

Although adding adjuvant plus concurrent chemotherapy to RT conferred superior survival over radiotherapy alone in the Intergroup 0099 study, the relative contribution of concurrent and adjuvant chemotherapy components has been inadequately assessed. Patients who were enrolled based on stage alone could have limited events making the studies on adjuvant chemotherapy frequently under-powered to show any benefit. The use of neoadjuvant chemotherapy is limited by the number of cycles generally permissible as definitive RT will be significantly delayed by more than six to nine weeks. These findings suggest that in the individual patient, the traditional risk profiles in therapeutic decision-making may not fully exploit all the potential therapeutic effects derived from the maximal integration of both modalities.

Towards individualized therapy: risk stratification

The addition of cisplatin to RT can lead to increase in both acute and late toxicities,

potentially narrowing the ultimate therapeutic gain. This point is well illustrated by the recently updated result from the Hong Kong NPC 9901 trial (Lee et al. 2010). In the updated result published in 2010, the investigators found that despite patients randomized to combined chemotherapy and RT experienced a statistically significant reduction in deaths due to disease progression, they also experienced a statistically significant increase in deaths due to treatment-related toxicities and other causes. The authors has also noted a "worrisome increase" in non-cancer deaths in the combined chemotherapy and RT arm, including infection, second malignancy and suicide. The increase in non-cancer deaths narrowed the resultant gain in overall survival (Lee et al. 2010).

The ability to identify a group of patients who cannot benefit from the addition of chemotherapy can render a more personalized therapy and maximize the therapeutic ratio. One possible approach to fine tune the choice of therapy is to develop a risk stratification model, which may include other biological and molecular markers that may help to individualize the best therapeutic option.

In NPC patients, pre-therapy EBV DNA in serum or plasma has been proven to correlate with cancer stage (Lo, Chan, Lo et al. 1999), clinical outcome (Lo, Chan et al. 2000) and prognosis (Lo, Chan, Chan et al. 1999). Post-therapy EBV DNA has even better correlation with prognosis and has been used to monitor recurrence during post-therapy surveillance (Lin et al. 2004; Chan, Lo et al. 2002; Hong et al. 2004). Raised EBV DNA has been shown to predate clinical recurrence by 3 to 7 months (Lo, Leung et al. 2000; Ngan et al. 2001; Chan et al. 2004). Detectable / high level of post-therapy EBV DNA in plasma can predict a poor progression-free or

overall survival when compared with those with undetectable / low DNA level (Lin et al. 2004; Chan, Lo et al. 2002), and may be a marker of subclinical residual disease.

Targeting high-risk patients (patients with a significant likelihood of harboring occult distant metastasis, defined by residual detectable post-therapy plasma EBV DNA) using intensive chemotherapy given in the adjuvant setting may be able to reduce distant metastasis and improve survival to level of statistical significance by eradicating low-burden micro-metastasis. Sparing low-risk patients defined by the same criteria from potential chemotherapy toxicity is also an advantage. To this end, our center has recently initiated the use of plasma EBV DNA as a screening tool to select for NPC patients at high risk of DM at completion of RT for enrolment into a randomized adjuvant chemotherapy trial (Hong Kong NPC study group 0502 adjuvant study, ClinicalTrials.gov number, NCT00370890).

Predictive markers (e.g. plasma EBV DNA) may be useful to stratify patients that will benefit from more intensive therapy and sparing lower risk patients from unnecessary toxicity. We have recently demonstrated that even patients with early stage NPC could be segregated by pre-therapy EBV DNA levels into a poor-risk subgroup with survival similar to that of stage III disease (Leung et al. 2006). These patients should be candidates for more intensive therapy, as supported by clinical observations from other group (Chua et al. 2003).

Chemotherapy in recurrent or metastatic disease

The traditional chemotherapy drugs with activity in head and neck cancers include cisplatin, carboplatin, 5-FU, methotrexate, and bleomycin. The response rate of

single agents ranged from 15% to 31% (Chan et al. 1998). Carboplatin as single agent in NPC showed a response rate of 44% and was well tolerated (Chi et al. 1997). Mitoxantrone demonstrated a response rate of 25% in a large multicenter phase II trial in NPC (Dugan et al. 1993).

In head and neck cancer, combination chemotherapy regimens have consistently demonstrated higher response rate than single agent chemotherapy, and therefore recent trials have focused on the use of multi-drug combinations. Early experiences of combination chemotherapy in recurrent or metastatic NPC suggested that NPC was highly chemo-responsive and platinum containing regimen appeared to be most effective in producing complete remission (Decker et al. 1983; Choo and Tannock 1991). Platinum-based combinations have consistently produced higher response rates compared with monotherapy or non-platinum therapy (Wang and Tan 1991; Au and Ang 1994; Stein et al. 1996; Yeo et al. 1996) (e.g. the combination of ifosfamide, 5-FU and leucovorin (Chua et al. 2000). Newer chemotherapy drugs including taxanes (paclitaxel and docetaxel), gemcitabine, capecitabine, irinotecan, vinorelbine and oxaliplatin, all demonstrated comparable response and generally improved side effect profile (summarized in Table 1.3)(Au, Tan, and Ang 1998; Yeo et al. 1998; Tan et al. 1999; Pan et al. 2000; McCarthy et al. 2002; Foo et al. 2002; Ngan et al. 2002; Ma et al. 2002; Jiang et al. 2005; Chua, Sham, and Au 2003; Poon et al. 2005; Chua, Sham, and Au 2005; Ma and Chan 2005; Zhang et al. 2005; Wang et al. 2006; Ma et al. 2009). Among the platinum-based doublets, cisplatin-gemcitabine has consistently produced both the highest overall response rate (64-93%) and complete response rate (14-21%) (Ngan et al. 2002; Ma et al. 2002; Jiang et al. 2005), which is a prerequisite for a potential cure.

More intensive chemotherapy regimens combining three or more agents have been attempted to improve treatment response. This is however achieved at the cost of increased toxicity and even treatment related death (Boussen et al. 1991; Su et al. 1993; Chi et al. 1994; Siu, Czaykowski, and Tannock 1998; Taamma et al. 1999; Hasbini et al. 1999; Leong et al. 2005) (Table 1.4).

The natural history and management of metastatic NPC has long been an area of controversy. Distant metastases in patients with NPC have been conventionally regarded as incurable and the aim of treatment has largely been palliative. However, the experience from our center and from other investigators in the French (Fandi et al. 2000) and Canadian (Choo and Tannock 1991) series all suggested that a small proportion of patients with metastatic NPC treated with aggressive chemotherapy had achieved long term disease free survival, suggesting the curative potential of chemotherapy, at least in a small subset of metastatic NPC (Chan et al. 1998).

Table 1.3
Platinum-based doublets or new agents in metastatic nasopharyngeal carcinoma.

Investigators	Year of Publication	Patient number	Regimen	Response rate (%)	Complete response (%)	Toxic death (%)	Reference
Wang and Tan	1991	25	Cisplatin + 5-FU	76	8	4	(Wang and Tan 1991)
Au and Ang	1994	24	Cisplatin + 5-FU	66	13	No	(Au and Ang 1994)
Stein et al	1996	18	Cisplatin + Ifosfamide	59	15	6	(Stein et al. 1996)
Yeo et al	1996	42	Carboplatin + 5-FU	38	17	No	(Yeo et al. 1996)
Au et al	1998	24	Paclitaxel	22	0	No	(Au, Tan, and Ang 1998)
Yeo et al	1998	27	Carboplatin + paclitaxel	59	11	No	(Yeo et al. 1998)
Tan et al	1999	32	Carboplatin + paclitaxel	75	3	3	(Tan et al. 1999)
Airoldi et al	2002	12 (pre-treated)	Carboplatin + paclitaxel	25	0	0	(Airoldi et al. 2002)
Ngeow et al	2010	30 (pre-treated)	Docetaxel	37	0	3	(Ngeow et al. 2010)
McCarthy et al	2002	9	Cisplatin + docetaxel	22	0	No	(McCarthy et al. 2002)
Chua et al	2005	19	Cisplatin + docetaxel	63	6	11	(Chua, Sham, and Au 2005)
Foo et al	2002	25 (untreated) 27 (pretreated)	Gemcitabine	28 48	4 3.7	No	(Foo et al. 2002)
Zhang et al	2008	32	Gemcitabine	44	0	No	(Zhang et al. 2008)

Table 1.3 (cont'd)
Platinum-based doublets or new agents in metastatic nasopharyngeal carcinoma.

Investigators	Year of Publication	Patient number	Regimen	Response rate (%)	Complete response (%)	Toxic death (%)	Reference
Ngan et al	2002	44	Cisplatin + gemcitabine	73	20	2	(Ngan et al. 2002)
Ma et al	2002	18	Gemcitabine	34	6	No	(Ma et al. 2002)
		14	Cisplatin + gemcitabine	64	14		
Jiang et al	2005	15	Cisplatin + gemcitabine	93	21	-	(Jiang et al. 2005)
Chua et al	2003	17	Capecitabine	24	6	No	(Chua, Sham, and Au 2003)
	2008	49		37	6	No	(Chua et al. 2008)
Ciuleanu et al	2008	23 (pretreated)	Capecitabine	48	9	No	(Ciuleanu et al. 2008)
Li et al	2008	48	Cisplatin + capecitabine	62.5	6.3	No	(Li et al. 2008)
Poon et al	2004	28 (platinum refractory)	Irinotecan	14	0	4	(Poon et al. 2005)
Pan et al	2000	11	Vinorelbine	18	0	No	(Pan et al. 2000)
Wang et al	2006	39 (cisplatin resistant)	Gemcitabine + vinorelbine	36	1	No	(Wang et al. 2006)
Ma et al	2009	42	Gemcitabine + oxaliplatin	56	2.4	No	(Ma et al. 2009)

Updated and modified from Ma BBY and Chan ATC (Ma and Chan 2005)

Table 1.4
Intensive chemotherapy regimens containing three or more agents in metastatic nasopharyngeal carcinoma.

Investigators	Year of Publication	Patient number	Regimen	Response rate (%)	Complete response (%)	Toxic deaths (%)	Reference
Boussen et al	1991	49	Cisplatin + bleomycin + 5-FU	79	19	-	(Boussen et al. 1991)
Su et al	1993	25	Cisplatin + bleomycin + 5-FU	40	3	12	(Su et al. 1993)
Chi et al	1994	35	Cisplatin + 5-FU + leucovorin	80-100	13-15	No	(Chi et al. 1994)
Siu et al	1998	90	CAPABLE	41-86	6-22	8	(Siu, Czaykowski, and Tannock 1998)
Taamma et al	1999	26	Cisplatin + bleomycin + Epirubicin + 5-FU	78	35	12	(Taamma et al. 1999)
Hasbini et al	1999	44	Cisplatin + Epirubicin + mitomycin + 5-FU	52	13	9	(Hasbini et al. 1999)
Leong et al	2005	32	Carboplatin + gemcitabine + paclitaxel	78	6	-	(Leong et al. 2005)

CAPABLE: cyclophosphamide + doxorubicin + cisplatin + methotrexate + bleomycin

Updated and modified from Ma BBY and Chan ATC (Ma and Chan 2005)

Molecular targeted therapy

Although there have been reports of long term survivors among those who achieved complete response to conventional chemotherapy (Fandi et al. 2000), recurrent or metastatic NPC still remains an incurable disease. Better systemic therapy is needed to improve the survival. In recent years, the field of cancer therapy has witnessed the emergence of novel targeted strategies that inhibit specific cancer pathways and key molecules in tumor growth and progression. With a potentially superior therapeutic index, molecular targeted agents may complement the use of conventional chemotherapy or radiotherapy in this disease.

As molecular targeted cancer therapeutics become more common, assessing the intended target will be more often deemed necessary for prediction of clinical response, independent of the traditional Tumor-Nodal-Metastases (TNM) stage (Ludwig and Weinstein 2005). Targeted therapies and their associated biomarkers will often "co-evolve", as in the example of HER2/neu in breast cancer. Before the advent of trastuzumab (Herceptin), which targets HER2/neu, HER2/neu positivity was considered simply as a negative prognostic indicator independent of TNM stage.

Hypoxia and human cancer

Ambient air is 21% Oxygen (150 mmHg). However, most mammalian tissues exist at 2% - 9% oxygen (on average 40 mmHg). Hypoxia is usually defined as < 2% oxygen, and severe hypoxia (or anoxia) is defined as < 0.02% oxygen (Bertout, Patel, and Simon 2008). Most solid tumors larger than one mm^3 contain regions of low oxygen tension (hypoxia) due to an imbalance in oxygen supply and consumption.

Two types of hypoxia can be distinguished in solid tumors: (a) diffusion limited (chronic) hypoxia, and (b) perfusion limited (acute) hypoxia. Within solid tumors diffusion limited hypoxia develops at distances beyond the diffusion capacity of oxygen from blood vessels (typically 100-150μm), leaving cells chronically deprived of oxygen and nutrients. Perfusion limited or acute hypoxia is often transient and may be due to severe functional and structural abnormalities of the tumor vasculatures. These abnormalities cause disturbances in the blood supply, leading to temporal shutdown of vessels, gradients of oxygen and nutrients, and even reversal of blood flow. In most tumors, both types of hypoxia coexist and contribute to greater or lesser extent (Hoogsteen, Marres, van der Kogel et al. 2007).

Hypoxia and radiation resistance

It has been appreciated for more than 50 years that hypoxia protects cells from killing by irradiation. The pioneering work of Gray and colleagues demonstrated that the sensitivity to radiation damage of cells and tissues depended on the presence of oxygen at the time of irradiation (Gray et al. 1953). The difference in radiation sensitivity between the aerobic and hypoxic cells, which is known as the oxygen enhancement ratio and is defined as the ratio of doses to produce the same level of cell kill under hypoxic to aerobic conditions, is normally in the range 2.5 to 3.0 for mammalian cells. The reason for the universality of this effect is that oxygen reacts chemically with the fundamental biological lesion produced by ionizing radiation, a radical in DNA, thereby "fixing" (making permanent) the damage. In the absence of oxygen, much of the radical damage can be restored to its undamaged form by hydrogen donation from nonprotein sulfhydryls in the cells (Brown 1999).

With the availability of polarographic oxygen electrodes in 1980s, investigators began to directly measure tumor hypoxia in patients with head and neck cancer and carcinoma of the cervix. They demonstrated that most human solid tumors have median pO_2 levels lower than their normal tissue of origin. Furthermore, they have shown that the more hypoxic tumor had an inferior outcome to radiotherapy (Brizel et al. 1997; Hockel et al. 1993; Nordsmark, Overgaard, and Overgaard 1996).

Tumor hypoxia is also a problem for chemotherapy

Hypoxic cells *in vitro* are universally resistant to ionizing radiation, but not to anticancer drugs in general (apart from few exceptions). However, in a solid tumor *in vivo*, a number of factors associated directly or indirectly with tumor hypoxia contribute to resistance to anticancer drugs (Brown 1999).

Hypoxia causes cells to stop or slow their progression through the cell cycle. This effect is not only the result of a generalized decrease in ATP or energy status of the cell but is likely to be caused by specific proteins induced under hypoxic conditions. Because most anticancer drugs are most effective against rapidly proliferating cells, this hypoxia induced inhibition of proliferation will lead to decreased cell killing. Furthermore, the concentration of anticancer drugs will be higher closer to blood vessels than further away. This is a consequence of both the geometry of diffusion distance and also because of the reactivity of anticancer drugs that limit their diffusion away from the blood vessels.

Hypoxia might also contribute to drug resistance in other ways. One is through amplification of genes conferring drug resistance or through the induction of various

hypoxic stress proteins that appear to be responsible for drug resistance. Another factor that can affect response to chemotherapy is the extracellular pH, which is likely to be lower in the hypoxic areas of the tumor. Such trans-membrane pH gradients inhibit the intracellular accumulation of weak bases like Adriamycin.

It is a well-established phenomena that hypoxia will cause a gradient of reduced cell killing by most anticancer drugs as a function of distance from the vasculature. This is supported by evidence from experimental tumors and spheroids (Durand 1989).

Tumor hypoxia increases malignant progression and metastases

There is evidence that hypoxia, by selecting for cells with mutant p53 and with a diminished apoptotic potential, might predispose tumors to a more malignant phenotype (Graeber et al. 1996). Hypoxia and the tumor microenvironment have also been shown to directly cause mutations and genomic instability (Reynolds, Rockwell, and Glazer 1996). Tumor hypoxia also stimulates tumor progression by promoting angiogenesis through the induction of proangiogenic proteins such as vascular endothelial growth factor.

Clinical studies in soft tissue sarcoma and carcinoma of the cervix have shown that hypoxia is an independent and highly significant prognostic factor predicting the metastatic spread of tumor (Brizel et al. 1996; Hockel et al. 1996). Interestingly, hypoxia predicted for distant failure not only in patients treated with radiotherapy but also in those treated with surgery alone. These studies suggest that hypoxia alters the fundamental and physiologically important pathways that result in more aggressive tumor behavior in a wide variety of tumors.

Clinical significance of measuring tumor oxygenation

There is now clear evidence that the oxygenation status of cells in tumors can influence the response to therapy. It follows naturally that if one could accurately measure the oxygenation status of individual tumors one should be able to better predict treatment outcome and select appropriate therapies for each individual patient (Horsman 1998; Hoogsteen, Marres, van der Kogel et al. 2007).

A number of methods are currently available or under development for the detection of tumor hypoxia in clinical setting. They include invasive techniques such as polarographic needle electrodes, minimally invasive methods such as exogenous or endogenous hypoxia markers, and radiologic and nuclear medicine imaging techniques (Hockel and Vaupel 2001; Hoogsteen, Marres, Bussink et al. 2007). The following is a selected list:

1) Invasive microsensor techniques to measure tissue pO_2 directly, e.g. polarographic oxygen electrodes, luminescence-based optical sensors.
2) Electron paramagnetic resonance oximetry
3) Intravascular O_2 detection techniques, e.g. cryospectrophotometry, near-infrared spectroscopy, phosphorescence imaging.
4) Nuclear magnetic resonance spectroscopy and imaging techniques, e.g. ^{1}H-MRI, ^{19}F-magnetic resonance relaxometry.
5) Non-invasive detection of sensitizer adducts, e.g. ^{18}F-Fluoromisonidazole PET, ^{123}I-Iodoazomycin-arabinoside SPECT.
6) Immunohistochemical techniques to detect exogenous administered tissue

hypoxia labeling markers e.g. pimonidazole and EF5.

The search of simple test for clinical use

The development of simple and reliable tests to estimate tumor hypoxia would be of clinical importance for the identification of subgroups of patients that could benefit from hypoxia targeting therapeutic strategies. Previous clinical studies of tumor hypoxia have concentrated on direct measurement with a polarographic electrode, or by injection of a hypoxia-labeling marker, such as pimonidazole, into patient's blood prior to biopsy and subsequent detection of the marker by immunohistochemistry. The recent development of scintigraphic and magnetic resonance imaging of hypoxia-labeling markers are promising new approaches.

In head and neck squamous cell cancer, using direct measurement of tumor pO2, a low pre-treatment pO2 has been shown to predict poor response to radiation and shorter survival (Nordsmark, Overgaard, and Overgaard 1996; Brizel et al. 1997). In NPC, using the hypoxia imaging agent fluorine-18 fluoromisonidasole with positron emission tomography system, tumor hypoxia was demonstrated in 100% of primary tumor and 58% of cervical lymph nodes metastases (Yeh et al. 1996). However, these techniques can only be applied in-vivo and on a prospective basis. In search of a simple test that would detect evidence of hypoxia even on archival tissue material, immunohistochemical detection of proteins induced by clinical relevant levels of hypoxia represents an appealing option. Such intrinsic marker of hypoxia would have the advantage of being assessable on routine clinical biopsies without the need for specialist equipment or administration of exogenous hypoxia markers.

Intrinsic hypoxia markers and the hypoxia-angiogenesis pathway

In the last few years, there has been remarkable progress in understanding the changes of cellular function as a result of tissue hypoxia. More recent studies are providing evidence that tumor hypoxia may also influence malignant progression through effects on signal transduction pathways and the regulation and transcription of various genes. Knowledge of the molecular biology of hypoxia has led to the investigation of hypoxia-induced proteins as intrinsic markers of hypoxia.

Hypoxia inducible factors (HIF)

The transcriptional complex hypoxia-inducible factor-1 (HIF-1) plays a pivotal role in essential adaptive responses to hypoxia, and its expression increases exponentially with decreases in levels of cellular oxygen. HIF-1 has emerged as an important mediator of gene expression patterns in many tumors and also a promising therapeutic target (Semenza 2010). HIF-1 is a heterodimer composed of HIF-1α and HIF-1β subunits. HIF-1β is constitutively expressed, whereas HIF-1α is protected from ubiquitination and proteasomal degradation under hypoxic conditions (Maxwell et al. 1999). Another member of the family showing close sequence homology and similar properties to HIF-1α has also been described and is named HIF-2α (also known as endothelial PAS domain protein-1) (Wiesener et al. 1998).

The hypoxia inducible factors HIF-1α and HIF-2α essentially function as the oxygen sensor in tissue. They dimerize with HIF-1β subunit to bind to a hypoxia-responsive element and activate a wide array of genes, including those involved in anaerobic metabolism, cell cycle control, stress adaptation, angiogenesis, and tissue invasion. These can result in profound alterations on tumor and cellular phenotype (Semenza

2000).

Carbonic anhydrase IX (CA IX)

Carbonic anhydrases form a large family of zinc metalloenzymes of great physiological importance. As catalysts of the reversible hydration of carbon dioxide to carbonic acid, they participate in a variety of biological processes, including respiration, calcification, acid base balance, bone resorption, formation of aqueous humor, cerebrospinal fluid, saliva and gastric acid. The membrane linked isoform carbonic anhydrase IX (CA IX) is a novel member of the carbonic anhydrase family that codes for a transmembrane glycoprotein with a suggested function in maintaining the acid-base balance and intercellular communication (Opavsky et al. 1996). CA IX can confer a variety of features of the transformed phenotype when transfected into NIH 3T3 cells (Pastorek et al. 1994).

Vascular endothelial growth factor (VEGF)

Angiogenesis, the development of new blood vessels from a preexisting vasculature, is a key pathways involved in tumor growth and metastases. Tumors cannot grow greater than 1-2 mm^3 in the absence of angiogenesis because the lack of oxygen in the centre of the tumor results in cell apoptosis and necrosis. Hypoxia is a key signal for the induction of angiogenesis, and one of the key angiogenic factors regulated by hypoxia is vascular endothelial growth factor (VEGF) (Ferrara 1999). VEGF is one of the most well studied markers of tumor angiogenesis and its expression has been shown to be of prognostic significance in most human tumors studied (Poon, Fan, and Wong 2001).

The molecular hypoxia-angiogenesis pathway in tumor

Recently it has been shown that hypoxia induces the expression of HIF-1α and HIF-2α, which then up-regulates the expression of downstream genes CA IX and VEGF (Wykoff et al. 2000; Beasley et al. 2001; Jones et al. 2001), illustrated in Figure 1.3. In cervical cancer, CA IX expression was demonstrated to correlate with tumor hypoxia as measured by needle electrode (Loncaster et al. 2001). CA IX positive cells in SiHa cervical xenografts were found to be clonogenic, resistant to killing by ionizing radiation and preferentially able to bind the hypoxia marker pimonidazole (Olive et al. 2001). HIF-1α expression was shown to overlap with the hypoxia-labeling marker EF5 in cervical cancer xenograft (Vukovic et al. 2001). HIF-1α and CA IX are thus potential endogenous markers of tumor hypoxia. In addition to hypoxia, major genetic or epigenetic alterations resulting in oncogene gain of function or tumor suppressor gene loss of function also lead to increased HIF-1 activity, suggesting HIF-1 activation represent a common final pathway in cancer pathogenesis and clonal selection (Semenza 2000; Maynard and Ohh 2007).

Figure 1.3

The molecular hypoxia-angiogenesis pathway in tumor.

Hypoxia was shown to induce hypoxia inducible factor (HIF) expression, which then up-regulates downstream genes like carbonic anhydrase IX (CA IX) and vascular endothelial growth factor (VEGF). The overexpression of these genes will promote metabolic adaptation and angiogenesis in tumor that eventually contribute to a more aggressive tumor phenotype with increased invasion and metastases (Semenza 2000; Maynard and Ohh 2007).

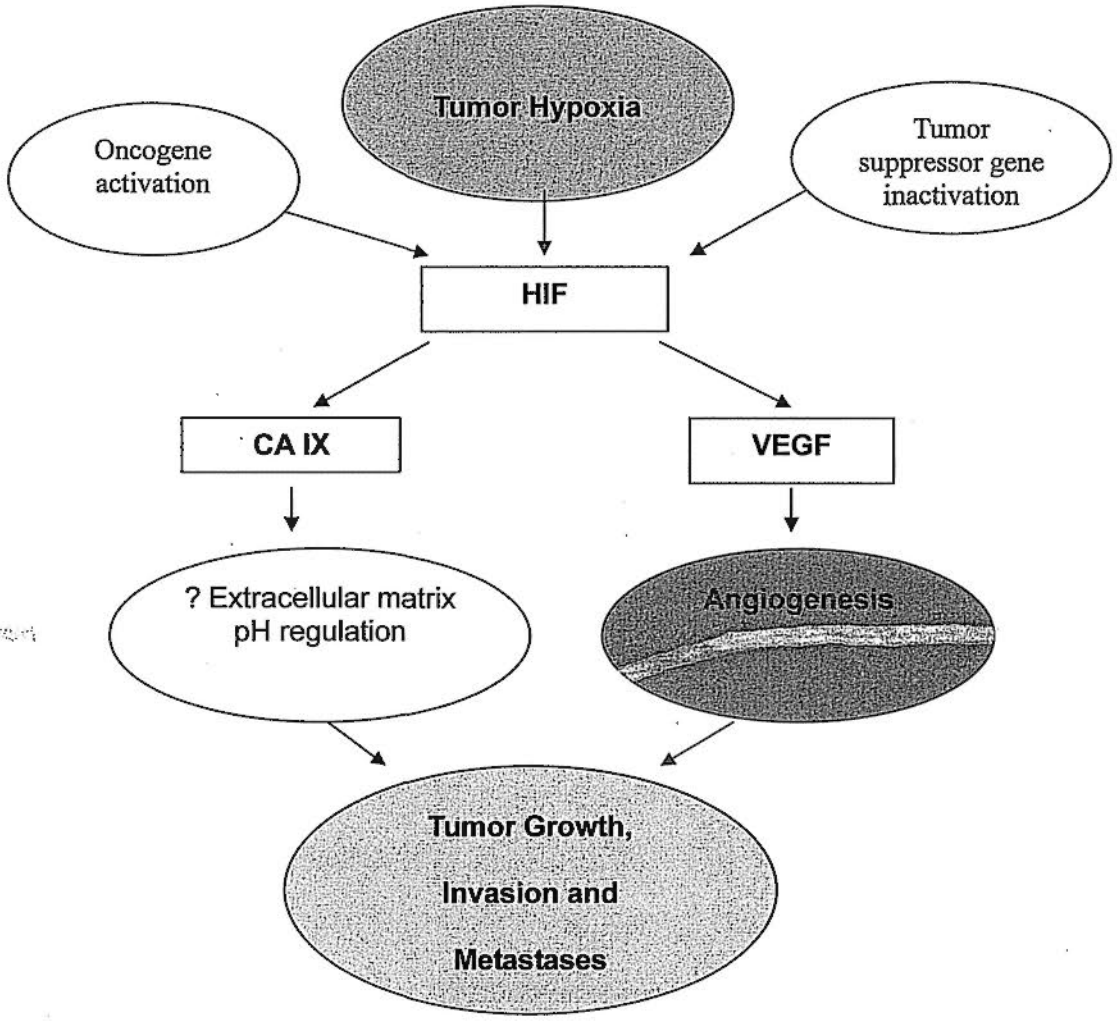

Chapter 2

Objectives and Hypotheses

OBJECTIVES

Part 1: New targets and biomarkers in NPC (study No 1, 2, 3 and 4)

1) To study the pattern of treatment failure and metastasis in NPC.

2) To study hypoxia regulated gene expression profile in NPC.

3) To study the expression of hypoxia regulated proteins and their clinical significance in NPC.

4) To investigate the relationship of plasma osteopontin, hypoxia and response to radiotherapy in NPC.

Part 2: New therapeutic approaches in NPC (study No 5, 6 and 7)

5) To investigate sequential strategy of neoadjuvant chemotherapy followed by concurrent chemoradiotherapy in NPC.

6) To evaluate the preclinical activities of sunitinib, a novel VEGF receptor tyrosine kinase inhibitor and antiangiogenesis agent, in NPC cell lines and xenograft model.

7) To evaluate the clinical activities of sunitinib in a phase 2 clinical trial in NPC patients.

RESEARCH HYPOTHESES

Part 1: New targets and biomarkers in NPC

1) Distant metastasis is the major cause of treatment failure after successful local control in NPC, and patients with different sites of metastases have different survival.

2) Hypoxia induces global changes in gene expressions patterns in NPC that

contributes to the clinical hypoxic tumor phenotype.

3) Hypoxia regulated proteins are detectable in NPC tumor biopsies and their expressions correlate with clinical outcome.

4) Plasma osteopontin is associated with distant metastasis and is predictive of response to radiotherapy in NPC.

Part 2: New therapeutic approaches in NPC

5) The sequential therapy of neoadjuvant chemotherapy followed by concurrent chemoradiotherapy is a tolerable new therapeutic approach in advanced NPC, which can reduce distant metastasis and improve patient survival, when compared with chemoradiotherapy alone.

6) Sunitinib, a novel multi-targeted receptor kinase inhibitor of VEGF, is an active agent in preclinical models of NPC.

7) Sunitinib is an active anti-angiogenesis agent in NPC patients in the clinic.

Chapter 3

Study 1: Pattern of Failures and Metastases

BACKGROUND

As discussed in chapter 1, the local control rate in NPC has been improved significantly in recent series, largely due to advances in tumor localization and high precision radiotherapy delivery. Distant metastasis (DM) has now emerged as the predominant mode of treatment failures. While a significant proportion of local or regional recurrence can be successfully salvaged by surgery or re-irradiation, the vast majority of patients with distant metastases will succumb to the disease. Despite an impressive high response rate to systemic chemotherapy of up to 60-70% (Chan et al. 1998), the overall prognosis for metastatic NPC remains dismal. The reported median duration of survival after the first diagnosis of metastasis has ranged from 5 to 11 months only (Ahmad and Stefani 1986; Vikram et al. 1986; Leung et al. 1991; Teo, Kwan, Lee et al. 1996; Geara et al. 1997; Ong et al. 2003).

It is recognized that metastatic NPC forms a heterogeneous group with a wide range of survival. Several reports have previously described metastatic NPC patients who achieved long-term disease free survival after aggressive multimodality therapy (Teo, Kwan, Lee et al. 1996; Chan et al. 1998; Fandi et al. 2000; Choo and Tannock 1991). To better understand this heterogeneity, we planned this retrospective study to describe the pattern of failure and the time course of the pattern of failures in NPC after primary RT. We also aimed to identify the predictive factors of DM, so that we can improve the patient selection for additional systemic therapy to reduce the risk of DM.

PATIENTS AND METHODS

Patients

The Hong Kong Nasopharyngeal Carcinoma Study Group (HKNPCSG) consist of representatives from all the five oncology centers under the Hospital Authority in Hong Kong, based at the Queen Elizabeth Hospital (QEH), Prince of Wales Hospital (PWH), Tuen Mun Hospital (TMH), Queen Mary Hospital (QMH), and Pamela Youde Nethersole Eastern Hospital (PYNEH). Data on patients treated at the five centers were retrospectively collected and pooled for this study. During the period from January 1996 to December 2000, there were a total of 2915 patients with confirmed histological diagnosis of NPC without evidence of distant metastasis at presentation (Stage M0), who were treated by curative-intent radiotherapy in one of the five oncology centers in Hong Kong: 628 at QEH, 690 at PWH, 618 at TMH, 519 at QMH, and 460 at PYNEH.

The histology diagnosis in 98.5% of the patients was poorly differentiated or undifferentiated carcinoma (World Health Organization, WHO, type 2 or 3 histology (International histological classification of tumours No 19 1978)). Table 3.1 summarised the patient characteristics. The median follow up duration for the entire cohort was 3.1 years (range = <0.1 to 6.6 years) at the time of data collection.

Clinical staging and treatment

All patients underwent routine clinical staging procedures by clinical examination, CT scan of nasopharynx and upper neck, endoscopic examination of the nasopharynx, chest radiograph, complete blood counts and serum biochemistry including alkaline

phosphatase level. Magnetic resonance imaging (MRI) of the nasopharynx and neck was performed in 33% of patients (because of resource limitation during the period). The stage definition in this study was according to the AJCC/UICC 1997 stage-classification for NPC (Fleming et al. 1997). Details of nodal involvement were routinely recorded in purpose-specific diagrams, allowing retrospective determination of nodal stage according to the 1997 stage-classification if this was not applied initially. The practice of screening by radiologic imaging for distant metastases was not mandatory, and was conducted only for patients with suspicious clinical symptoms or abnormal baseline investigations. Routine imaging screening for distant metastases was however routinely performed for patients with N3b stage disease in two study centers (QMH and PWH).

The Ho's technique was used in the primary radiotherapy (RT) for most (88.7%) patients during the study period. The RT techniques had been described in detail in a previous publication (Teo, Yu et al. 1996). The median dose to the primary tumor was 66 Gy. A "parapharyngeal boost" of 10-20Gy was given to patients with parapharyngeal extension of disease (Teo, Lee, and Yu 1996), and intra-nasopharyngeal brachytherapy boost was given selectively to patients with T1 or T2a disease either for residual disease or on an adjuvant basis (Teo, Kwan, Yu et al. 1996), and conformal radiotherapy boost given to some patients with advanced T-stage disease. 681 (23%) of patients with advanced-stage disease received cisplatin based chemotherapy either in the neoadjuvant, concurrent or adjuvant settings (Table 3.1).

Statistical analysis

The clinical endpoints included local failure (LF, relapses at nasopharynx), regional failure (RF, relapses at regional neck lymph node), distant metastasis (DM), and death. Patients who developed DM were further categorized into three groups: (1) "DM-only": those had distant metastases without local or regional failure. (2) "LF/RF $\rightarrow$ DM": those with local or regional failure preceding the diagnosis of distant metastasis for more than two months. The two months period was the usual time required to complete the full staging investigations for confirming the extent of distant metastases. (3) "LF/RF + DM": those with distant metastases concurrent with or followed by local or regional failure.

All time-to-event endpoints were calculated from the first day of primary RT to the date of occurrence of that event, or censored at the date of last follow-up. The time interval from primary RT to first DM in different subgroups was compared by the Student's t-test. The overall survival (OS) of different subgroups were plotted by the Kaplan Meier method and compared with the log rank test. The predictive factors for distant metastases were analyzed by the time to first distant metastasis with the Kaplan Meier method and the log rank test. Cox proportional hazard model was used for the multivariate analysis. The clinical parameters used in the analysis included patient's age, sex, histology type, UICC T-stage and UICC N-stage. Age was analyzed as a continuous variable. The use of chemotherapy was not analyzed in this study as it was selected for advanced disease and the selection criteria were not exactly uniform among centers. The statistical analysis was performed with SAS version 8.02. All significance tests were two sided with $p < 0.05$ as significant.

RESULTS

Clinical outcome

Among the study cohort of 2915 patients treated with curative-intent RT with or without chemotherapy, 1705 (58%) patients were alive without evidence of disease, 608 (21%) patients were alive with disease, and 45 patients were alive with unknown disease status. A total of 408 (14%) patients had died of NPC, of whom 21 patients had died of treatment related complications. Seventy-five patients had died of intercurrent illness. Seventy-four patients died of unknown cause that could not be determined. A total of 338 patients (12%) had developed local failure (LF), 100 (3%) had developed regional failure (RF) and 476 (16%) had developed distant metastases (DM). Combined local-regional and distant failures occurred in 3% of patients. Distant metastasis was the most common mode of failure, with 5-year actuarial rate of 14.9% in this reprospective study cohort.

Time course of distant failure in different patient subsets

The time course of DM in different subsets of patients was shown in Table 3.2 and was illustrated by the Kaplan-Meier overall survival curves in Figures 3.1 and 3.2. There appeared to be marked heterogeneity in the overall survival among the metastatic failure at different sites (Table 3.2 and Figure 3.2). In particular, patients with lung metastasis alone had a median overall survival of 3.9 years, which is significantly longer than other sites of pure distant metastases ($p < 0.0001$ by log rank test). Lung metastasis was also associated with a significantly longer median time interval from primary RT to metastasis compared to that of distant metastases at other sites ($p = 0.0034$)

For the 97 patients with both DM and LF/RF during their course of disease, there was

a trend towards a longer median time interval from primary RT to first distant metastasis in the LF/RF → DM group than in the LF/RF + DM group (1.7 years versus 1.1 years, p = 0.073, Table 3.2 and Figure 3.1). There was however no significant difference in the overall survival between the L/R → DM group and the L/R + DM group (p = 0.13, log rank test, Figure 1). The overall survival curve of the L/R + DM group also largely overlapped with that of the pure DM group.

The independent prognostic significance of pure lung metastasis

The baseline clinical characteristics of the forty-one patients with pure lung metastasis were compared with that of the entire cohort, and no significant difference was found (data not shown). To confirm the independent prognostic significance in the overall survival of this group, Cox regression model was constructed and included all the baseline clinical parameters. The overall survival for this group with pure lung metastasis remained highly significant (p = 0.0003) even after adjustment for the other significant prognostic factors of OS (Table 3.3).

Predictive factors of distant metastases

The potential clinical characteristics at the time of primary diagnosis that may be predictive of the subsequent risk of DM were analyzed by both univariate (Table 3.4) and multivariate model (Table 3.5). These factors had also been analyzed across the different subgroups of DM. The significant predictive factors identified were fairly consistent in the different subgroups of DM. In summary, UICC N-stage was the strongest independent predictor for distant metastases, followed by UICC T-stage. Advanced age and male sex were also significant independent risk factors for DM.

Table 3.1

Clinical characteristics of 2915 NPC patients in the study cohort.

Characteristics	Number of patients (%)
Age	
< 40	694 (23.8)
≥ 40	2221 (76.2)
Sex	
Male	2099 (72.0)
Female	816 (28.0)
Histology type	
WHO type 1 (keratinizing carcinoma)	10 (0.3)
WHO type 2 (nonkeratinizing carcinoma)	280 (9.6)
WHO type 3 (undifferentiated carcinoma)	2593 (88.9)
UICC T-stage	
T1	467 (16.0)
T2	1476 (50.6)
T3	469 (16.1)
T4	503 (17.3)
UICC N-stage	
N0	804 (27.6)
N1	1223 (42.0)
N2	517 (17.7)
N3	371 (12.7)
UICC overall stage grouping	
I	199 (6.8)
II	1174 (40.3)
III	741 (25.4)
IV	801 (27.5)
Use of Chemotherapy	
Neoadjuvant	244 (8.4)
Concurrent	420 (14.4)
Adjuvant	237 (8.1)
Any chemotherapy	681 (23.4)
Use of Boost	
Parapharyngeal boost	1493 (51.2)
Intracavitary brachytherapy	320 (10.9)
Any boost	1786 (61.3)

NPC: nasopharyngeal carcinoma; WHO: World Health Organization; UICC: International Union Against Cancer

Table 3.2

Time course for different pattern of NPC failures.

Modes of failure *	Number of patients	Median time interval from primary RT to first failure (years) (25 – 75 percentile)	Median overall survival (OS) from primary RT (years) (95% C.I.)
DM only	379	1.1 (0.63 – 1.96)	2.1 (1.96 – 2.45)
Bone only	84	0.8 (0.40 – 1.30)	1.7 (1.30 – 2.54)
Liver only	61	1.0 (0.65 – 1.82)	1.9 (1.53 – 2.19)
Lung only	41	1.6 (1.03 – 2.35)	3.9 (3.10 – #)
More than one organ	139	1.1 (0.61 – 2.02)	2.3 (1.99 – 2.91)
Others/Unclassified	54	1.2 (0.78 – 1.94)	1.87 (1.53 – 2.45)
DM with LF/RF			
LF/RF → DM	59	1.7 (1.01 – 2.42)	2.6 (2.21 – 4.09)
LF/RF + DM	38	1.1 (0.51 – 1.56)	2.5 (1.54 – 2.81)

* LF: local failure; RF: regional (neck) failure; DM: distant metastases; LF/RF: local and/or regional failure; LF/RF → DM: local and/or regional failure preceded the diagnosis of DM for more than two months; LF/RF + DM: local and/or regional failure occurred within two months of the diagnosis of DM or after the diagnosis of DM.

Inadequate number of events beyond median.

Table 3.3

Cox regression model: overall survival of pure lung metastasis vs non-lung metastasis in NPC, adjusted for other significant prognostic factors.

Factors	P-value	Hazard ratio	95% C.I. for hazard ratio
Age	0.025	1.01	1.002 – 1.02
Histology	0.012	1.28	1.06 – 1.56
UICC T-stage	0.026	1.16	1.02 – 1.32
UICC N-stage	<0.0001	1.49	1.31 – 1.71
Lung metastasis	0.0003	0.41	0.25 – 0.66

Table 3.4

Predictive factors of distant metastases in NPC: univariate analysis.

Factors	(1) Pure DM		(2) LR + DM		(3) LR -> DM		(4) Pure DM: Lung only		(5) Pure DM: Non Lung	
	Hazard Ratio	P-value	Hazard Ratio	P-value	Hazard Ratio	P-value	Hazard Ratio	P-value	Hazard Ratio	P-value
Age	1.02	< 0.0001	0.99	0.46	1.00	0.78	1.03	0.0081	1.01	0.0011
Sex	0.67	0.0011	0.73	0.40	0.84	0.55	0.68	0.30	0.67	0.0021
Histology	0.98	0.83	0.45	0.019	1.08	0.66	0.96	0.86	0.99	0.87
UICC T-stage	1.40	< 0.0001	1.53	0.0086	1.13	0.38	1.20	0.26	1.42	< 0.0001
UICC N-stage	1.72	< 0.0001	1.99	< 0.0001	1.60	0.0003	1.39	0.036	1.77	< 0.0001

Table 3.5

Predictive factors of distant metastases in NPC: multivariate analysis.

Factors	P-value	Hazard ratio	95% C.I. for hazard ratio
(1) Pure DM			
UICC N-stage	<0.0001	1.67	1.51 – 1.84
UICC T-stage	<0.0001	1.29	1.16 – 1.43
Age	<0.0001	1.02	1.01 – 1.02
Sex	0.012	0.73	0.57 – 0.93
(2) L/R + DM			
UICC N-stage	<0.0001	1.95	1.43 – 2.65
UICC T-stage	0.017	1.48	1.07 – 2.04
(3) L/R → DM			
UICC N-stage	0.0003	1.60	1.24 – 2.06
(4) Pure DM – Lung			
Age	0.0059	1.03	1.01 – 1.06
(5) Pure DM – Non Lung			
UICC N-stage	<0.0001	1.71	1.54 – 1.90
UICC T-stage	<0.0001	1.31	1.17 – 1.47
Age	0.0011	1.01	1.01 – 1.02
Sex	0.019	0.73	0.57 – 0.95

Figure 3.1

Overall survival for the different patterns of distant metastases in NPC (DM only: distant metastases without local-regional failure, LF/RF → DM: local and/or regional failure preceding distant metastases, LF/RF + DM: local and/or regional failure accompanied by distant metastases).

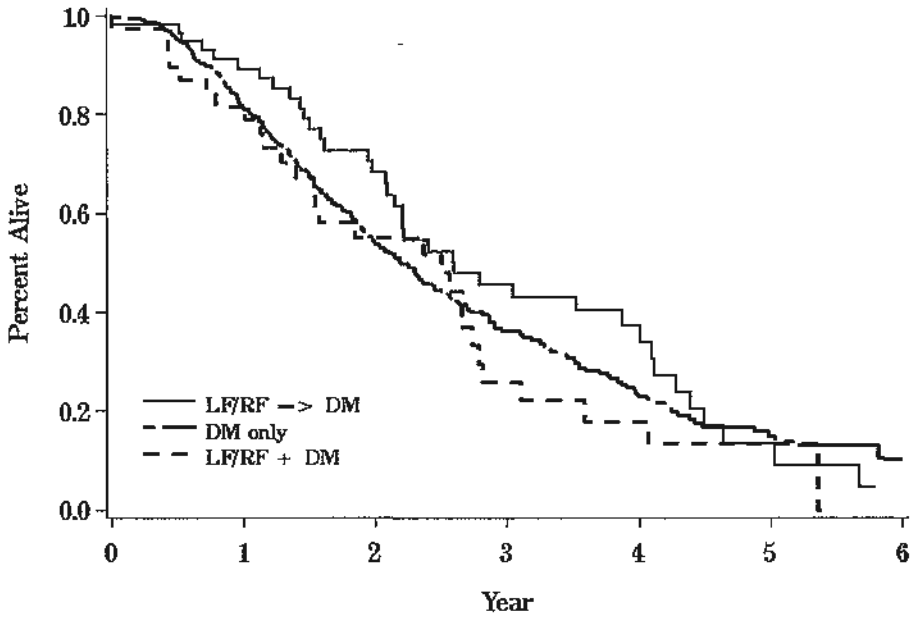

Figure 3.2

Overall survival of NPC patients with pure distant metastases by metastatic sites.

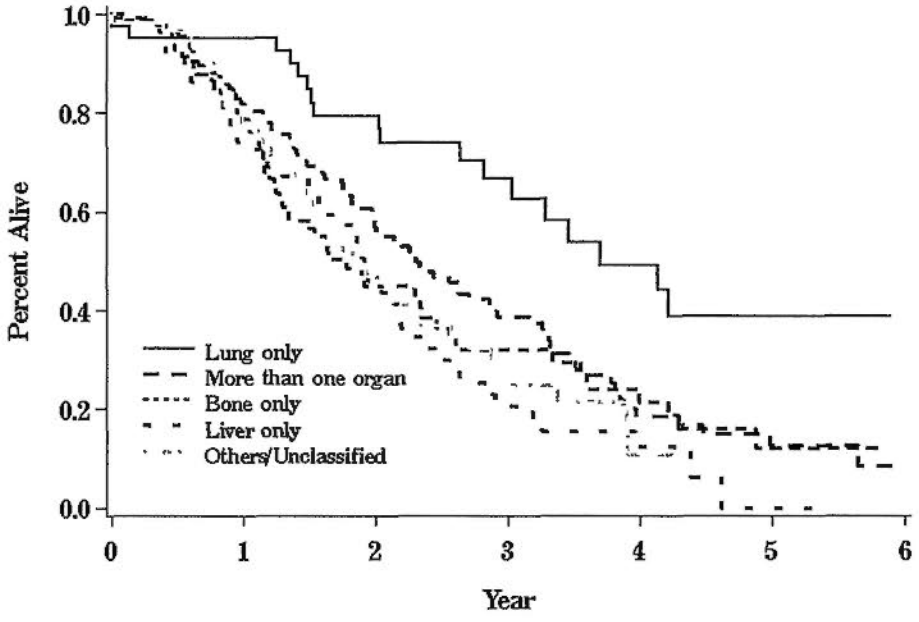

DISCUSSION

In this study, we have described the clinical course of DM in a large cohort of NPC patients treated with conventional 2-dimensional (2D) RT technique from 1996 to 2000 in Hong Kong. With the prospect of further improvement in local control with the increasing application of 3-dimensional high-precision radiotherapy, distant failure is expected to become an even more outstanding problem. This point is well exemplified by recent studies that reported excellent local control in advanced stage disease with the use of concomitant radiotherapy and chemotherapy (Cheng et al. 2001), or intensity modulated radiotherapy (IMRT) with or without chemotherapy (Lee et al. 2002). Both studies had consistently demonstrated the increased burden of distant failures in NPC despite achieving an excellent local control.

For patients who developed distant metastases, we have demonstrated a marked heterogeneity in the time course and survival in different metastatic sites. In particular, patients with lung metastasis alone appeared to belong to a distinctive good prognostic group with both a longer progression free survival and overall survival. However, the predictive factor for this distinctive prognostic group cannot be identified from the available clinical parameters. We postulate that it may be associated with a unique biological behavior of NPC in this particular group. Future study of molecular markers in NPC should aim to identify this significant prognostic group.

In a recent report that proposed a prognostic index score to predict the survival in metastatic NPC, the authors identified both liver metastasis and lung metastasis, among others, as independent and significant negative prognostic factors for metastatic survival (Ong et al. 2003). The findings are in disparity with that of an earlier report from our group which suggested that while liver metastasis was

associated with a shorter metastatic survival, patients with lung metastasis had a significantly longer metastatic survival (Teo, Kwan, Lee et al. 1996). The discrepancies between these reports and our current results are likely to be due to the different methods used to assess the survival outcome in metastatic NPC. The previous reports all looked at metastatic survival (MS, defined as the time from the first diagnosis of distant metastasis to the time of death), whereas in the current study we looked at the overall survival (OS, calculated from the first day of primary RT to the time of death). We believe that OS is a more solid and appropriate outcome measure for this study. This is in consideration of the commonly held view that distant metastases actually originate from micro-metastases that were already present at the time of primary radiotherapy treatment, an integral part of the disease at the time of first diagnosis. On the other hand, the definition of MS is influenced by the timing of clinical diagnosis of distant metastases. The definition of this clinical time-point tends to be influenced by the interval between follow-up visits as well as the site of metastasis. Without routine surveillance imaging for distant metastases, skeletal metastases may be more amenable to detection by clinical symptoms at an earlier stage of its natural history compared to pulmonary and hepatic metastases. Furthermore, the duration of MS also depends on the disease free interval (DFI), which would again be heavily influenced by the primary treatment given. The use of OS (= DFI + MS) as the outcome measure will minimize these potential biases.

The natural history and management of metastatic NPC has long been an area of controversy. DM in patients with NPC have been conventionally regarded as incurable and the aim of treatment has largely been palliative. This view found support from the experience in treating head and neck cancer at other sites, and observations from the historical reports on distant metastases in NPC. The literature

had consistently reported high distant metastases rate in NPC, and poor survival after the diagnosis of metastasis. The reported median survival after the diagnosis of metastasis had ranged from 5 to 11 months (Ahmad and Stefani 1986; Vikram et al. 1986; Leung et al. 1991; Teo, Kwan, Lee et al. 1996; Geara et al. 1997; Ong et al. 2003). However, the experience from our center (Kwan et al. 1996; Teo, Kwan, Lee et al. 1996) and from other investigators in the French (Fandi et al. 2000) and Canadian (Choo and Tannock 1991) series all suggested that a small proportion of patients with metastatic NPC treated with aggressive chemotherapy had achieved long term disease free survival, suggesting the curative potential of chemotherapy, at least in a small subset of metastatic NPC (Chan et al. 1998). We recommend an aggressive approach to manage metastatic NPC patients with good performance status, especially if the metastasis is confined to the intrathroacic site, where which long-term survival is a realistic goal after multimodality treatment.

The results of the current study support the previous reports that the incidence of distant metastases after local-regional salvage was significant (20-34%) and as such, is the major determinants in the overall survival of these patients (King, Teo, and Li 1992; Yang et al. 1996). A previous study from the US Radiation Therapy Oncology Group (RTOG) head and neck database also reported that tumors of the hypopharynx and nasopharynx had a higher propensity to metastatic dissemination at the time of initial diagnosis, and until effective methods to treat disseminated disease were developed, the effect of local control on survival would not be readily achieved (Leibel et al. 1991). Future research should aim to identify the subgroup of patients after successful local-regional salvage that was at high risk of distant metastases. This group should be investigated by incorporating systemic therapy to their local-regional treatment, not only for the enhancement of local control, but also more

importantly for eradicating microscopic metastasis to improve the overall survival. In this regards, the recent development in high-sensitivity tumor markers, such as circulating plasma EBV DNA, may be useful to identify residual disease after radiotherapy (Chan, Lo et al. 2002).

The current study has also confirmed the significant predictive factors for DM, namely advanced UICC N-stage and T-stage disease, in agreement with previous reports from our group and others in the literature (Lee et al. 1992; Teo, Yu et al. 1996; Geara et al. 1997; Sham, Choy, and Choi 1990). This study also demonstrated advanced age and male sex to be independent significant risk factors of distant metastases. Future prospective studies should target advanced UICC N-stage and T-stage diseases for testing new strategy of systemic therapy to reduce the risk of DM.

CONCLUSION

In a contemporary cohort of 2915 NPC patients treated in five oncology centers in Hong Kong in 1996-2000, we confirmed that distant metastasis (16%) is the leading cause of treatment failures after primary radiotherapy, followed by local failure (12%) and regional failure (3%). The patterns and management of local failures will be further addressed by my colleagues (Yu et al. 2005). The following chapters of this thesis will focus on a better understanding on the possible molecular mechanism leading to tumor metastasis in NPC (hypoxia and angiogenesis, in chapters 4-6, study No 2-4) and developing new therapeutic approaches to combat distant metastases in order to improve the overall treatment outcome in NPC (neoadjuvant chemotherapy and antiangiogenesis therapy, in chapters 7-9, study No 5-7).

Chapter 4

Study 2: Hypoxia Regulated Gene Expression Profile

BACKGROUND

As explained in chapter 1, tumor hypoxia is well known to be associated with resistance to RT and chemotherapy, as well as a more malignant tumor phenotype with increased invasiveness, metastases, and poorer survival (Gray et al. 1953; Brizel et al. 1996; Hockel et al. 1996). The transcriptional complex of hypoxia-inducible factor-1 (HIF-1) has emerged as an important mediator of gene expression patterns in tumors (Semenza 2000, 2010). HIF-1 plays a pivotal role in essential adaptive responses to hypoxia and its expression increases exponentially with decreased level of cellular oxygen. Genes that are up-regulated by micro-environmental hypoxia through activation of HIF include erythropoietin, glucose transporters, glycolytic enzymes, and angiogenic factors. Among them, both carbonic anhydrase IX (CA IX) and vascular endothelial growth factor (VEGF) are up-regulated by hypoxia via HIF-1 dependent pathways (Wykoff et al. 2000; Beasley et al. 2001; Jones et al. 2001).

Clinical studies have shown that hypoxia is an independent prognostic indicator of poor patient survival in different tumor types (Nordsmark, Overgaard, and Overgaard 1996; Brizel et al. 1996). Because this observation also holds true for surgically treated patients (Hockel et al. 1996), it suggests that there are fundamental biological differences between hypoxic and non-hypoxic tumor cells. A major mechanism by which hypoxia confers its effect is by differential regulation of gene expression. In a clinical study, we have found that the markers HIF-1α, CA IX and VEGF were frequently over-expressed in about 60% of patients' tumor samples. We also showed that tumors with a hypoxic phenotype, as defined by the coexpression of HIF-1α and

CA IX, were associated with poor survival. Furthermore, tumors with both hypoxic and angiogenic phenotype (defined by the overexpression of VEGF) had the worst outcome after RT (refer to chapter 5, study 3). In the current study, we further investigated the expression of these hypoxic markers at both the mRNA and protein levels in NPC cell lines. We also investigated the global differential gene expression in normoxic and hypoxic-treated NPC cells by Affymetrix GeneChip Array expression analysis. We demonstrated that hypoxia induced coordinated up- and down-regulation of a broad range of genes involved in distinct biological pathways. We investigated genes not previously reported that may be of special relevance in NPC, since there is known variation in the global transcriptional response to hypoxia among different cell types (Chi et al. 2006). We believe that recognition of the pattern of the differential gene expressions in the hypoxic cells will lead to a better understanding of the hypoxic tumor phenotype in the clinical settings.

MATERIALS AND METHODS

Culture of tumor cell lines and hypoxia treatment

Four nasopharygneal carcinoma (NPC) cell lines (CNE-2, C666-1, HONE-1 and HK1) were employed. The CNE-2 cell line (Sizhong, Xiukung, and Yi 1983) and HONE-1 cell line (Glaser et al. 1989) were established from poorly-differentiated nasopharyngeal carcinomas. C666-1 was established from undifferentiated nasopharyngeal carcinoma and consistently carried the Epstein-Barr virus in long-term cultures (Cheung et al. 1999). The HK1 cell line was established from a well-differentiated squamous nasopharyngeal carcinoma (Huang et al. 1980). CNE-2 and HONE-1 cells were cultured in RPMI-1640 medium supplemented with 5% fetal bovine serum (FBS) and antibiotics (100 units/ml penicillin and 10 μg/ml streptomycin), while HK1 and C666-1 cells were cultured in RPMI-1640 medium

supplemented with 10 % FBS and antibiotics. Cell cultures were incubated at 37°C in a humid atmosphere of 5% CO_2 and 95% air (normoxia). Hypoxia was created by culturing cells in a hypoxia chamber (Galaxy R CO_2 incubator, RS Biotech Laboratory Equipment Ltd., Ayrshire, Scotland) containing 0.1% O_2, 5% CO_2 and 94.9% N_2. All culture medium and reagents were purchased from GIBCO BRL (Grand Island, NY).

Western immunoblotting

NPC cell lines growing at log-phase were used in the experiments. Cells were cultured under normoxic or hypoxic condition for 16 hours. Cells were scraped off from culture flasks and lysed in urea buffer containing 7 M urea, 10% glycerol, 10 mM Tris-HCl (pH 6.8), 1% SDS, 5 mM dithiothreitol (DTT) and 1× complete protease inhibitor cocktail (Roche Diagnositcs GmbH, Mannheim, Germany). Protein concentrations were measured by a RC DC Protein Assay (Bio-Rad Laboratories, Inc., Hercules, CA, USA). Fifty μg of cellular proteins were separated by 4-12% SDS-polyacrylamide gel electrophoresis (Bio-Rad Laboratories, Inc., Hercules, CA, USA). The separated proteins were electrophoretically transferred to Hybond ECL nitrocellulose membrane (Amersham Pharmacia Biotech Inc, Piscataway). Membranes were blocked with 5% nonfat milk in Tris-buffered saline containing 0.1% Tween-20 at room temperature for 1 hour and then incubated with mouse anti-human HIF-1α antibody (Tranduction Laboratories, Lexington, KY), rabbit anti-human HIF-2α antibody (Stressgene Biotechnologies, Victoria, BC Canada) or mouse anti-human CA IX antibody M75 (Pastorekova et al. 1992) overnight at 4°C with gentle shaking. Horseradish peroxide conjugated anti-mouse or anti-rabbit IgG (DAKO, Ely, UK) was used as a secondary antibody. After washing, the enhanced chemiluminescence detection system ECL (Amersham Biosciences, Buckinghamshire, UK) was used to visualize the appropriate bands. Actin (Calbiochem, Merck KGaA, Darmstadt,

Germany) was used as an internal control to verify equal protein loading in each NPC cell line during experiment.

RNA purification

Cells were incubated under normoxic or hypoxic condition for 16 hours (4 to 24 hours for time course experiments). Cells were then lysed by TRIzol Reagent (Invitrogen, Carlsbad, CA) and RNA was extracted according to manufacturer's instruction. To avoid genomic DNA contamination, extracted RNA was then purified with RNeasy kit (QIAGEN Inc., Valencia, CA USA). The quantity and quality of RNA was determined by optical density (OD) measurement at 260 and 280 nm. The integrity of RNA was checked by visual inspection of the two rRNAs 28S and 18S on an agarose gel. For RNA used for microarray analysis, the quality of RNA was further checked by Agilent Technologies 2100 Bioanalyzer.

Reverse transcription-PCR (RT-PCR)

Semi-quantitative RT was performed by using random hexamers and MuLV reverse transcriptase (GeneAmp RNA PCR kit, Applied Biosystems, Foster City, CA), as reported previously (Tao et al. 2002). The RT reaction was started with 10 minutes incubation at room temperature, 1 hour at 42 °C, and 5 minutes at 99°C and followed by 5 minutes at 5°C. PCR was performed using AmpliTaq Gold (Applied Biosystems). The PCR program started with an initial denaturation at 95°C for 10 min, followed by 20-30 cycles (94°C for 30 s, 55°C or 60°C for 30 s, and 72°C for 30 s) of amplification, with a final extension at 72°C for 10 min. The RT-PCR product was electrophoresed on a 2% agarose gel containing ethidium bromide.

Enzyme-linked immunosorbent assay for VEGF

Cells were seeded onto 6-well plates. Sub-confluent cultures were incubated in RMPI-1% FBS under normoxia or hypoxic condition for various time intervals (4 to 48 hours). At the end of incubation, culture medium was collected and span at 3000 rpm for 3 minutes to remove cell debris. Aliquots of the supernatant were stored at –80°C until processing. VEGF concentrations in cell culture supernatant were quantified by Quantikine® human VEGF enzyme-linked immunosorbent assay (ELISA) kit (R & D Systems, Inc., Minneapolis, MN). Cells were washed with cold PBS and then lysed in lysis buffer. The amount of total protein in each well was quantified. VEGF secretions by cells were normalized by total protein amount in each well.

Microarray analysis

Identification of differentially expressed genes between normoxic and hypoxic treated NPC cells was carried out using GeneChip® Human Genome U133A and U133B Arrays (Affymetrix, Santa Clara, CA), which represents greater than 39,000 transcripts derived from approximately 33,000 human genes. The microarray analysis was performed following the manufacturer's instruction (Affymetrix), as previously described (Tsui et al. 2004). In brief, 10 μg of total RNA was used to synthesize cDNA. The cDNA was then used as a template to generate biotinylated cRNA by *in vitro* transcription. The cRNA was subsequently fragmented. The quality and size distribution of the total RNA, cRNA and fragmented cRNA was checked on an Agilent 2100 Bioanalyzer (Agilent, Amstelveen, the Netherlands), using RNA 6000 Pico assay. The fragmented cRNA was hybridized to the GeneChip arrays. The arrays were then washed and stained and finally scanned with a laser scanner. The scanned images were processed with GeneChip® Microarray Suite 5.0 (Affymetrix).

The comparison between expression profiles of the normoxic and hypoxic treated

NPC cells was performed using GeneSpring® software version 7 (Silcongenetics, Redwood, California). Gene expression data were first normalized by GC-RMA (robust multichip average) preprocessor. Normalized values below 0.001 were set to 0.001. The normalized expression values were then compared between normoxic and hypoxic CNE-2 cells, as well as between normoxic and hypoxic HONE-1 cells. Fold-change differences were calculated to identify the up- and down-regulated genes. Transcripts with a 1.8-fold or more difference in the expression levels were defined as differentially expressed. RT-PCR analyses were performed for a selection of up-regulated and down-regulated genes to confirm their differential expressions.

We used several online tools that are designed to assist investigators to classify the functional roles of the differentially expressed genes. The FatiGO (Al-Shahrour, Diaz-Uriarte, and Dopazo 2004) (http://www.fatigo.org) utilize the Gene Ontology (GO) database provided by the GO Consortium (http://www.geneontology.org/) (Creating the gene ontology resource: design and implementation 2001). The annotations were further checked at the NetAffx Analysis Centre database (Liu et al. 2003) (http://www.affymetrix.com/ analysis/index.affx). Fisher's exact test was used to compare the percentage distribution of differential regulated genes with GO annotation in each functional category. We also utilized GenMapp 2.0 (Gladstone Institutes 2004, http://www.GenMapp.org) to visualize microarray data in pre-defined biological pathways (Dahlquist et al. 2002; Salomonis et al. 2007).

RESULTS

Expression of cellular HIF-1α, HIF-2α, CA IX proteins in NPC cells

The effects of hypoxia on the protein expression of some known hypoxia markers

including HIF-1α, HIF-2α, and CA IX were examined in four NPC cell lines. After exposure to hypoxic conditions for 16 hours, cellular proteins were subjected to Western blotting analysis. As shown in Figure 4.1, HIF-1α protein levels were significantly increased after hypoxia treatment in all cell lines examined. It was also observed that the HIF-1α protein from hypoxic NPC cells has lower electromobility than that from normoxic NPC cells. By contrast, HIF-2α protein levels did not vary among the four cell lines after exposure to hypoxia (Figure 4.1A). Hypoxia-induced CA IX protein expression was observed in HONE-1, CNE-2 and HK1 cells but not in C666-1 cells.

Secretion of VEGF by NPC cells

The effects of hypoxia on the secretion of VEGF, a HIF-1-regulated gene, in NPC cells were also investigated. NPC cell lines were incubated in normoxia and hypoxia conditions for 4 to 48 hours. Culture medium was collected and the amount of cellular proteins in each well was quantified. The results showed that secretion of VEGF was up-regulated by hypoxia in C666-1, HONE-1 and CNE-2 cells (Figure 4.2A, B and C), and the induction only became pronounced after 24 hours of hypoxia exposure. VEGF secretion was not significantly changed in HK1 cells after exposure to hypoxia (Figure 4.2D). This demonstrates the heterogeneity of the response to hypoxia, even for well described genes such as VEGF and CA IX.

mRNA expression of HIF-1α, HIF-2α, CA IX and VEGF in NPC cells

After hypoxia treatment for 16 hours, the mRNA levels of HIF-1α, HIF-2α and VEGF in all four NPC cell lines were unchanged (Figure 4.1B). CA IX mRNA was not detected in C666-1 cells with or without hypoxia treatment. Up-regulation of CA IX mRNA was detected in HONE-1, CNE-2 and HK1 cell lines after hypoxia treatment,

which correlated with the increased protein levels. However, as indicated by the increase of protein levels of VEGF after 24 hours, so there was an increase in mRNA levels of VEGF in C666-1, HONE-1 and CNE-2 cells but not in HK1 cells after 24 hours of hypoxia treatment (Figure 4.1B). This result suggests that the increase of cellular CA IX protein and VEGF protein secretion was mediated at least partly by a transcriptional-dependent way derived from an increase of mRNA levels, but the early changes in VEGF were mainly post-translational.

Microarray analysis of hypoxia treated NPC cell lines

Gene expression profiles of normoxic and hypoxia-treated NPC cell lines (CNE-2 and HONE-1) were obtained by microarray analysis using Affymetrix U133A and U133B Human Genome Arrays. A total of 17796, 16544, 18334 and 17336 probe sets (transcripts) were present in samples of normoxic CNE-2 cells, hypoxic CNE-2 cells, normoxic HONE-1 cells and hypoxic HONE-1 cells, respectively. There were 816 (396 up-regulated and 420 down-regulated) and 1397 (584 up-regulated and 813 down-regulated) differentially expressed (1.8 fold or more) gene transcripts in hypoxic-treated CNE-2 and HONE-1 cells respectively. The hypoxia regulated genes comprised of 4.6% - 7.6% of all measured transcripts. Altogether, 222 gene transcripts (1.3%) were commonly up-regulated and 137 genes transcripts (0.8%) down-regulated in both hypoxic-treated cell lines. Genes that were more than 2.5 fold up-regulated or 2.5 fold down-regulated upon hypoxia in these cell lines are listed in Table 4.2 (90 genes) and Table 4.3 (15 genes) respectively.

Validation of differential regulated genes by RT-PCR

For selected differentially expressed candidate genes, we performed RT-PCR to validate their expression levels. The genes include 10 up-regulated genes (HIG2,

BNIP3, E2IG5, EFNA3, ELF3, JMJD1A, MAFF, EFNA1, GADD45B and LOX) and 4 down-regulated genes (RRS1, IFRD1, EIF5 and RFP). The RT-PCR results confirmed the microarray findings in CNE-2 and HONE-1 cells (Figure 4.3). RT-PCR analysis of these genes was also performed in C666-1 and HK1 cells and the results of most of the genes were similar to that in CNE-2 and HONE-1 cells except ELF3, GADD45B and LOX were unchanged in C666-1 cells and EIF5 was unchanged in both C666-1 and HK1 cells (Figure 4.3).

Biological functions of differential regulated genes by hypoxia

To gain further insight into the biological functions of the hypoxia-modulated genes, we utilized the online tool FatiGo to classify these genes according to the biological process in Gene Ontology (GO) terms. Hypoxia induced coordinated up- and down-regulation of distinct sets of genes in several biological processes. The biological processes involved by the 222 commonly up-regulated genes include apoptosis (15 genes), carbohydrate metabolism (13 genes), cell cycle, communication and differentiation (33 genes), defense and immune response (10 genes), metabolism of macromolecules (22 genes), regulation of transcription (25 genes), response to stress and stimulus (8 genes), and transport (10 genes). Among the 137 commonly down-regulated genes, the biological processes involved are apoptosis (8 genes), biosynthesis and metabolism of macromolecules (20 genes), cell growth and differentiation (13 genes), DNA repair (5 genes), immune response (1 genes), regulation of translation (5 genes), regulation of transcription (9 genes), RNA processing (14 genes), and transport (6 genes). The complete list and functional categories of the differentially expressed genes by hypoxia in NPC cell lines are summarized in supplementary Table S1 (up-regulated genes) and Table S2 (down-regulated genes) (Appendix C, supplementary tables).

The biological processes most frequently involved by the 222 up-regulated genes and 137 down-regulated genes are compared in Figure 4.4. Hypoxia induced significant up-regulation of genes in the biological processes of carbohydrate metabolism, cell communication, defense and immune response, and response to external stimulus. Hypoxia also caused significant down-regulation of genes in the biological processes of biosynthesis, metabolism, ribosome biogenesis, RNA processing, and translation. However, there is similar distribution of up- or down-regulation of gene expressions in the categories of apoptosis, transcription, and transport (Figure 4.4).

Hypoxia up-regulated genes in NPC

The common hypoxia up-regulated genes (supplementary Table S1) included many genes that have previously been associated with hypoxia response but also a few less well described genes. The up-regulated genes included genes involved in carbohydrate metabolism (e.g. aldolase C [ALDOC], phosphofructokinase [PFKFB3 and PFKFB4]) and transport (e.g. solute carrier family [SLC2A1 and SLC2A3]), angiogenesis (e.g. adrenomedullin [ADM], endothellin 2 [END2]), cell signaling (e.g. ephrin-A1 and ephrin-A3 [EFNA1 and EFNA3], lysyl oxidase [LOX]), defense and immune response (e.g. v-fos FBJ murine osteosarcoma viral oncogene homolog [FOS]), response to stress (e.g. hypoxia-inducible protein 2 [HIG2]), and regulation of transcription (e.g. E74-like factor 3 [ELF3], jumonji domain containing 1A and 2B [JMJD1A and JMJD2B], v-maf musculoaponeurotic fibrosarcoma oncogene homolog F and K [MAFF and MAFK]).

Hypoxia down regulated genes in NPC

Among the hypoxia repressed genes were a large group of genes whose expression may reflect a physiological alteration that halts cellular metabolism, proliferation and

translation activities as the cells try to preserve energy consumption under hypoxic stress (supplementary Table S2). These included genes linked to biosynthesis and metabolism of macromolecules (e.g. RRS1 ribosome biogenesis regulator homolog [RRS1]), cell proliferation (e.g. ret finger protein [RFP]) and differentiation (e.g. interferon-related developmental regulator 1 [IFRD1]), DNA repair (anti-silencing function 1 homolog A [ASF1A], general transcription factor IIH - polypeptide 2 [GTF2H2], polymerase epsilon 2 [POLE2], replication factor C3 [RFC3], translin [TSN]), RNA processing, and regulation of translation (e.g. eukaryotic translation initiation factor 5 [EIF5]).

Hypoxia responsive apoptosis genes in NPC

We specifically examined genes regulated by hypoxia in the apoptosis pathway, which involved many well-known apoptosis genes as well as novel genes. As illustrated in the GenMapp apoptotic pathway with microarray data from HONE-1 cells, there is both up- and down-regulation of gene expression in the apoptosis pathway (Figure 4.5). Nine of the 15 up-regulated genes were known to be pro-apoptotic (e.g. BIK, BNIP3, BTG1, E2IG5, EGLN3, RHOB), but the other six up-regulated genes were anti-apoptotic (e.g. GADD45B, IER3, NOL3, SOCS3). Similarly, three of the 8 down-regulated genes were pro-apoptotic and four others were anti-apoptotic (Table 4.4). Therefore, the net effect of hypoxia on the cellular apoptosis machinery in NPC cells appeared to be complex and not easily predictable.

Comparative study with other array-based hypoxia experiments

We compared our list of hypoxia regulated genes in NPC with previously published array-based studies investigating hypoxia regulated genes in several other cell types (Denko et al. 2003; Sonna et al. 2003; Subarsky and Hill 2003; Ning et al. 2004;

Greijer et al. 2005; Vengellur et al. 2005; Weinmann et al. 2005; Chi et al. 2006). As annotated in the references column in Table 4.2, 38 of the ninety up-regulated genes in NPC shown in Table 4.2 were previously identified to be up-regulated by hypoxia in other studies. In Table 4.3, only two of the fifteen down-regulated genes in NPC were also previously identified in other studies.

Weimann et al recently compared whole cell RNA from hypoxia-tolerant NCI H460 cells selected by 10 consecutive cycles of hypoxia and reoxygenation to whole cell RNA from control NCI H460 cells grown under normoxia using the Affymetrix Human genome U133A array. They found 82 genes of the 22,283 probe sets were up-regulated while 156 genes down-regulated after hypoxia selection (Weinmann et al. 2005). Since our experiments shared the same Affymetrix gene chip and probe sets, it was possible to directly compare these two expression datasets. We found a group of genes that were consistently up-regulated in both short term hypoxia treatment and after chronic hypoxia selection in all three cell lines. These genes were involved in transport (SLC2A1, SLC16A3), cell motility (MARCKS, TPBG), protein binding (TIPARP) and transcription (HEY1). The result of this comparison was shown in Table 4.5.

Table 4.1 Primers used for RT-PCR

Gene	Primer sequence	Product size (bp)	Temp °C	cycles
HIF-1α	CATGGAAGGTATTGCACTGC	452	60	30
	CACACATACAATGCACTGTGG			
HIF-2α	AACAGCAAGAGCAGGTTCC	258	60	30
	GTGCTGCCCAGGTAGAAG			
CA9	CAATATGAGGGGTCTCTGACTACAC	249	60	30
	GGAATTCAGCTGGACTGGCTCAGCA			
VEGF	CCTCCGAAACCATGAACTTT	509	60	30
	GGGAACGCTCCAGGACTTAT			
BNIP3	CAGGGCTCCTGGGTAGAACT	194	55	25
	GCCCTGTTGGTATCTTGTGG			
GADD45β	AACATGACGCTGGAAGAGCT	247	55	25
	AGAAGGACTGGATGAGCGTG			
E2IG5	GGCAGCAGGAAGCTGTTTTA	215	60	25
	CTTCCTTTTGAAGCGACCTG			
HIG2	CAAGCTGAGCACCGTTGTAA	241	55	25
	CCACCACACCCAGCTAACTT			
EFNA3	CATGCGGTGTACTGGAACAG	180	60	28
	GCTCACCATGTACAGCACGTA			
ELF3	ATGGCTGCAACCTGTGAGAT	176	60	25
	CAGCTGGCCTTCTCTGTACC			
JMJD1A	GGGGAGGAGGTTTCTCAGTC	173	60	25
	ATTCCCCATCAAATTCCACA			
MAFF	TCTGTGGATCCCCTATCCAG	246	60	28
	CTTCTGCTTCTGCAGCTCCT			
EFNA1	CACACCGTCTTCTGGAACAG	165	55	20
	CTCATGCTCCACCAGGTACA			
EIF5	TACAAGATGCCCCGTCTGAT	227	55	25
	CCATCCAACATGTCTTGCAG			
RFP	GCTTCAAGGAGCAAATCCAG	191	55	25
	CAGGAGGCGATACTCATGCT			
RRS1	ACGTGTCCCAAAGGAAACTG	165	55	25
	TGGAGGCTGGAGAGAGTCAT			
IFRD1	GCACAGACGCACGAGTAAAA	203	60	25
	AGGCTGAACATTTCGATGCT			
LOX	CGACCCTTACAACCCCTACA	234	60	25
	CTGGCCAGACAGTTTTCCTC			

Table 4.2 Hypoxia up-regulated genes (>2.5-fold) in NPC cell lines.

Gene symbol	Gene Title	Genbank	Fold change		Reference
			CNE-2	HONE-1	
ADM	adrenomedullin	NM_001124	19.7	27.4	(Denko et al. 2003; Sonna et al. 2003)
AK3	adenylate kinase 3	AK026966	3.0	4.0	(Sonna et al. 2003)
ALDOC	aldolase C, fructose-bisphosphate	NM_005165	6.9	12.4	(Denko et al. 2003; Sonna et al. 2003; Greijer et al. 2005)
ARRDC3	arrestin domain containing 3	AB037797	4.1	12.3	
BHLHB2	basic helix-loop-helix domain containing, class B, 2	BG326045	9.7	24.9	(Sonna et al. 2003)
BNIP3	BCL2/adenovirus E1B 19kDa interacting protein 3	U15174	5.1	12.0	(Denko et al. 2003; Subarsky and Hill 2003; Greijer et al. 2005)
BNIP3L	BCL2/adenovirus E1B 19kDa interacting protein 3-like	AF060922	4.8	4.5	(Denko et al. 2003; Ning et al. 2004)
BTG1	B-cell translocation gene 1, anti-proliferative	AL535380	2.6	3.4	(Denko et al. 2003)
C10orf10	chromosome 10 open reading frame 10	AL136653	11.1	17.4	
C10orf75	chromosome 10 open reading frame 75	AU151788	9.6	2.3	
CA9	carbonic anhydrase IX	NM_001216	3.8	7.7	(Denko et al. 2003; Sonna et al. 2003; Subarsky and Hill 2003; Vengellur et al. 2005)
CCNG2	cyclin G2	L49506	6.2	7.8	(Denko et al. 2003; Subarsky and Hill 2003)
CDKN1C	cyclin-dependent kinase inhibitor 1C (p57, Kip2)	R78668	3.7	3.1	
CLECSF2	C-type (calcium dependent, carbohydrate-recognition domain) lectin, superfamily member 2 (activation-induced)	BC005254	2.6	2.6	
CLK1	CDC-like kinase 1	AI251890	2.9	5.0	
CLK3	CDC-like kinase 3	NM_003992	2.8	2.9	
CNOT8	CCR4-NOT transcription complex, subunit 8	AF180476	4.5	2.9	
DDIT4	DNA-damage-inducible transcript 4	NM_019058	2.8	5.9	
DHRS3	dehydrogenase/reductase (SDR family) member 3	NM_004753	2.7	2.5	
DSIPI	delta sleep inducing peptide, immunoreactor	AL110191	3.0	3.2	
DUSP1	dual specificity phosphatase 1	NM_004417	3.2	4.3	(Sonna et al. 2003)
E2IG5	growth and transformation-dependent protein	NM_014367	3.6	5.7	
EDN2	endothelin 2	NM_001956	6.6	33.4	(Denko et al. 2003; Subarsky and Hill 2003)
EFNA1	ephrin-A1	NM_004428	6.8	14.6	(Denko et al. 2003)
EFNA3	ephrin-A3	AW189015	3.7	2.9	
EGLN3	egl nine homolog 3 (C. elegans)	NM_022073	11.5	56.8	
ELF3	E74-like factor 3 (ets domain transcription factor, epithelial-specific)	U73844	4.9	7.2	
ENO2	enolase 2 (gamma, neuronal)	NM_001975	30.1	53.5	(Sonna et al. 2003)
ERO1L	ERO1-like (S. cerevisiae)	BE966748	3.6	4.7	
FAM13A1	family with sequence similarity 13, member A1	NM_014883	5.5	6.5	
FLJ10134	hypothetical protein FLJ10134	NM_018004	4.1	14.9	
FLJ12953	hypothetical protein FLJ12953 similar to Mus musculus D3Mm3e	AK023015	3.0	3.6	
FOS	v-fos FBJ murine osteosarcoma viral oncogene homolog	BC004490	7.6	23.9	
FOSL2	FOS-like antigen 2	N36408	6.3	22.7	
FOXD1	forkhead box D1	NM_004472	3.2	3.5	
FOXO3A	forkhead box O3A	N25732	2.7	2.0	
FUT11	fucosyltransferase 11 (alpha (1,3) fucosyltransferase)	AI754928	6.6	8.9	
GADD45B	growth arrest and DNA-damage-inducible, beta	AF078077	13.9	13.6	(Sonna et al. 2003; Subarsky and Hill 2003)
GOLGIN-67	golgin-67	AF204231	3.9	2.9	
HES1	hairy and enhancer of split 1, (Drosophila)	BE973687	5.3	20.3	
HEY1	hairy/enhancer-of-split related with YRPW motif 1	NM_012258	4.1	13.8	(Weinmann et al. 2005)

Table 4.2 (continued) Hypoxia up-regulated genes (>2.5-fold) in NPC cell lines.

Gene symbol	Gene Title	Genbank	Fold change		Reference
			CNE-2	HONE-1	
HIG2	hypoxia-inducible protein 2	NM_013332	23.4	34.2	
HK2	hexokinase 2	AI761561	6.9	12.6	(Sonna et al. 2003; Ning et al. 2004; Greijer et al. 2005)
IER3	immediate early response 3	NM_003897	5.5	10.7	
IGFBP3	insulin-like growth factor binding protein 3	M31159	4.7	11.3	(Denko et al. 2003; Sonna et al. 2003; Subarsky and Hill 2003)
INSIG1	insulin induced gene 1	NM_005542	6.0	5.2	
INSIG2	insulin induced gene 2	AL080184	8.0	12.8	
ITGA5	integrin, alpha 5 (fibronectin receptor, alpha polypeptide)	NM_002205	3.2	5.1	(Denko et al. 2003)
JMJD1A	jumonji domain containing 1A	AA524505	4.6	9.1	
JMJD2B	jumonji domain containing 2B	BE256900	2.9	3.6	
LOX	lysyl oxidase	NM_002317	8.6	22.7	(Denko et al. 2003; Sonna et al. 2003)
LOXL2	lysyl oxidase-like 2	NM_002318	3.0	3.2	
Lrp2bp	low density lipoprotein receptor-related protein binding protein	AA886870	27.5	32.0	(Denko et al. 2003)
MAFF	v-maf musculoaponeurotic fibrosarcoma oncogene homolog F (avian)	AL021977	2.6	4.2	(Sonna et al. 2003)
MAFK	v-maf musculoaponeurotic fibrosarcoma oncogene homolog K (avian)	BG231691	2.9	2.1	
MIG-6	mitogen-inducible gene 6	AL034417	5.8	4.8	(Subarsky and Hill 2003)
MOBKL2A	MOB1, Mps One Binder kinase activator-like 2A (yeast)	BE396735	2.6	4.4	
MUC1	mucin 1, transmembrane	NM_002456	2.7	3.1	(Denko et al. 2003)
MXI1	MAX interactor 1	NM_005962	9.3	12.0	(Denko et al. 2003; Sonna et al. 2003)
NDRG1	N-myc downstream regulated gene 1	NM_006096	9.1	64.3	(Sonna et al. 2003; Subarsky and Hill 2003; Greijer et al. 2005; Vengellur et al. 2005)
NFIL3	nuclear factor, interleukin 3 regulated	NM_005384	3.3	7.9	
NOL3	nucleolar protein 3 (apoptosis repressor with CARD domain)	AI912351	3.0	3.7	
P4HA2	procollagen-proline, 2-oxoglutarate 4-dioxygenase (proline 4-hydroxylase), alpha polypeptide II	NM_004199	2.6	3.7	
PAG	phosphoprotein associated with glycosphingolipid-enriched microdomains	AK000680	9.7	17.5	
PBEF1	pre-B-cell colony enhancing factor 1	AA873350	5.8	5.1	(Ning et al. 2004)
PDK1	pyruvate dehydrogenase kinase, isoenzyme 1	AU146532	3.5	6.5	(Sonna et al. 2003; Vengellur et al. 2005)
PFKFB3	6-phosphofructo-2-kinase/fructose-2,6-biphosphatase 3	NM_004566	10.1	27.8	(Denko et al. 2003; Sonna et al. 2003)
PFKFB4	6-phosphofructo-2-kinase/fructose-2,6-biphosphatase 4	AL038787	11.9	9.2	(Denko et al. 2003; Sonna et al. 2003)
PGK1	phosphoglycerate kinase 1	BE856250	10.1	9.0	(Denko et al. 2003; Sonna et al. 2003; Subarsky and Hill 2003; Ning et al. 2004; Greijer et al. 2005)
PLOD2	procollagen-lysine, 2-oxoglutarate 5-dioxygenase (lysine hydroxylase) 2	AI754404	3.8	9.5	(Denko et al. 2003; Ning et al. 2004)

Table 4.2 (continued) Hypoxia up-regulated genes (>2.5-fold) in NPC cell lines.

Gene symbol	Gene Title	Genbank	Fold change		Reference
			CNE-2	HONE-1	
RAB20	RAB20, member RAS oncogene family	NM_017817	2.6	6.2	
RAB40C	RAB40C, member RAS oncogene family	AW007215	6.6	7.9	
RAI3	retinoic acid induced 3	AA156240	2.9	3.5	
RARA	retinoic acid receptor, alpha	AI806984	3.1	5.0	
SEMA4B	sema domain, immunoglobulin domain (Ig), transmembrane domain (TM) and short cytoplasmic domain, (semaphorin) 4B	AK026133	3.2	3.8	
SERPINE1	serine (or cysteine) proteinase inhibitor, clade E (nexin, plasminogen activator inhibitor type 1), member 1	AL574210	3.0	4.8	(Denko et al. 2003; Sonna et al. 2003; Ning et al. 2004; Vengellur et al. 2005)
SERTAD2	SERTA domain containing 2	BG107456	2.4	3.0	
SLC2A1	solute carrier family 2 (facilitated glucose transporter), member 1	NM_006516	4.8	9.2	(Weinmann et al. 2005)
SLC2A14	solute carrier family 2 (facilitated glucose transporter), member 14	AA778684	9.0	31.2	
SLC2A3	solute carrier family 2 (facilitated glucose transporter), member 3	NM_006931	8.5	33.2	
SLC6A8	solute carrier family 6 (neurotransmitter transporter, creatine), member 8	NM_005629	7.6	6.4	(Denko et al. 2003; Sonna et al. 2003; Greijer et al. 2005; Vengellur et al. 2005)
STC1	stanniocalcin 1	AW003173	2.7	46.1	(Subarsky and Hill 2003)
STC2	stanniocalcin 2	BC000658	4.7	5.9	
TBC1D3	TBC1 domain family, member 3	AL136860	3.5	2.5	
TIPARP	TCDD-inducible poly(ADP-ribose) polymerase	AL556438	3.7	4.3	(Weinmann et al. 2005)
TPBG	trophoblast glycoprotein	NM_006670	3.7	2.9	(Weinmann et al. 2005)
TRA1	tumor rejection antigen (gp96) 1	AI684643	3.0	2.7	(Ning et al. 2004)
WSB1	WD repeat and SOCS box-containing 1	AI377135	6.7	4.4	
ZNF292	zinc finger protein 292	AA972711	3.5	5.2	
ZNF395	zinc finger protein 395	NM_017606	4.6	3.6	

Table 4.3 Hypoxia down-regulated genes (> 2.5-fold) in NPC cell lines.

Gene symbol	Gene Title	Genbank	Fold change		Reference
			CNE-1	HONE-1	
C6orf93	chromosome 6 open reading frame 93	AI458051	-3.0	-3.2	
DBR1	debranching enzyme homolog 1 (S. cerevisiae)	AK000116	-3.3	-2.6	
EIF5	eukaryotic translation initiation factor 5	AK026933	-2.7	-6.0	
FLJ20249	hypothetical protein FLJ20249	BE794289	-2.6	-3.7	
HSPC111	hypothetical protein HSPC111	NM_016391	-3.2	-2.9	(Sonna et al. 2003)
HSPC196	hypothetical protein HSPC196	AF151030	-3.3	-3.6	
IFRD1	interferon-related developmental regulator 1	NM_001550	-3.1	-5.6	
LOC129401	mitotic phosphoprotein 44	AL529634	-2.6	-2.9	
MGC4399	mitochondrial carrier protein	BC004991	-3.3	-2.8	
POLR1B	polymerase (RNA) I polypeptide B, 128kDa	BC004882	-2.9	-5.9	
RFP	ret finger protein	AF230394	-2.6	-4.2	(Chi et al. 2006)
RIOK1	RIO kinase 1 (yeast)	BC006104	-2.8	-3.7	
RRS1	RRS1 ribosome biogenesis regulator homolog (S. cerevisiae)	BC001811	-2.9	-7.8	
SOCS4	suppressor of cytokine signaling 4	BF446961	-2.5	-3.1	
TFRC	transferrin receptor (p90, CD71)	N76327	-2.6	-6.7	

Table 4.4 Apoptosis genes regulated by hypoxia in NPC cells.

Gene Symbol	Gene Title	Apoptosis regulation*	Genbank	Fold change CNE-2	Fold change HONE-1
	Up-regulated				
BIK	BCL2-interacting killer (apoptosis-inducing)	+	NM_001197	2.9	2.0
BNIP3	BCL2/adenovirus E1B 19kDa interacting protein 3	+	U15174	5.1	12.0
BNIP3L	BCL2/adenovirus E1B 19kDa interacting protein 3-like	+	AF060922	4.8	4.5
BTG1	B-cell translocation gene 1, anti-proliferative	+	AL535380	2.6	3.4
E2IG5	growth and transformation-dependent protein	+	NM_014367	3.6	5.7
EGLN3	egl nine homolog 3 (C. elegans)	+	NM_022073	11.5	56.8
GADD45B	growth arrest and DNA-damage-inducible, beta	-	AF078077	13.9	13.6
IER3	immediate early response 3	-	NM_003897	5.5	10.7
IGFBP3	insulin-like growth factor binding protein 3	+	M31159	4.7	11.3
MTP18	mitochondrial protein 18 kDa	-	AF060924	1.8	2.2
NOL3	nucleolar protein 3 (apoptosis repressor with CARD domain)	-	AI912351	3.0	3.7
PPP1R15A	protein phosphatase 1, regulatory (inhibitor) subunit 15A	+	U83981	2.0	2.1
RHOB	ras homolog gene family, member B	+	AI263909	2.8	2.4
SOCS3	suppressor of cytokine signaling 3	-	AI244908	1.8	2.8
TGFB1	transforming growth factor, beta 1 (Camurati-Engelmann disease)	-	BC000125	2.2	2.1
	Down-regulated				
BAG2	BCL2-associated athanogene 2	-	AF095192	-2.3	-3.0
BIRC4	baculoviral IAP repeat-containing 4	-	BF109251	-2.2	-2.2
CUL3	cullin 3	+	AF062537	-1.9	-2.4
CUL5	cullin 5	+	BF435809	-2.0	-2.7
FAIM	Fas apoptotic inhibitory molecule	-	NM_018147	-1.8	-2.0
MGC5297	hypothetical protein MGC5297	?	NM_024091	-2.2	-2.3
PSEN1	presenilin 1 (Alzheimer disease 3)	-	NM_007318	-1.9	-1.9
UTP11L	UTP11-like, U3 small nucleolar ribonucleoprotein	+	NM_016037	-2.1	-1.9

* Apoptosis regulation: "+" = pro-apoptotic; "-" = anti-apoptotic

Table 4.5 Comparison of genes modulated by hypoxia[1] in CNE-2, HONE-1 and NCI H460 cell lines.

	Probe Set	Gene Symbol	Gene Title
	a) Commonly up-regulated genes (CNE-2 and NCI H460)		
*	201250_s_at	SLC2A1	solute carrier family 2 (facilitated glucose transporter), member 1
*	201670_s_at	MARCKS	myristoylated alanine-rich protein kinase C substrate
*	202855_s_at	SLC16A3	solute carrier family 16 (monocarboxylic acid transporters), member 3
	203325_s_at	COL5A1	collagen, type V, alpha 1
*	203476_at	TPBG	trophoblast glycoprotein
	203665_at	HMOX1	heme oxygenase (decycling) 1
	204284_at	PPP1R3C	protein phosphatase 1, regulatory (inhibitor) subunit 3C
*	212665_at	TIPARP	TCDD-inducible poly(ADP-ribose) polymerase
*	44783_s_at	HEY1	hairy/enhancer-of-split related with YRPW motif 1
	b) Commonly up-regulated genes (HONE-1 and NCI H460)		
*	201250_s_at	SLC2A1	solute carrier family 2 (facilitated glucose transporter), member 1
*	201669_s_at	MARCKS	myristoylated alanine-rich protein kinase C substrate
*	201670_s_at	MARCKS	myristoylated alanine-rich protein kinase C substrate
*	202855_s_at	SLC16A3	solute carrier family 16 (monocarboxylic acid transporters), member 3
*	202856_s_at	SLC16A3	solute carrier family 16 (monocarboxylic acid transporters), member 3
	203186_s_at	S100A4	S100 calcium binding protein A4 (calcium protein, calvasculin, metastasin, murine placental homolog)
*	203476_at	TPBG	trophoblast glycoprotein
	204584_at	L1CAM	L1 cell adhesion molecule
	204679_at	KCNK1	potassium channel, subfamily K, member 1
	209373_at	BENE	BENE protein
*	212665_at	TIPARP	TCDD-inducible poly(ADP-ribose) polymerase
*	44783_s_at	HEY1	hairy/enhancer-of-split related with YRPW motif 1
	c) Commonly down-regulated genes (CNE-2 and NCI H460)		
	209505_at	NR2F1	nuclear receptor subfamily 2, group F, member 1
	209967_s_at	CREM	cAMP responsive element modulator
	221727_at	PC4	activated RNA polymerase II transcription cofactor 4
	d) Commonly down-regulated genes (HONE-1 and NCI H460)		
	203137_at	WTAP	Wilms tumor 1 associated protein
	204977_at	DDX10	DEAD (Asp-Glu-Ala-Asp) box polypeptide 10
	218016_s_at	POLR3E	polymerase (RNA) III (DNA directed) polypeptide E (80kD)

* Genes modulated by hypoxia in all three cell types

[1] Hypoxic CNE-2 and HONE-1 cells were treated in 0.1% O_2, 5% CO_2 and 94.9% N_2 for 16 h. Hypoxia tolerant NCI H460 cells were selected by 10 consecutive cycles of hypoxia and reoxygenation.

Figure 4.1

(A) Protein expression of HIF-1α, HIF-2α and CA IX in NPC cells after exposure to hypoxia. NPC cells were subjected to normoxic (-) or hypoxia (H) treatment for 16 hours. At the end of incubation, cells were collected and lysed. Total cell lysates were analyzed by SDS-PAGE followed by immunoblotting with appropriate antibodies. These are typical blots taken from 3 separate experiments.

(B) Expression of mRNA of HIF-1α, HIF-2α, CA9 and VEGF in NPC cells after exposure to hypoxia. NPC cells were incubated in normoxic (-) or hypoxia (H) treatment for 16 hours and 24 hours. At the end of incubation, cells were collected and total RNA was extracted. RT-PCR was then performed. The PCR amplified cDNA derived from HIF-1α (16 hr hypoxia), HIF-2α (16 hr hypoxia), CA9 (16 hr hypoxia), VEGF (16 hr and 24 hr hypoxia) and β-actin (16 hr hypoxia) were separated by 1.8 % agarose gel electrophoresis containing ethidium bromide. These are representative gel pictures taken from 3 separate experiments.

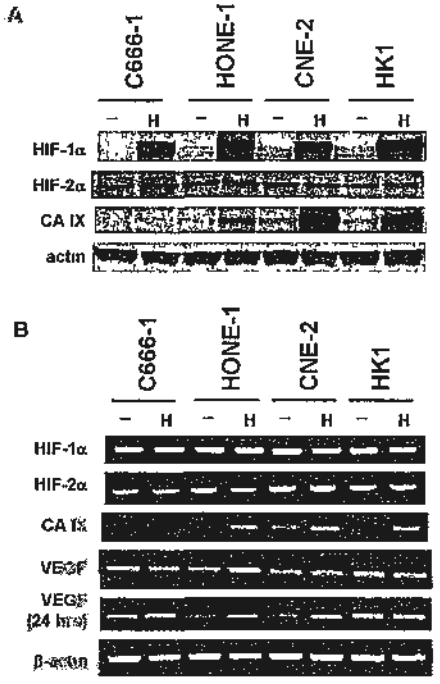

Figure 4.2

VEGF secretion by NPC cells after exposure to short term chronic hypoxia. NPC cells were incubated in normal (solid line) or hypoxia (dotted line) condition for 4 to 48 hours. At the end of incubation, culture medium was collected and VEGF secretion to culture medium was quantified by a VEGF ELISA kit. Cells in each well were collected and lysed. Total proteins were then quantified. VEGF secretion was then normalized by total protein in each well. A: C666-1 cells, B: HONE-1 cells, C: CNE-2 cells, and D: HK1 cells.

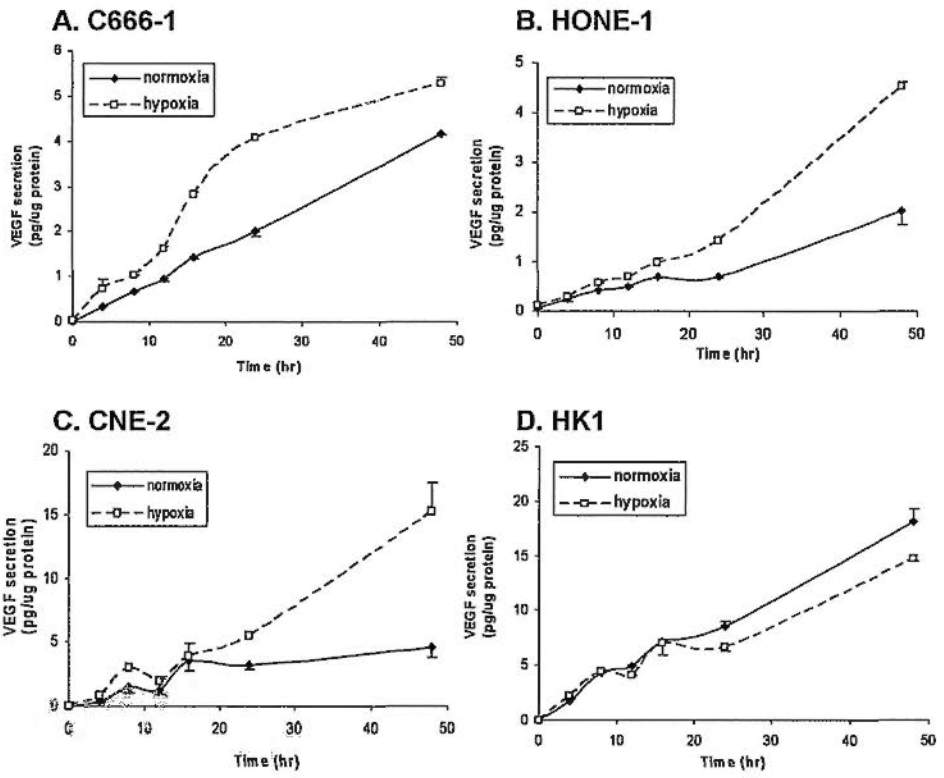

Figure 4.3

RT-PCR analyses of 13 differentially expressed genes in CNE-2, HONE-1, C666-1 and HK1 cells. NPC cells were incubated in normoxic (-) or hypoxia (H) treatment for 16 hours. At the end of incubation, cells were collected and total RNA was extracted. RT-PCR was then performed. The PCR amplified cDNA were separated by 2 % agarose gel electrophoresis containing ethidium bromide.

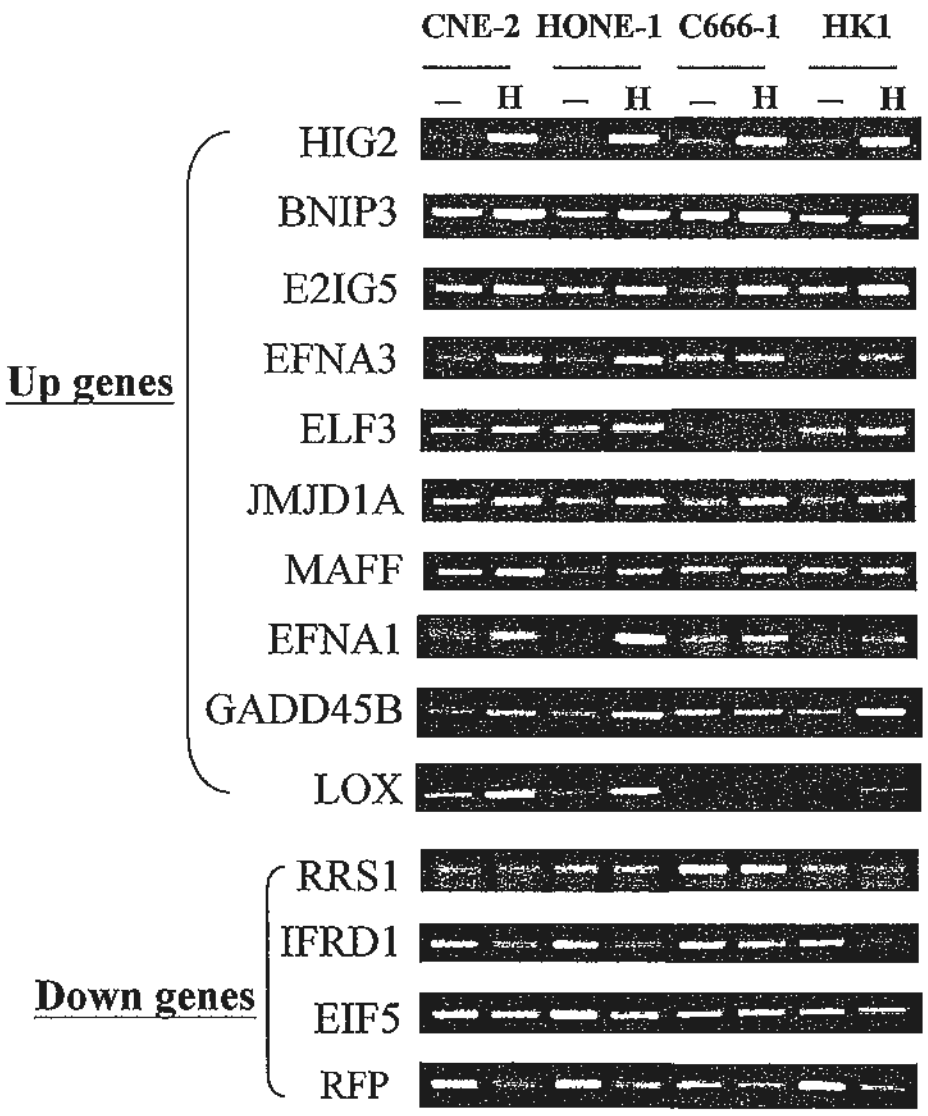

Figure 4.4

Biological processes most frequently involved by the 222 up-regulated and 137 down-regulated genes under hypoxia according to the Gene Ontology (GO) classification. The percentage distribution of up- and down-regulated genes with GO annotation in each category of biological process was shown, and each asterisk (*) represent a significant differential regulation in the category compared ($p < 0.05$ by Fisher's exact test).

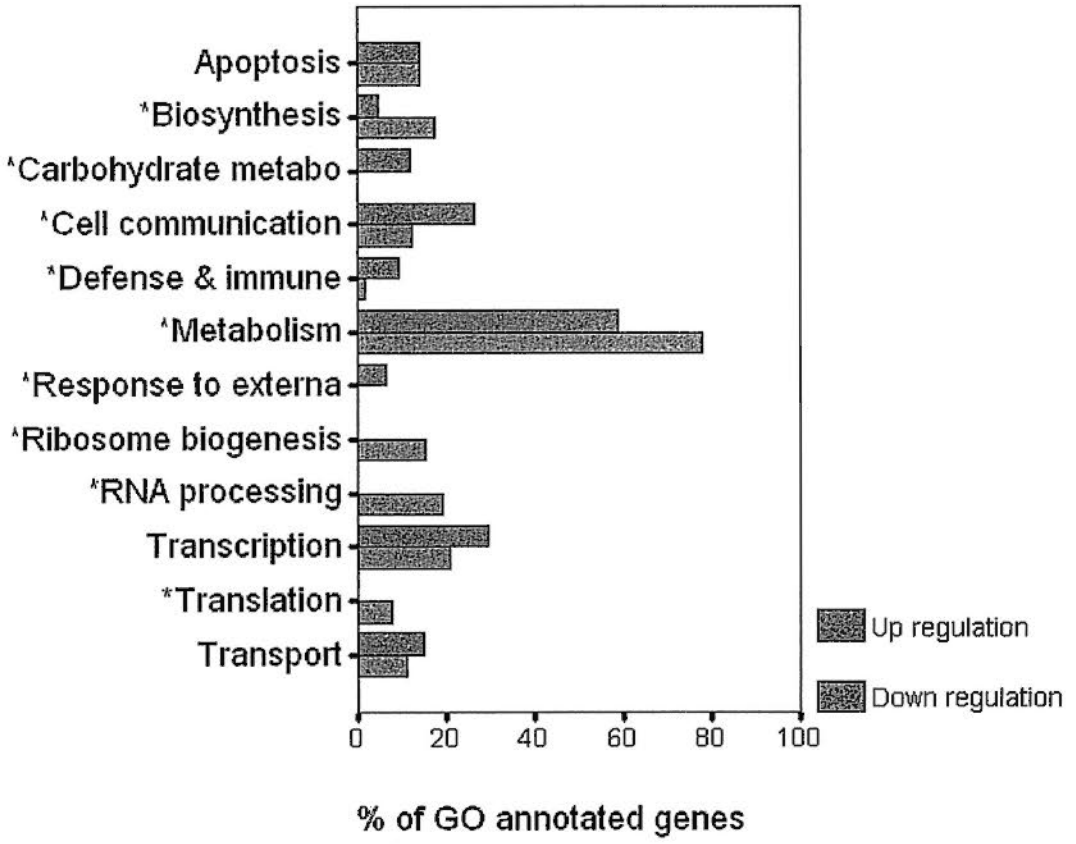

Figure 4.5

Differential gene expressions in the apoptosis pathway produced by GenMapp (Salomonis et al. 2007). The fold changes identified by microarray expression analysis of HONE-1 cells under normoxic versus hypoxic conditions are indicated adjacent to each box. Each box represents a gene, with red color indicating up-regulation, and green color indicating down-regulation.

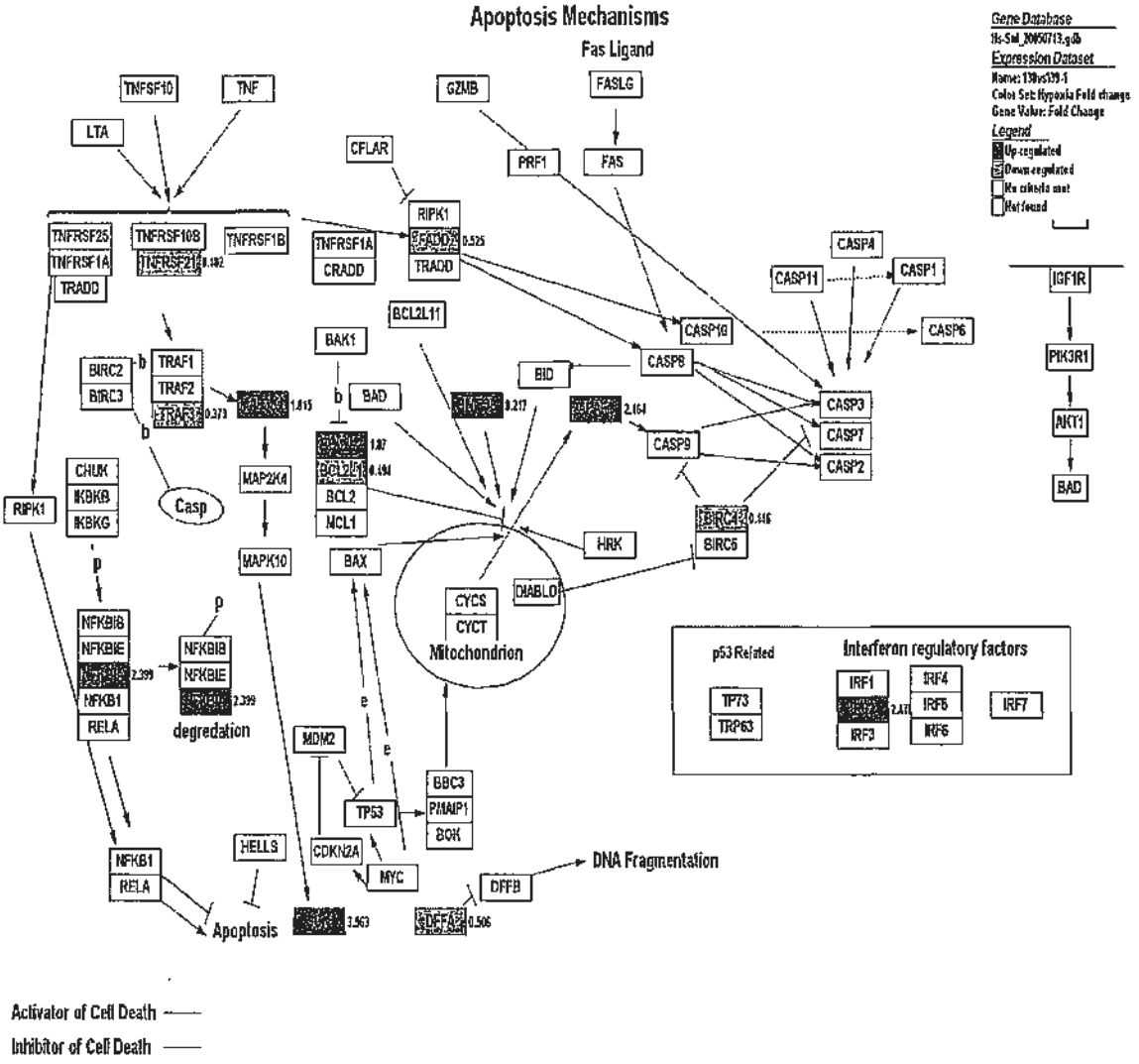

Figure 4.6

A GenMapp view (Salomonis et al. 2007) of the differential gene expressions in the translation factor pathway (data shown were from HONE-1 cells). Each box represents a gene, with red color indicating up-regulation, and green color indicating down-regulation. Numbers adjacent to box indicate fold changes.

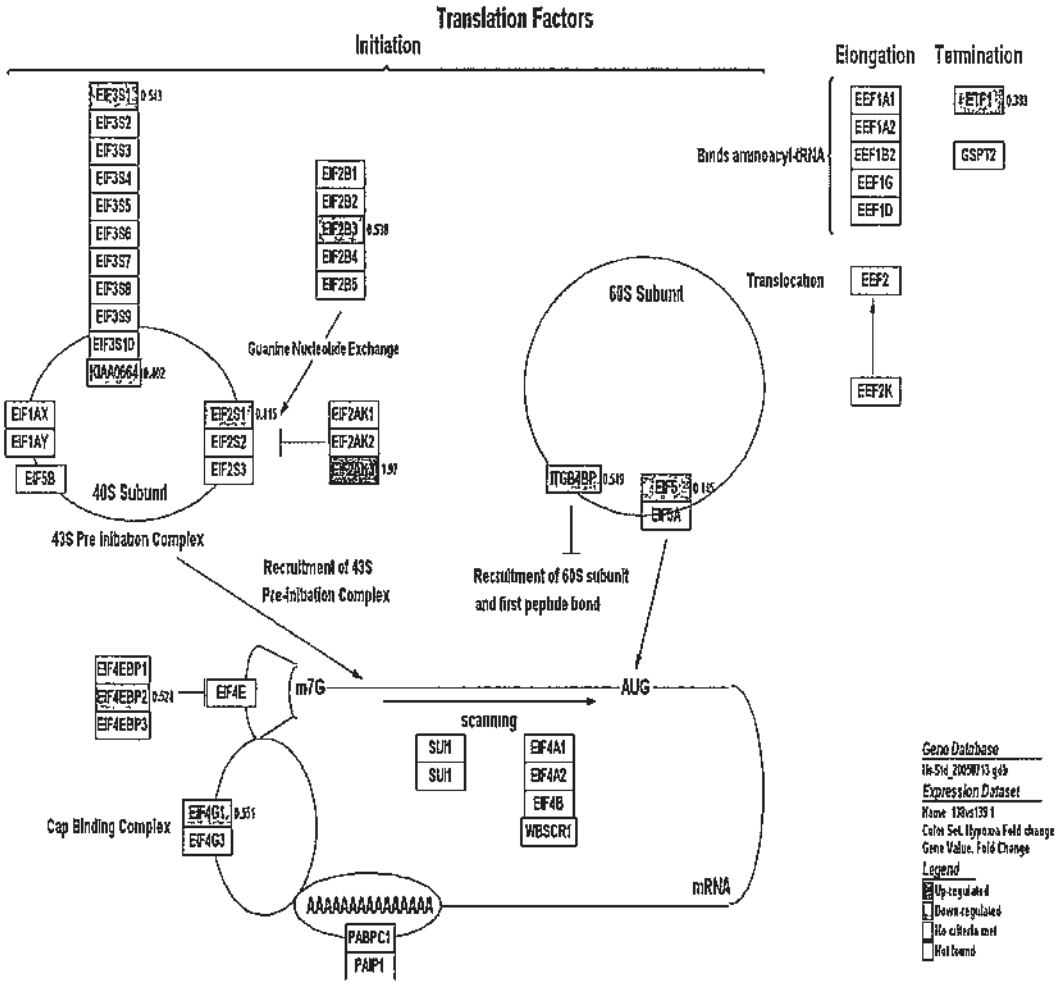

DISCUSSION

In 4 NPC cell lines, we have shown that the protein level of HIF-1α was induced but in contrast, hypoxia did not induce significant change in the protein level of HIF-2α. Hypoxia incubation also significantly increased protein level of CA IX and VEGF in 3 of 4 NPC cell lines. Our findings in NPC are consistent with the known hypoxia induction of HIF-1α, CA IX and VEGF protein in other tumor types reported in the literature (Wykoff et al. 2000; Beasley et al. 2001; Jones et al. 2001). The lack of hypoxic induction of HIF-2α in NPC cell lines suggested that this marker may not play a significant role in relation to hypoxia induced changes in NPC tumor cells. This was also reflected in our clinical study in that HIF-2α was only scarcely expressed in the tumor cells of clinical samples in NPC (see chapter 5, study 3). In that study, HIF-2α was more frequently found to be expressed in tumor associated stromal cells or macrophages. Other investigators have also found that HIF-2α was mainly expressed in stromal cells instead of tumor cells, and suggested that the HIF-2α mediated hypoxic pathway may play a significant role in tumor associated macrophages (Leek et al. 2002; Onita et al. 2002).

Od special note, we observed that the time course of hypoxia induced mRNA changes in NPC cells differed for CA IX and VEGF. Compared to CA IX mRNA induction, hypoxia induced up-regulation of VEGF mRNA was only evident after a more prolonged (>24 hours) incubation under hypoxia. This subtle difference in the temporal relationship of CA IX and VEGF to hypoxia induction may partly explain the lack of correlation in the expression pattern of the two markers at the microscopic level in NPC tumors in our clinical study (see chapter 5, study 3). Similar observation of the differential regulation of CA IX and VEGF by hypoxia has also been reported by

other investigators in superficial versus invasive bladder cancer (Turner et al. 2002). The mechanism for selective modulation of genes in the hypoxia pathway may be variable and included methylation of CA IX (Cho et al. 2000).

Based on extrapolation of the expression profiling data from our microarray experiments, we estimated that between 2-5% of the NPC genome is transcriptionally responsive to hypoxia. Hypoxia regulated genes are involved in diverse biological processes. However, we observed a pattern of coordinated up- or down-regulation of genes in distinct biological processes. Thus, despite a general down-regulation of genes involved in cellular metabolism, biosynthesis, RNA processing and translation, there is selective up-regulation of genes involved carbohydrate metabolism to turn on glycolytic pathway and anaerobic metabolism. Other hypoxia up-regulated genes were involved in angiogenesis, cell communication, defense and immune response, response to stress and external stimulus. These findings suggest that cancer cells can undergo adaptive changes that allow them not only to survive but even to proliferate or leave the adverse hypoxic environment.

Hypoxia has been known to inhibit macromolecule biosynthesis in an oxygen dependent manner to conserve energy utilization. We observed the selective down-regulation of a group of genes involved in translation control (eukaryotic translation initiation factor 3 /subunit 1 alpha [EIF3S1], eukaryotic translation initiation factor 5 [EIF5], eukaryotic translation termination factor 1 [ETF1], G elongation factor /mitochondrial 1 [GFM1], protein-kinase /interferon-inducible double stranded RNA dependent inhibitor /repressor of P58 [PRKRIR]) in NPC cells under hypoxia (supplementary Table S2 and Figure 4.6), which may mediate inhibition of protein

synthesis under hypoxia. Interestingly, a recent study revealed that a class of candidate genes, including EIF5 and activating transcription factor 4 [ATF4], is hypoxia induced and regulated at the translational level in hypoxic HeLa cells (Blais et al. 2004). However, the contribution of suppression of individual translational control genes to the overall suppression of translation will require further study.

Hypoxia has been associated with genetic instability and tumor progression. It has been shown previously that alterations in the expression of DNA repair genes in response to hypoxic stress may account for a proportion of such genetic instability (Koshiji et al. 2005; Bindra et al. 2005). Our expression data in NPC indicated that hypoxia repressed the expression of five genes involved in DNA repair (ASF1A, GTF2H2, POLE2, RFC3 and TSN) (supplementary Table S2). This suggests that regulation of DNA repair is an integral part of the hypoxic response. Further studies on the role of these DNA repair genes will provide molecular insights into the mechanisms underlying hypoxia-induced genetic instability.

Our microarray data on the differential gene regulations illustrated the complexity involved in the apoptosis pathway in NPC (Table 4.4). Hypoxia can induce (as well as repress) both the pro- and anti-apoptotic molecules in a cell and the final balance is not readily predictable. It is known that severe and prolonged hypoxia may initiate apoptosis, whereas under acute and mild hypoxia cells may adapt to this environmental stress and will survive. Fine tuning of the regulation of apoptosis by hypoxia is influenced by HIF-1 in combination with many other factors, which may determine whether HIF-1 might shift the balance towards apoptosis or act as an anti-apoptotic factor (Greijer and van der Wall 2004). In addition, different cell types

may influence the balance of apoptotic mechanisms. Because hypoxia can be an early event in tumor development, it can acts as an early selection pressure on tumor cells to become resistant to hypoxia-induced apoptosis. This acquired resistance to apoptosis can in turn contribute to the aggressive phenotype that is characteristic of clinical hypoxic tumors. A better understanding of the regulation of apoptosis by hypoxia in solid tumors and the mechanisms of resistance to apoptosis might lead to more specific treatments for solid tumors.

It should be acknowledged that our in vitro experimental system for hypoxia may not be an ideal representation for all the possible physiological or pathological conditions inside the body. Different cells in the human body often have diverse energy requirement, operate in different microenvironment and are normally exposed to different range of oxygen concentration. As our objective was to study the full extent of hypoxia modulated gene expression, we used 0.1% O_2 to define a state of severe hypoxia, which was previously adopted in several studies (Wykoff et al. 2000; Beasley et al. 2001; Jones et al. 2001; Weinmann et al. 2005). Other studies used mild level of hypoxia (5% - 0.5% O_2) (Chi et al. 2006) or even anoxia (< 0.1% O_2) (Ameri et al. 2004), which may modulate a different set of gene expression profile. HIF-1 was previously shown in vitro, in a variety of cell culture system, to be activated at a cut off point of about 5% O_2 (40 mmHg), and to progressively increase its activity with a decrease in O_2 gradient down to 0.2% - 0.1% O_2 (1.6 – 0.8 mmHg), close to anoxia (Pouyssegur, Dayan, and Mazure 2006). Recently, it was shown that the oxygen sensor Factor-Inhibiting HIF-1 (FIH) controls expression of distinct genes through the bifunctional transcriptional character of HIF-1α (Dayan et al. 2006), and a working model of two sets of HIF-1-regulated genes was proposed. In this model

the bifunctional transcriptional nature of HIF-1α will, in an FIH-dependent or FIH-independent manner, regulate two sets of genes according to the pO_2 gradient (Pouyssegur, Dayan, and Mazure 2006).

We presented a comprehensive analysis of the genomic response to hypoxia in NPC cell lines. We have identified distinct functional classes whose expressions are significantly modulated by hypoxia. One limitation of our study is that we only performed microarray experiments in CNE-2 and HONE-1 cell lines. The results of our microarray analysis must be viewed as preliminary. Our findings should be followed by further functional studies and eventually to be confirmed in tumor tissues. However, we were able to replicate and validate most of the findings by RT-PCR in the other NPC cell lines (HK1 and C666-1, Figure 4.3). Moreover, the results of hypoxia markers expression from our in-vitro cell line experiments were corroborated by protein expression analysis in our clinical study using patients' biopsy samples (chapter 5, study 3).

Several groups have used genomic approach to identify gene expression profile in hypoxia (Denko et al. 2003; Sonna et al. 2003; Subarsky and Hill 2003; Ning et al. 2004; Greijer et al. 2005; Vengellur et al. 2005; Weinmann et al. 2005; Chi et al. 2006). Among the different cell types examined *in vitro*, the different level and duration of hypoxia used, and the resultant gene profile have underscored both the heterogeneity and complexity of gene expression changes in hypoxia. From these analyses one can conclude that there is a core set of genes that are modulated consistently by hypoxia but a large number of genes exhibited cell-type-specific changes. Our result demonstrated that there is a significant component of down regulation in addition to

up regulation of gene expressions modulated by hypoxia. In the process of generation of apoptosis-resistant phenotype of hypoxia selected cells, down regulation of pro-apoptotic genes will have the same bearing as up-regulation of anti-apoptotic genes. Unlike the well known list of hypoxia induced (up-regulated) genes, the group of hypoxia repressed genes has been less well defined in the past. This should become the focus of future study in order to provide a more comprehensive picture of the hypoxic tumor phenotypes.

Recently, Giaccia's group found that the expression of lysyl oxidase (LOX) was elevated in hypoxic human tumor cells in microarray experiments. They went on to demonstrate that LOX expression was regulated by HIF and hypoxia in human breast and head and neck cancer tumors. Patients with high LOX-expressing tumors had poor distant metastasis-free and overall survivals. Inhibition of LOX eliminated breast cancer metastasis in mice. Their findings indicate that LOX is essential for hypoxia-induced metastasis (Erler et al. 2006; Erler et al. 2009). We also found that LOX and lysyl oxidase-like 2 (LOXL2) were highly up-regulated by hypoxia in NPC cell lines (Table 4.2 and S1, also Figure 4.3). We are conducting further studies to investigate the role of LOX in NPC.

CONCLUSION

This study has provided a global and mechanistic view to the molecular changes underlying the clinical hypoxic tumor phenotype in NPC. These data further contributed to our understanding on the possible link between tumor hypoxia, angiogenesis and distant metastases in NPC (Chapter 1, Figure 1.3).

Chapter 5

Study 3: Biomarkers of Hypoxia and Angiogenesis

BACKGROUND

As introduced in chapter 1 and discussed in the previous chapter, tumor hypoxia has long been known to be associated with resistance to chemotherapy and radiotherapy as well as a more malignant tumor phenotype with increased invasiveness, metastases, and poorer survival (Gray et al. 1953; Hockel et al. 1996; Brizel et al. 1996). The development of simple and reliable tests to estimate tumor hypoxia would be of clinical importance for the identification of subgroups of patients that could benefit from hypoxia targeting therapeutic strategies (Hoogsteen, Marres, van der Kogel et al. 2007). Previous clinical studies of tumor hypoxia concentrated on direct measurement with a polarographic electrode, or by injection of a hypoxia labeling marker, such as pimonidazole, into patient's blood prior to biopsy and subsequent detection of the marker by immunohistochemistry. The recent development of non-invasive radiologic and nuclear medicine imaging of hypoxia markers are promising new approaches. In head and neck squamous cell cancer, using direct measurement of tumor pO2, a low pre-treatment pO2 has been shown to predict poor response to radiation and shorter survival (Nordsmark, Overgaard, and Overgaard 1996; Brizel et al. 1997). In NPC, using the hypoxia imaging agent fluorine-18 fluoromisonidasole with positron emission tomography system, tumor hypoxia was demonstrated in 100% of primary tumor and 58% of cervical lymph nodes metastases (Yeh et al. 1996). However, these techniques can only be applied in-vivo and on a prospective basis. In search of a simple test that would detect evidence of hypoxia even on archival tissue material, immunohistochemical detection of proteins induced

by clinical relevant levels of hypoxia represents an appealing option. Such intrinsic marker of hypoxia would have the advantage of being assessable on routine clinical biopsies without the need for specialist equipment or administration of exogenous hypoxia markers.

The transcriptional complex hypoxia-inducible factor-1 (HIF-1) plays a pivotal role in essential adaptive responses to hypoxia, and its expression increases exponentially with decreases in levels of cellular oxygen. HIF-1 has recently emerged as an important mediator of gene expression patterns in many tumors (Semenza 2000). HIF-1 is a heterodimer composed of HIF-1α and HIF-1β subunits. HIF-1β is constitutively expressed, whereas HIF-1α is protected from ubiquitination and proteasomal degradation under hypoxic conditions (Maxwell et al. 1999). Another member of the family showing close sequence homology and similar properties to HIF-1α has been described and is named HIF-2α (also known as endothelial PAS domain protein-1) (Wiesener et al. 1998).

Carbonic anhydrase IX (CA IX) is a novel member of the carbonic anhydrase family that codes for a transmembrane glycoprotein with a suggested function in maintaining the acid-base balance and intercellular communication (Opavsky et al. 1996). CA IX can confer a variety of features of the transformed phenotype when transfected into NIH 3T3 cells (Pastorek et al. 1994). Vascular endothelial growth factor (VEGF) is one of the most well studied markers of tumor angiogenesis and its expression has been shown to be of prognostic significance in most human tumors studied.

Previous studies have shown that hypoxia induces the expression of HIF-1α, which

then up-regulates the expression of downstream genes CA IX and VEGF (Wykoff et al. 2000; Beasley et al. 2001; Jones et al. 2001). In cervical cancer, CA IX expression was demonstrated to correlate with tumor hypoxia as measured by needle electrode (Loncaster et al. 2001). HIF-1α expression was shown to overlap with the hypoxia-labeling marker EF5 in cervical cancer xenograft (Vukovic et al. 2001). HIF-1α and CA IX are thus potential endogenous markers of tissue hypoxia.

In this clinical and translational study, we aimed to investigate the expression pattern of HIF-1α, HIF-2α, CA IX and VEGF in NPC biopsies, and to correlate the level of expression with clinicopathological characteristics and survival outcome.

MATERIALS AND METHODS

Patients and samples

Formalin-fixed, paraffin-embedded biopsy tissues of 90 consecutive NPC patients recruited between 1994 and 1997 in a randomized controlled trial of chemo-radiation in locally advanced NPC (Chan, Teo et al. 2002) were retrieved. Patients with biopsy-proven, previously untreated NPC with Ho's N2 or N3 stage, or N1 stage with lymph node size >= 4 cm (Ho's staging)(Ho 1978), and without distant metastases (M0), were eligible for the trial. Eligible patients were randomized to receive either standard radiotherapy alone or the same radiotherapy given concurrently with weekly cisplatin 40mg/m^2 for up to eight weeks (Chan, Teo et al. 2002). After completion of treatment patients were followed up every 8 weeks during the first year, every 12 weeks for the second year and third year, and every 16 to 24 weeks thereafter. Patients who developed local or distant recurrence were subjected to any treatment considered appropriate in the opinion of the attending physician including surgery,

chemotherapy or radiotherapy. Informed consent for immunohistochemical study of biological markers was obtained at the time of biopsy. All biopsies were taken via a nasopharyngeal endoscope for diagnostic purposes before the start of treatment. Flanking sections from each tumor biopsy were studied by immunohistochemistry for the expression of HIF-1α, HIF-2α, CA IX and VEGF.

Immunohistochemistry (IHC)

The HIF-1α, HIF-2α, CA IX and VEGF proteins in tissue sections were detected by IHC using the murine monoclonal antibodies ESEE 122 (Talks et al. 2000), EP 190b (Talks et al. 2000), M75 (Pastorekova et al. 1992) and VG1 (Turley et al. 1998) respectively according to previously described methodology (Talks et al. 2000; Wykoff et al. 2000; Wykoff et al. 2001; Turley et al. 1998).

HIF-1α and HIF-2α

IHC staining was performed on 4-5 um paraffin sections. The slides were first placed in 60°C oven for 15 minutes. They were then deparaffinized in citroclear twice for 10 minutes and rehydrated through a series of graded alcohols and distilled water. After being placed in Tris buffered saline (TBS) buffer for 5 minutes, the slides were transferred to a jar containing 1 mM EDTA pH 8.0 buffer and placed in a preheated 60°C water bath for overnight incubation to achieve antigen retrieval. To block endogenous peroxidase activity, DAKO Peroxidase block solution was applied for 5 minutes. After two washes in TBS buffer, Triton-X 100 0.2% in TBS was applied for 10 minutes. For HIF-1α, the primary antibody ESEE 122 was applied at 1:40 dilution for 30 minutes. For HIF-2α, the primary antibody EP 190b was applied neat for 30 minutes. Secondary labeled polymer from the Envision HRP Kit (DAKO) was applied for 30 minutes. The peroxidase reaction was developed using diaminobenzidine

(DAB) chromogen kit from DAKO for 10 minutes. After washing, the slides were lightly counter-stained with Haematoxylin and mounted.

CA IX

Sections were deparaffinized and rehydrated. Endogenous peroxidase was quenched with DAKO Peroxidase block solution applied for 5 minutes. Normal human serum at 10% in TBS was then applied for 15 minutes. After knocking off excess blocking serum from the slides, the primary antibody M75 was applied at 1:50 for 30 minutes. Secondary polymer from the Envision HRP Kit (DAKO) was applied for 30 minutes. Diaminobenzidine (DAKO) was applied for 8 minutes. The slides were then counter-stained with Haematoxylin and mounted.

VEGF

The paraffin sections were baked in a 60°C oven for 15 minutes before deparaffinization. Antigen retrieval was achieved by pressure-cooking in Tris-EDTA pH 9.0 buffer (preparation: 12.2 gm Tris base, 1.48 gm EDTA in 2 L distilled water) for 3 minutes. DAKO Peroxidase block solution was applied for 5 minutes. Primary antibody VG1 was applied in 1:10 dilution for 30 minutes. Secondary polymer from the Envision HRP Kit (DAKO) was applied for 30 minutes, followed by diaminobenzidine (DAKO) for 5 minutes. The slides were counter-stained with Haematoxylin and mounted.

For all the above IHC staining, positive control slides from a tissue block with known positive staining for the respective primary antibody was included with each run. Negative control was achieved by substituting the primary antibody with TBS. In the case of VEGF, the universal presence of serum (which contains VEGF) in the blood vessel lumens of each section also served as a good internal positive control.

Scoring method

All slides were evaluated independently by two investigators (E.P.H. and F.P.) who were blinded to the patient's clinical data. Difference in scores between the two observers was resolved at a conference microscopy. Each slide was examined at low (x40) and high (x250) power to study both the staining pattern and distribution. The staining pattern of individual cells was classified into membranous, nuclear or cytoplasmic. The percentage of tumor cells showing positive staining for each antibody under study was scored. Staining intensity was not incorporated in our scoring method as we noted that it was more or less constant. The staining pattern of stromal cells and normal epithelium in the same tissue section was also assessed. The following grading system was adopted to score the number of positive stained macrophages in the tumor or stroma with HIF-2α: 0 - none seen in section; +/- very occasional single cell positive: + few positive cells either in foci or scattered; ++ moderate numbers either in foci or scattered; +++ large numbers of positive cells.

Statistical analysis

All statistical analysis and graphs were performed with the statistical package SPSS Release 9.0.0 (SPSS Inc., Chicago, IL). Correlation among the markers was analyzed using Spearman's correlation. Association between HIF-1α, HIF-2α, CA IX, VEGF expression and the various clinicopathological parameters was analyzed using Chi-squared test. Overall survival was defined from the day of randomization to the day of death or last follow-up. Progression free survival was defined from the day of randomization to the day of progression or last follow-up. Univariate analysis of overall survival and progression free survival was performed by the Kaplan-Meier

method and Log rank test. The Cox proportional hazards model was used for multivariate analysis. For all tests, a two-sided $p < 0.05$ was considered significant.

RESULTS

Patient cohort

The clinicopathological characteristics of the ninety NPC patients are presented in Table 5.1. The median duration of follow-up for this cohort was 4.13 years (range 0.52 to 6.21 years) at the time of analysis. To date, there have been four local recurrences, 30 distant metastases and 26 deaths.

Expression pattern of hypoxia markers

Table 5.2 summarizes the expression pattern of HIF-1α, HIF-2α, CA IX and VEGF in the tumor, stroma and normal epithelium in the NPC biopsy tissues.

HIF-1α

The tumor cells showed typical nuclear staining of HIF-1α in 52/90 (58%) of cases. Overall, the percentage of positive cells in tumor ranged from 0 to 90% (median, 1%; mean, 8.4%; Figure 5.1a). In the stroma, 12 cases (13%) showed nuclear staining. The normal epithelium showed focal staining in 16/60 (27%) of cases, including 7 cases of nuclear stain, 4 cases of cytoplasmic stain, and 5 cases of mixed nuclear and cytoplasmic stain pattern.

HIF-2α

The tumor cells were mostly negative and only showed focal nuclear stain in 6/89 (7%) of cases. Scanty focal cytoplasmic stain of tumor was noted in 6/89 (7%) of cases (of

which three cases showed focal nuclear stain as well). Focal cytoplasmic staining was observed in the stroma of 12/89 (13%) of cases. The normal epithelium showed focal staining in 9/57 (16%) of cases (cytoplasmic 6, nuclear 2, mixed cytoplasmic and nuclear 1).

In contrast, a striking pattern of HIF-2α expression in tissue infiltrating macrophages was observed in both the tumor and stroma (Summarized in Table 5.3). We generally observed a higher number of HIF-2α expressing macrophages in the stroma than the corresponding tumor.

CA IX

In the tumor, 51/90 (57%) of cases showed the characteristic membranous staining pattern of CA IX. Overall, the percentage of positively stained tumor cells ranged from 0 to 80% (median 1%; mean 7.5%; Figure 5.1b). The tumor typically showed a periluminal and peri-necrotic distribution of membranous staining for CA IX. Tumor nuclear staining pattern was observed in only 4/90 (5%) of cases. Only two cases showed positive staining of CA IX in stroma, including one nuclear and one cytoplasmic pattern.

A distinctive pattern of focal membranous staining of CA IX in the basal cells was observed in 30/57 of cases of normal epithelium (including both respiratory epithelium and squamous epithelium), and another 2 cases of normal epithelium revealed a focal nuclear staining. Additionally, para-tumoral dysplastic lesions frequently demonstrated focal positive staining, independently of tumor stain.

VEGF

The near universal presence of serum within the blood vessel lumens and in the interstitial space at area of broken tissues served as strong internal positive control. For the same reason only areas of intact tumor cells were scored. In the tumor, 54/90 (60%) of cases showed cytoplasmic staining for VEGF. Overall, the percentage of positive cells in tumor ranged from 0 to 100% (median, 5%; mean, 23%; Figure 5.1c). In the normal epithelium, 50/66 (76%) of cases showed cytoplasmic staining of VEGF. Of special note, in the respiratory epithelium it was the upper ciliated cells that showed positive cytoplasmic stain. In contrast, the oral squamous type epithelium was less often stained and it was the basal cells showed positive cytoplasmic stain. In general, the staining intensity of the tumor was weaker than or equal to that in the corresponding normal epithelium.

Co-expression of hypoxia markers

As serial flanking sections from each tumor were studied for all four markers, we had the opportunity to observe if there was any pattern of co-expression among the markers. A frequent observation was that if the same tumor was stained positive for HIF-1α, it was also positive for CA IX and VEGF as well, though at the microscopic level the positively stained cells of each marker usually did not overlap. This is well illustrated in the photomicrographs in Figure 5.2a to 5.2c, which demonstrated the expression of the three markers respectively in the same flanking tumor section. Indeed, by Spearman's rank sum test, tumor HIF-1α expression correlated significantly with that of CA IX expression (correlation coefficient = 0.28; $p = 0.008$) and also with VEGF expression (correlation coefficient = 0.31; $p = 0.003$), though the correlation coefficients were small. However, tumor CA IX expression did not

correlate with VEGF expression (correlation coefficient = -0.014; p = 0.899; Table 5.4).

Expression in tumor and normal epithelium

There was a significant correlation between HIF-1α expression in tumor and in the corresponding normal epithelium in the same section of the tumor (correlation coefficient = 0.40; p = 0.0023). A strong correlation between VEGF expression in tumor and in the corresponding normal epithelium was also evident (correlation coefficient = 0.45; p = 0.0003). On the other hand, no significant correlation between CA IX expression in tumor and in the corresponding normal epithelium was found (correlation coefficient = 0.09; p = 0.49).

Clinical correlation and survival analysis

For clinical correlation and survival analysis, a cut off expression level of 5% was used throughout for HIF-1α, CA IX and VEGF. Tumor with less than 5% positive cells for the marker was defined as low expression. Tumor with 5% or more positive cells was defined as high expression. This 5% level was chosen based on both the median score and a practical consideration so that borderline staining would be regarded as low expression. For HIF-2α, because the tumor cells only showed infrequent staining, we used the score of positively stained macrophages in tumor or stroma for analysis (negative = 0; positive = +/-, +, ++, +++).

No significant association was observed for the expression of HIF-1α, HIF-2α, CA IX or VEGF with any of the following clinicopathological parameters: gender, histology type, Ho's T stages, Ho's N stages, Ho's overall stages, lymph node size, treatment

arm, local recurrences and distant metastases ($p > 0.05$ by Chi-squared test, data not shown).

On univariate analysis, high tumor HIF-1α expression was associated with poor overall survival (OS) but this only reached borderline significance (Log rank test, $p = 0.06$; Figure 5.3a), and a non-significant trend of poor progression free survival (PFS) (Log rank test, $p = 0.11$). On the other hand, no significant association between HIF-2α, CA IX or VEGF expression with respect to OS or PFS was found (Table 5.5a). None of the other parameters, including gender, age, histology type, Ho's T stages, Ho's N stages, and lymph node size, reached statistical significance by univariate analysis for OS or PFS (data not shown).

Overall effect of tumor hypoxic and angiogenic profile on survival

Since hypoxia induces the expression of HIF-1α, which then up-regulates the expression of downstream genes CA IX and VEGF (Wykoff et al. 2000; Beasley et al. 2001; Jones et al. 2001), HIF-1α and CA IX has been suggested to be endogenous markers of tumor hypoxia (Loncaster et al. 2001; Vukovic et al. 2001). We therefore proposed to define a model of tumor hypoxic and angiogenic profile based on the co-expression of HIF-1α, CA IX and VEGF. We defined tumors with a high expression of both HIF-1α and CA IX as having a hypoxic profile, and those with high VEGF expression as possessing an angiogenic profile. By the above definition, 20 of the 90 patients had a hypoxic tumor profile. This group was found to have a significantly worse PFS (Log rank test, $p = 0.04$; Figure 5.3b) and a marginally significant worse OS ($p = 0.06$). 10 of the 90 patients had both a hypoxic and angiogenic tumor profile by the above definition. This group was found to have a significantly worse PFS (Log

rank test, p = 0.0095; Figure 5.3c) but not a worse OS (p = 0.1; summarized in Table 5.5a).

Multivariate analysis

The analysis of PFS in the original phase III randomized trial of concurrent chemo-radiation versus radiotherapy alone has been reported (Chan, Teo et al. 2002). The current analysis on hypoxia markers was based on the same survival data from the clinical trial. Although the PFS was not significantly different between the two treatment arms in the overall comparison, it was significantly prolonged in the subgroup of patients with advanced tumor and node stages (Chan, Teo et al. 2002). Therefore we have incorporated treatment arm as a potential prognostic and/or confounding factor in the multivariate analysis. In Cox's proportional hazard model, we only entered parameters that with $p<0.1$ in univariate analysis (i.e. HIF-1α, tumor hypoxic profile, tumor hypoxic and angiogenic profile) and treatment arm as covariates. HIF-1α or tumor hypoxic profile was not significant independently of treatment arm. Only the hypoxic and angiogenic profile retained its significance independently of treatment arm on PFS (p = 0.022 for hypoxic and angiogenic profile, p = 0.027 for treatment arm, Table 5.5b).

Table 5.1

Clinical characteristics of NPC patients in the study cohort.

Charateristics		No. of patients (N=90)
Age (Years)		
Median	45	
Range	21-67	
< 40		25
≥ 40		65
Sex		
Male		73
Female		17
Histology		
Poorly differentiated squamous carcinoma		3
(WHO II)		87
Undifferentiated carcinoma (WHO III)		
Ho's T stage		
1		20
2		48
3		22
Ho's N stage		
1		7
2		51
3		32
LN size		
>3 cm		29
<= 3 cm		61
Ho's overall staging		
II		7
III		51
IV		32
Treatment arm		
Chemoradiotherapy		48
Radiotherapy alone		42
Duration of follow-up (Years)		
Median	4.13	
Range	0.52 - 6.21	
Failure pattern		
Local recurrence	4	
Distant metastases	30	
Death	26	

Table 5.2

Expression pattern of HIF-1α, HIF-2α, CA IX and VEGF in NPC biopsies. The number and percentages of positive staining over total number of evaluable cases was shown. Positive staining pattern was further classified into membranous, nuclear or cytoplasmic.

	Tumor		Stroma		Normal epithelium	
HIF-1α	Nuclear	52 / 90 (58%)	Nuclear	12 / 90 (13%)	Nuclear Cytoplasmic Nuclear & cytoplasmic All = 16 / 60 (27%)	7 4 5
HIF-2α	Nuclear Cytoplasmic	6 / 89 (7%) 6 / 89 (7%)	Cytoplasmic	12 / 89 (13%)	Nuclear Cytoplasmic Nuclear & cytoplasmic All = 9 / 57 (16%)	2 6 1
CA IX	Membranous Nuclear	51 / 90 (57%) 4 / 90 (4%)	Membranous Nuclear	1 / 90 (1%) 2 / 90 (2%)	Membranous Cytoplasmic All = 32 / 57 (56%)	30 2
VEGF	Cytoplasmic	54 / 90 (60%)	negative		Cytoplasmic	50 / 66 (76%)

Table 5.3

Expression pattern of HIF-2α in tissue infiltrating macrophages.

(The number of cases in each grade was shown)

Grading*	negative	+/-	+	++	+++	Total (N)
Macrophage in tumor	65	14	9	0	1	89
Macrophage in stroma	31	26	20	9	3	89

* Grading: +/-, very occasional single cell positive: +, few positive cells either in foci or scattered; ++, moderate numbers either in foci or scattered; +++, large numbers of positive cells.

Table 5.4

Correlations between HIF-1α, CA IX and VEGF expression in NPC.

Spearman's rho Correlation coefficient Significance (p)	**HIF-1α**	**CA IX**	**VEGF**
HIF-1α	-	0.280 (0.008 **)	0.313 (0.003 **)
CA IX	-	-	-0.014 (0.899)
VEGF	-	-	-

** Correlation is significant at the 0.01 level (2-tailed).

Table 5.5

(a) Univariate and (b) multivariate analysis of overall and progression free survival for hypoxia markers.

	Overall survival			Progression free survival		
	Risk Ratio	**95% C.I.**	**p value**	**Risk Ratio**	**95% C.I.**	**p value**
(a) Univariate analysis						
HIF-1α	2.12	0.96 – 4.70	0.06	1.72	0.87 – 3.39	0.12
CA IX	1.39	0.64 – 3.01	0.40	1.28	0.65 – 2.52	0.48
VEGF	1.12	0.52 – 2.41	0.78	1.52	0.76 – 3.04	0.24
HIF-1α + CA IX (Hypoxic profile)	2.13	0.95 – 4.80	0.06	2.06	1.00 – 4.23	0.04 *
HIF-1α + CA IX + VEGF (hypoxic and angiogenic profile)	2.22	0.84 – 5.88	0.10	2.87	1.25 – 6.59	0.01 *
(b) Multivariate analysis						
Treatment arm (RT versus chemo-RT)	4.08	1.70 – 9.79	0.002*	2.19	1.09 – 4.39	0.027*
HIF-1α + CA IX + VEGF (hypoxic and angiogenic profile)	2.32	0.87 – 6.18	0.09	2.66	1.15 – 6.14	0.022*

C.I.: confidence interval
*: $p < 0.05$

Table 5.6a
Clinical correlation of immunohistochemical detection of HIF-1α or HIF-2α in selected tumor types and patient outcome

Authors (Reference)	Tumor type (stage)	Treatment(s)	No. of patients	Hypoxia marker	Prognostic significance of hypoxia marker expression [a]	
					Univariate analysis	Multivariate analysis
(Birner et al. 2000)	Cervix cancer (stage pT1b)	Surgery +/- adjuvant RT	91	HIF-1α	OS, DFS	OS, DFS
(Haugland et al. 2002)	Cervix cancer (stages IB-III)	Radical RT	41	HIF-1α	Correlate with tumor oxygenation (by Eppendorf pO2 histograph) DFS: n.s.	n/a.
(Bachtiary et al. 2003)	Cervix cancer (stages IB-IIIB)	Radical RT	67	HIF-1α	Response to RT, PFS, CSS	PFS, CSS
(Burri et al. 2003)	Cervix cancer (stages IB-IIIB)	Radical RT	78	HIF-1α	LPFS, OS	OS
(Hutchison et al. 2004)	Cervix cancer (stages IB-IVA)	Radical RT	99	HIF-1α	n.s.	n/a
(Ishikawa et al. 2004)	Cervix cancer (stages IIIB)	Radical RT	38	HIF-1α	RFS, MFS	n/a
(Mayer et al. 2004)	Cervix cancer (stages IB-IVB)	heterogeneous	38 (34 for survival analysis)	HIF-1α	No correlation with pO2 n.s.	n/a

[a] Higher marker expression is correlated with poorer outcome, except otherwise specified

Abbreviations: PDT: photodynamic therapy; RT: radiotherapy; Chemo: chemotherapy; CRT: chemoradiation; OS: overall survival; CSS: cancer specific survival; DFS: disease-free survival; DSS: disease-specific survival; RFS: relapse-free survival; LPFS: local progression free survival; LRFS: local relapse-free survival; LFFS: local failure free survival; MFS: metastases-free survival; CR: complete response; LC: local control; n/a: not available; n.s.: not significant.

Table 5.6b (cont'd)
Clinical correlation of immunohistochemical detection of HIF-1α or HIF-2α in selected tumor types and patient outcome

Authors (Reference)	Tumor type (stage)	Treatment(s)	No. of patient	Hypoxia marker	Prognostic significance of hypoxia marker expression	
					Univariate analysis	Multivariate analysis
(Sivridis et al. 2002)	Endometrial cancer (stage I)	Surgery +/- adjuvant RT	81	HIF-1α HIF-2α	OS n.s.	OS n/a
(Birner, Schindl et al. 2001)	Ovarian cancer (Stage I-IV)	Surgery +/- adjuvant chemo	102	HIF-1α HIF-1α + P53	n.s. OS	n.s. OS
(Schindl et al. 2002)	Breast cancer (LN+)	Surgery +/- adjuvant therapy	206	HIF-1α	DFS, OS	DFS, OS
(Bos et al. 2003)	Breast cancer (stage I-II)	Surgery +/- adjuvant therapy	150 (81 LN-)	HIF-1α	LN- only: DFS, OS	LN- only: DFS, OS
(Gruber et al. 2004)	Breast cancer (LN+)	Surgery +/- adjuvant therapy	77	HIF-1α	MFS, DFS OS: n.s.	T1/2 tumors only: MFS, DFS.
(Dales et al. 2005)	Breast cancer	Surgery	745	HIF-1α	MFS, OS	MFS, OS
(Vleugel et al. 2005)	Breast cancer	Surgery +/- adjuvant therapy	166	HIF-1α	DFS	n/a
(Schoppmann et al. 2006)	Breast cancer (stage I-IV)	Surgery +/- adjuvant therapy	119	HIF-1α	DFS, OS	DFS, OS
(Generali, Berruti et al. 2006)	Breast cancer (T2-4N0-1)	Neoadjuvant chemo + Surgery + adjuvant therapy	187	HIF-1α	Response to chemo, DFS	Response to chemo
(Trastour et al. 2007)	Breast cancer	Surgery +/- adjuvant therapy	132	HIF-1α	DFS, DMFS, OS	DFS, DMFS

Table 5.6c (cont'd)
Clinical correlation of immunohistochemical detection of HIF-1α or HIF-2α in selected tumor types and patient outcome

Authors (Reference)	Tumor type (stage)	Treatment(s)	No. of patients	Hypoxia marker	Prognostic significance of hypoxia marker expression[a]	
					Univariate analysis	Multivariate analysis
(Aebersold et al. 2001)	Oropharyngeal cancer	Radical RT +/- Chemo	98	HIF-1α	LFRS, DFS, OS	LFFS, DFS, OS
(Beasley et al. 2002)	Head and neck cancer	Surgery +/- adjuvant RT (35%)	79	HIF-1α	[b] Improved DFS and OS ([b]HIF-1α expression associated with better outcome)	[b] Improved DFS and OS
				HIF-2α	n.s.	n/a
(Koukourakis et al. 2002)	Head and neck cancer (locally advanced)	Chemo-RT	75	HIF-1α	Response to Chemo-RT, LRFS, OS	n.s
				HIF-2α	Response to Chemo-RT, LRFS, OS	LRFS, OS
(Kyzas et al. 2005)	Head and neck cancer	Surgery	81	HIF-1α	n.s.	n/a
(Winter et al. 2006)	Head and neck cancer	Surgery +/- adjuvant RT (85%)	140	HIF-1α	DFS, DSS	DFS, DSS
				HIF-2α	n.s.	n/a
(Koukourakis et al. 2006)	Head and neck cancer	RT (CHART 59%, conventional 41%)	198	HIF-2α	LC, OS	LC, OS
(Birner, Gatterbauer et al. 2001)	Oligodendrogliomas (supratentorial)	Surgery +/- RT / Chemo	51	HIF-1α	OS	OS

Table 5.6d (cont'd)
Clinical correlation of immunohistochemical detection of HIF-1α or HIF-2α in selected tumor types and patient outcome

Authors (Reference)	Tumor type (stage)	Treatment(s)	No. of patient	Hypoxia marker	Prognostic significance of hypoxia marker expression[a]	
					Univariate analysis	Multivariate analysis
(Koukourakis, Giatromanolaki, Skarlatos et al. 2001)	Esophageal cancer (early stage but inoperable)	PDT +/- RT	37	HIF-1α	Response to PDT LRFS, OS: n.s.	n/a
				HIF-2α	n.s.	
(Sohda et al. 2004)	Esophageal cancer (stage I-IV)	Chemo-RT	65	HIF-1α	Response to Chemo-RT	n/a
(Matsuyama et al. 2005)	Esophageal cancer	Surgery	215	HIF-1α	DFS OS: n.s.	n.s.
(Griffiths et al. 2007)	Gastric and gastroesophageal junction cancer (stage 0-IV)	Surgery	177	HIF-1α	n.s.	n.s.
(Volm and Koomagi 2000)	Non-small cell lung cancer (stage I-IIIA)	Surgery	96	HIF-1α	Improved OS	Improved OS
(Giatromanolaki, Koukourakis, Sivridis, Turley et al. 2001)	Non-small cell lung cancer (operable)	Surgery	108	HIF-1α HIF-2α	n.s. OS	n.s. OS
(Swinson et al. 2004)	Non-small cell lung cancer (stage I-IIIA)	Surgery	172	HIF-1α	OS	OS

Table 5.7a
Clinical correlation of immunohistochemical detection of CA IX in selected tumor types and patient outcome

Authors (Reference)	Tumor type (stage)	Treatment(s)	No. of patient	Hypoxia marker	Prognostic significance of hypoxia marker expression[a]	
					Univariate analysis	Multivariate analysis
(Chia et al. 2001)	Breast cancer	Surgery + adjuvant therapy	103	CA IX	RFS, OS	OS
(Brennan et al. 2006)	Breast cancer (stage II)	Surgery + adjuvant therapy	400	CA IX	RFS, DSS, OS	DSS
(Generali, Fox et al. 2006)	Breast cancer (T2-4N0-1)	Neoadjuvant chemo + Surgery + adjuvant therapy	183	CA IX	DFS, OS	n.s.
(Hussain et al. 2007)	Breast cancer	Surgery	144	CA IX	OS	OS
(Trastour et al. 2007)	Breast cancer	Surgery +/- adjuvant therapy	132	CA IX	DFS	DFS, MFS
(Giatromanolaki, Koukourakis, Sivridis, Pastorek et al. 2001)	Non-small cell lung cancer	Surgery	107	CA IX	OS	OS
(Swinson et al. 2003)	Non-small cell lung cancer (stage I-III)	Surgery	175	CA IX	OS	OS.
(Kim et al. 2004)	Non-small cell lung cancer (stage I-II)	Surgery	75	CA IX	DFS, OS	DFS, OS

[a] Higher marker expression is correlated with poorer outcome

Abbreviations: RT: radiotherapy; Chemo: chemotherapy; CHART: Continous Hyperfractionated Accelerated Radiotherapy; ARCON: accelerated radiotherapy with carbogen and nicotinamide. FDM: freedom of distant metastases; OS: overall survival; DFS: disease-free survival; DSS: disease-specific survival; RFS: relapse-free survival; MFS: metastases-free survival; LC: local control; n/a: not available; n.s.: not significant.

Table 5.7b(cont'd)
Clinical correlation of immunohistochemical detection of CA IX in selected tumor types and patient outcome

Authors (Reference)	Tumor type (stage)	Treatment(s)	No. of patient	Hypoxia marker	Prognostic significance of hypoxia marker expression[a]	
					Univariate analysis	Multivariate analysis
(Loncaster et al. 2001)	Cervix cancer (stage I-IV)	RT	130	CA IX	DSS, MFS	DSS, MFS
(Hedley et al. 2003)	Cervix cancer (stage Ib-IV)	RT +/- chemo	102	CA IX	n.s.	n.s.
(Koukourakis, Giatromanolaki, Sivridis et al. 2001)	Head and neck cancer	RT + chemo	75	CA IX	Response to chemo-RT, LRFS, OS	n/a
(De Schutter et al. 2005)	Head and neck cancer	RT +/- chemo (5%)	67	CA IX	n.s.	n.s.
(Jonathan et al. 2006)	Head and neck cancer	ARCON	58	CA IX	LC, FDM	n.s.
(Winter et al. 2006)	Head and neck cancer	Surgery +/- adjuvant RT (85%)	149	CA IX	n.s.	n/a
(Koukourakis et al. 2006)	Head and neck cancer	RT (CHART 59%, conventional 41%)	198	CA IX	LC, OS	LC, OS

Figure 5.1 (a, b, c)

Distribution for tumor expression scores of (a) HIF-1α, (b) CA IX, and (c) VEGF in NPC.

Figure 5.1 (a)

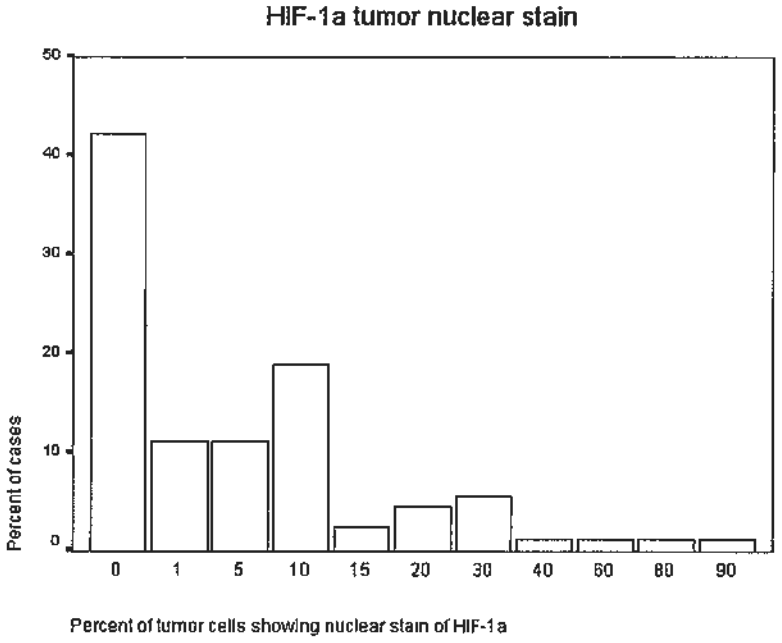

Figure 5.1 (b)

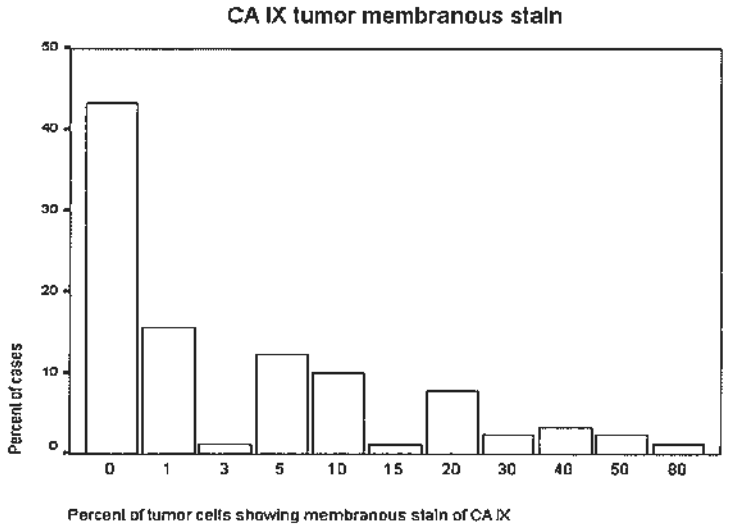

Figure 5.1 (c)

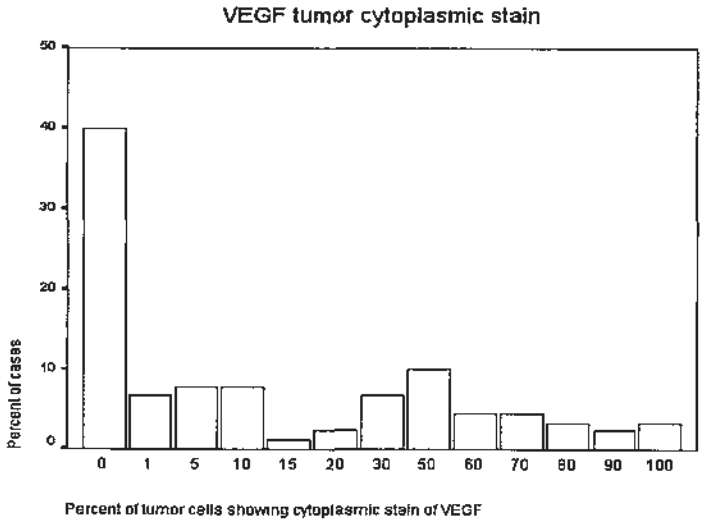
VEGF tumor cytoplasmic stain
Percent of cases
50
40
30
20
10
0
0
1
5
10
15
20
30
50
60
70
80
90
100
Percent of tumor cells showing cytoplasmic stain of VEGF

Figure 5.2 (a to f)

Expression of (a) CA IX (b) HIF-1α (c) VEGF in tumor cells in the same flanking tissue sections. Note the perinecrotic distribution of positive stained tumor cells (N = necrosis); x250. (d) Expression of HIF-1α in tumor cells showing nuclear staining pattern; x200. (e) Expression of HIF-2α in tissue infiltrating macrophages; x400. (f) Expression of CA IX in the basal cells of normal epithelium in NPC biopsy tissue; x200. (All immunoperoxidase with diaminobenzidine, Haematoxyline counter stain).

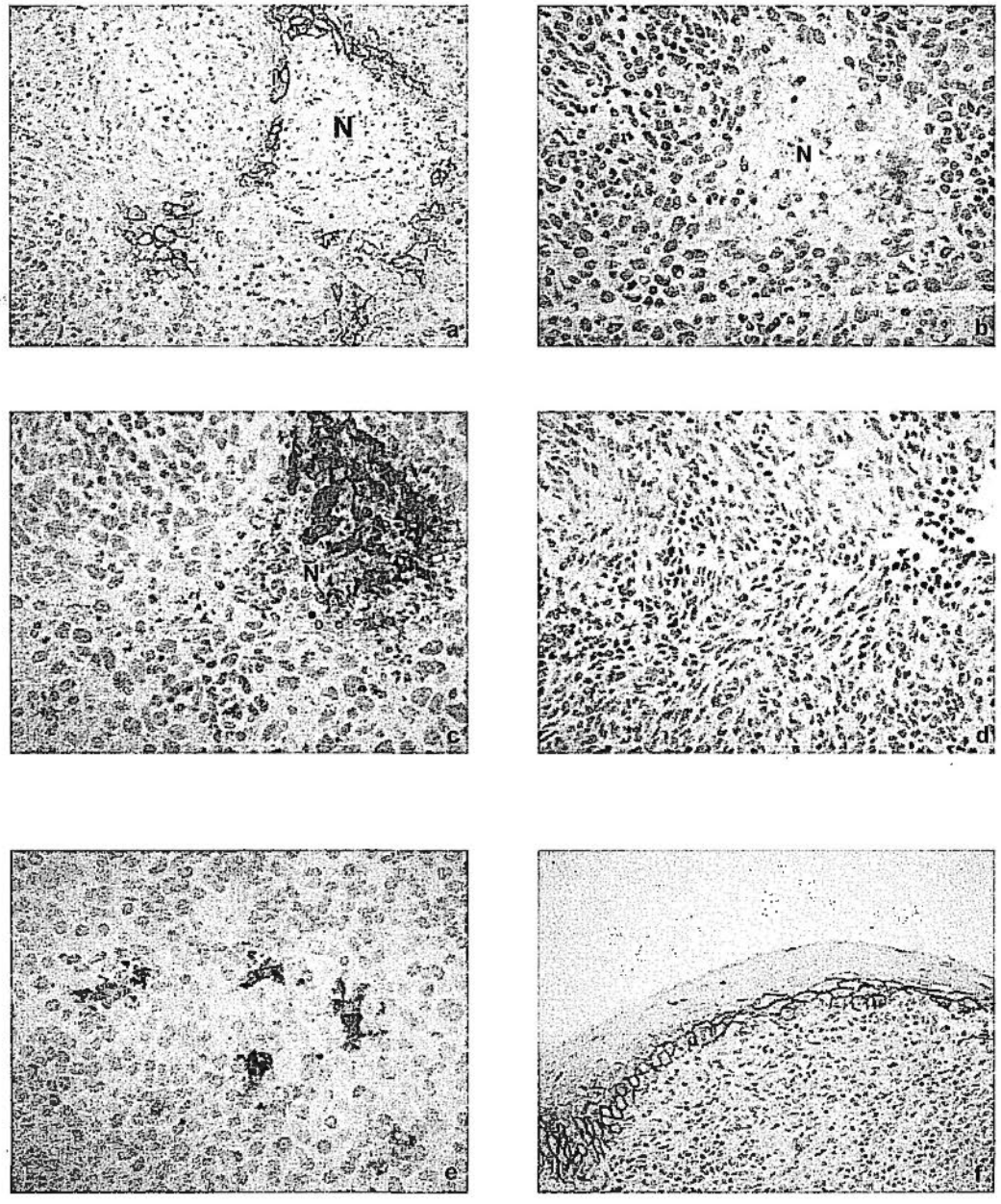

Figure 5.3 (a, b, c)

Survival curves for (a) OS stratified by tumor HIF-1α expression. (b) PFS stratified by tumor hypoxic profile. (c) PFS stratified by tumor hypoxic and angiogenic profile.

Figure 5.3 (a)

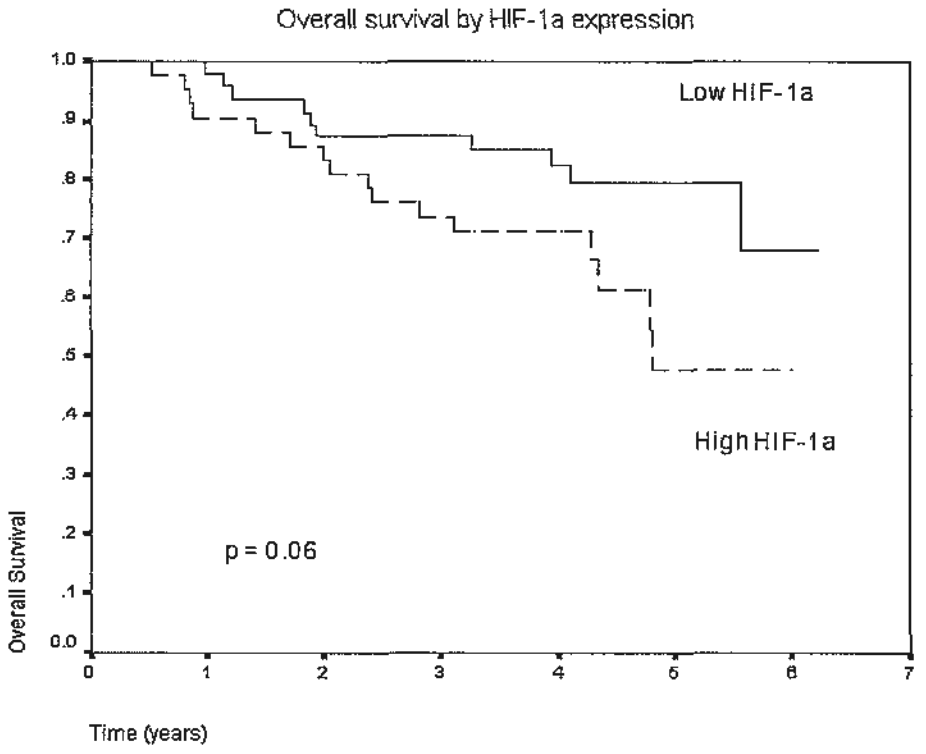

Figure 5.3 (b)

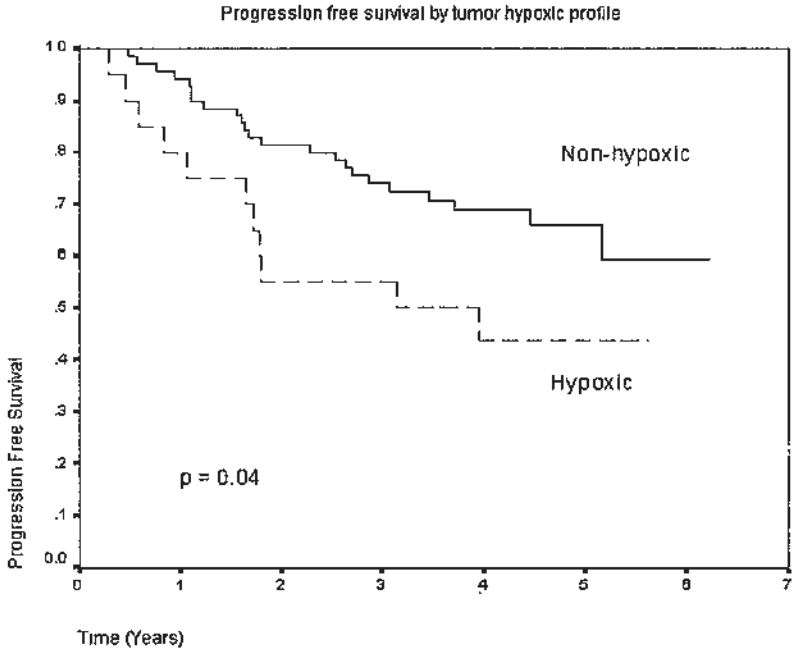

Figure 5.3 (c)

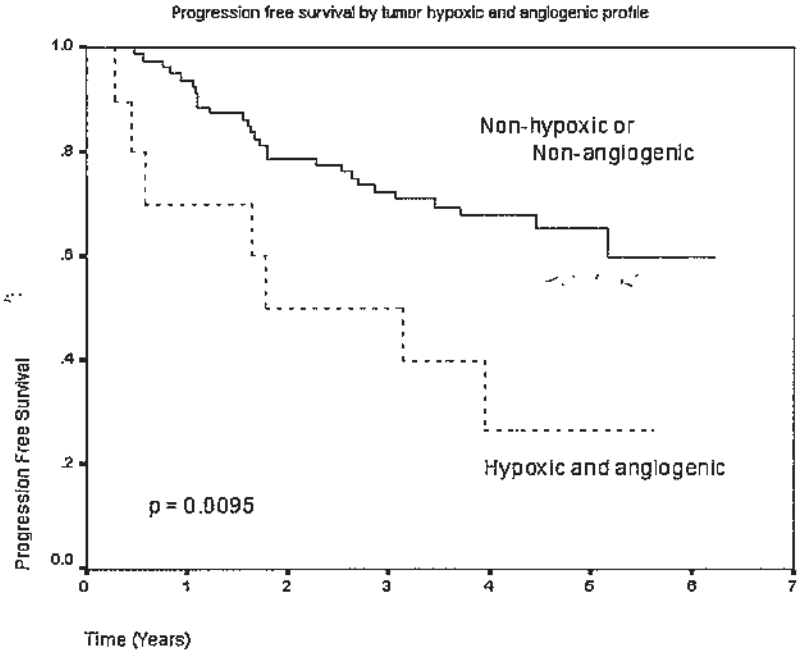

DISCUSSION

To our knowledge, this is the first study to determine the expression pattern of the hypoxia markers HIF-1α, HIF-2α and CA IX in NPC. It is also the first attempt to study the co-expression of all three hypoxia markers HIF-1α, HIF-2α and CA IX together with the angiogenesis marker VEGF simultaneously in the same tissue sample from a cohort of NPC patients with long-term follow-up and survival data.

In our study cohort, we observed that HIF-1α was expressed in 58%, HIF-2α in 7%, CA IX in 57% and VEGF in 60% of tumors from NPC biopsy specimens. Our observations are similar to the findings by other investigators in other human tumors (Zhong et al. 1999; Talks et al. 2000; Ivanov et al. 2001). Taken together these results suggest that over-expression of the hypoxia markers HIF-1α, HIF-2α, CA IX and the angiogenic factor VEGF are general phenomena in human malignancy. Furthermore, we have found that tumor expression of HIF-1α correlates significantly with that of CA IX and with VEGF. This co-expression of HIF-1α with CA IX, and of HIF-1α with VEGF in clinical tumor is in concordance with previously described *in-vitro* findings in cell lines. The *in-vitro* hypoxia experiments have already shown that both CA IX and VEGF are downstream genes of HIF-1α and that their protein levels are up-regulated by HIF-1α under conditions of hypoxia (Wykoff et al. 2000; Jones et al. 2001).

On the other hand, we found that tumor CA IX expression did not correlate with VEGF expression. The reason may be that VEGF and CA IX transcripts have a short half-life after reperfusion and since VEGF protein is secreted and has a rapid clearance, VEGF will be subjected to rapid change with changes in intermittent oxygenation. In contrast CA IX protein has a half-life of over 24 hours (Turner et al. 2002) so would reflect an integration of hypoxia over longer periods of time. Both are regulated by HIF but may reflect different time courses of events.

Another interesting finding was that HIF-1α was expressed in 27%, HIF-2α in 16%, CA IX in 56% and VEGF in 76% of the (morphologically) normal epithelium present in the same section of the tumor. Moreover, the expression of HIF-1α and VEGF in tumor correlates significantly with its expression in the corresponding normal epithelium. It was often observed that the positively stained normal epithelium was close or adjacent to the underlying tumor. It should be pointed out that the morphologically normal epithelium adjacent to tumor was probably not equivalent to their counterpart in a healthy person without NPC. We have not studied, and it would be interesting to know, the expression pattern of these markers in the normal nasopharyngeal epithelium of a healthy individual. Previous studies on the

expression of HIF-1α and HIF-2α in normal human tissue and cancer demonstrated that these markers were mostly negative in the normal tissues but were over-expressed in most human tumors (Zhong et al. 1999; Talks et al. 2000). The expression of CA IX in normal adult tissues was shown to be restricted to certain highly specialized cells e.g. bile duct and gastric mucosa (Ivanov et al. 2001). Our observations suggest that the normal epithelium near the tumor probably share the same micro-environmental hypoxia so that they over-express the same marker. The growth of tumor may have created local circulatory shunts, and/or caused increased O_2 consumption diverting oxygen away from normal tissues.

We observed a striking pattern of HIF-2α expression in tissue infiltrating macrophages within both tumor and stroma of NPC. Talks et al have previously described similar observation in other tumor types (Talks et al. 2000). Morphological identification of these cells as macrophages was confirmed by CD68 co-expression. It is well known that NPC is characterized by harboring Epstein-Barr virus genes in the tumor cells and an intense infiltration of leukocytes in the stroma. These infiltrating cells are mainly composed of T lymphocytes and macrophages. The mechanism and role of this intense lymphoid infiltrates in NPC has been extensively studied (Tang et al. 2001). A strong association of macrophages infiltration with angiogenesis and

prognosis in invasive breast cancer has been reported (Leek et al. 1996). Leek et al also described the relation of HIF-2α expression in tissue infiltrating macrophages to tumor angiogenesis and the oxidative thymidine phosphorylase pathway in human breast cancer (Leek et al. 2002). Our observation provides further support to the recognized contribution to tumor angiogenesis coming from tumor associated stromal microenvironment.

A significant association between tumor necrosis and CA IX expression was previously observed by other investigators (Wykoff et al. 2001; Beasley et al. 2001; Chia et al. 2001). We did observe that CA IX expression followed a peri-necrotic pattern of distribution. However, necrosis was an infrequent finding in our biopsy specimens, probably reflecting the fact that the endoscopists often avoid taking biopsy from the necrotic area of a tumor.

There have been other studies on the expression of HIF-1α, HIF-2α and CA IX in a number of common human cancers. HIF-1α and HIF-2α were found to be over-expressed in most human cancers and their metastases (Zhong et al. 1999; Talks et al. 2000). HIF-1α over-expression was shown to be a marker of unfavorable prognosis in early stage cervical cancer (Birner et al. 2000). HIF-1α expression was

shown to predict resistance to photodynamic therapy in esophageal cancer (Koukourakis, Giatromanolaki, Skarlatos et al. 2001), and was also found to be a novel predictive and prognostic parameter in oropharyngeal cancer treated by radiotherapy (Aebersold et al. 2001). In ovarian cancer, the over-expression of HIF-1α in combination with P53 indicated a dismal prognosis (Birner, Schindl et al. 2001). Over-expression of HIF-1α indicated a shorter overall survival in oligodendrogliomas (Birner, Gatterbauer et al. 2001). In non-small cell lung cancer, HIF-2α expression was shown to be independent prognosticator of poor outcome (Giatromanolaki, Koukourakis, Sivridis, Turley et al. 2001). However, another study in non-small cell lung cancer found that HIF-1 positive tumors had significantly longer median survival (Volm and Koomagi 2000).

CA IX over-expression has also been shown in a number of common human tumors (Ivanov et al. 2001). In breast cancer, CA IX expression was associated with a worse relapse free survival and overall survival (Chia et al. 2001). In cervical cancer, CA IX expression was shown to correlate with tumor hypoxia as measured by direct needle electrode, supporting its role as an intrinsic marker of tumor hypoxia, and was associated with poor prognosis (Loncaster et al. 2001). In non-small cell lung cancer, CA IX expression was shown to be a significantly poor prognosticator independent of

angiogenesis (Giatromanolaki, Koukourakis, Sivridis, Pastorek et al. 2001). CA IX was also shown to relate to poor vascularization and resistance of squamous cell head and neck cancer to chemoradiotherapy (Koukourakis, Giatromanolaki, Sivridis et al. 2001).

After the publication of our study results in 2002, the prognostic impact of HIF-1α, HIF-2α and CA IX expression by IHC has been the subjects of numerous studies in various tumor types. Table 5.6 and 5.7 summarized the findings from other studies on the prognostic impact of HIF-1α, HIF-2α and CA IX in selected tumor types. In general, higher expression of hypoxia markers were correlated with poor clinical outcome and survival, with few exceptions. For a review, see (Maynard and Ohh 2007; Vaupel and Mayer 2007; Semenza 2010; Griffiths et al. 2005)

Interestingly, in the first study from the Oxford group (Beasley et al. 2002), overexpression of HIF-1α was found to be associated with an improved disease free survival (DFS) and overall survival (OS) in 79 surgically treated head and neck cancer patients. In a subsequent expanded study of 140 patients reported by the same group, which also included 73 of the 79 patients from the first study, HIF-1α was however associated with a worse DFS and disease specific survival (DSS)(Winter et al. 2006).

The contradictory findings between the two studies may be explained in part by differences in study design, technical differences in assay, larger patient numbers and longer follow up. The group finally concluded that overexpression of HIF-1α should be considered to be associated with decreased survival in patients of head and neck cancer (Winter et al. 2006).

In head and neck cancer, VEGF over-expression was shown to be associated with poor disease free and overall survival (Smith et al. 2000), a marker of tumor invasion and metastases (Sauter et al. 1999). In NPC, expression of VEGF was found to have significant association with angiogenesis and lymph node metastases (Wakisaka et al. 1999), as well as distant metastases (Guang-Wu et al. 2000).

NPC is distinct from other head and neck cancer in that it is highly sensitive to radiation and chemotherapy. In our study cohort of locally advanced non-metastatic NPC, HIF-1α expression was only associated with a borderline significant trend of poor overall survival, while no significant association with survival outcome was found for HIF-2α, CA IX or VEGF. The overall treatment result in this cohort was excellent in that all patients achieved complete remission after their primary treatment, despite their initial locally advanced stage. After a median follow up of 4.13 years, the median

survival was still not reached yet. Because of the relatively small numbers of clinical events occurred at the time of this analysis, we cannot exclude the potential prognostic significance of HIF-2α, CA IX, and VEGF in NPC, which have been reported by other authors in other tumor types. Another limitation of our study is that we used small biopsy tissue to determine the expression of the hypoxia markers, hoping it would reflect the hypoxia status of the whole tumor. Although this may be far from satisfactory, in NPC this is usually the only pathological material available to the clinician to base their treatment decision on.

Hypoxia is known to induce HIF-1α expression, which then up-regulates downstream genes CA IX and VEGF (Wykoff et al. 2000; Beasley et al. 2001; Jones et al. 2001). HIF-1α and CA IX has been suggested to be endogenous markers of tumor hypoxia (Loncaster et al. 2001; Vukovic et al. 2001; Olive et al. 2001). We therefore proposed to define a model of tumor hypoxia and angiogenic profile based on the co-expression of HIF-1α, CA IX and VEGF. In fact our model predicted that tumors with a hypoxic profile (high expression of both HIF-1α and CA IX) were associated with a significantly worse PFS. Tumors with both hypoxic and angiogenic profile (high HIF-1α, CA IX and VEGF expression) were associated with a significantly worse PFS, and this remained significant in multivariate analysis.

CONCLUSION

Hypoxia is increasingly being recognized as an important therapeutic target in cancer (Brown 2001; Hoogsteen, Marres, van der Kogel et al. 2007). In head and neck cancer, several researchers have recently proposed HIF 1α as one of the most promising biomarker that helps to guide the choice and intensity of treatment (individualized therapy) (Hoogsteen, Marres, Bussink et al. 2007; Eckert, Schubert, and Taubert 2010; Prestwich, Dyker, and Sen 2010). A whole panel of bioreductive drugs targeting at tumor hypoxia have been developed and some have entered into clinical trials with promising preliminary results (Stratford and Workman 1998). As we have established that HIF-1α, CA IX and VEGF are expressed in the majority of NPC, this represents a potential new therapeutic target for further studies.

The result of this translational study has confirmed the clinical importance of hypoxia and angiogenesis in NPC and also supported these as potential therapeutic targets in NPC. As a follow up, we have investigated the hypoxia targeting agent tirapazamine (Hong et al. 2009) and the HIF-1 inhibitor YC-1 (Hong et al. 2010) in NPC. In chapter 6, we will further study the relationship of osteopontin, hypoxia and response to radiotherapy in NPC (study 4). In chapter 8 and 9, we will explore the targeting of VEGF and angiogenesis in a preclinical (study 6) and clinical study (study 7) in NPC.

Chapter 6

Study 4: Plasma Osteopontin, Hypoxia and Response to Radiotherapy

BACKGROUND

As introduced in chapter 1 and discussed in previous two chapters, tumor hypoxia has long been recognized as an important determinant of clinical outcome in radiotherapy (Gray et al. 1953). Eppendorf electrode measurements of tumor oxygenation have defined an adverse effect of tumor hypoxia on prognosis after radiotherapy in head and neck cancer (Nordsmark, Overgaard, and Overgaard 1996; Nordsmark et al. 2005). A recent study of ^{18}F-MISO PET scan to assess tumor hypoxia has suggested the potential utility of this investigation to predict clinical benefit in patients undergoing hypoxia-targeting therapy (Rischin et al. 2006). However, the limited availability and technical complexities of these methods of hypoxia determination would likely preclude a wider clinical application. Hence the availability of a simple, widely usable, and robust method of assessing tumor oxygenation that will correlate with clinical outcome is urgently needed.

The immunohistochemical detection of proteins involved in the hypoxic response of

tumor cells has been studied as a method to estimate hypoxia in clinical tumor specimens. In particular, the transcription factor, hypoxia inducible factor 1-alpha (HIF-1a), and the genes up regulated by HIF-1 such as carbonic anhydrase 9 (CA9), have been studied as endogenous markers of tumor hypoxia in head and neck cancer (Aebersold et al. 2001; Koukourakis et al. 2006) and by our group in NPC (refer to chapter 4 and 5). The level of both proteins is increased under hypoxia conditions, and both can be detected in routine paraffin sections by immunohistochemistry. These retrospective clinical studies have consistently demonstrated that high tumor expression of one of these hypoxia markers were associated with a poorer outcome after radiotherapy. For a complete review, see (Vordermark and Brown 2003; Vaupel and Mayer 2007; Semenza 2010). Recent reviews of the available clinical and experimental data regarding the prognostic impact and comparability with other methods of hypoxia detection have pointed out that these endogenous markers have the potential to indicate therapeutically relevant levels of hypoxia within tumors (Brown and Le 2002; Vordermark and Brown 2003; Hoogsteen, Marres, Bussink et al. 2007).

The search for circulating hypoxia markers has always been of clinical interest. Recently, Le et al have shown that hypoxia exposure stimulated osteopontin (OPN)

secretion in head and neck cancer cell line. Furthermore, they were able to demonstrate that high level of plasma OPN correlated with tumor hypoxia (pO2 as measured by Eppendorf electrode) and was associated with poor clinical outcome in head and neck cancer patients (Le et al. 2003). An expanded follow up study has further confirmed high plasma OPN as an independent predictor for tumor control and overall survival (Petrik et al. 2006).

In head and neck squamous cell carcinoma (HNSCC), two studies from the DAHANCA group have provided further evidence on the role of osteopontin as a potential hypoxia biomarker. In the study by Nordsmark et al, 67 patients with advanced HNSCC were studied for pre-treatment plasma osteopontin measured by ELISA, tumor oxygenation status using pO2 needle electrodes, and tumor osteopontin, HIF-1a and CA9 by IHC. Plasma OPN was found to correlate inversely with median tumor pO2. High plasma OPN, high HIF-1a and high proportion of tumor pO2 $\leq$ 2.5 mm Hg related significantly with poorer loco-regional control (Nordsmark et al. 2007). In the study by J Overgaard et al, plasma OPN level was evaluated in 320 patients with stored plasma samples from the 414 originally included patients of the randomized DAHANCA 5 trial (Overgaard et al. 2005). In this study, high level of plasma OPN was associated with poor prognosis in HNSCC patients treated with RT.

This could be reversed by giving such patients the hypoxic sensitizer nimorazole together with RT. The study indicated that OPN is a predictor for clinical relevant hypoxia and may predict the patients who may benefit from hypoxic modification.

Although the clinical significance of plasma or serum OPN has been widely studied in various tumor types (Singhal et al. 1997; Fedarko et al. 2001; Bramwell et al. 2006; Koopmann et al. 2004; Hotte et al. 2002; Ramankulov, Lein, Kristiansen, Loening et al. 2007; Ramankulov, Lein, Kristiansen, Meyer et al. 2007; Ang et al. 2005; Pass et al. 2005; Kim et al. 2002; Schorge et al. 2004; Shimada et al. 2005; Kim et al. 2006; Zhang et al. 2006; Wu et al. 2007; Chang et al. 2007), only one study reported elevated plasma OPN level in a cohort of non-metastatic NPC (Wong et al. 2005). However, the relationship to treatment response was not studied. To define the implications of elevated plasma OPN levels in NPC patients, we sought to investigate the response of a panel of NPC cell lines to in-vitro hypoxia, with or without reoxygenation, regarding the accumulation and secretion of this protein in NPC cells. We determined plasma OPN in patient cohort that included newly diagnosed NPC, as well as recurrent and metastatic NPC. We also included cohorts of non-NPC head and neck cancer (HNC) patients and healthy control subjects as disease and normal control, respectively. We further explored the relationship of plasma OPN with clinical

response to RT in NPC.

MATERIALS AND METHODS

Culture of tumor cell lines and hypoxia /re-oxygenation treatment

Four NPC cell lines (CNE-2, C666-1, HONE-1 and HK1) were employed as previously described (chapter 4) (Sung et al. 2005; Sung et al. 2007). The CNE-2 cell line (Sizhong, Xiukung, and Yi 1983) and HONE-1 cell line (Glaser et al. 1989) were established from poorly differentiated nasopharyngeal carcinomas. C666-1 was established from undifferentiated nasopharyngeal carcinoma and consistently carried the Epstein-Barr virus in long-term cultures (Cheung et al. 1999). The HK1 cell line was established from a well-differentiated squamous nasopharyngeal carcinoma (Huang et al. 1980). CNE-2 and HONE-1 cells were cultured in RPMI-1640 medium supplemented with 5% fetal bovine serum (FBS) and antibiotics (100 units/ml penicillin and 10 μg/ml streptomycin), while HK1 and C666-1 cells were cultured in RPMI-1640 medium supplemented with 10 % FBS and antibiotics. Cell cultures were incubated at 37°C in a humid atmosphere of 5% CO_2 and 95% air (normoxia). Hypoxia was created by culturing cells in a hypoxia chamber (Galaxy R CO_2 incubator, RS Biotech Laboratory Equipment Ltd., Ayrshire, Scotland) containing 0.1% O_2, 5% CO_2 and 94.9% N_2. Re-oxygenation of cells was achieved by exposure to normoxia

condition after hypoxia. All culture medium and reagents were purchased from GIBCO BRL (Grand Island, NY).

Enzyme-linked immunosorbent assay (ELISA) for osteopontin

NPC cells were seeded onto 6-well plates. Sub-confluent cultures were incubated in RMPI-1% FBS under normoxia or hypoxic condition for various time intervals (4 to 48 hours). At the end of incubation, culture medium was collected and spun at 3000 rpm for 3 minutes to remove cell debris. Aliquots of the supernatant were stored at –80°C until processing. Cells were then washed with cold PBS and then lysed in lysis buffer. The amount of total protein in each well was quantified. For plasma samples, blood was drawn from healthy control subjects or patients into EDTA-tubes and then span at 3000 rpm for 10 minutes. Supernatant (plasma) was collected and stored at -80°C until used. Plasma was diluted ten-fold before assayed. Osteopontin concentrations in cell culture supernatant or plasma were quantified by TiterZyme® EIA human Osteopontin Enzyme Immunometric Assay Kit (Assay Designs, Inc. Ann Arbor, USA) according to the manufacturer's instruction. The intra-assay and inter-assay precision (expressed as percent coefficient of variation) ranged from 3.1% to 8.6% and 6.3% to 10.3% (from low to high OPN concentration) respectively. Osteopontin secretions by NPC cells were normalized by total protein amount in each well and expressed in

ng/μg cellular protein. Osteopontin levels in plasma were expressed in ng/ml.

Western immunoblotting of osteopontin in tumor cell lines

After incubation, NPC cells were scraped off from culture flasks and lysed. Cellular proteins were separated by SDS-polyacrylamide gel electrophoresis. The separated proteins were electrophoretically transferred to nitrocellulose membrane. After blocking with 5% non-fat milk powder in TBST, the membrane was incubated with primary antibody for overnight at 4°C. After washing, the membrane was incubated with horseradish peroxide conjugated secondary antibodies (DAKO) for 1 hour at room temperature. After washing, the enhanced chemiluminescence detection system (ECL, Amersham Biosciences, Little Chalfont, Buckinghamshire, UK) was used to visualize the protein bands. The primary antibodies used were rabbit anti-human osteopontin antibody (Assay Designs, Inc. Ann Arbor, USA) and mouse anti-human hypoxia-inducible factor (HIF)-1α antibody (Transduction Laboratories, Lexington, KY). Actin was used as an internal control to verify equal protein loading of NPC cells during experiment.

RNA purification and reverse transcription-PCR (RT-PCR)

After incubation and treatment, NPC cells were then lysed by TRIzol Reagent

(Invitrogen, Carlsbad, CA) and RNA was extracted according to manufacturer's instruction. RT was performed by using random hexamers and MuLV reverse transcriptase (GeneAmp RNA PCR kit, Applied Biosystems, Foster City, CA), as reported previously (Sung et al. 2007). The RT reaction was started with 10 minutes incubation at room temperature, 1 hour at 42 °C, and 5 minutes at 99°C and followed by 5 minutes at 4°C. PCR was performed using AmpliTaq Gold (Applied Biosystems). The PCR program started with an initial denaturation at 95°C for 10 min, followed by 30 cycles (94°C for 30 s, 60°C for 30 s, and 72°C for 30 s) of amplification, with a final extension at 72°C for 10 min. The RT-PCR product was electrophoresed on a 2% agarose gel containing ethidium bromide.

Patients and samples

Plasma samples were collected from consecutively consenting patients of newly diagnosed and untreated nasopharyngeal or head and neck cancer attending oncology clinics at Department of Clinical Oncology of Prince of Wales Hospital. Written informed consent of blood collection for research purpose was obtained from all patients before blood taking. The control plasma samples were collected from volunteer staff members in good health without evidence of cancer. Additional plasma samples were collected during a phase 1 clinical trial of chemotherapy (cisplatin and

fluorouracil combined with antiviral agent ganciclovir) in patients with recurrent or metastatic nasopharyngeal cancer. The studies on human subjects were approved by the institutional ethics committee.

Statistical analysis

Descriptive statistics (mean, standard error of mean, standard deviation, median and range) were used to summarize the distribution of plasma OPN levels. One-sample Kolmogorov-Smirnov test was used to test for normal distribution of plasma OPN level within each group, and the result suggested a normal distribution. Correlations between plasma OPN level and clinical characteristics were analyzed by Pearson's (for continuous variables) or Spearman's (for categorical variables) correlation coefficient. Student's t-test was used to compare the mean plasma OPN of patient group against that of healthy control. Mann-Whitney U test was used to compare the difference of plasma OPN of patient group with that of healthy control. Response to RT according to plasma OPN level was compared by Fisher's exact test (as dichotomized variable divided by the median) and logistic regression (as a continuous variable). Univariate and multivariate logistic regression models were used to test for confounding covariates. All statistical analyses were performed with SPSS for Windows release 11.5 (SPSS Inc, Chicago, IL, USA). Statistical significance was set

at $P < 0.05$ (except where a Bonferroni correction was made to adjust for multiple testing in subgroup analysis, and the significance was set at $P < 0.05/n$, n = number of subgroups). All reported P values were two sided.

RESULTS

Effect of hypoxia on osteopontin secretion and expression in NPC cells

Four NPC cell lines were incubated in normoxia or hypoxia condition for 4-48 hours (Figure 6.1). Osteopontin secretion by NPC cells were quantified by ELISA. The results showed that only CNE-2 secreted osteopontin into culture medium (Figure 6.1a) while the osteopontin secretion by the other three NPC cell lines was undetectable under all conditions (data not shown). Hypoxia treatment did not significantly increase the osteopontin secretion by CNE-2 cells (Figure 6.1a). Cellular HIF-1α and osteopontin protein in NPC cells was detected by Western blotting. Hypoxia treatment (4-48 hours) significantly increased the cellular HIF-1α protein levels in NPC cell lines with peaks at 4 hours of hypoxia for HONE-1, C666-1 and HK1 cells and 16 hours of hypoxia for CNE-2 cells, HIF-1α protein levels were then declined progressively with longer incubation time. However, hypoxia did not change the cellular osteopontin protein levels in NPC cells (Figure 6.1b). The molecular weight of HIF-1α protein detected was between 100 and 150 kDa and that of OPN

was between 50 and 75 kDa. The osteopontin mRNA levels in hypoxic NPC cells were determined by RT-PCR. The primers for osteopontin can detect bands for osteopontin transcript variant 1 (product size 242 bp) and variant 2 (200 bp) in NPC cell lines. The data suggested that 16 hours of hypoxia did not significantly change the osteopontin mRNA levels (Figure 6.1c).

Effect of hypoxia/re-oxygenation on osteopontin levels in NPC cells

Since hypoxia followed by re-oxygenation may occur in some regions of hypoxic tumors (perfusion-limited hypoxia), and previous report suggested that reoxygenation rather than hypoxia may cause increased OPN production in certain cell types, we also studied the effect of hypoxia (16 hours) followed by re-oxygenation (2-48 hours) on cellular osteopontin protein levels in NPC cells. Our results showed that reoxygenation following hypoxia did not change the cellular osteopontin protein levels in NPC cells (Figure 6.1d).

Plasma osteopontin in healthy control, patients of nasopharyngeal and head and neck cancer

Plasma OPN was measured in 29 healthy control subjects, 44 nasopharyngeal cancer (NPC) and 22 head and neck cancer (HNC) patients (Table 6.1). The mean

and median plasma OPN of healthy control were 523 ng/ml and 513 ng/ml respectively. The mean and median plasma OPN of head and neck cancer patients were 728 ng/ml and 695 ng/ml respectively, which were significantly higher (even after Bonferroni correction) than that of healthy control ($p<0.001$ for the comparison of means by student's t-test, and $p = 0.002$ for the comparison of difference by Mann-Whitney U test, Table 6.2). The mean and median plasma OPN of all 44 NPC patients were 705 ng/ml and 582 ng/ml respectively, which were however not significantly different from that of healthy control ($p = 0.062$ by student's t-test, and $p = 0.073$ by Mann-Whitney U test).

Among the NPC or HNC patients, either tested as a combined group ($n = 66$) or as separate groups, there was no significant correlation between plasma OPN level and the following clinical parameters: gender, age, body weight, T-stage, N-stage, UICC stages (data not shown). However, plasma OPN level was significantly correlated with the presence of distant metastases (Spearman's correlation coefficient = 0.28, $p= 0.024$). Therefore we divided the 44 NPC patients into three clinical subgroups: (a) Loco-regional NPC, which represented the newly diagnosed, previously untreated, non-metastatic NPC. (b) Local recurrent NPC (rNPC). This group comprised of local recurrent NPC after previous radiotherapy without distant metastases. (c) metastatic

NPC (mNPC). All patients in group (a) were treated with curative radiotherapy with or without chemotherapy. Patients in group (b) or (c) were treated with palliative chemotherapy. Table 6.1 summarized the clinical characteristics of study patients.

The distribution of plasma OPN level in these three distinct clinical groups of NPC is shown in box and whisker plots in Figure 6.2. Plasma OPN levels in loco-regional NPC, either newly diagnosed NPC or recurrent disease (rNPC), were not significantly different from healthy control (Table 6.2 and Figure 6.2). In contrast, the plasma OPN levels in NPC patients with distant metastases (mNPC) were significantly higher (even after Bonferroni correction) that of healthy control ($p<0.001$ for the comparison of means by student's t-test, and $p < 0.005$ for the comparison of difference by Mann-Whitney U test, Table 2).

Plasma osteopontin and response to radiotherapy in NPC

There were 32 patients in group (a) with newly diagnosed loco-regional and non-metastatic NPC. All received curative RT with or without concurrent chemotherapy, except one patient who refused RT (this patient was excluded from the following analysis). Patients with stage I to II disease were treated with RT alone (n=10), and patients with stage III to IVB disease were given weekly cisplatin

concurrent with RT (concurrent chemoradiation, n=21), according to departmental clinical protocol (Chan, Teo et al. 2002). Response in primary tumor was evaluated by nasopharyngoscopy and biopsy at 6 weeks after completion of RT. Nodal response was evaluated by clinical examination at end of RT. Response was classified according to World Health Organization (WHO) response criteria (Miller et al. 1981). At the end of planned RT, 20 patients achieved complete response, 10 patients had partial response and one had progressive disease. Of the 10 patient with residual tumor at end of RT, 9 were successfully salvaged by additional radiotherapy delivered to residual tumor bed (six in the neck, and three in the nasopharynx including one followed by nasopharyngectomy). After a median follow up of 2.0 years for this cohort (n=31), 7 patients relapsed and 3 patients died (all from NPC recurrence). The response to planned RT (complete response vs partial response/progressive disease) was found to be a significant predictor of relapse ($p = 0.036$; odd ratio = 7.5, 95% C.I. 1.14 to 49.3).

When plasma OPN were dichotomized into high (> median 545 ng/ml) and low level (≤ median), NPC patients with high plasma OPN at diagnosis were found to be significantly less likely to achieve complete response after RT compared to those with low plasma OPN. The complete response rate was 40% (6/15) versus 88% (14/16)

for high versus low plasma OPN respectively (p=0.009, Fisher's exact test). When plasma OPN was analyzed as a continuous variable, plasma OPN remained a significant predictor for tumor response after RT (p=0.010, logistic regression). For NPC patients treated with concurrent chemoradiation (n=21), plasma OPN was also a significant predictor of response to concurrent chemoradiation. The complete response rate was 20% (2/10) versus 82% (9/11) for high versus low plasma OPN respectively (p=0.009, Fisher's exact test). When plasma OPN was analyzed as a continuous variable, plasma OPN remained a significant predictor for tumor response after concurrent chemoradiation (p=0.025, logistic regression).

The ability of plasma OPN and other clinical characteristics to predict the response to RT was further tested in both univariate and multivariate logistic regression models. On univariate analysis, T stage, N stage, UICC overall stage and plasma OPN were significant predictors of complete response to RT (Table 6.3a). When we incorporated these significant predictors from univariate analysis into a multivariate model, plasma OPN remained a significant and independent predictor of response to RT (Table 6.3b).

Impact of plasma osteopontin on relapse and survival in NPC

After a median follow up of 2 years, in the cohort of 31 NPC treated with curative intent RT (n=10) or concurrent chemoradiation (n=20), seven patient relapsed (including 3 local recurrences and 4 distant metastases) and 3 patient died (all from NPC recurrence). There were no significant differences in the relapse free survival or overall survival when stratified by high versus low plasma OPN (data not shown).

Table 6.1

Patient characteristics in each study cohort.

	Loco-regional nasopharyngeal cancer (NPC)	Local recurrent nasopharyngeal cancer (rNPC)	Metastatic nasopharyngeal cancer (mNPC)	Head and neck cancer (HNC)
Number of subjects (N)	32	5	7	22
Gender				
Male	26	4	6	18
Female	6	1	1	4
Age (years)				
Range	25 - 76	40 - 52	31 - 52	21 - 80
Median	48	43	45	60
Body weight (kg)				
Range	47.6 – 118.2	34.4 - 92	51.5 – 75	39.4 – 78
Mean	65.8	63	66.3	53
T stage				
T1	6	0	2	0
T2	9	0	2	6
T3	12	1	2	4
T4	5	4	1	12
N stage				
N0	11	3	0	12
N1	8	1	0	1
N2	6	1	2	7
N3	7	0	5	2
M stage				
M0	32	5	0	22
M1	0	0	7	0
UICC overall stage				
I	5	0	0	0
II	5	0	0	3
III	13	1	0	3
IV	9	4	7	16
Histology				
Squamous cell carcinoma				17
Poorly differentiated				1
Lymphoepithelial like or undifferentiated carcinoma	32	5	7	4
Site of primary tumor				
Nasopharynx	32	5	7	-
Hypopharynx/oropharynx	-	-	-	6
Larynx	-	-	-	8
Nasal	-	-	-	2
Tonsil	-	-	-	2
Others	-	-	-	4
Primary treatment				
Radiotherapy	10	0	0	4
Concurrent chemoradiation	21	0	0	17
Chemotherapy	0	5	7	0
Surgery	0	0	0	1
Others	1 (refused treatment)	0	0	0

Table 6.2

Comparison of plasma osteopontin levels in healthy control, patients with nasopharyngeal cancer and head and neck cancer.

Plasma osteopontin (ng/ml)	**Healthy control (Control)**	**Loco-regional nasopharyngeal cancer (NPC)**	**Local recurrent nasopharyngeal cancer (rNPC)**	**Metastatic nasopharyngeal cancer (mNPC)**	**Head and neck cancer (HNC)**
Number of subjects (N)	29	32	5	7	22
Mean	**523**	**578**	**614**	**1349**	**728**
Standard error of mean	25	28	188	375	53
Standard deviation	135	160	420	992	248
*Student's t-test**	-	*p = 0.15*	*p = 0.35*	*p < 0.001*	*p < 0.001*
Median	**513**	**545**	**501**	**894**	**695**
Minimum	278	333	228	379	405
Maximum	836	1015	1317	3200	1276
*Mann-Whitney U test**	-	*P = 0.18*	*P = 0.87*	*P = 0.005*	*P = 0.002*

* p value for the comparison of each patient group with reference to healthy control.

Table 6.3

Prediction of complete response to radiotherapy by patient's pre-treatment characteristics.

(a) Univariate analysis

Pre-treatment characteristics	P value	Odds ratio	95% C.I.
Gender	0.303	-	-
Age	0.799	-	-
Body Weight	0.161	-	-
T stage	0.011*	4.5	1.4 – 14.4
N stage	0.010*	2.8	1.3 – 6.3
UICC overall stage	0.009*	6.7	1.6 – 28
Treatment (concurrent chemotherapy)	0.065	-	-
Plasma osteopontin (high vs low)	0.011*	10.5	1.7 – 63.9

(b) Multivariate analysis

Pre-treatment characteristics	P value	Odds ratio	95% C.I.
T stage	0.039*	14.9	1.1 - 194
N stage	0.84	-	-
UICC overall stage	0.66		
Plasma osteopontin (high vs low)	0.019*	169	2.3 – 12345

* denote $p < 0.05$

Figure 6.1

(a) Osteopontin (OPN) secretion by NPC cells after exposure to hypoxia. CNE-2 cells were incubated in normoxic (solid line) or hypoxic (dotted line) condition for 4 to 48 hours. At the end of incubation, cultured medium was collected and OPN secretion to cultured medium was quantified by an OPN ELISA kit. Cells in each well were collected and the cellular proteins were then quantified. OPN secretion was then normalized by total protein in each well.

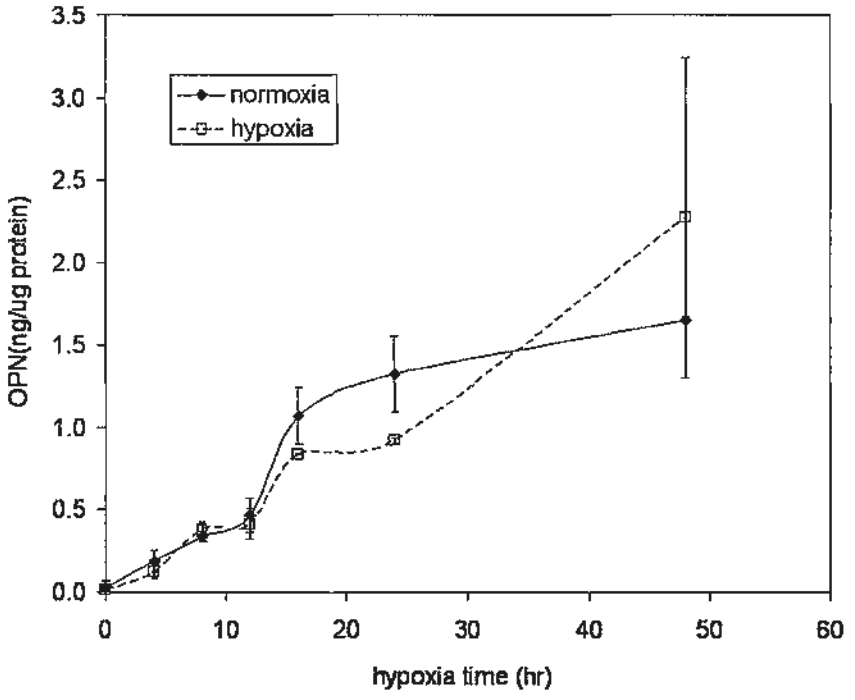

Figure 6.1

(b) Cellular OPN levels in NPC cells after exposure to hypoxia. NPC cells were subjected to hypoxic treatment for 4 to 48 hours. At the end of incubation, cells were collected and lysed. Total cell lysates were analyzed by SDS-PAGE followed by immunoblotting with anti-HIF-1α, anti-OPN or anti-actin antibodies. Actin was used as an internal control to verify equal protein loading.

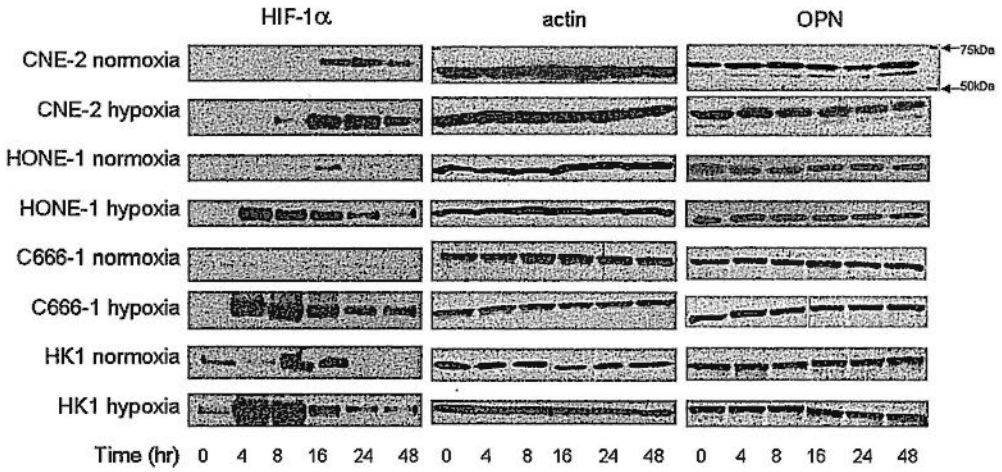

Figure 6.1

(c) Expression of OPN mRNA in NPC cells after exposure to hypoxia. NPC cells were incubated in normxia (-) or hypoxia (H) condition for 16 hours. At the end of incubation, cells were collected and total RNA was extracted. RT-PCR was then performed. The PCR amplified cDNA derived from OPN and GAPDH were separated by 1.8 % agarose gel electrophoresis containing ethidium bromide.

Figure 6.1

(d) Cellular OPN levels in NPC cells after exposure to hypoxia/re-oxygenation. NPC cells were subjected to hypoxia (H) treatment for 16 hours followed by 2 to 48 hours of re-oxygenation (R). At the end of incubation, cells were collected and lysed Total cell lysates were analyzed by SDS-PAGE followed by immunoblotting with anti-OPN antibody

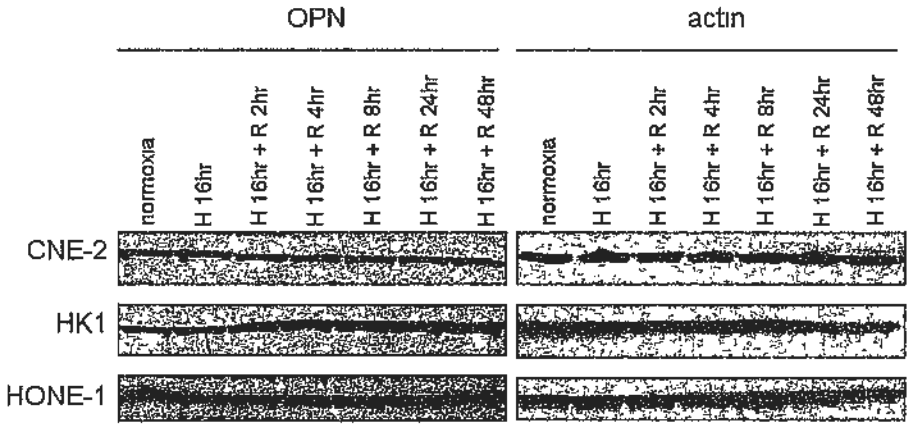

Figure 6.2

Distribution of plasma osteopontin (OPN) levels in healthy control subjects (control), patients of loco-regional nasopharyngeal cancer (NPC), loco-regional recurrent nasopharyngeal cancer (rNPC), metastatic nasopharyngeal cancer (mNPC), or head and neck cancer (HNC) by box and whisker plots.

(Box = the range of the middle 50% of OPN level; line inside box = median; whiskers = 5th and 95th percentile; circles = data points outside the whiskers)

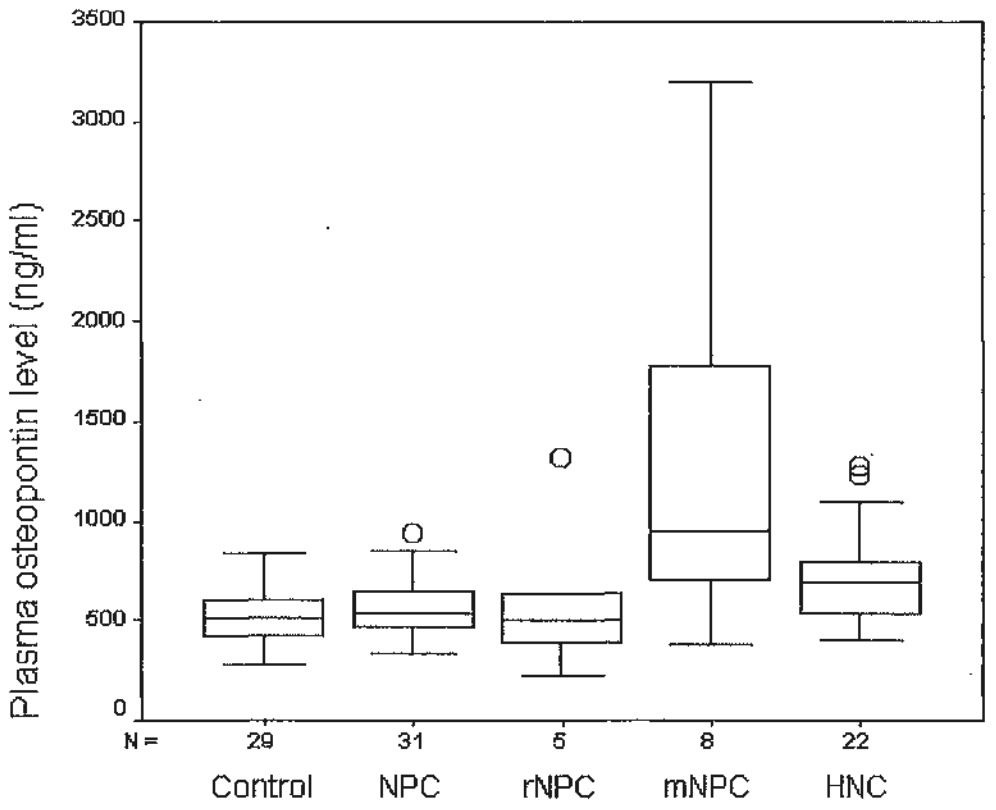

DISCUSSION

Recent reports have proposed OPN as a promising secreted and circulating biomarker of tumor hypoxia. In their original report identifying osteopontin as a potential hypoxia marker, Le et al showed the expression of osteopontin gene was inversely related with the expression of the von-Hippel-Lindau (VHL) gene which has a central role in the degradation of the transcription factor subunit HIF-1α and therefore linked to the hypoxic response of cells (Le et al. 2003). Their data suggested that cells with low VHL expression had intermediate to high OPN protein levels, and cells with high VHL expression had low OPN protein levels. Le et al also investigated the level of intracellular and secreted OPN proteins in one head and neck squamous cell carcinoma cell line SCC4 after exposure to either normoxia or different time course of hypoxia (<0.05% oxygen). Based on the experiment from a single cell line, the authors suggested that hypoxia and reoxygenation stimulated OPN extracellular secretion (Le et al. 2003).

In this study, we investigated the effect of hypoxia on osteopontin secretion and expression in a panel of 4 well characterized NPC cell lines (chapter 4, study 2) (Sung et al. 2005; Sung et al. 2007). Of the 4 NPC cell lines used, three of them are established from poorly differentiated or undifferentiated nasopharyngeal carcinoma.

C666-1 also carried the Epstein-Barr virus (EBV) in long-term cultures. In Southern China, most of NPCs are considered as undifferentiated carcinomas of the nasopharyngeal type (95%) and are strongly associated with the EBV (Tao and Chan 2007). Our results showed that osteopontin was expressed by all 4 NPC cell lines under normoxia but was only secreted by CNE2. However, hypoxia has no significant effect on either the intracellular mRNA and protein expression or the extracellular secretion of OPN in NPC cell lines. Reoxygenation also had no effect on intracellular OPN protein expression. In order to validate the hypoxic condition created by the hypoxia chamber, we had also examined the expression of the levels of HIF-1α protein, which is known to be induced by hypoxia, in the NPC cell lines. The Western blotting results showed that HIF-1α protein was elevated in all 4 NPC cell lines after hypoxia treatment. In addition, we also observed that a moderate induction of HIF-1α protein level in some of the NPC cell lines during incubation in normoxia condition. This moderate elevation may be due to the stress/starvation created by incubating cells in medium with only 1% FBS, as this was not seen when cells were incubated in 5% or 10% FBS in our previous report (see chapter 4, study 2) (Sung et al. 2007).

This difference between the NPC cell lines and the SCC4 cell line could be explained by the genetic background of the cell lines investigated. While the VHL gene was not

mutated (Sun et al. 1995) or methylated (Wong et al. 2003) in NPC, the VHL status of the other cell lines has not been published. Recent in-vivo and in-vitro studies by other investigators also supported that hypoxia induced OPN up-regulation is not consistent and may be cell type specific (Said et al. 2005; Lukacova et al. 2006). Said et al studied osteopontin secretion from cultured cell lines. Of 6 cell lines tested, only 3, A549 (human lung carcinoma), HT1080 (human fibrosarcoma) and U87 (human malignant glioma) showed detectable OPN under aerobic condition. No increase of OPN in the medium during 24 h hypoxia but moderate increases during subsequent reoxygenation were observed in these three cell lines. In FaDu (human pharyngeal carcinoma), HT 29 and HCT 116 (human colorectal carcinoma cells), OPN levels were undetectable under all conditions (Said et al. 2005). Sorensen et al also showed that OPN was up regulated by hypoxia in SiHa (human uterine cervix squamous cell carcinoma) cells but not in $FaDu_{DD}$ (pharyngeal squamous cell carcinoma, a subline of FaDu) cells (Sorensen et al. 2007).

Another possible explanation for the discrepancy between high plasma OPN levels in patients with hypoxic tumors and a lack of protein secretion during hypoxia in tumor cell cultures may be the contribution of non-tumor cells. At present, the exact source(s) of the elevated OPN in the serum or plasma of cancer patients remains

unclear. Osteopontin is a secreted phosphoprotein that can be expressed at high level by T-lymphocytes, epidermal cells, bone cells, macrophages, endothelial cells and tumor cells in remodeling processes such as inflammation, ischemia-reperfusion, bone resorption, arteriosclerosis and tumor progression (Wai and Kuo 2007). Although OPN may be expressed in tumor cells, OPN in blood may be derived from several possible tissue sources, including activated secretary epithelia, remodeling of bone or vascular bed, activated immune cells and/or tumor cells. In pancreatic adenocarcinoma, activated tumor infiltrating macrophages have been suggested as a primary source of OPN (Koopmann et al. 2004). In a recent study of advanced head and neck cancer patients, no correlation was found between plasma OPN and tumor OPN expression (Nordsmark et al. 2007).

Despite the uncertainty on the possible source(s) and mechanism(s) of elevated plasma osteopontin in health and disease states, plasma osteopontin has been extensively investigated as a biomarker of advanced disease in multiple tumor types (Singhal et al. 1997; Fedarko et al. 2001; Bramwell et al. 2006; Koopmann et al. 2004; Hotte et al. 2002; Ramankulov, Lein, Kristiansen, Loening et al. 2007; Ramankulov, Lein, Kristiansen, Meyer et al. 2007; Ang et al. 2005; Pass et al. 2005; Kim et al. 2002; Schorge et al. 2004; Shimada et al. 2005; Kim et al. 2006; Zhang et al. 2006; Wu et al.

2007; Chang et al. 2007), and has been implicated as an important mediator in tumor metastasis, as summarized in a recent review (Wai and Kuo 2007). Our results showed that plasma OPN was not elevated in localised NPC (either newly diagnosed or recurrent) but was increased in metastatic NPC. This supports for a role of osteopontin in tumor metastasis.

We also demonstrated that high plasma OPN was a significant negative predictor of response to radiotherapy in NPC. This suggests that high plasma OPN may be a biomarker of radiation resistance. In NPC patients treated with concurrent chemoradiation, the fact that plasma OPN remains a significant negative predictor of radiotherapy response suggests that alternative strategy other than addition of chemotherapy should be explored in future to overcome the poor response to radiotherapy associated with a high plasma OPN level. However, because of the small sample size and lack of long term follow up, we could not address the impact on relapse and survival in this pilot study. Our observations and hypothesis should therefore be confirmed in a larger clinical study in NPC.

Our clinical data indicated that in patients with loco-regional NPC, plasma OPN was not different from that in healthy control but nevertheless was predictive of

radiotherapy response. Taken together with the in-vitro data of the lack of hypoxia induction of OPN in NPC cell lines, our findings challenged the view that OPN secretion is directly caused by the effect of low oxygen tension on tumor cells. However, it was still possible that plasma OPN was related to intratumoral hypoxia and prognostic, but was not secreted directly from the tumor cells. Defining the exact mechanism of elevated plasma OPN levels in cancer and the relationship to tumor hypoxia will required further investigations.

Recently, Vordermark et al showed that the commercially available OPN ELISA systems produce different absolute plasma OPN levels, compromising any direct comparison of individual patient data with published results (Vordermark et al. 2006). It appeared that the discrepancy may be related to difference in epitope recognition site of the different capture antibodies provided with individual ELISA kits. In addition, the type of blood sample used (e.g. plasma versus serum) and variations in sample processing and storage may also affect the results of ELISA. To further complicate the measurement of plasma OPN, it is known that OPN exist in various forms due to post-translational modifications such as glycosylation, sulfation, and phosphorylation. There are at least three differentially spliced isoforms of human OPN. The use of various combinations of antibodies raised against four different portions of human

OPN in a total of six separate ELISA systems has been shown to recognize distinct truncated or glycosylated forms of OPN (Kon et al. 2000). However, the potential functional differences among those isoforms are largely unknown and the differential expression of OPN fragments in various disease states is not well characterized. Therefore prospective validation study for each specific tumor type is required before plasma OPN could be widely used in the clinic to guide clinical decision.

CONCLUSION

This study showed that in a panel of NPC cell lines, prolonged hypoxia with or without reoxygenation did not lead to increased cellular OPN mRNA/protein production or increased OPN secretion. This finding challenged the view that OPN secretion is directly caused by low oxygen tension. The clinical data showed for the first time that plasma OPN predicted complete response to radiotherapy in NPC. Our results suggested that elevated plasma OPN is a biomarker of distant metastasis, and pre-treatment plasma OPN level may be a useful biomarker of response to RT in NPC.

Page

SECTION III

NEW THERAPEUTIC APPROACHES IN NASOPHARYNGEAL CARCINOMA

Chapter 7

Study 5: Targeting Distant Metastasis - Neoadjuvant Chemotherapy

BACKGROUND

As discussed in chapter 1, the current standard therapy of NPC is RT alone in early stage and concurrent chemoradiotherapy (CRT) in advanced stage. This is based on the results that CRT with or without adjuvant chemotherapy demonstrated improved overall survival compared with RT alone in several large scale phase III studies including the intergroup 0099 trial and meta-analysis (Baujat et al. 2006; Chan et al. 2010)(summarized in chapter 1, Table 1.1 and 1.2). However, adjuvant chemotherapy is often poorly tolerated after an intensive course of chemoradiation (Agulnik and Siu 2005). Randomized trials of neoadjuvant chemotherapy followed by radiotherapy alone have resulted in encouraging response rates and improvement in disease free survival but not overall survival (Chan et al. 1995; VUMCA-I 1996; Chua et al. 1998; Ma et al. 2001; Hareyama et al. 2002; Chua et al. 2005) Since the use of chemotherapy in the neoadjuvant setting has been shown to improve progression free survival (PFS), and as concurrent therapy to RT to improve overall survival (OS) in advanced NPC, the development of a sequential schedule of neoadjuvant chemotherapy followed by CRT would seem a logical strategy in an attempt to

maximize the benefit from both approaches. In fact, this "neoadjuvant-concurrent" strategy has been pursued by several groups in uncontrolled phase II studies, all reported favourable outcomes (Rischin et al. 2002; Oh et al. 2003; Chan et al. 2004).

The taxanes (paclitaxel and docetaxel) have demonstrated considerable single agent activity in NPC (Au, Tan, and Ang 1998; Ngeow et al. 2010). The combination of paclitaxel and carboplatin has yielded high response rates in metastatic NPC (Yeo et al. 1998; Tan et al. 1999; Airoldi et al. 2002), and has demonstrated encouraging activity and safety profile in the neoadjuvant setting of NPC (Chan et al. 2004). Docetaxel is associated with less neurotoxicity than paclitaxel and can therefore be more tolerably combined with cisplatin. Docetaxel in combination with cisplatin has been investigated in NPC (McCarthy et al. 2002; Chua, Sham, and Au 2005) and is expected to be more active in the neoadjuvant setting.

With the experience of a weekly cisplatin schedule from a completed phase III study of CRT in NPC (Chan, Teo et al. 2002; Chan, Leung et al. 2005) and the evidence from other cancers that this may be the best tolerated schedule of CRT (Morris et al. 1999), the schedule of weekly cisplatin 40 mg/m^2 up to 8 weeks concurrently with RT was used in the present protocol.

The primary endpoint of this study was to compare the toxicities in patients with advanced NPC treated with CRT with or without neoadjuvant docetaxel and cisplatin. Secondary endpoints were to compare the tumor response, PFS, OS, and the quality of life of patients between the two treatment arms.

PATIENTS AND METHODS

Patient eligibility and randomization

Eligible patients had biopsy proven, previously untreated, loco-regionally advanced NPC of International Union Against Cancer (UICC) 1997 stages III to IVB. Additional eligibility criteria included evaluable disease, Eastern Cooperative Oncology Group (ECOG) performance status grade 0 or 1, ≥18 years old, adequate bone marrow reserve (white blood cell count and platelet count ≥ the lower limit of normal) and renal function (serum creatinine <1.5 times the upper limit of normal or creatinine clearance ≥50 ml/min), absence of hypercalcaemia or second malignancy.

All patients provided written informed consent before study enrolment. The study protocol was approved by the Clinical Research Ethics Committee of The Chinese University of Hong Kong and was conducted in compliance with the principles of the

Declaration of Helsinki (2000).

After informed patient consent, the registration and randomization procedure was carried out through telephone at the central office of the Comprehensive Cancer Trials Unit (CCTU) of The Chinese University of Hong Kong. A computer program was used to generate the allocation list. Patients were stratified for stage (stage III versus IV) and randomized in 1:1 ratio to either one of the two treatment arms: (1) neoadjuvant chemotherapy followed by cisplatin-radiotherapy (CRT), or (2) CRT alone (Fig 7.4).

Chemotherapy

In the experimental arm, the neoadjuvant chemotherapy schedule was docetaxel 75 mg/m^2 as intravenous (I.V.) infusion over 1 hour on day 1 and cisplatin 75 mg/m^2 I.V. over 1 hour with hydration on day 1. Docetaxel was preceded by premedication with oral dexamethasone 8 mg twice daily for 3 days starting one day before the infusion. Cycles were repeated every 3 weeks for 2 cycles. This was followed by radiotherapy (RT) delivered concurrently with cisplatin 40 mg/m^2 IV over 2 h from week 7-14 (Fig 7.5). In the control arm, RT concurrent with cisplatin 40 mg/m^2 was given from week 1-8 without the neoadjuvant chemotherapy (Chan, Teo et al. 2002; Chan, Leung et al.

2005).

Neoadjuvant chemotherapy was delayed by one week if the absolute neutrophil count (ANC) was <1.5 x 10^9/L or platelet count was <75 x 10^9/L. Both cisplatin and docetaxel were reduced to 65 mg/m^2 if the nadir ANC was <0.5 x 10^9/L or platelet count was <50 x 10^9/L. No growth factor support was used. During CRT, cisplatin was delayed by one week if ANC was < 1.5 x 10^9/L or platelet count was < 75 x 10^9/L until the counts recovered. Cisplatin was stopped if there were any grade 4 toxicites. RT delays were strongly discouraged. Enteral tube feeding was used as required at the investigators' discretion.

Radiotherapy

RT was planned and delivered by the Ho's technique (Chan, Teo et al. 2002; Chan et al. 2004). The same RT technique was used for both arms. The nasopharynx and adjacent region were treated to 66 Gy in 33 fractions over 6.6 weeks by a shrinking-field technique (two lateral facial-cervical ports to 40 Gy in 20 fractions over 4 weeks, followed by a three-port plan to another 26 Gy in 13 fractions over 2.6 weeks, with 6MV photons). The cervical lymphatics were treated by a separate anterior photon port. For patients with parapharyngeal disease, a boost dose to the

nasopharyngeal and parapharyngeal region was delivered by an ipsilateral postero-lateral port, giving 20 Gy in 10 fractions over 2 weeks. Palpable residual nodes at completion of RT were boosted to 7.5 Gy in two fractions with an electron field. Patients with persistent NP disease at 6 weeks after completion of CRT were given intracavitary brachytherapy using paired iridium-192 sources, delivering a dose of 18 Gy in four fractions in 15 days. Those with cytological proven residual neck nodes were referred for radical neck dissection.

From 1 March 2004, the protocol was amended to adopt Intensity Modulated Radiation Therapy (IMRT) technique to treat all T3/4 disease in both arms, in concordance with the change to adopt IMRT as standard departmental protocol in advanced NPC. The prescribed dose was 66 Gy in 33 fractions in 6.6 weeks to the Gross Tumor Volume (GTV) with margins. Details of the IMRT techniques used had been described previously (Kam et al. 2004).

Assessment and follow up

All patients had tp complete the pre-treatment screening investigations within 28 days before randomization. Staging procedures included computed tomography (CT) scan and magnetic resonance imaging (MRI) of nasopharynx and neck, chest X-ray,

ultrasound scan of abdomen, and radionuclide bone scan.

Routine complete blood pictures, serum biochemistry and adverse events were evaluated on day 1 and day 10 of neoadjuvant chemotherapy and weekly during CRT, and were graded according to the National Cancer Institute Common Toxicity Criteria (NCI-CTC) version 2.0. Response to neoadjuvant therapy was evaluated before commencement of CRT by endoscope of the nasopharynx, physical examination, and CT scan. Response after CRT was evaluated by endoscope of the nasopharynx and biopsy, physical examination, and CT scan at 6 weeks after completion of CRT. Response was classified according to World Health Organization (WHO) response criteria (Miller et al. 1981).

All patients were followed up every 3 months in the first two years, then every 6 months in the 3rd and 4th year, and yearly thereafter. The following assessments were performed at each follow up visit: (1) history and physical examination, (2) nasopharyngoscopy, (3) late RT toxicity of the skin, subcutaneous tissue, and salivary gland using the Radiation Therapy Oncology Group (RTOG) and European Organisation for Research and Treatment of Cancer (EORTC) late radiation morbidity scoring schema (Cox, Stetz, and Pajak 1995).

Quality of life assessment

The EORTC QLQ-C30 core questionnaire (Aaronson et al. 1993) together with the head and neck cancer (H&N35) module (Bjordal et al. 1999) were administered at baseline, on day 1 of each cycle of neoadjuvant chemotherapy, weekly during CRT and at each follow up visits.

Statistical analysis

The incidence of toxicity was the primary endpoint. We calculated in this study the 95% confidence intervals (C.I.) for the incidence of toxicities with an adjustment of the type I error for multiple comparisons of about 10 commonly encountered hematologic and non-hematologic toxicities. Using 30 patients in each arm, we would be able to exclude at least 20% difference using the lower bound of the 95% C.I. in a reasonable range of toxicities commonly found in most NPC trials i.e. around 0-25%. Therefore, about 30 patients in each of the two arms would allow us to exclude a difference of 20% on one-side of 95% confidence interval with 80% power. Secondary endpoints include tumor response, PFS, OS, and quality of life. The accrual goal was 60 patients.

OS was defined as the duration from the date of randomization to the date of death due to any cause or censored at the date of last follow-up. PFS was defined as the duration from the date of randomization to the date of disease progression or censored at the date of last follow-up. The survival analysis was based on intention-to-treat principle and included all randomized patients (ITT cohort, n=65). Analysis of toxicities and responses was based on per protocol treatment cohort (n=60). Chi-square test was used to compare the adverse events and other categorical variables between the two treatment arms. The progression free and overall survival curves were computed by Kaplan-Meier method and compared by log-rank test. The hazard ratios and the corresponding 95% C.I. were calculated by using Cox's proportional hazard model. For quality of life scores, a difference or change of 10 units or more on a 0 to 100 scale was regarded as clinically important. Test of differences between the two arms were performed by Wilcoxon test.

RESULTS

Patients

From November 2002 to November 2004, 68 patients were screened and 65 were randomly assigned to one of the two study arms. 34 patients were randomized to neoadjuvant chemotherapy arm and 31 patients to control arm (Fig 7.1). The two

treatment arms were well balanced in the baseline characteristics (Table 7.1). All patients in the neoadjuvant arm received the allocated treatment but five patients in the control arm did not receive the allocated treatment. Of these five patients, two withdrew consent before treatment commencement, one was diagnosed to have dermatomyositis, one mandated IMRT mode of radiotherapy (before protocol amendment to include IMRT as standard), and one required further investigation for lung lesion (which was later confirmed to be related to old tuberculosis on CT scan of thorax). Of the two patients who withdrew study consent after randomization, one seeked herbal medicine for one month and then received CRT. The other patient seeked herbal medicine for one year before development of distant metastases and subsequently received palliative chemotherapy. All other three patients received CRT. Altogether, four of the five patients who withdrew from study received CRT as per standard institutional protocol, which was the same as the control arm that they were originally allocated. All five patients were followed and included in the ITT analysis.

Treatment administration

All patients in the neoadjuvant arm completed the scheduled two cycles of neoadjuvant chemotherapy. The median duration from day 1 of cycle 1 to day 1 of cycle 2 neoadjuvant chemotherapy was 21 days (range from 21-27 days), and from

day 1 of cycle 2 chemotherapy to day 1 of RT was 24 days (range from 20-28 days). The mean relative dose intensities of cisplatin and docetaxel during neoadjuvant chemotherapy and that of weekly cisplatin during CRT were shown in Figure 7.2. In the neoadjuvant arm, 100%, 97%, 94%, 88%, 74%, 35%, 7%, 3% of patients completed 1, 2, 3, 4, 5, 6, 7 and 8 weeks of cisplatin during CRT, respectively. The corresponding numbers for the control arm were 100%, 96%, 92%, 84%, 76%, 48%, 20%, 0%. The proportion of patients who completed cisplatin at different time points during CRT were comparable in the two arms ($p = 0.94$).

All patients in both arms completed RT to the prescribed dose. Twenty-nine percent in the neoadjuvant arm and 23% in the control arm were treated with IMRT plan. The mean RT total dose was 78.4 Gy (+/- standard deviation, S.D., 8.6 Gy) in the neoadjuvant arm and 76.5 Gy (+/- S.D. 7.4 Gy) in the control arm. The mean RT overall treatment time was 58.8 days (+/- S.D. 7.6 days) in the neoadjuvant arm and 56.6 days (+/- S.D. 6.6 days) in the control arm.

Acute toxicity

There was no grade 5 toxicity (death) during treatment. The main grade 3/4 adverse events during neoadjuvant chemotherapy were hematological (Table 7.2). Although

grade 3/4 neutropenia occurred in 97% of patients during neoadjuvant docetaxel-cisplatin chemotherapy, the rate of febrile neutropenia was only 12%, which were all uncomplicated. During the CRT phase, no significant differences were observed in the rates of grade 3/4 neutropenia, other hematological or non-hematologic toxicities between the two study arms. The mean time to first onset of grade 3/4 neutropenia during CRT was also similar in both arms (33 ± 2.8 days in neoadjuvant arm and 33 ± 14.7 days in control arm).

Efficacy

Responses after neoadjuvant chemotherapy and cisplatin-RT were summarized in Table 7.3. After a median follow-up of 4.3 years, we observed a total of 20 disease progressions and 17 deaths in the ITT population. The pattern of failure according to treatment arm was summarized in Table 7.5. The 3-year progression free survival for neoadjuvant versus control arm was 88.2% and 59.5% (hazard ratio 0.49; 95% C.I.=0.20 to 1.19; p=0.12)(Fig 7.3a). The 3-year overall survival for neoadjuvant versus control arm was 94.1% and 67.7% (hazard ratio 0.24; 95% C.I.=0.078 to 0.73; p=0.012) (Fig 7.3b).

The survival analysis was repeated based on the per protocol treatment cohort by

excluding the five patients who did not receive the allocated treatment. The result of this per protocol analysis was similar to the ITT cohort. The 3-year progression free survival for neoadjuvant chemotherapy versus control arm was 88.2% and 63.5% (hazard ratio 0.55; 95% C.I.=0.21 to 1.44; p=0.23). The 3-year overall survival for neoadjuvant chemotherapy versus control arm was 94.1% and 69.2% (hazard ratio 0.26; 95% C.I.=0.081 to 0.83; p=0.022).

Late toxicity

No significant differences were observed in the cumulative incidence of grade 3 or above late radiation morbidity or adverse events during follow up between the two study arms (Table 7.4).

Quality of life

Compliance with quality of life questionnaire was 100% in both arms (34 pts in neoadjuvant arm and 26 pts in control arm) at baseline and 4 week post-treatment, 94.1% (32) at 12 months and 88.2% (30) at 24 months in the neoadjuvant arm, and 76.9% (20) at 12 months and 65.4% (17) at 24 months in control arm. The decrease was because of patient's death or disease progression. The frequency of missing response per each item was low, ranged from none to 2/24 (8%) for items on

sexuality. Most items have no missing value.

No significant difference was observed in the global quality of life scores in the two treatment arms (Figure 7.6, mean change in score was -8.59 at 4 weeks, 3.89 at 12 months and 1.79 at 24 months in neoadjuvant arm; -4.00 at 4 weeks, 1.75 at 12 months and 5.73 at 24 months in control arm). Regarding physical functioning, patients in the neoadjuvant arm had slightly more deterioration at 4 weeks post CRT (mean change score, -42.9 vs. -27.7; p=0.0499), with increase in symptom score of appetite (mean change score, 18.6 vs. -5.3; p=0.023) and constipation (mean change score, 24.5 vs. -3.8; p=0.0075) as compared with control arm. However, the differences in these items were no longer significant by 12 and 24 months post treatment. No significant difference was observed in other QLQ-C30 function domains or symptom subscales between the two arms. In the H&N35 module, the only significant difference was an increase of nutritional supplements in neoadjuvant arm compared with control arm (mean change score, 10.0 vs. -23.5; p=0.025) at 24 months post-treatment.

Table 7.1

Baseline characteristics of all randomized patients in the intent-to-treat cohort.

Characteristics*	**Neoadjuvant arm** (n=34)	**Control arm** (n=31)
Age, years		
Median	50	45
Range	31-70	32-70
Gender, n (%)		
Male	21 (61.8)	24 (77.4)
Female	13 (38.2)	7 (22.6)
ECOG Performance Status, n (%)		
0	29 (85.3)	26 (83.9)
1	5 (14.7)	5 (16.1)
UICC T-classification, n (%)		
T1	2 (5.9)	2 (6.4)
T2	12 (35.3)	7 (22.6)
T3	13 (38.2)	15 (48.4)
T4	7 (20.6)	7 (22.6)
UICC N-classification, n (%)		
N0	8 (23.5)	4 (12.9)
N1	4 (11.8)	8 (25.8)
N2	13 (38.2)	12 (38.7)
N3	9 (26.5)	7 (22.6)
UICC stage, n (%)		
III	19 (55.9)	19 (61.3)
IV	15 (44.1)	12 (38.7)

* ECOG, Eastern Cooperative Oncology Group; UICC, International Union Against Cancer.

Table 7.2

Summary of grade 3 and 4 adverse events during treatment.*

	Neoadjuvant arm (n=34)		**Control arm** (n=26)		P value**
	Grade 3	Grade 4	Grade 3	Grade 4	
(a) During neoadjuvant chemotherapy, n (%)					
Hematologic:					
Neutropenia	6 (17.6)	27 (79.4)			
Neutropenic fever	4 (11.8)	0			
Non-hematological:					
Fatigue	2 (5.9)	0			
Nausea/Vomiting	3 (8.8)	0			
(b) During cisplatin-radiotherapy, n (%)					
Hematologic:					
Anaemia	3 (8.8)	0	5 (19.2)	0	0.23
Thrombocytopenia	1 (2.9)	2 (5.9)	0	1 (3.8)	0.44
Neutropenia	8 (23.5)	1 (2.9)	3 (11.5)	1 (3.8)	0.30
Neutropenic fever	1 (2.9)	0	1 (3.8)	0	0.16
Non-hematologic:					
Anorexia/nausea/vomiting	3 (8.8)	0	2 (7.7)	0	0.87
Dehydration/renal	8 (23.5)	0	6 (23.1)	0	0.96
Fatigue	5 (14.7)	0	2 (7.7)	0	0.40
Electrolytes	10 (29.4)	0	9 (34.9)	0	0.66
Mucositis/odynophagia	8 (23.5)	0	2 (7.7)	0	0.11
Transfusion	5 (14.7)	0	4 (15.4)	0	0.94

* Adverse events were graded according to the National Cancer Institute Common Toxicity Criteria (NCI-CTC), version 2.0.

** P values, calculated with the use of Fisher's exact test, are for the difference in the incidence of Grade 3 and 4 adverse events between the two treatment arms.

Table 7.3

Response to neoadjuvant chemotherapy and cisplatin-radiotherapy.*

	Response Rate				P value+
	Neoadjuvant arm (n=34)		Control arm (n=26)		
After neoadjuvant chemotherapy, n (%)	**NP** (n=34)	**LN**** (n=26)			
CR	8 (23.5)	14 (53.8)			
PR	20 (58.8)	8 (30.8)			
SD	6 (17.6)	4 (15.4)			
PD	0	0			
Combined response	**NP + LN** (n=34)				
CR	6 (17.6)				
ORR (CR + PR)	26 (76.5)				
After cisplatin-radiotherapy, n (%)	**NP** (n=34)	**LN**** (n=26)	**NP** (n=26)	**LN**** (n=24)	
CR	32 (94.1)[a]	21 (80.8)[b]	22 (84.6)[a]	16 (66.7)[b]	0.22 [a] 0.26 [b]
PR	2 (5.9)	4 (15.4)	4 (15.4)	8 (33.3)	
SD	0	1 (3.8)	0	0	
PD	0	0	0	0	
Combined response	**NP + LN** (n=34)		**NP + LN** (n=26)		
CR	28 (82.4)		16 (61.5)		0.07
ORR (CR + PR)	33 (97.1)		26 (100)		0.38

* NP, nasopharynx; LN, regional neck lymph nodes; CR, complete response; PR, partial response; SD, stable disease; PD, progressive disease; ORR, overall response rate.

** Patients with N0 at baseline were excluded for the calculation of LN response.

+ P values, calculated with the use of Chi-squared test, are for the difference in the response rate between the two treatment arms.

[a] difference in the CR rate of NP between the two treatment arms.

[b] difference in the CR rate of LN between the two treatment arms.

Table 7.4

Late radiation morbidity and adverse events.*

	Neoadjuvant arm (n=34)		Control arm (n=26)		P value **
Late Radiation Morbodity, n (%)	Grade 3	Grade 4	Grade 3	Grade 4	
Esophagus	1 (2.9)	0	0	0	0.38
Eye	0	0	0	1 (3.8)	0.24
Mucous membrane	3 (8.8)	0	0	0	0.12
Salivary glands	11 (32.4)	0	8 (30.8)	0	0.89
Skin	4 (11.8)	0	5 (19.2)	0	0.49
Subcutaneous tissue	7 (20.6)	0	3 (11.5)	0	0.35
Total (Any)	26 (76.5)	0	16 (61.5)	1 (3.8)	0.17
Late Adverse Events, n (%)	Grade 3	Grade 4	Grade 3	Grade 4	
CNS hemorrhage	0	0	0	1 (3.8)	0.24
Conjunctivitis/Keratitis	0	0	0	1 (3.8)	0.24
Dysphagia	0	0	0	1 (3.8)	0.24
Ear	3 (8.8)	0	1 (3.8)	0	0.44
Epistaxis	0	1 (2.9)	0	0	0.38
Fatigue	1 (2.9)	0	0	0	0.38
Hepatic	0	0	1 (3.8)	0	0.24
Hearing	1 (2.9)	2 (5.9)	3 (11.5)	0	0.73
Hypoxia	0	1 (3.8)	0	0	0.38
Irregular menses	0	0	1 (3.8)	0	0.24
Lymphoedema (submental)	0	0	1 (3.8)	0	0.24
Musculoskeletal	1 (2.9)	0	2 (7.7)	0	0.72
Pain	1 (2.9)	0	0	0	0.38
Pulmonary	1 (2.9)	0	4 (15.4)	0	0.07
Second cancer (primary site)	0	2 (5.9) (Breast, tongue)	0	1 (3.8) (colon)	0.72
Transfusion	3 (8.8)	0	0	0	0.12
Total (Any)	11 (32.4)	6 (17.6)	13 (50.0)	4 (15.4)	0.23

* Late radiation morbidity was graded according to Radiation Therapy Oncology Group and European Organisation for Research and Treatment of Cancer (RTOG/EORTC) scoring schema. Late adverse events were graded according to National Cancer Institute Common Toxicity Criteria (NCI-CTC) version 2.0.

** P values, calculated with the use of Fisher's exact test, are for the difference in the incidence of Grade 3 and 4 events between the two treatment arms.

Table 7.5

Pattern of failure according to treatment arm

Site of any failures, n (%)	**Neoadjuvant arm (n=34)**	**Control arm* (n=31)**	**Control arm** (n=26)**
Progression	8 (23.5)	12 (38.7)	9 (34.6)
Locoregional	5 (14.7)	3 (9.7)	3 (11.5)
nasopharynx	5 (14.7)	1 (3.2)	1 (3.8)
neck lymph node	3 (8.8)	2 (6.5)	2 (7.7)
Distant metastases	4 (11.8)	9 (29.0)	6 (23.1)
Death	4 (11.8)	13 (41.9)	10 (38.5)

The intention-to-treat (ITT) cohort and per protocol treatment cohort were the same for the neoadjuvant arm.

* includes all randomized patients in ITT cohort.

** includes only patients who received allocated treatment (per protocol treatment cohort).

Figure 7.1

CONSORT chart showing the flow of trial participants.

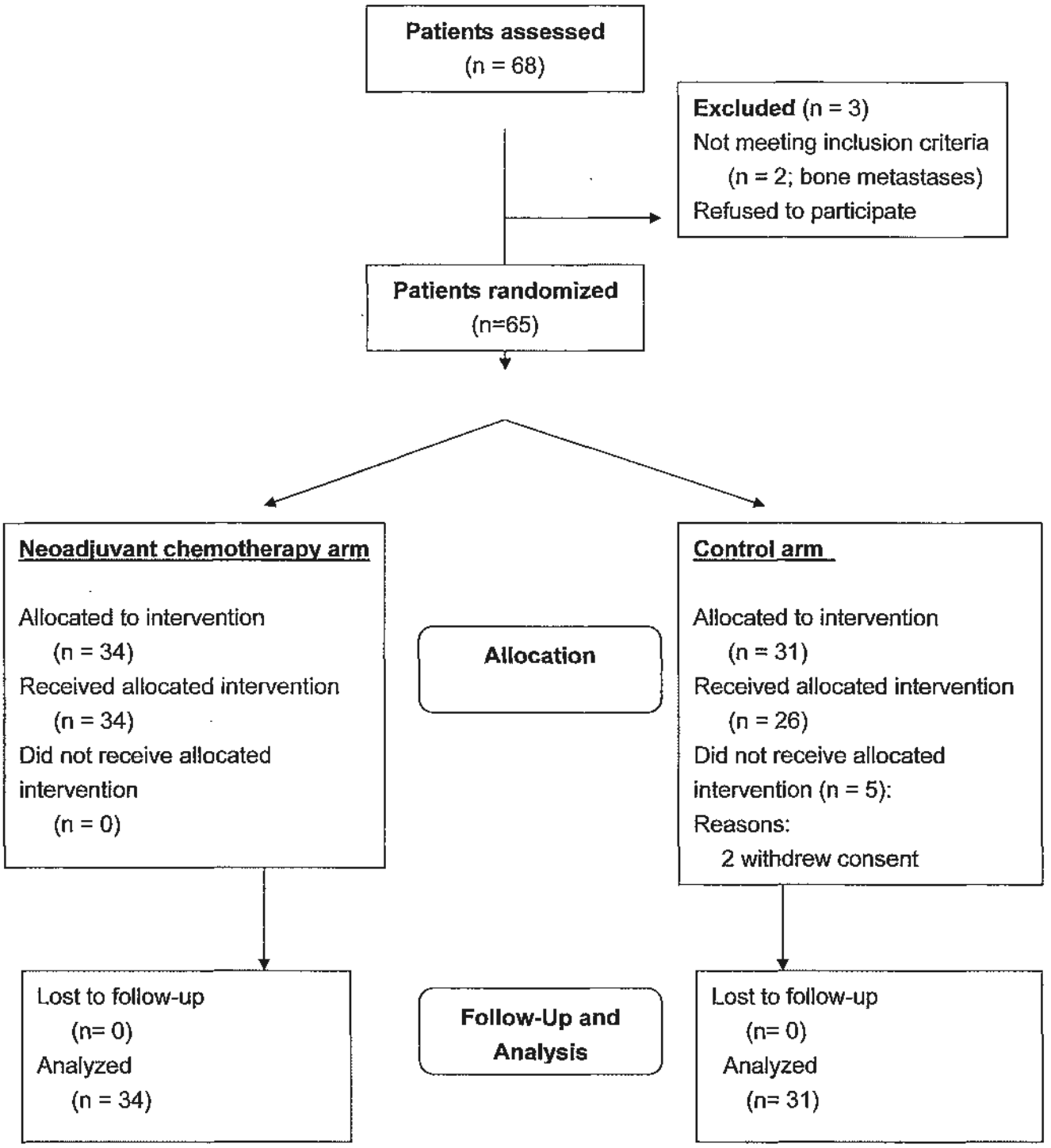

Figure 7.2

Mean relative dose intensities of cisplatin and docetaxel delivered during two cycles of neoadjuvant chemotherapy and eight weeks of cisplatin-radiotherapy (C = cisplatin 75 mg/m^2, D = docetaxel 75 mg/m^2, P = cisplatin 40 mg/m^2)

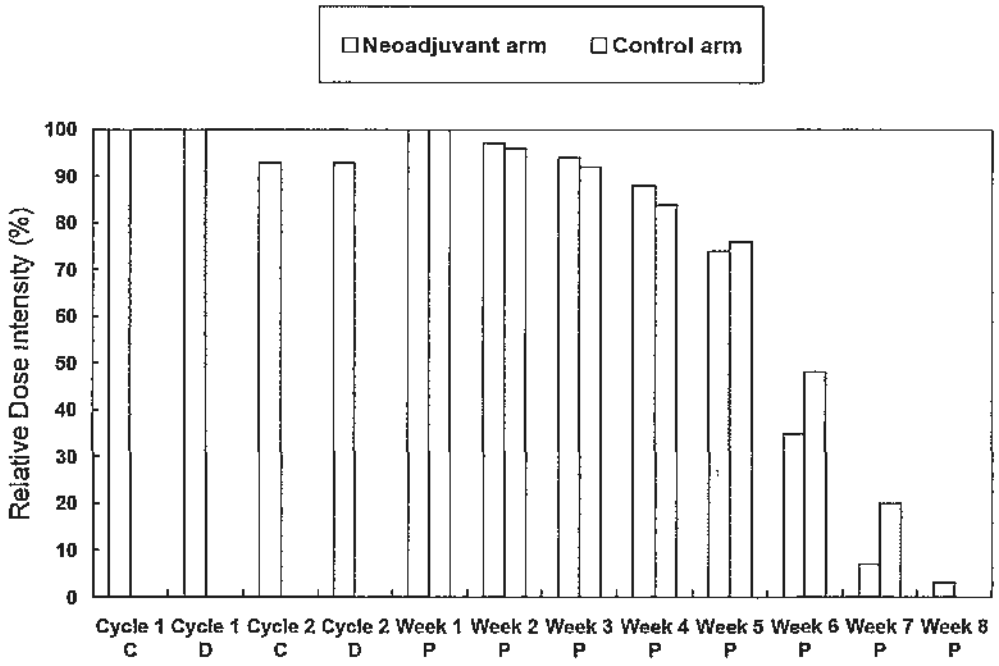

Figure 7.3

Survival curves for the two treatment arms.

a) Progression free survival. There was a trend for improvement of progression free survival in favour of neoadjuvant arm (log rank test, p=0.11).

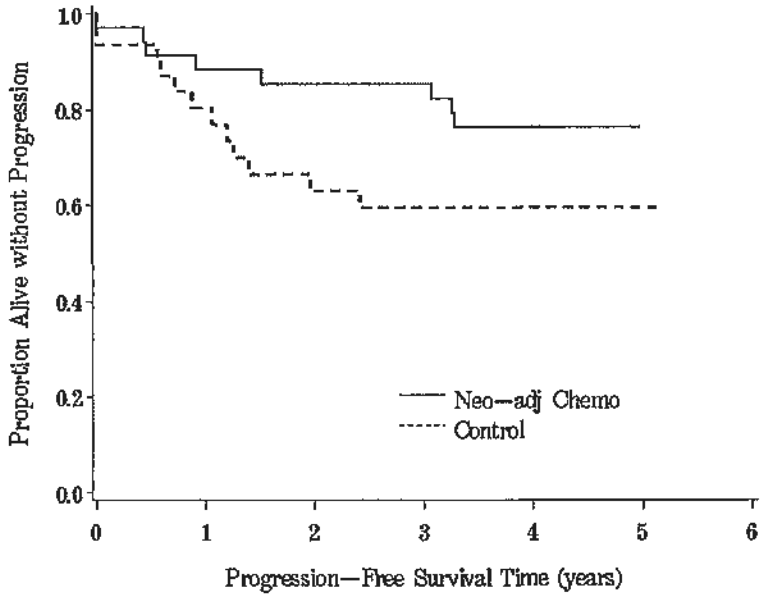

b) Overall survival. There was a significant improvement of overall survival in favour of neoadjuvant arm (log rank test, p=0.0066).

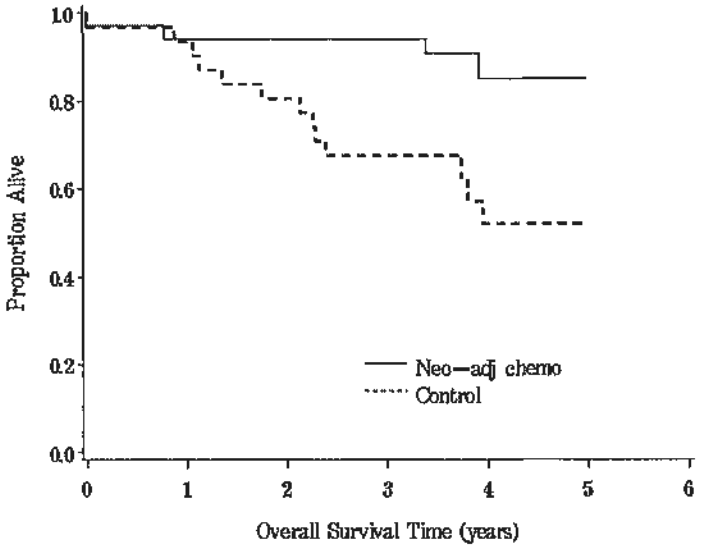

Figure 7.4

Randomisation chart (DC = docetaxel-cisplatin, RT = radiotherapy).

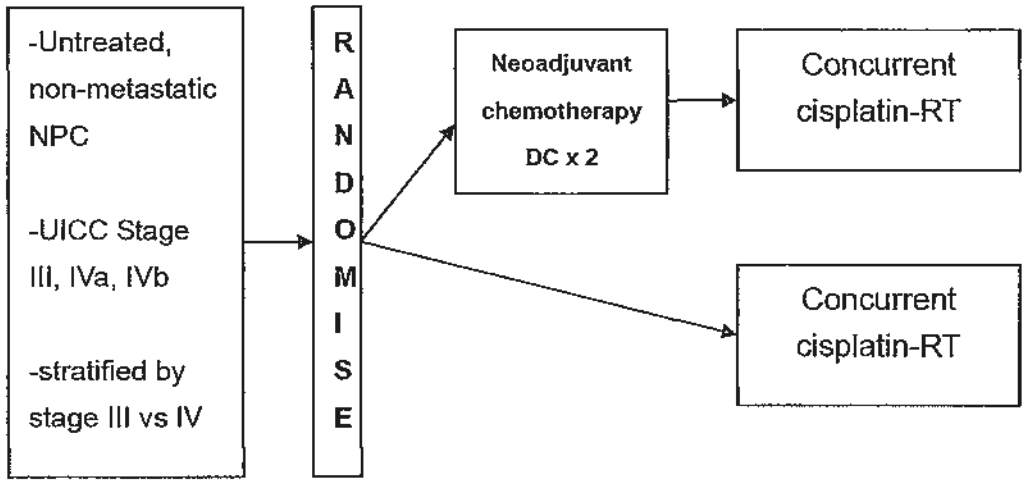

Figure 7.5

Treatment schema (D = docetaxel 75 mg/m^2, C = cisplatin 75 mg/m^2, P = cisplatin 40 mg/m^2, RT = radiotherapy).

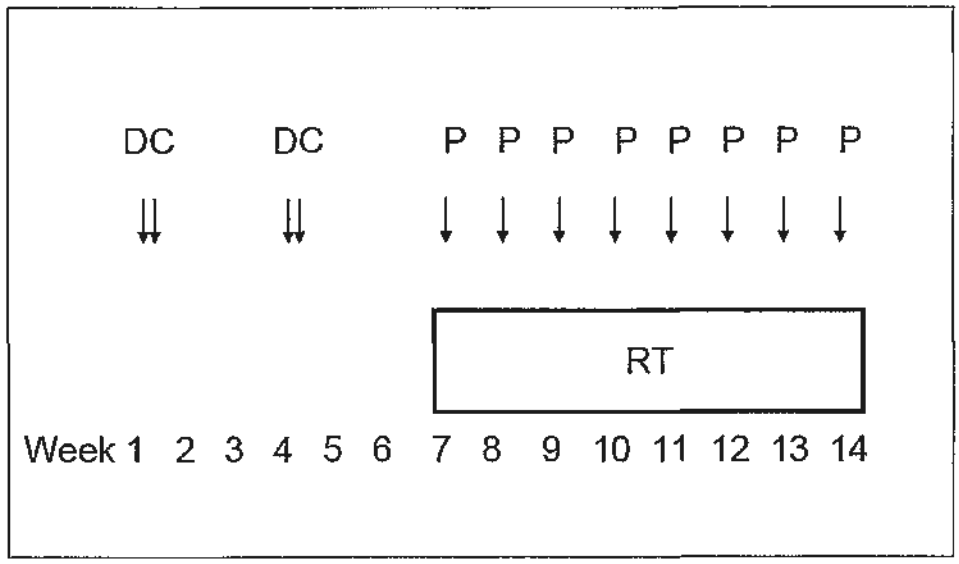

Figure 7.6

Changes in the global quality of life scores in the two treatment arms at 4 weeks, 12 months and 24 months. No significant difference was observed at each time point.

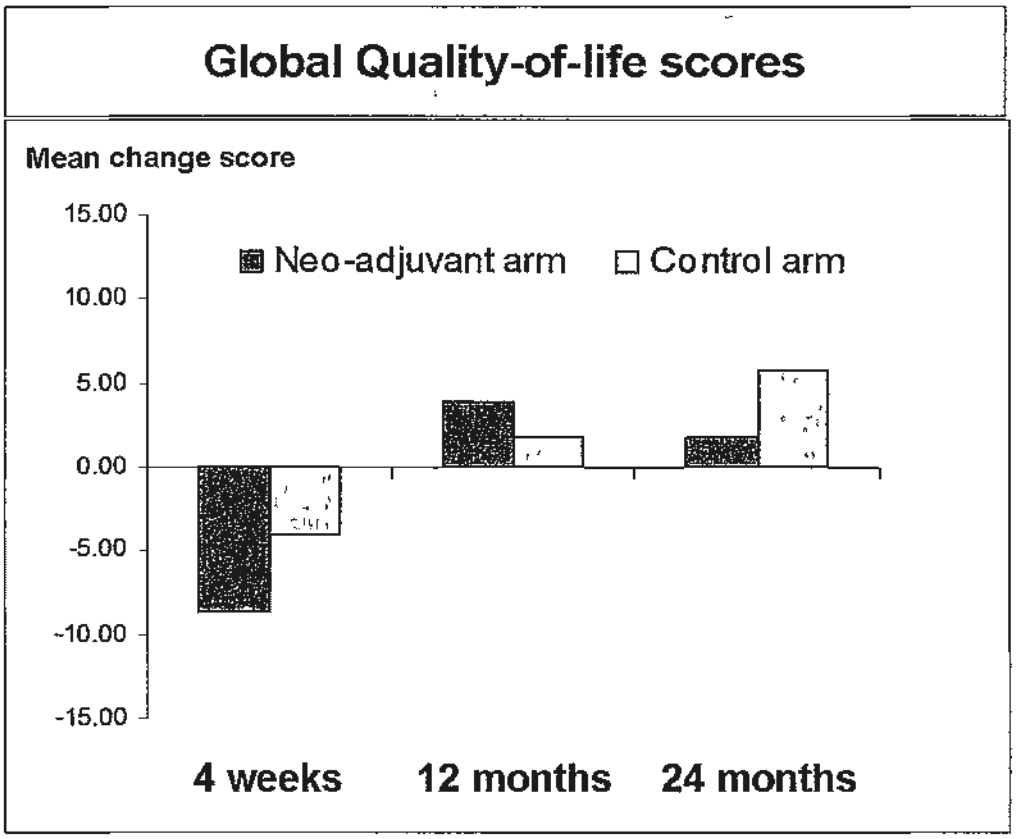

DISCUSSION

As explained in chapter 1, there has been a renewed interest in the re-exploration of neoadjuvant chemotherapy in advanced NPC. This has resulted from two observations. First, more effective chemotherapy regimens incorporating new agents have become available (summarized in Chapter 1, Table 1.3). The second has been the observation that with the use of high precision radiotherapy delivery such as with IMRT, coupled with the wide adoption of concurrent chemoradiation, the local control rate in NPC has improved and distant metastases has emerged as the predominant mode of treatment failures (discussed in chapter 3, study 1)(Hui et al. 2004; Kam et al. 2004).

Despite no significant improvement in overall survival was seen in all the published neoadjuvant chemotherapy trials, the body of available clinical evidence strongly supports neoadjuvant chemotherapy in terms of improvement in progression free survival (Chan et al. 1995; VUMCA-I 1996; Chua et al. 1998; Ma et al. 2001; Chua et al. 2005; Hareyama et al. 2002). Benefit has been seen in reduction of both local and distant failures (Chua et al. 2005). It is recognized that the selection and dosage of drugs may be crucial, as an over-toxic schedule has been shown to impair the delivery of subsequent radiotherapy and any possible benefit on survival may be

offset by increased treatment-related mortality as evidenced in the VUMCA experience (VUMCA-I 1996).

Several uncontrolled single arm phase 2 studies (Rischin et al. 2002; Oh et al. 2003; Ozturk et al. 2007; Xie et al. 2007), including our own report (Chan et al. 2004), have explored this sequential schedule of neoadjuvant chemotherapy followed by CRT approach in NPC. The results have been encouraging and toxicity has been acceptable. Except for the feasibility of this approach, it is difficult to draw further conclusion from these uncontrolled phase 2 data. There is also concern about the additional toxicity, cost, prolonged treatment duration, compliance, and impact on late physical function and quality of life that could result from this approach.

The results from this randomized phase 2 study suggest that neoadjuvant docetaxel and cisplatin chemotherapy followed by CRT is a highly feasible sequential strategy for advanced NPC. The increased acute toxicity during the neoadjuvant chemotherapy was mainly hematological (neutropenia and neutropenia fever) which was uncomplicated and manageable. Most importantly, this did not compromise the delivery of subsequent CRT. The hematological toxicity could be further ameliorated with the use of growth factor support and prophylactic antibiotics. The comparable

late toxicities and quality of life scores in both arms are encouraging. The preliminary results on pattern of failures suggest that the potential benefit of neoadjuvant chemotherapy is in the reduction of distant metastases (11.8% in the neoadjuvant arm versus 23.1-29.0% in the control arm, Table 7.5). There is a suggestion of a positive impact on progression free and overall survival although this needs to be confirmed in a definitive phase 3 trial.

[^{18}F]-fluorodeoxyglucose positron emission tomography (PET) was compared with conventional staging procedures (i.e. chest X-ray, abdominal ultrasound and bone scan) in the staging of advanced NPC and it was suggested that PET may be more sensitive in detecting distant metastases (Liu et al. 2006; Liu et al. 2007). Sixty-three of the 65 patients enrolled in this trial also participated in a parallel study of PET-CT scan and tumor marker study (Ma et al. 2006). No distant metastases were detected on PET-CT after conventional staging procedures at study entry. Therefore it would be unlikely that there was significant imbalance of occult distant metastases between the two treatment arms.

During the course of our study, two phase 2 studies have reported on the efficacy and toxicity of docetaxel and cisplatin combination as first line chemotherapy in patients

with recurrent or metastatic NPC.(McCarthy et al. 2002; Chua, Sham, and Au 2005) Hematological toxicity was reported to be severe but manageable in both studies without growth factor support. Interestingly, the combination was concluded as active with an overall response rate (ORR) of 62.5% and complete response (CR) rate of 6.3% in one study of 19 patients (Chua, Sham, and Au 2005), but was regarded as of low efficacy (22% ORR and no CR) in the other study which was prematurely terminated after accrual of only nine patients (McCarthy et al. 2002). This discrepancy was most likely a result of case selection. Our result concurs with the former study that docetaxel and cisplatin is an active regimen in NPC. Although this regimen may be better tolerated in the neoadjuvant setting as shown in our study, the use of growth factor support and/or prophylactic antibiotic to alleviate the hematological toxicity (neutropenia and neutropenic fever) is highly recommended.

Unlike the traditional cisplatin and infusional 5-flourouracil combination (PF), docetaxel and cisplatin combination can be conveniently given as out-patient without the need for a central venous catheter device. A recent phase 2 study from MD Anderson Cancer Centre has tested docetaxel and carboplatin combination as neoadjuvant therapy in NPC. Their result also confirmed that this regimen could be more conveniently given in the out-patient setting and was devoid of serious

non-hematological toxicity (Johnson, Garden et al. 2004).

Our study adopted a pure concurrent chemoradiotherapy as control arm. We used weekly cisplatin during the CRT. However, any conclusion on tolerability of this schedule may not necessarily be extrapolated to the intergroup regimen using high dose cisplatin regimen (100 mg/m^2 every 3 weeks) followed by 3 cycles of adjuvant chemotherapy (Al-Sarraf et al. 1998), another commonly used schedule in other trials (Wee et al. 2005; Lee, Lau et al. 2005).

It remains to be proven in head and neck cancer and in NPC, whether the addition of any neoadjuvant chemotherapy regimen to concurrent chemoradiotherapy improves the overall survival when compared to concurrent chemoradiotherapy alone in a phase 3 setting (Adelstein and Leblanc 2006; Glynne-Jones and Hoskin 2007). To answer the latter question, several phase 3 studies comparing a sequential approach of neoadjuvant chemotherapy followed by chemoradiotherapy versus chemoradiotherapy alone are ongoing in head and neck cancer (Specenier and Vermorken 2007; Cruz et al. 2008).

In NPC, a GORTEC multicenter phase 3 trial of neoadjuvant chemotherapy (TPF)

followed by concurrent weekly cisplatin-RT versus weekly cisplatin-RT alone has been ongoing. In a slightly different approach, the ongoing 0501 randomised phase 3 trial of the Hong Kong NPC study group is comparing the sequential strategy of induction-concurrent versus concurrent-adjuvant chemotherapy schedule in advanced NPC. These phase 3 studies designed with PFS as the primary endpoint, will define whether this sequential strategy of neoadjuvant (induction) chemotherapy followed by concurrent chemoradiation will become the future standard of care.

CONCLUSION

Our randomized phase 2 study showed that a sequential strategy of neoadjuvant chemotherapy followed by CRT was well tolerated with a manageable toxicity profile that allowed subsequent delivery of full dose CRT. Preliminary results suggested a positive impact on survival. However, the limitation of a randomized phase 2 study designed with the incidence of toxicity as the primary endpoint should be noted. Phase 3 studies to definitively test this neoadjuvant-concurrent strategy are ongoing.

Chapter 8

Study 6: Targeting Tumor Angiogenesis - Preclinical Study

BACKGROUND

In previous chapters, we have demonstrated that hypoxia was a regulator of VEGF expression in NPC cells (chapter 4, study 2). We have further showed that overexpression of VEGF in NPC tumor biopsies (>60% cases) was associated with expression of hypoxia markers (e.g. HIF-1a and CA IX), and poor outcome after radiotherapy (chapter 5, study 3). Other studies have also implicated the significance of VEGF/VEGFR signaling in NPC pathogenesis (Murono et al. 2001; Ma et al. 2003; Foote et al. 2005; Krishna, James, and Balaram 2006). VEGF receptors (Flt-1 and KDR), as well as its ligand VEGF, were widely expressed in 66 - 90% of NPC tumors and correlated with clinical features and poor prognosis in NPC patients (Sha and He 2006). Although the expression of VEGF receptors (Flt-1 and KDR) cannot be captured in *in vitro* models of NPC for reasons to be investigated (Xiao et al. 2007), preclinical studies have demonstrated the effectiveness of anti-angiogenesis therapy (Qian et al. 1998; Qian et al. 1999). In NPC patients, VEGF has been associated with angiogenesis and lymph node metastases (Wakisaka et al. 1999), as well as distant metastases (Guang-Wu et al. 2000). Finally, serum levels of VEGF were significantly

elevated in male patients with metastatic NPC (Qian et al. 2000).

The expression of PDGF receptor and c-kit has been detected in NPC tumors, cell lines or tumor xenograft (Bar-Sela et al. 2003; Sheu et al. 2005; Sheu et al. 2007; Mocanu et al. 2007). Although the functional involvement of these receptors in NPC pathogenesis remains to be elucidated in details, a preclinical study with STI571 (imatinib mesylate, with known inhibitory activity against the tyrosine kinase abl, or the chimeric bcr-abl, as well as PDGF receptor and c-kit) (Sheu et al. 2007) showed that it can inhibit NPC cell growth as well as c-kit activation. Similarly, inhibition of PDGFR-β activation has been demonstrated with STI571 in an *in vivo* model of NPC (Mocanu et al. 2007). Combination of STI571 with cisplatin, but not STI571 alone, has been shown to significantly reduce the growth of an NPC xenograft model (HONE-1) (Sheu et al. 2007), suggesting STI571 may not be the best agent to target PDGF receptor and c-kit in NPC.

Sunitinib malate (Sutent®, SU11248, Pfizer, NY, USA) is an orally available, multi-targeted receptor tyrosine kinase (RTK) inhibitor of vascular endothelial growth factor receptors (VEGFR1-3), platelet-derived growth factor receptors (PDGFRα and PDGFRβ), stem cell factor receptor (c-kit), glial cell-line derived neurotrophic factor

receptor (REarranged during Transfection; RET). Sunitinib is currently approved for the treatment of advanced renal cell carcinoma (RCC) and imatinib resistant or intolerant gastrointestinal stromal tumour (GIST) in multiple countries. Preclinical and/or clinical studies have demonstrated the effectiveness of this agent as many of these RTKs are key players in the progression of some of these tumour types, linking the multi-RTK-inhibitory effects of sunitinib with its antitumour activity (Mendel et al. 2003; Potapova et al. 2006; Christensen 2007; Faivre et al. 2007; Chow and Eckhardt 2007).

Sunitinib selectively inhibits signaling through VEGF, PDGF and c-kit receptors. It may exert direct antitumor activity against tumor cells that rely on these RTKs for proliferation and/or survival, but it is also able to indirectly inhibit tumor growth by inhibiting angiogenesis. The latter antitumor mechanism is supported by inhibitory effect of sunitinib on VEGFR and PDGFR (Mendel et al. 2003; Potapova et al. 2006; Christensen 2007). Therefore, sunitinib-mediated inhibition of these multi-RTK targets, even in the absence of potential activating mutations, is anticipated to result in broad antitumor efficacy in NPC. Based on the above information, we hypothesized that sunitinib would exhibit antitumor activity in preclinical models of NPC. The combination of sunitinib with chemotherapy agent may offer additive antitumor activity

owing to the different modes of action of sunitinib and chemotherapy.

MATERIALS AND METHODS

Drugs, chemicals and antibodies

Sunitinib was obtained from Pfizer Pharmaceuticals (New York, USA). Cisplatin (Mayne Pharma Pty, Ltd, VIC, Australia) and docetaxel (Taxotere®, sanofi-aventis, France) was obtained as commercial products from our hospital pharmacy. RPMI medium and fetal bovine serum (FBS) was from Hyclone, Thermo Fisher Scientific (Logan, Utah, USA). Sodium pyruvate (10mM), penicillin (50 IU/ml) and streptomycin (50 µg/ml), and 3-(4,5-dimethylthiazol-2-yl)-2, 5-diphenyltetrazolium bromide (MTT) were from Invitrogen (Gaithersburg, MD, USA). Supersignal West Pico Chemiluminescence Western blotting detection reagent was from PIERCE, Thermo Fisher Scientific (Rockford, IL, USA). Antibodies for phospho-c-kit (Tyr719) and cleaved PARP were obtained from Cell Signaling Technology (Danvers, MA, USA). Anti-phospho-PDGFRβ (Try716) was from Upstate, Millipore (Billerica, MA, USA). Anti-ß-actin antibody was from Calbiochem, Merck (Gibbstown, NJ, USA). PDGFRβ, c-kit, RET and pi-RET (Tyr1062) were from Santa Cruz Biotechnology (Santa Cruz, CA, USA).

Drug preparation and cell culture

Sunitinib was dissolved in DMSO at a stock concentration of 30 mM and stored in aliquots at -20°C as recommended by the manufacturer. Cisplatin was prepared as a 1 mg/ml stock solution in 0.9% NaCl and docetaxel was prepared as a 40 mg/ml stock solution in 13% ethanol. Drug aliquots were diluted in corresponding medium just before addition to cell cultures. Human NPC cell lines (HK-1, CNE-2, HONE-1, CNE-1, and C666-1) were cultured at 37°C, 5% CO_2 in RPMI with 10% fetal bovine serum (FBS). CNE-2 (Sizhong, Xiukung, and Yi 1983) and HONE-1 cell line (Glaser et al. 1989) were established from poorly differentiated nasopharyngeal carcinomas. C666-1 was established from undifferentiated nasopharyngeal carcinoma and consistently carried the Epstein-Barr virus in long-term cultures (Cheung et al. 1999). CNE-1 (Xiao et al. 2007) and HK-1 (Huang et al. 1980) cell lines was established from well-differentiated squamous nasopharyngeal carcinomas.

Proliferation assay

NPC cells were cultured in 48-well plates (300-7000 cells per well) in respective culture medium. Sunitinib or cisplatin in complete medium was added to the cells 24 hours after plating and incubated at 37°C with 5% CO_2 for 72 hours. Cell proliferation was assessed by MTT assay as previously described (Sung et al. 2005). Percentage

of cell growth inhibition was calculated as $(OD_{vehicle} - OD_{drug})/OD_{vehicle}$ x 100%. The IC_{50} value was defined as the drug concentration resulting in 50% of maximal growth inhibition as determined from the dose-response curve generated by the PRISM4 Software (GraphPad, California, USA). Each assay was repeated in more than three independent experiments.

Western blot analysis

NPC cells were treated at various drug doses according to the individual study. Cell lysates were collected for Western blotting as previously described (Lui et al. 2007). Fifty μg of total protein (100 μg for PDGFRβ) was used. For the detection of apoptosis, cleaved poly(ADP-ribose) polymerase (PARP) expression was analysed with cleaved PARP antibody. The blot was developed with SuperWest Pico chemiluminescent substrate by autoradiography. Each assay was repeated in three independent experiments.

Cell cycle analysis

Cell cycle analysis was performed as previously described (Wong et al. 2009). NPC cell lines HONE-1 or CNE-2 were plated in 100-mm^2 Petri dishes at 3-4x10^5 and treated with increasing concentrations of sunitinib. Cells were collected at 24 hour

after drug treatment and fixed with 70% cold ethanol. DNA staining was performed with a solution containing RNase (0.2 mg/ml) and propidium iodide (0.05 μg/ml). Analysis was performed using a FACScan flow cytometer while data of cell cycle were processed with CELLQuest software (Becton Dickinson). Assay was repeated in three independent experiments.

Tumor xenograft studies

All xenograft experiments were conducted under license from the Hong Kong Department of Health and according to approval given from the Animal Experimentation Ethics Committee of the Chinese University of Hong Kong. Female athymic nude mice (nu/nu) of six-week old weighing about 20 g were supplied and housed by the Laboratory Animal Services Centre of the Chinese University of Hong Kong. CNE-2 cells (6×10^5 cells resuspended in 50 μl of HBSS-buffer) were inoculated subcutaneously into the flanks of the nude mice. When tumors were established (reaching a tumor volume of 50-80 mm^3), animals were randomized into 2 groups. The mice in each group were given either the vehicle control (carboxymethylcellulose sodium 0.5% (w/v)) or sunitinib (80 mg/kg) by oral gavage for five days a week for 2 weeks. Docetaxel 10mg/kg was applied to the mice by intraperitoneal injection (in a volume of 200 μl of 0.9% NaCl) every 2 days. Control group received the 200 μl 0.9%

NaCl. The body weight of the mice and tumor size were measured (by a digital caliper) and recorded every 2 days. Tumor volume was calculated using the equation $V = (a \times b^2)/2$, where *a* is the longest dimension and *b* the perpendicular diameter of the tumor. Fractional tumor volume was calculated as the ratio of the original tumor volume before drug treatment/ tumor volume post drug treatment.

Microvessel density (MVD)

Tumor specimens for MVD evaluation were fixed in 10% buffered formalin before routine processing and sectioning. General tissue morphology and pathological changes were examined by haematoxylin and eosin (H&E) staining. Tumor microvessel densities were assessed by counting 5 areas of IHC stained microvessels using rat against mouse anti-CD34 antibody (1:100 dilution, sc-18917, Santa Cruz Biotechnology Inc. Santa Cruz, CA 95060, USA.). The average MVD expressed as number of MVD / x200 field was calculated for each xenograft specimen.

Statistical analysis

The difference between treatment and control groups were compared by the unpaired t-test with Welch correction. Chi-squared test was used to compare the *in vivo* tumor

response in Table 8.2. Mann-Whitney U test was used to compare the median MVD between control and sunitinib treated tumors. Statistical analyses were performed using PRISM4 software (GraphPad, La Jolla, CA). Results were considered statistically significant with $P < 0.05$.

RESULTS

Molecular targets identification of sunitinib in NPC cell lines

The basal level of protein expression for the receptor tyrosine kinase targets of sunitinib including total and phosphorylated PDGFR, c-kit and RET, were studied in a panel of five NPC cell lines (HK1, CNE-2, HONE-1, CNE-1 and C666-1). As shown in Figure 8.1, HONE-1 and CNE-2 cells showed the highest level of expression for phosphorylated PDGFRβ. HK1, CNE-2 and C666-1 showed the highest expression for phosporylated c-kit. C666-1, HK1, HONE-1 and CNE-1 showed the highest expression of phosphorylated RET. Based on the these results of target identification, we have chosen HONE-1 and CNE-2, both derived from poorly differentiated NPC, for subsequent preclinical evaluation of sunitinib.

Dose dependent inhibition of NPC cell proliferation by sunitinib

The effect of sunitinib on cell growth was assessed by MTT assay. A panel of five

human NPC cell lines (HK1, CNE-2, HONE-1, CNE-1, and C666-1 at 0.3-7.0 x 10^4 cell/well in complete RPMI medium) were treated with sunitinib (at increasing concentrations from 0-60 μM) or vehicle control (DMSO) for 72 hours. Sunitinib demonstrated a steep dose response relationship with dose-dependent growth inhibition in all five NPC cell lines (Fig 8.2a). The IC_{50} of sunitinib ranged from 2-7.5 μM, and the maximal achievable growth inhibition was ≥ 97% in all NPC cell lines tested (Table 8.1).

Effect of sunitinib on cell cycle progression and apoptosis in NPC

Significant cell cycle arrest was observed at the G_0/G_1 phase when HONE-1 and CNE-2 cells were treated with sunitinib for 24 hours (Fig 8.2b and 8.2c). This was accompanied by a concomitant reduction of cell populations at S and G_2/M phases. Sunitinib also induced apoptosis in NPC cells as evidenced by the induction of PARP cleavage as early as 24 hrs (Fig 8.2d).

***In vitro* activity of sunitinib in combination with chemotherapy**

Sunitinib was found to moderately enhance the growth inhibitory effect of cisplatin in both HONE-1 and CNE-2 cells, when treated with sunitinib alone, cisplatin alone, or the combination ($p < 0.01$, Fig 8.3a and 8.3b). However, the combination effect was

less than additive when compared with either agent alone, and there was no synergism. Similar result was observed when sunitinib was combined with docetaxel, in which the combination also showed a less than additive effect (data not shown).

***In vivo* activity of sunitinib in NPC xenograft**

Nude mice bearing established CNE-2 tumors (average tumor volume of about 50-80 mm^3) were given either vehicle control or sunitinib by oral gavage for 5 days/week for 2 weeks. Sunitinib demonstrated significant growth inhibition of NPC tumor in a CNE-2 xenograft model in nude mice. The growth inhibition of sunitinib was found to be dose-dependent, increasing from 20 mg/kg to 40 mg/kg and was maximal at the highest dose of 80 mg/kg (data not shown). The tumor growth of sunitinib-treated group was significantly suppressed in comparison with the control group (Fig 8.4a). There was no significant difference in body weight of the mice between sunitinib-treated and control groups (Fig 8.4b), indicating a good tolerability of sunitinib at 80mg/kg repeated dosing in mice. No gross toxicity was observed except for a general pale coloration in the sunitinib-treated animals (Fig 8.4c), which was a known phenomena due to a yellow discoloration imparted by the sunitinib compound itself.

We next examined the number of tumors having response to sunitinib treatment by calculating the ratio of pre-treatment tumor size / post-treatment tumor size for each individual tumor (fractional tumor volume). A fractional tumor volume of ≤ 1 indicates reduction in tumor size when compared to its pre-treatment size. Our cumulative results showed that upon sunitinib treatment (80 mg/kg), 9/33 (27%) tumors had a fractional tumor volume ≤ 1 compared to 0/31 (0%) in the vehicle treated control ($p=0.002$, Chi-squared test). Among the 9 tumors with measurable response to sunitinib, 1 tumor had a complete regression (Table 8.2).

Sunitinib treatment induced a significant reduction in MVD in CNE2 NPC xenograft as compared with vehicle treated control (Figure 8.5). The median MVD was 6.7 in the sunitinib treated tumors versus 18.6 in the vehicle treated control tumors ($p=0.0007$, Mann-Whitney U test). Moreover, extensive area of necrosis was frequently observed under the microscope in the sunitinib treated tumor xenograft (Figure 8.6) while necrosis was only rarely seen in the control tumor xenograft.

When sunitinib was combined with docetaxel at each of their efficacious dose, the antitumor efficacy of sunitinib alone and the combination was found to be similar, and the anti-tumor efficacy of sunitinib alone was higher than docetaxel alone. However

the combination of sunitinib and docetaxel induced acute toxicity with death of mice occurred in the combination group before the end of experiments (data not shown).

Table 8.1

Summary of the average IC_{50} values of sunitinib and the maximum growth inhibition (at 60 μM of sunitinib) in a panel of human NPC cell lines (HK1, CNE-2, HONE-1, CNE-1, and C666-1). Similar results were obtained in more than three independent experiments.

Cell lines	**Average IC_{50} (μM)**	**Maximum Growth Inhibition (at 60 μM)**
HK1	2.06 ± 0.29	97.8 ± 0.8%
CNE-2	3.45 ± 0.11	98.7 ± 0.5%
HONE-1	4.07 ± 1.07	97.1 ± 1.1%
CNE-1	2.60 ± 0.38	98.3 ± 0.5%
C666-1	7.57 ± 1.74	98.5 ± 0.4%

Table 8.2

Summary of *in vivo* tumor response in NPC xenografts. Fractional tumor volume represents change in tumor volume compared to its pretreatment volume, and value less than one indicates response to drug treatment.

Treatment arm	No of tumors with fractional tumor volume ≤ 1 (%)
(1) Vehicle control	0/31 (0%)
(2) Sunitinib (80 mg/kg)	*9/33 (27%)

(* among the 9 tumors that are responding to sunitinib, one demonstrated complete regression with a fractional tumor volume = 0).

Figure 8.1

Basal expression level of total and phosphorylated PDGFRβ, c-kit and RET in NPC cell lines. Both total and phosphorylated forms of PDGFRβ, c-kit and RET were detected by immunoblotting in a panel of 5 human NPC cell lines (HK1, CNE-2, HONE-1, CNE-1 and C666-1). Beta-actin was used as a control.

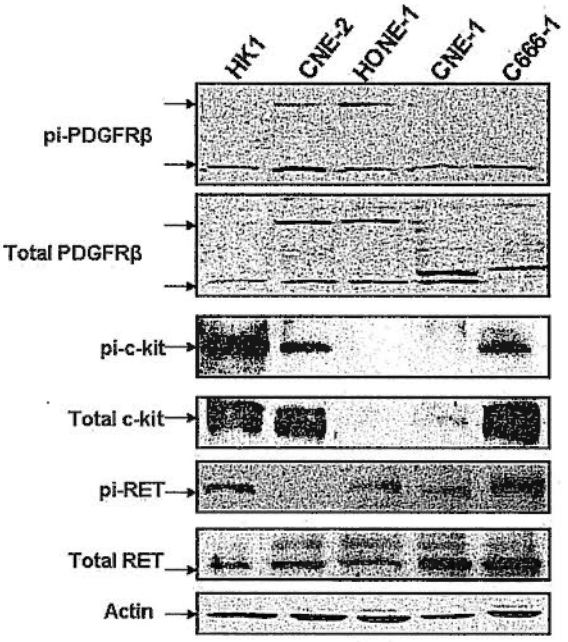

Figure 8.2 (a)

(a) Dose-dependent inhibition of NPC cell proliferation by sunitinib. A panel of 5 human NPC cell lines, HK1, CNE-2, HONE-1, CNE-1, and C666-1 (0.3-7.0 x 10^4 cells/well in complete RPMI medium), were treated with sunitinib (0-60 μM) / vehicle control (DMSO) for 72 hours. The effect of sunitinib on cell growth was assessed by MTT assay. Similar results were obtained in more than three independent experiments.

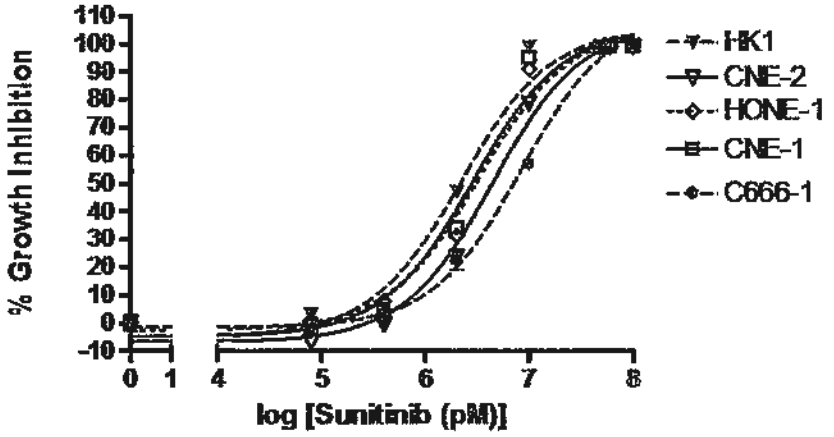

Figure 8.2 (b, c)

Sunitinib induces G_0/G_1 arrest in NPC cell lines. HONE-1 (b) and CNE-2 cells (c) were treated with sunitinib (3 μM) or corresponding DMSO control for 24 hours. Cell cycle arrest at G_0/G_1 phase was observed in sunitinib-treated cells, when compared to DMSO control. Similar results were obtained in three independent experiments.

Figure 8.2 (b)

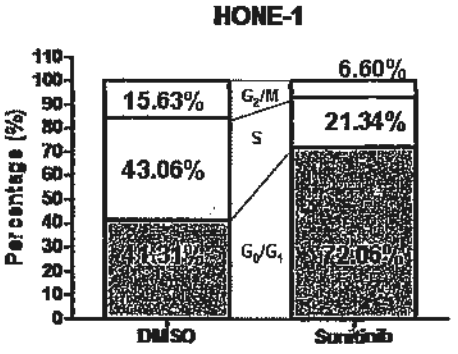

Figure 8.2 (c)

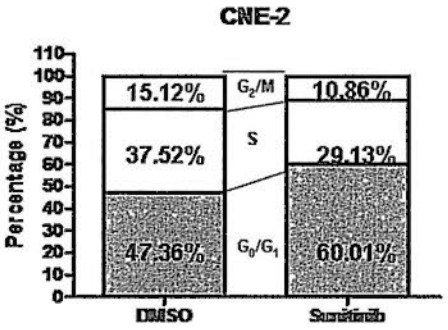
CNE-2
Percentage (%)
110
100
90
80
70
60
50
40
30
20
10
0
15.12%
37.52%
47.36%
G2/M
S
G0/G1
10.86%
29.13%
60.01%
DMSO

Figure 8.2 (d)

(d) Sunitinib induces PARP cleavage in HONE-1 and CNE-2 cells. HONE-1 and CNE-2 cells were treated with sunitinib (3 μM) or corresponding DMSO control for 24 hours. Sunitinib-treated cells expressed a higher level of cleaved PARP expression when compared to DMSO control. Similar results were obtained in three independent experiments.

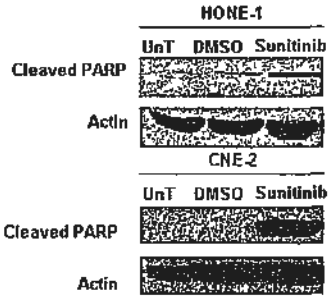

Figure 8.3 (a, b)

Sunitinib moderately enhanced the cytotoxic effects of cisplatin in (a) HONE-1 and (b) CNE-2 cells. HONE-1 and CNE-2 cells were treated with sunitinib (3 μM) and cisplatin (0.35 μg/ml) for 72 hours. Corresponding DMSO control + cisplatin vehicle control (9 mg/ml NaCl, 1mg/ml mannitol) was used as control. By MTT assay, sunitinib was found to moderately enhance the growth inhibitory effect of cisplatin in both HONE-1 and CNE-2 ($p<0.01$). Similar results were obtained in three independent experiments.

Figure 8.3 (a)

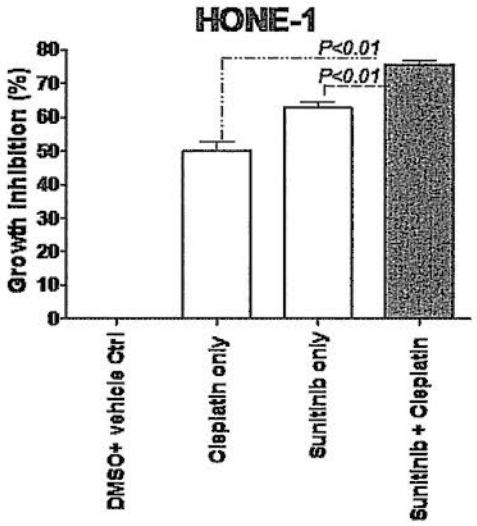

Figure 8.3 (b)

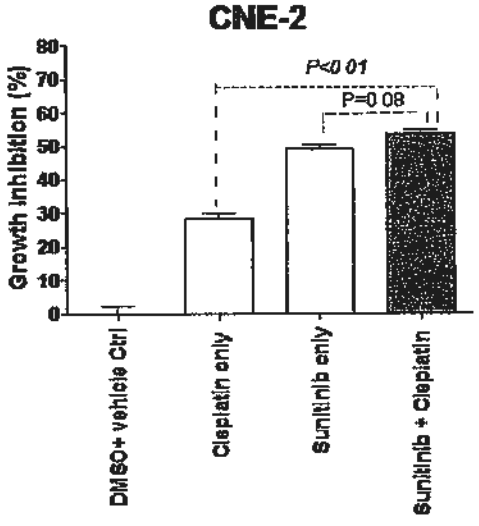
CNE-2
Growth inhibition (%)
80
70
60
50
40
30
20
10
0
P<0.01
P=0.08
DMSO+ vehicle Ctrl
Cisplatin only
Sunitinib only
Sunitinib + Cisplatin

Figure 8.4 (a)

Sunitinib inhibits *in vivo* tumor growth in a CNE-2 xenograft model in nude mice. Nude mice bearing established CNE-2 tumors (average tumor volume of about 50-80 mm^3) were given either vehicle control (0.5% CMC (w/v), n = 12 tumors) or sunitinib (80 mg/kg, n = 16 tumors) by oral gavages for 5 days/week for 2 weeks. The body weight of the mice and tumor size were measured and recorded every 2 days.

(a) The tumor growth of sunitinib-treated group was significantly reduced in comparison with the control group (* P<0.05, ** P<0.01).

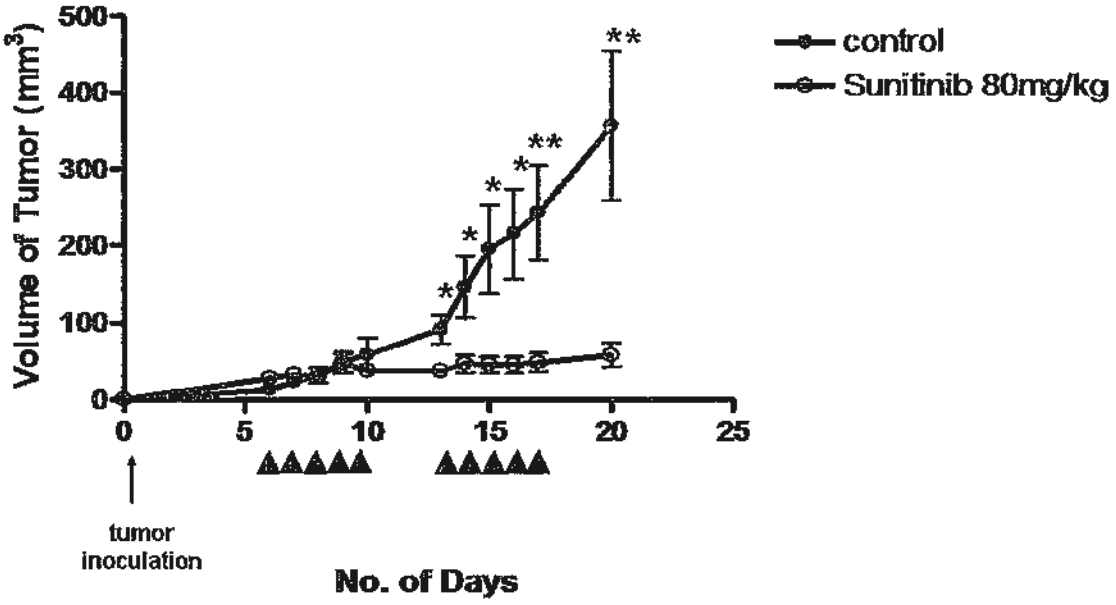

Figure 8.4 (b)

(b) No significant difference was observed in body weight of the mice between sunitinib-treated and control groups.

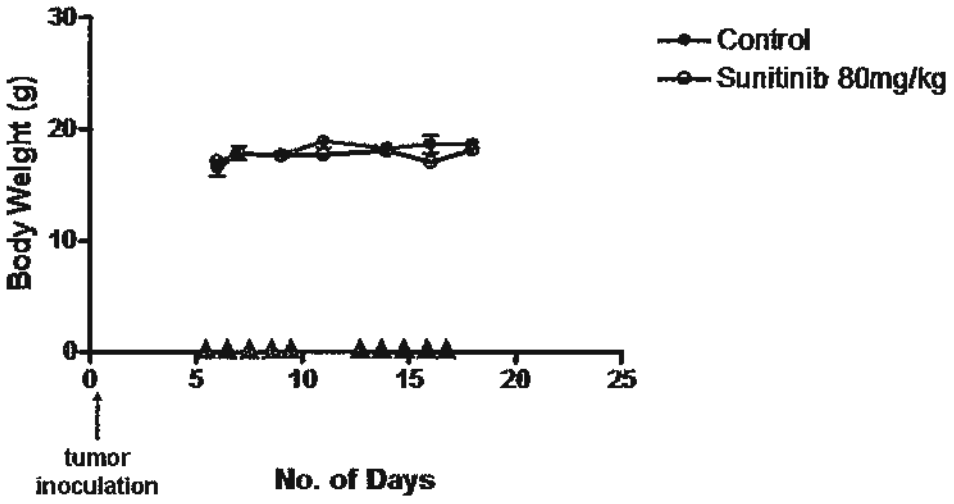

Figure 8.4 (c)

(c) Representative nude mice with CNE-2 xenograft at day 20 after vehicle control / sunitinib treatment.

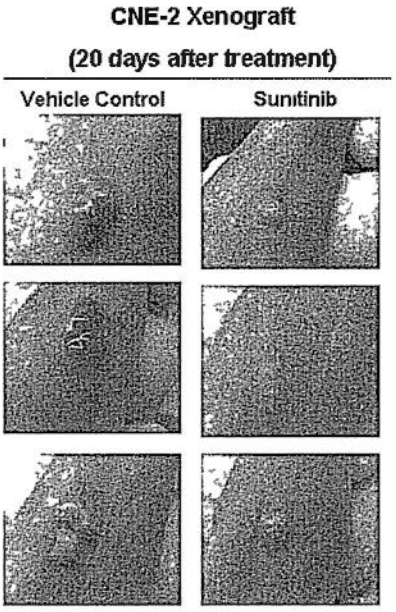

Figure 8.5

CD34 immunostaining for microvessel density (MVD) in CNE-2 NPC xenograft at day 20 after (a) vehicle control, and (b) sunitinib treatment.

(a) Vehicle control

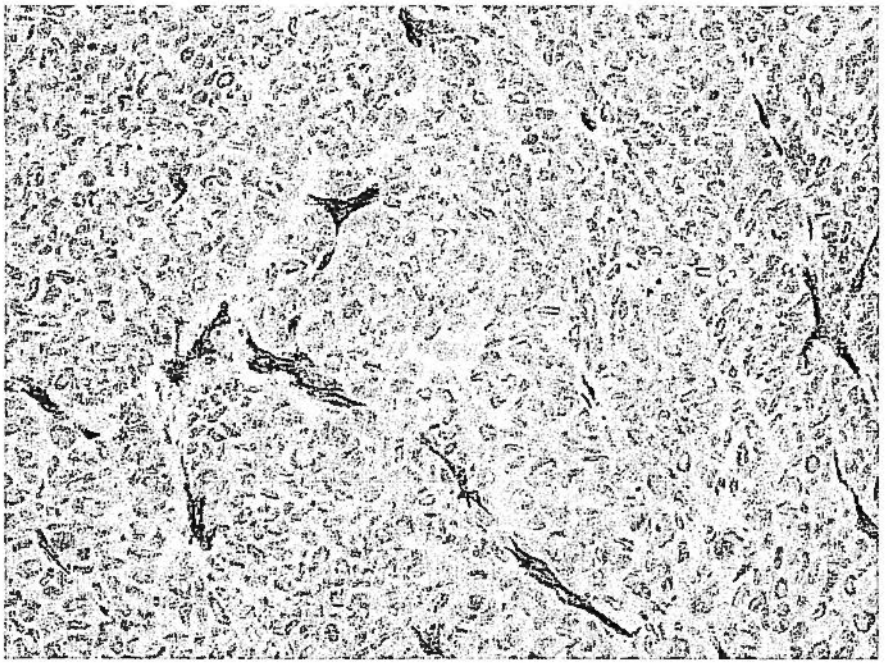

(b) Sunitinib treatment

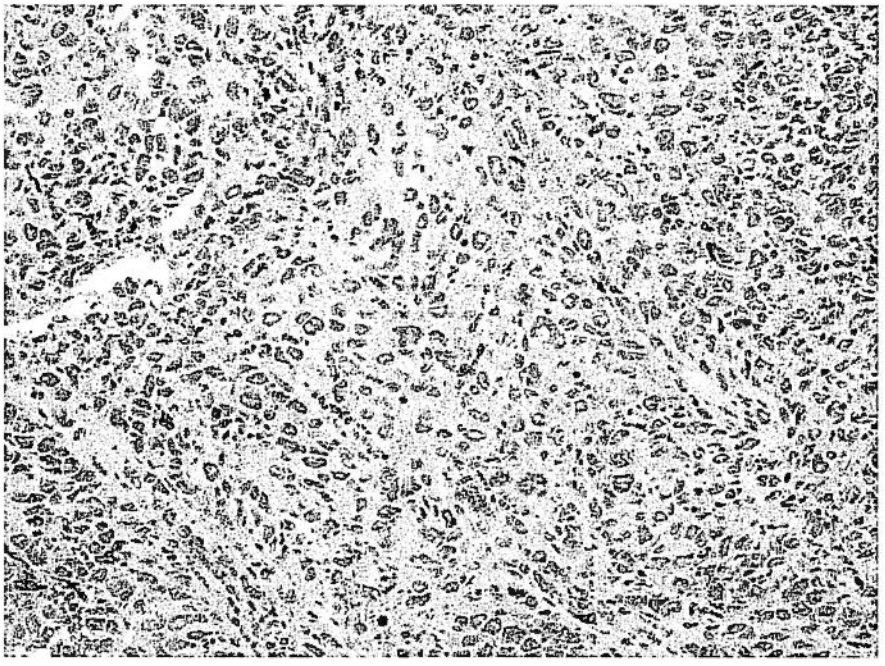

Figure 8.6

Extensive area of necrosis (N) within the tumor (T) in the sunitinib treated NPC xenograft (Haematoxylin and Eosin stain, x200 magnification).

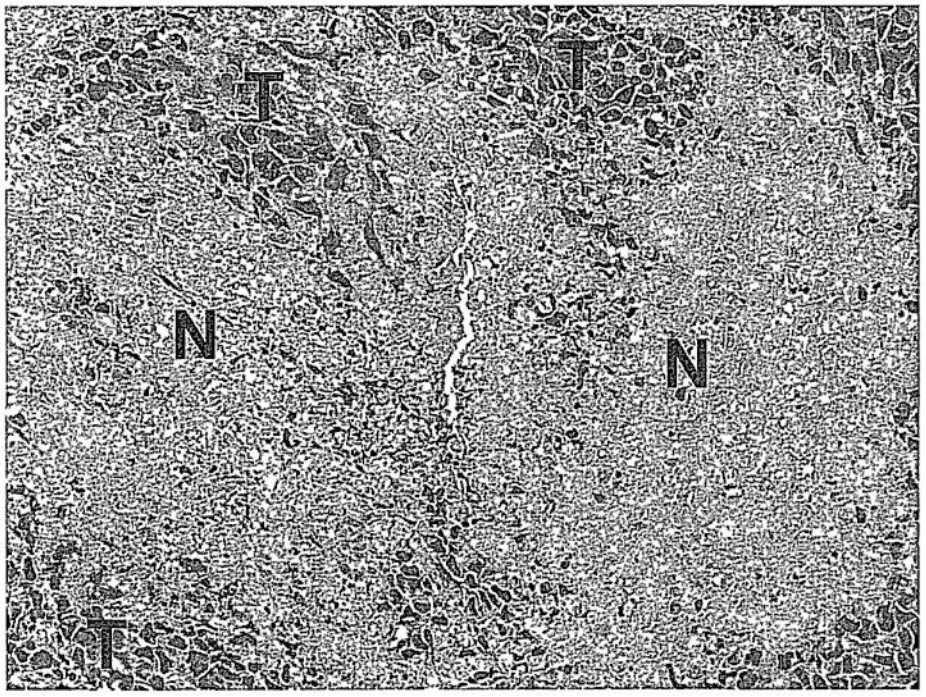

DISCUSSIONS

Following the success story of imatinib in chronic myelogeneous leukemia (CML) and GIST, receptor tyrosine kinase inhibitors are a new and promising class of therapeutic agents for the treatment of solid tumors and hematological malignancies. Sunitinib, a small-molecule multi-targeted tyrosine kinase inhibitor with activity against VEGFR, PDGFR, c-kit, and RET, is approved for the treatment of advanced RCC and imatinib-resistant GISTs, and is currently evaluated for the treatment in a variety of solid tumors and acute myelogenous leukemia (Faivre et al. 2007; Chow and Eckhardt 2007).

In this preclinical study, we evaluated the growth inhibitory activity of sunitinib as a single agent or in combination with cisplatin or docetaxel in NPC cell lines and xenografts. We found that the IC_{50} values of sunitinib in NPC cell lines ranged from 2-7.5 μM, and the maximum growth inhibition was greater than 97% at sunitinib concentration of 60 μM. The data indicated the effectiveness of sunitinib in inhibiting NPC cell growth. This is further supported by our *in vivo* finding that sunitinib alone was effective in suppressing tumor growth in nude mice without significant toxicity. Results from this preclinical study suggested that sunitinib is a promising agent for NPC.

NPC cells exhibited sensitivity towards sunitinib in the low micromolar (μM) range in our cell line study, similar to previously reported in small cell lung cancer (SCLC) and hematologic malignancies (Abrams, Lee et al. 2003; Ikezoe et al. 2006). Although some studies demonstrated sunitinib sensitivity in the nanomolar (nM) range in certain cancer cell lines, the underlying molecular mechanism contributing to the higher *in vitro* sensitivity in these cells is not fully understood. In some cases, higher sensitivity towards sunitinib may be contributed by differences in the experimental conditions (e.g. ligand-dependent proliferation or serum free medium) (O'Farrell et al. 2003; Abrams, Lee et al. 2003; Mendel et al. 2003; Maris et al. 2008). Nevertheless, the *in vivo* model of NPC demonstrated good sensitivity towards sunitinib treatment at 80mg/kg. Our *in vivo* effective dose (at 80 mg/kg) of sunitinib was similar to several previous studies in several other tumor models, where 40-80 mg/kg was known to induce substantial inhibition of target RTK phosphorylation (Abrams, Lee et al. 2003; Abrams, Murray et al. 2003; Murray et al. 2003; Cumashi et al. 2008; Guerin et al. 2008; Sonpavde et al. 2008; Mendel et al. 2003).

Sunitinib induced cell cycle arrest at the G_0/G_1 phase in NPC cells. This may have explained the lack of synergism when we combined sunitinib with cisplatin or

docetaxel in NPC cells. Because the cytotoxic cisplatin or docetaxel were expected to be most active in dividing cells, the halting of cell cycle progression by sunitinib is likely to contribute to the lack of additive or synergistic effect on cell growth with cisplatin/docetaxel. On the other hand, as sunitinib is usually administered as 4-weeks on and 2-weeks off (4/2) schedule, and clinical tumor progression was often observed during the 2-week off drug period. One could explore a sequential administration schedule of giving cytotoxic chemotherapy during the 2 week off-drug period of sunitinib. In this way, one may potentially exploit the synchronous burst in tumor cell proliferation and/or accelerated repopulation after stopping sunitinib. A recent study in tumor xenografts showed that sunitinib treatment improved microhemodynamics and blood flow in tumor vessels that escape therapy leading to improved vascular delivery of chemotherapy (Czabanka et al. 2009). Further studies are warranted to explore the best administration sequence to fully utilize this potential chemosensitizing effect of sunitinib.

CONCLUSION

We showed that single agent sunitinib induced significant *in vitro* and i*n vivo* growth inhibition in NPC cell lines and xenograft model. On the other hand, data from our preclinical NPC model suggested that concurrent administration of sunitinib with

chemotherapy may lead to significant toxicity in host without further improvement in the therapeutic ratio. Alternatively, based on the effect of sunitinib in NPC cell cycle progression, one may explore a sequential administration schedule when attempt to combine sunitinib with chemotherapy.

Based on the promising preclinical activities of single agent sunitinib in this study, we conducted a phase 2 clinical trial to investigate the clinical efficacy and safety of single agent sunitinib in NPC patients in the next study (chapter 9, study 7).

Chapter 9

Study 7: Targeting Tumor Angiogenesis - Clinical Study

BACKGROUND

As discussed in chapter 1, a wide range of chemotherapeutic agents has been tested in the treatment of locally recurrent or metastatic NPC (summarized in chapter 1, Table 1.3 and 1.4). Although the activity of platinum-based chemotherapy in patients with recurrent or metastatic NPC is high, with response rates over 50%, the duration of response and survival time are limited and palliative second-line chemotherapy is only reserved for good performance patients (Ma and Chan 2005). A small number of publications have reported the outcome of treatments given to recurrent or metastatic NPC patients who progressed after palliative platinum-based chemotherapy (Airoldi et al. 2002; Chua, Sham, and Au 2003). Patients with recurrent or metastatic NPC have few therapeutic options once they have progressed on platinum-based chemotherapy. There is therefore a clear unmet need for new anti-cancer agents in this indication. Targeted biologics are now becoming available for clinical uses which offer the promise of new treatment options for this patient group (Chan, Hsu et al. 2005).

Angiogenesis, the development of new blood vessels from a preexisting vasculature,

is a key pathway involved in tumor growth and metastases. Tumors cannot grow greater than 1-2 mm^3 in the absence of angiogenesis because the lack of oxygen in the centre of the tumor results in cell apoptosis and necrosis. Hypoxia is a key signal for the induction of angiogenesis, and one of the key angiogenic factors regulated by hypoxia is vascular endothelial growth factor (VEGF) (Ferrara 1999). A substantial numbers of studies have demonstrated a strong association between elevated tumor expression of VEGF and advanced disease or poor prognosis in various cancers. This supports the pivotal role of VEGF in regulating tumor angiogenesis. In head and neck cancer, VEGF over-expression was shown to be associated with poor disease free and overall survival (Smith et al. 2000), a marker of tumor invasion and metastases (Sauter et al. 1999).

The expression of VEGF was significantly associated with angiogenesis and lymph node metastases (Wakisaka et al. 1999), as well as distant metastases in NPC patients (Guang-Wu et al. 2000). In chapter 5 (study 3), we have demonstrated that overexpression of VEGF was present in over 60% of clinical biopsies of NPC, which was co-expressed with hypoxia markers HIF-1a and CA IX, and associated with poor outcome after radiation treatment. Other studies have also highlighted the significant role of tumor angiogenesis in NPC (Rubio et al. 2000; Qian et al. 2000; Murono et al.

2001; Rubio et al. 2002; Ma et al. 2003; Foote et al. 2005). In preclinical studies, antiangiogenesis treatment has already demonstrated promising results in NPC (Qian et al. 1998; Qian et al. 1999; Qian et al. 2000).

Sunitinib malate (Pfizer, New York, NY, USA) is an orally administered small molecule that inhibits the tyrosine kinase activities of VEGF receptor (VEGFR1-3), platelet-derived growth factor receptor (PDGFR), KIT, FLT-3, and RET. Sunitinib exhibits direct antitumor activity against tumor cells dependent on those receptor signaling for proliferation/survival (Mendel et al. 2003). Sunitinib also has antiangiogenic activity through its inhibition of vascular endothelial growth factor receptor and platelet-derived growth factor receptor signaling (Osusky et al. 2004). In our previous preclinical study, sunitinib has demonstrated potent single agent activity in NPC cell lines and xenograft models (chapter 8, study 6).

The most commonly tested regimen of sunitinib is a 6-week cycle comprising daily treatment for 4 weeks followed by a 2-week rest period (Schedule 4/2). Recent reports suggested that a continuous daily regimen of sunitinib may provide the advantage of maintaining sustained antitumor activity and preventing tumor regrowth during the 2-week off-treatment period (Chow and Eckhardt 2007; Faivre et al. 2007).

This phase 2 clinical trial will evaluate the activity and safety of sunitinib administered in a continuous once-daily dosing schedule as second line single agent treatment in patients with recurrent or metastatic NPC.

PATIENTS AND METHODS

Patients

Eligibility criteria were age ≥18 years, histological proven NPC, recurrent or metastatic, and evidence of measurable disease based on Response Evaluation Criteria in Solid Tumors (RECIST) (Therasse et al. 2000). Additional eligibility criteria included disease progressed after at least one line of prior platinum-based chemotherapy and not amenable to potentially curative radiotherapy or surgery; Eastern Cooperative Oncology Group (ECOG) performance 0 to 2; and adequate bone marrow, renal and hepatic reserve. Patients were excluded if they had history of hemorrhage of ≥ grade 3 within 4 weeks of starting study treatment; second malignancy within the last 3 years; central nervous system metastases; uncontrolled hypertension; significant cardiovascular disease including myocardial infarction/unstable angina or congestive heart failure within 12 months; ongoing cardiac dysrhythmias or prolongation of the QTc interval to > 450 msec for males or > 470 msec for females; treatment with anticonvulsant agents or therapeutic doses of

warfarin; inability to swallow oral medications, or presence of active inflammatory bowel disease, partial or complete bowel obstruction or chronic diarrhea; pregnancy or breastfeeding.

All patients provided written informed consent before study enrolment. The study protocol was approved by the Clinical Research Ethics Committee of The Chinese University of Hong Kong and conducted in accordance with the Declaration of Helsinki (2000).

Study Procedures

Patients received sunitinib at a starting dose of 37.5 mg once daily for 4 consecutive weeks. Treatment cycles were repeated every 4 weeks. There would be no treatment break between cycles unless in the event of ≥ grade 3 toxicity. Patients were evaluated biweekly for serial laboratory testing and clinical assessment. 12-lead electrocardiograms were done at baseline, on day 1 of cycle 2 and at end of treatment or study withdrawal. Adverse events were graded according to the National Cancer Institute (NCI) Common Terminology Criteria for Adverse Events (CTCAE) version 3.0. Treatment was continued until disease progression, unacceptable toxicity, or withdrawal of consent. Dose reduction (to 25 mg daily and then to 12.5 mg daily)

was allowed in case of recurrent toxicity of ≥ grade 3. Computed tomography or magnetic resonance imaging were performed at screening and repeated every 3 cycles. Objective tumor response was assessed using RECIST. Patients were followed after treatment discontinuation for survival status.

Statistical Analysis

The primary endpoints were clinical benefit rate (CBR) and time-to-progression (TTP). Secondary endpoints included overall response rate, toxicity, progression free survival (PFS) and overall survival (OS). CBR was defined as the percent of patients with confirmed complete response (CR), partial response (PR), or stable disease (SD) lasting for at least 12 weeks on study according to RECIST. TTP was defined as the time from start of study treatment to first documentation of objective tumor progression. PFS was defined as the time form start of study treatment to first documentation of objective tumor progression, or to death due to any cause. OS was defined as the time from start of study treatment to date of death due to any cause. Time-to-event data was summarized using the Kaplan-Meier method. In an exploratory analysis, the association between hemorrhagic events and clinical risk factors were tested with Fisher's exact test. The statistical analysis was conducted with SAS 8.0 (SAS Institute Inc., Cary, NC).

The sample size was calculated based on clinical benefit rate (non-progression rate) using the Simon's Minimax two-stage phase II design (Simon 1989). We considered the study drug to be inactive if the non-progression rate is at most 50%, and considered the study drug as active if the non-progression rate is at least 70%. Therefore, assuming P0 = 0.50, P1= 0.70, and the type I error of 0.05 with power of 80%, we would recruit 23 patients in stage I. If we observed 12 or less non-progression, we would stop the study and conclude the study drug as inactive, otherwise we would proceed to stage II and accrue an additional 14 patients. If 23 or less of the 37 patients were non-progressors, the drug would be deemed inactive.

For patients who have recurrent or metastatic NPC receiving a second-line treatment, the median TTP is about 4 months. We postulated that the study drug would achieve a median time-to-progression of about 6 months and the corresponding lower limit of the 95% confidence interval should exceed 4 months in order to conclude that the study drug has sufficient anti-tumor activity. Assuming the time-to-progression follows an exponential distribution, we need to observe at least 20 events to achieve this level of accuracy for the 95% confidence interval. In order to observe enough events for the study, we would enter 37 patients and follow all patients for at least 3 months.

RESULTS

Patient and Treatment

Fourteen patients were enrolled from July 2007 to April 2008. Recruitment was stopped after two patients died of hemorrhagic events. Table 9.1 summarised the baseline characteristics of enrolled patients. All patients received prior definitive curative-intent radiotherapy (RT) to nasopharynx and neck, and nine patients also received concurrent chemotherapy with the radical RT. Two, 5, 4 and 3 patients had received 1, 2, 3 and 4 lines of prior chemotherapy respectively after recurrence. This represented a cohort of recurrent NPC heavily pre-treated with RT and chemotherapy.

Sunitinib treatment administration was summarised in Table 9.2. Patient received a median of 3 cycles (range 1-24) of sunitinib. All patients required dose interruption. Eight (57%) patients had dose reduced to 25 mg daily and two (14%) patients required further dose reduction to 12.5 mg daily. The reasons for dose reduction were for non-hematological toxicity in eight patients and hematological toxicity in two patients.

Safety

Adverse events (AE) encountered during study that were possibly related to the administration of sunitinib are summarised in Table 9.3. The most common treatment-related adverse events (all grades) included fatigue (71%), dermatological (71%), hemorrhage (64%), neutropenia (50%), pain (50%), odynophagia/glossitis (50%), hypertension (43%), mucositis (29%) and hypothyroidism (29%). Grade 3 or above non-hematological adverse events included hemorrhage (43%), fatigue (21%), dysphagia (14%), odynophagia/glossitis (7%) and hyponatremia (7%). Grade 3 or above hematologic toxicities were neutropenia (21%), leucopenia (29%), anemia (7%) and thrombocytopenia (7%).

Hemorrhagic events (all grades) occurred in 9 pts (64%), including epistaxis in 6 pts, hemoptyses in 3 pts and hemetemesis in 2 pts (Table 9.4). Prior RT to thorax was significantly associated with hemoptyses ($p=0.03$, Fisher's exact test).

Two patients with local disease recurrence developed grade 5 epistaxis/hemetemesis within first 4 weeks of sunitinib treatment. In both patients the local recurrent tumors had extended from the nasopharynx posterolaterally to invade the parapharyngeal space and completely encase the internal carotid artery on the pre-treatment MRI

scan (Figure 9.1a). In contrast, another two patients with local recurrence never developed any symptoms of bleeding from the upper aero-digestive tract during sunitinib treatment. In these two patients (who did not bleed) the local recurrent tumor in the nasopharynx had also extended also to the parapharyngeal space but the tumor had not extended any further posterolaterally into the carotid space (post-styloid space) to involve the wall of internal carotid artery.

Efficacy

Of the ten patients who had completed at least one post-baseline radiological assessment, tumor shrinkage was noted in five patients. Response could not be evaluated in the other four patients, since one died from hemorrhage, one withdrew consent because of toxicity and two had clinical deterioration prior to radiological assessment. Figure 9.2a shows the maximum percentage change of target tumor lesions. Percentages were calculated using the summed unidimensional measurements of target lesions per RECIST. The serial changes in radiologic tumor measurements of the target tumor lesions are illustrated in Figure 9.2b. Three patients received sunitinib for more than 12 cycles and their serial CT scan appearance of the target tumor lesions are shown in Figure 9.3.

By RECIST criteria, one patient achieved a confirmed partial response for duration of 5.6 months. A further three patient had stabilization of disease lasting for at least 12 weeks, giving a clinical benefit rate of 28.6% (4/14, 95% CI 4.4-52.7%) in the total intent-to-treat population. At the last follow up, one patient was still continuing on sunitinib treatment with stable disease and good symptom control after 24 cycles.

After a median follow up of 23.1 months, the median TTP was 4.4 months (95% CI 2.8 – 9.4), the median PFS was 3.5 months (95% CI 2.5 – 9.4) and the median OS was 10.5 months (95% CI 7.2 - 20.7). The actuarial one-year overall survival rate was 35.7%.

Table 9.1

Baseline characteristics of NPC patients.

	Sunitinib (n=14)	
Characteristic	No. of patients	%
Age (years)		
Median	51	
Range	35 - 75	
Gender		
Male	13	93
Female	1	7
ECOG performance status		
0	12	86
1	2	14
Disease stage at screening		
Local recurrence	4	29
Metastatic disease	13	93
Site of metastatic disease (n=13)		
Lung metastases	9	69
Liver metastases	8	62
Bone metastases	4	31
Lymph nodes	4	31
Others	3	23
Primary Radiotherapy (to NPC)		
Radiotherapy	14	100
Chemoradiotherapy	9	64
Prior therapy (for NPC recurrence)		
Palliative radiotherapy	3	21
Surgery	2	14
Chemotherapy	14	100
Number of lines of prior palliative chemotherapy		
1	2	14
2	5	36
3	4	29
4	3	21
Prior chemotherapy agents		
Cisplatin	9	64
Carboplatin	8	57
Oxaliplatin	5	36
Paclitaxel	6	43
Gemcitabine	11	79
5-Fluorouracil	3	21
Capecitabine	6	43
Ganciclovir	2	14

ECOG, Eastern Cooperative Oncology Group.

Table 9.2
Treatment administration of sunitinib.

	Sunitinib (n=14)	
Characteristic	No. of patients	%
Duration of treatment		
Median (days)	77	
Range	11 - 692	
Treatment delay	7	50
Treatment interruption	14	100
Dose reduction		
To 25 mg/day	8	57
To 12.5 mg/day	2	14
Primary reason for treatment discontinuation (n=13)		
Disease progression	9	70
Adverse events	2	15
Death	2	15

Table 9.3

Adverse events after sunitinib treatment in recurrent or metastatic NPC.

	Grade 1/2		Grade 3/4		Grade 5 (death)		Total (all grades)	
Adverse Event	**No.**	**%**	**No.**	**%**	**No.**	**%**	**No.**	**%**
Non-hematological								
Fatigue	7	50	3	21.4	-	-	10	71.4
Dermatological	10	71.4	-	-	-	-	10	71.4
Hemorrhage	3	21.4	4	28.6	2	14.3	9	64.3
Pain	7	50	-	-	-	-	7	50
Odynophagia/Glossitis	6	42.9	1	7.1	-	-	7	50
Hypertension	6	42.9	-	-	-	-	6	42.9
Hypothyroidism	4	28.6	-	-	-	-	4	28.6
Mucositis	4	28.6	-	-	-	-	4	28.6
Dysphagia	-	-	2	14.3	-	-	2	14.3
Diarrhea	2	14.3	-	-	-	-	2	14.3
Hyponatremia	-	-	1	7.1	-	-	1	7.1
Auditory	1	7.1	-	-	-	-	1	7.1
Dizziness	1	7.1	-	-	-	-	1	7.1
Limb edema	1	7.1	-	-	-	-	1	7.1
Fever	1	7.1	-	-	-	-	1	7.1
Heartburn	1	7.1	-	-	-	-	1	7.1
Pulmonary	1	7.1	-	-	-	-	1	7.1
Vomiting	1	7.1	-	-	-	-	1	7.1
Hematological								
Neutropenia	4	28.6	3	21.4	-	-	7	50
Leucopenia	2	14.3	4	28.6	-	-	6	42.9
Thrombocytopenia	1	7.1	1	7.1	-	-	2	14.3
Anemia	-	-	1	7.1	-	-	1	7.1

Table 9.4
Summary of hemorrhagic events in patients with recurrent or metastatic NPC during sunitinib treatment.

Hemorrhagic event	Grade	Patient characteristics			Radiotherapy treatment			Outcome
		Patient No	Local recurrence	Lung metastases	Primary RT for NPC	CRT	Palliative RT to other site	
Epistaxis	5	PW002	Yes	No	NP 60 Gy (2.5 Gy/fr) Neck 45.6 Gy (3.8 Gy/fr)	Yes	-	Died
	3	PW010	No	Yes	NP 66 Gy + boost 18 Gy (4.5 Gy x 4) Neck 66 Gy	No	-	Resolved
	3	PW005	No	No	NP 66 Gy + boost 8 Gy Neck 66 Gy + boost 7.5 Gy (3.75 Gy x 2)	Yes	-	Resolved
	2	PW014	No	Yes	NP/neck 66 Gy	Yes	-	Resolved
	1	PW008	No	Yes	NP 60 Gy + boost (2.4 Gy x 3 + 2 Gy x 3), neck 40 Gy	Yes	-	Resolved
	1	PW012	No	Yes	NP /neck 66 Gy PPS boost 20 Gy	No	-	Resolved
Hemetemesis	5	PW013	Yes	No	NP 70 Gy Neck 40 Gy	Yes	-	Died
	3	PW005	No	No	NP 66 Gy + boost 8 Gy Neck 66 Gy + boost 7.5 Gy (3.75 Gy x 2)	Yes	-	Resolved
Hemoptyses	3	PW001	No	Yes	NP /neck 66 Gy PPS boost 20 Gy	Yes	Mediastinum 50 Gy	Resolved
	3	PW007	No	Yes	NP/neck 66 Gy + boost 8 Gy	Yes	Thoracic spine 28 Gy (4 Gy/fr)	Resolved
	1	PW008	No	Yes	NP 60 Gy + boost (2.4 Gy x 3 + 2 Gy x 3), neck 40 Gy	Yes	-	Resolved

All radiotherapy was delivered in conventional fractionation of 2 Gray (Gy) per fraction (fr) unless otherwise specified.
RT, radiotherapy; CRT, concurrent cisplatin-radiotherapy; NP, nasopharynx; PPS, parapharyngeal space.

Figure 9.1

(a) Baseline MRI scan of a NPC patient with local recurrence.

Axial T1-weighted MRI post contrast showing a large recurrent carcinoma (arrow heads) in the left side of the nasopharynx which is extending posterolaterally into the parapharyngeal space and then even deeper into the carotid space. The left internal carotid artery (long arrow) is completely encased (and therefore probably invaded) by the carcinoma.

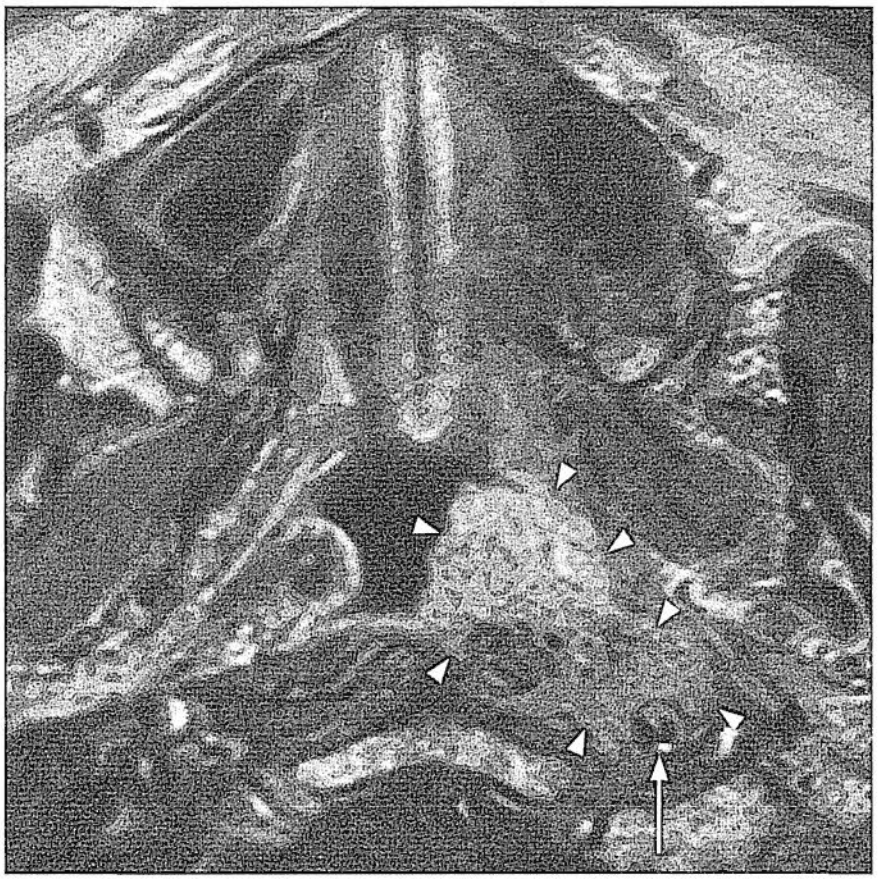

Figure 9.1

(b) MRI scan performed just before the patient developed a fatal hemorrhage.

Axial T1-weighted MRI post contrast following treatment showing that the recurrent carcinoma has undergone extensive tumor shrinkage with necrosis resulting in a large area of cavitation (arrow heads) which extends all the way down to the wall of the left internal carotid artery (long arrow). The artery now lies directly exposed to the nasopharyngeal airway. It is postulated that this resulted in the fatal hemorrhage from a carotid "blow-out".

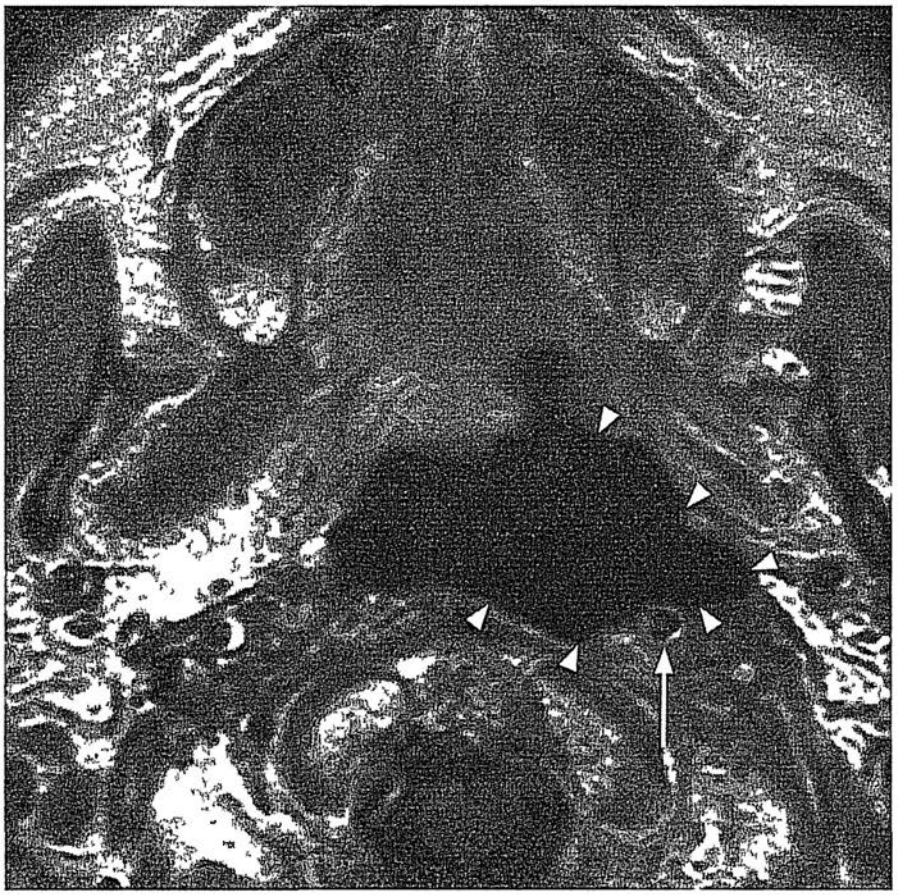

Figure 9.2

(a) Waterfall plot showing the best radiologic response of the target lesions by RECIST criteria for all evaluable patients. Patients experiencing a partial response are shown in yellow bar, while those with stable disease are shown in blue bar and progressive disease in red bar.

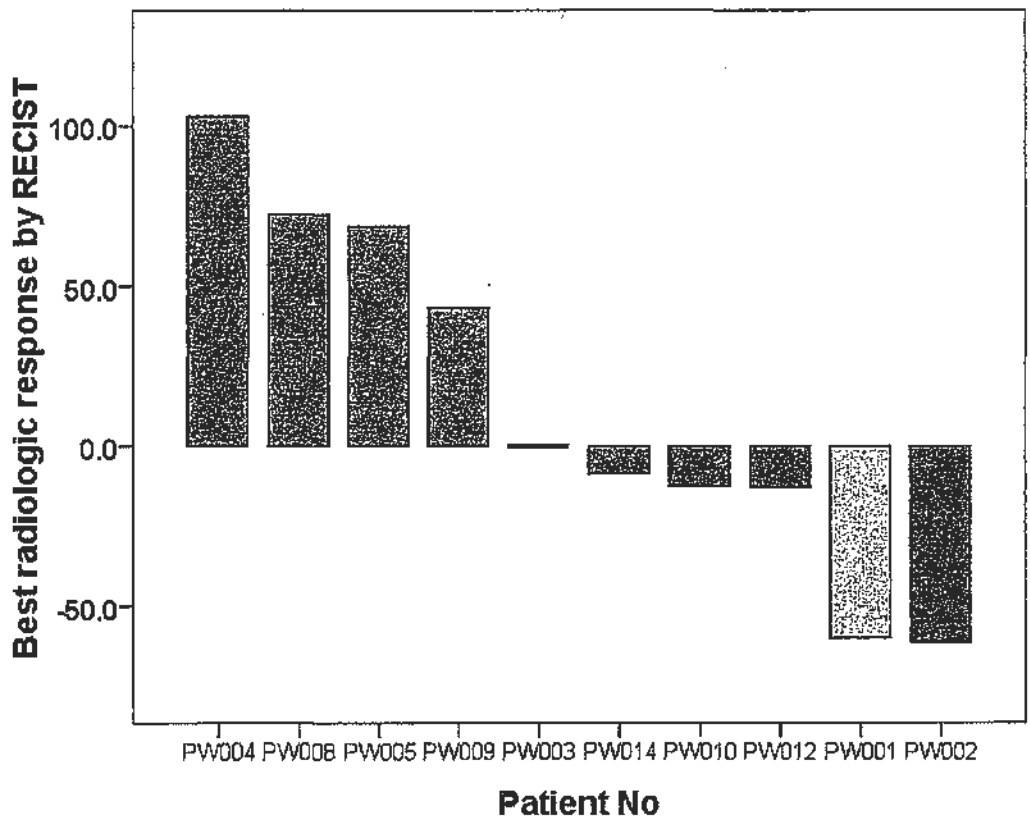

Figure 9.2

(b) Serial changes in radiological measurement of the target tumor lesions by RECIST criteria during treatment for all evaluable patients. Sunitinib was given in a continuous daily dosing schedule of 4-week cycles. All changes were compared with baseline measurement and expressed as percentage. Positive percentage represents an increase in tumor size while negative change represents a reduction of tumor size (*PW002 and PW003 withdrew from study before cycle 3 and their radiologic change were censored from cycle 1 and 2 respectively).

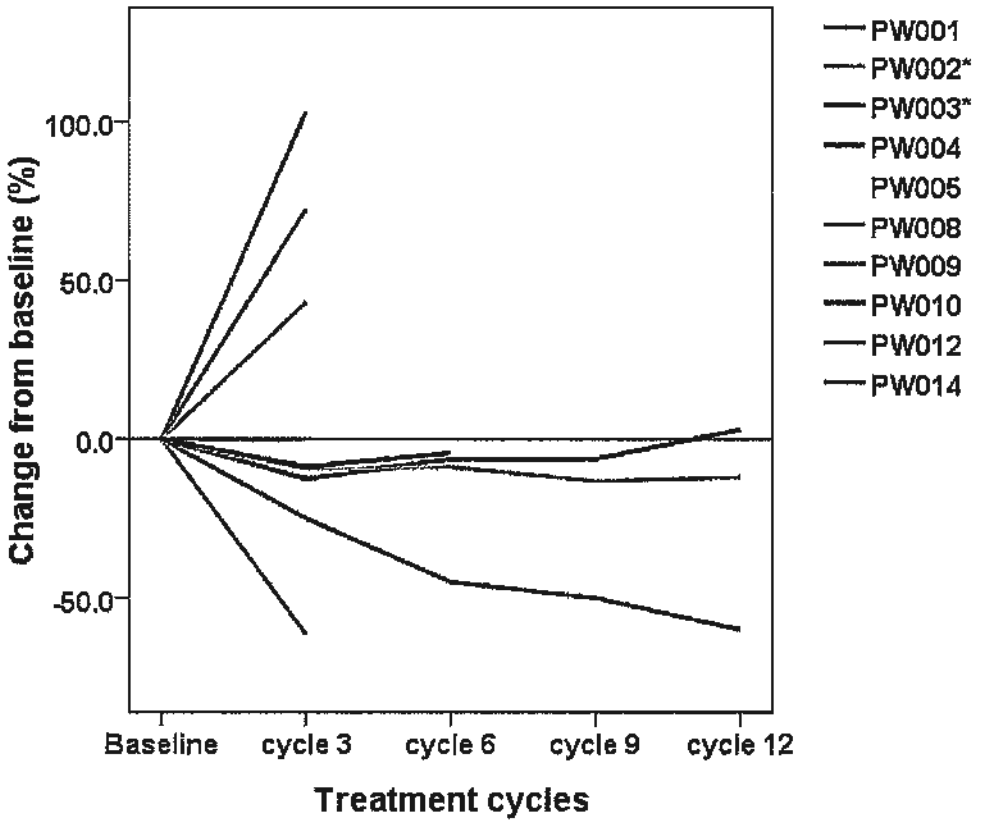

Figure 9.3

Serial CT scans showing the appearance of the target lesions before treatment (baseline), and after 12 weeks (cycle 3) and 48 weeks (cycle 12) of sunitinib treatment in the three NPC patients who received sunitinib for ≥ 12 cycles.

(a) PW001: significant tumor necrosis with cavitation after 3 cycles.

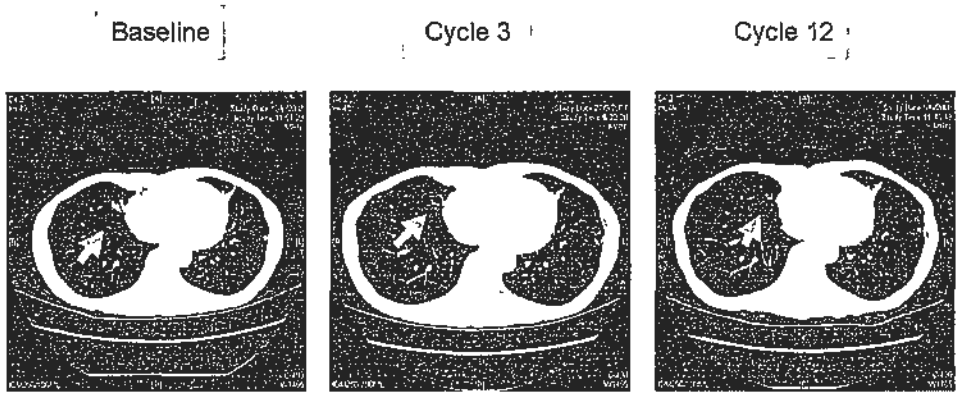

Figure 9.3

(b) PW010: prolonged disease stabilization for more than 12 months.

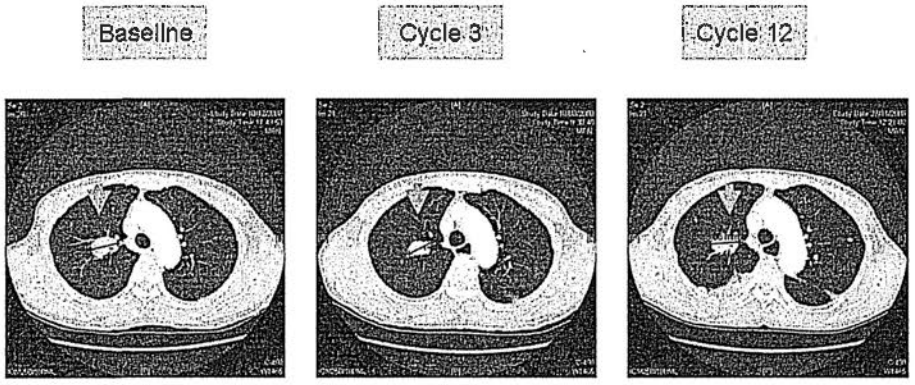

(c) PW012: prolonged disease stabilization for more than 12 months.

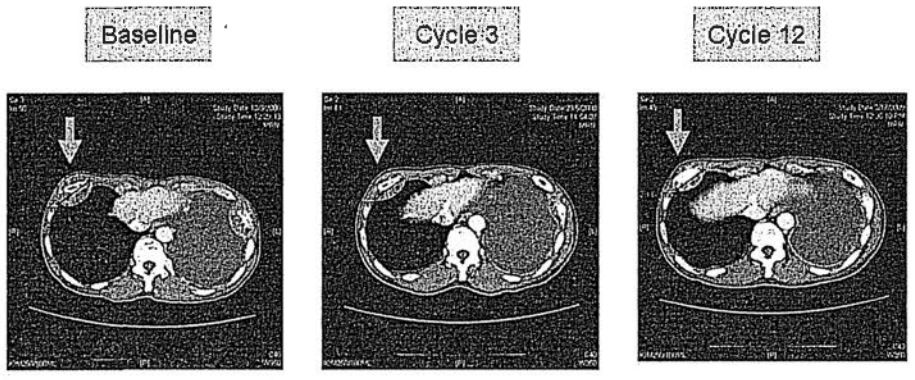

DISCUSSIONS

In the past few years, several new agents developed as angiogenesis inhibitors have been targeting the vascular endothelial growth factor receptor (VEGFR). At least four such agents have already obtained US Food and Drug Administration (FDA) approval for clinical use and many others have entered into clinical trials. Thus an increase in their use is expected in the near future. The FDA approved agents include the monoclonal antibody against VEGF bevacizumab (Genentech, South San Francisco, CA, USA) and the VEGFR tyrosine kinase inhibitors sunitinib (Pfizer, New York, NY, USA), sorafenib (Bayer Pharmaceuticals, West Haven, CT, USA) and pazopanib (GlaxoSmithKline, London, UK). These agents do not show the typical side effects of cytotoxic chemotherapy. However, a new toxicity pattern has been reported, including hemorrhage, thrombosis, hypertension, proteinuria, bowel perforation, impaired wound healing, cardiac impairment, hypothyroidism and reversible posterior leucoencephalopathy (Eskens and Verweij 2006; Elice et al. 2008; Verheul and Pinedo 2007; van der Veldt et al. 2008; Lordick et al. 2006; Hall et al. 2008; Pouessel and Culine 2008; Sher, Chu, and Wu 2009).

This is to our knowledge the first clinical study to explore the efficacy of sunitinib in patients with recurrent or metastatic NPC. Although the types of toxicities reported here are consistent with those seen in previous studies of single agent sunitinib in other cancer types, with the most common toxicities being fatigue, dermatological and gastrointestinal side effects, both the incidence and severity of hemorrhagic events was much more pronounced. However, the single-arm study design without a control group and the early suspension of the trial makes it difficult to determine true incidence of hemorrhagic events during antiangiogenesis therapy in NPC.

In our study, we observed a high incidence of non-hematological toxicities that mandated dose interruptions and/or dose reductions. A recent retrospective analysis has also highlighted that frequent dose interruptions are required for patients receiving oral kinase inhibitor therapy (sorafenib or sunitinib) in advanced renal cell carcinoma and suggested that the initial grade 3 or 4 adverse events presented in the literature appeared to have been underreported (La Vine et al. 2009). We hypothesized that the pre-existing late radiation toxicity prevalent in NPC who received prior high dose radiation (such as chronic xerostomia) could have predisposed NPC patients to development of odynophagia, glossitis or mucositis. We also observed a relative high incidence of hypothyroidism (which was almost universal in patients who took sunitinib beyond 3 months). The prior exposure of high dose radiation to neck could have predisposed NPC patients to subsequent development hypothyroidism during sunitinib treatment. We suggest that monitoring of thyroid function is mandatory during sunitinib treatment in patients who received prior radiation to the neck.

The mechanisms of interaction between antiangiogenic agents and ionizing radiation are complex and may involve multiple interactions between tumor stroma, vasculature and the tumor cells (Wachsberger, Burd, and Dicker 2003). Previous studies combining VEGF/VEGFR inhibition and radiation have reported greater than additive effect in a variety of tumor model systems *in vivo*. However, the role of VEGF in the repair of chronic or late radiation damage remains unclear. Radiation damaged vessels were shown to be more sensitive to VEGFR inhibition in tumor model system (Zips et al. 2005). Clinically, increased risk of ischemic bowel complications during

treatment with bevacizumab after previous pelvic irradiation has been reported (Lordick et al. 2006). Fatal bowel perforation within the area of irradiation occurred in a patient receiving sorafenib, suggesting its potential as radiosensitizer (Peters et al. 2008). In a phase 1 trial of bevacizumab with concurrent radiotherapy and capecitabine in locally advanced pancreatic cancer, three patients developed tumor-associated bleeding duodenal ulcers and one had a contained duodenal perforation among the first 30 patients treated. It was suggested that ulceration and bleeding in the radiation field possibly related to bevacizumab occurred when tumor involved the duodenal mucosa. No additional bleeding events occurred among the final 18 patients after patients with duodenal involvement by tumor were excluded (Crane et al. 2006). As antiangiogenesis therapy after radiation is becoming more frequent in daily clinical practice, clinicians should be alerted to monitor for potentially serious side effect arising from irradiated tissues.

In studies of non-small cell lung cancer, fatal pulmonary hemorrhages were also observed in a number of patients. All these fatal events occurred in patients with centrally located squamous cell lung cancer (Johnson, Fehrenbacher et al. 2004). Vascular disruption by inhibition of existing VEGF/VEGFR-dependent tumor blood vessels often lead to tumor necrosis and cavitations. It is hypothesized that presence or the development of tumor cavitations, probably a sign of antitumor activity of chemotherapy and bevacizumab, underlies these events. Patients with centrally located squamous cell lung cancer are therefore currently excluded from bevacizumab treatment.

In our previous preclinical study, sunitinib decreased tumor microvessel density and

induced significant tumor necrosis in a NPC xenograft model (chapter 8, Figure 8.5 and 8.6). In fact, tumor necrosis leading to cavitations has previously been reported patients treated in a phase 1 trial of sunitinib (Faivre et al. 2006). Infection in necrotic area of lung metastasis was reported in a NPC patient enrolled in the phase 1 trial (Faivre et al. 2006). Nasopharyngeal hemorrhage was previously reported in a phase 2 trial of sorafenib that enrolled patients with recurrent or metastatic squamous cell carcinoma of head and neck or nasopharyngeal carcinoma. However, in that study the author attributed the bleeding event as likely related to underlying malignancy instead of related to antiangiogenesis treatment (Elser et al. 2007).

In our study, two patients with local recurrence developed grade 5 hemorrhage during the first cycle of sunitinib treatment. These patients had not reported any bleeding symptoms prior to sunitinib treatment despite having previously received multiple chemotherapies. In one of the patients, significant tumor shrinkage (>60%) was found on the MRI study performed before the fatal hemorrhagic event (Figure 9.1b). The tumor necrosis has exposed the naked internal carotid artery to the nasopharyngeal cavity. The complete encasement of the artery on MRI prior to therapy suggests that invasion of the arterial wall was likely and this together with the direct exposure of the artery to the nasopharyngeal cavity likely contributed to the subsequent carotid blowout syndrome with torrential hemorrhage.

In a recent metaanalysis of 23 trials involving a total of 6779 patients, the risk of bleeding with vascular endothelial growth factor receptor tyrosine kinase inhibitors sunitinib and sorafenib was analysed (Je, Schutz, and Choueiri 2009). The incidence of bleeding events (all grades) was 16.7% and that of high grade bleeding was 2.4%.

The relative risk of all-grade bleeding events associated with sunitinib and sorafenib from four randomized controlled trials was 2.0 (95% CI 1.14-3.49; p=0.015). However, the relative risk of high grade bleeding were raised only slightly (1.16, 95% CI 0.70-1.92; p=0.555). The authors attributed this to the small number of events recorded and possible underreporting of rare events in clinical trials which are not usually designed to specifically address toxic events. A high incidence of hemorrhage (8/22, 36% and 10/17, 59%) was also reported in two phase 2 trial of sunitinib in head and neck cancers, of which most of the patients also received prior radiotherapy or chemoradiotherapy (Choong et al. 2009; Fountzilas et al. 2010). In the phase 2 study of sunitinib in recurrent or metastatic squamous cell carcinoma of the head and neck conducted by the GORTEC group, a high incidence of head and neck bleedings (13/38, 34%) was also observed, of which four were fatal hemorrhages (Machiels et al. 2010). The authors hypothesized that late toxicity owing to prior radiation therapy could have contributed to the complications, and proposed that patients with tumor situated within 5 mm of large blood vessels be excluded from studies of angiogenesis inhibitors.

CONCLUSION

Single agent sunitinib demonstrated modest clinical activity in a heavily pretreated cohort of NPC patients. However, our study is underpowered to demonstrate its efficacy because of premature study termination. However, the high incidence of high grade hemorrhagic events from the upper aero-digestive tract, area that were within the high dose zone of prior radiotherapy for NPC, is a cause of concern. In particular, patients with local tumor invading into the carotid sheath are at high risk of fatal hemorrhage. As a safety precaution, we propose to exclude NPC patients with

disease recurrence within previous radiation field and/or invading major vascular structure from future antiangiogenesis therapy. This study has also highlighted the importance of careful patient selection for antiangiogenesis therapy.

SECTION IV
CONCLUSIONS

Chapter 10

Summary and Future Directions

NPC has traditionally been treated by local radiotherapy with great success especially for early stage disease. The recognition of a high rate of distant metastases leads investigators to explore the incorporation of systemic therapy (principally chemotherapy) into the primary radiotherapy. Concurrent chemoradiation with or without adjuvant chemotherapy has been shown to improve the overall survival and disease free survival when added to radiotherapy in advanced NPC, and becomes the standard of care. The sequence of neoadjuvant chemotherapy followed by concurrent chemoradiation allows better maintenance of chemotherapy dose intensity, and has demonstrated excellent result in several phase II studies, and would be a reasonable approach to be explored in future randomized trials. With the increased understanding of the molecular mechanism in NPC, new therapies targeting tumor metastasis and angiogenesis can be explored.

In study 1 (chapter 3), using the clinical database of a contemporary cohort of 2915 NPC patients treated in five oncology centers in Hong Kong during 1996-2000, we confirmed that distant metastasis is the leading cause of treatment failures after primary radiotherapy. UICC N-stage, T-stage, advanced age and male sex were the significant and independent determinants for distant metastases. Future studies should target advanced UICC N-stage and T-stage diseases for testing new strategy of systemic therapy to combat the risk of distant failure. In studies 2-4 (chapter 4-6), we have focused on the understanding the molecular mechanism leading to tumor metastasis. In study 5-7 (chapter 7-9), we have focused on developing new

therapeutic approaches to combat distant metastases in order to improve the overall treatment outcome in NPC.

In study 2 (chapter 4), we found that hypoxia induced HIF-1α, CA IX and VEGF expression in NPC cells. Hypoxia also induced broad changes of both up- and down-regulated gene expressions involved in diverse biological processes in NPC cells. Elucidation of the coordinated functions modulated by hypoxia could lead to a better understanding of the clinical significance of the hypoxic tumor phenotype.

In study 3 (chapter 5), we showed that over-expression of HIF-1α, CA IX and VEGF is common in NPC biopsy samples, which is probably related to hypoxia up-regulated expression involving a HIF dependent pathway, and is associated with poor prognosis after conventional radiotherapy. These suggest that targeting the hypoxia pathway may be useful in the treatment of NPC.

In study 4 (chapter 6), we demonstrated that elevated plasma OPN is a biomarker of distant metastasis, and pre-treatment plasma OPN level may be a useful biomarker of response to radiotherapy in NPC.

In study 5 (chapter 7), in a randomized phase 2 clinical trial, we conformed that neoadjuvant chemotherapy followed by CRT was well tolerated with a manageable toxicity profile that allowed subsequent delivery of full dose CRT. Preliminary results suggested a positive impact on survival. A phase 3 study to definitively test this neoadjuvant-concurrent strategy is warranted. Currently, several phase 3 studies comparing a sequential approach of neoadjuvant chemotherapy followed by

chemoradiotherapy versus chemoradiotherapy alone are ongoing in head and neck cancer (Specenier and Vermorken 2007; Cruz et al. 2008). In NPC, a GORTEC multicenter phase 3 trial of neoadjuvant chemotherapy followed by concurrent weekly cisplatin-RT versus weekly cisplatin-RT alone has been started.

In study 6 (chapter 8), in a preclinical NPC model system, the antiangiogenesis agent sunitinib demonstrated potent *in vitro* and *in vivo* growth inhibition in NPC, partly by induction of apoptosis and cell cycle arrest. Sunitinib reduced microvessel density and caused significant tumor necrosis in NPC xenograft. When combined with chemotherapy, sequential instead of concurrent administration schedule should be further explored.

In study 7 (chapter 9), the antiangiogenesis agent sunitinib demonstrated modest clinical activity in a phase 2 clinical trials of heavily pretreated NPC patients. However, the high incidence of hemorrhage from upper aero-digestive tract in NPC patients who received prior high dose RT to the region is of concern. Recurrence within previously RT field and direct vascular invasion by tumors appeared to increase the risk of serious bleeding and we proposed that these high risk patients should be excluded from future antiangiogenesis therapy. Our result also highlighted the importance of careful patient selection for antiangiogenesis therapy.

Results from this series of combined clinical, translational and laboratory studies (studies 1 to 7) have redefined the role of hypoxia, angiogenesis and metastasis as new therapeutic targets in NPC. New biomarkers (HIF1, CA IX, VEGF, plasma OPN) and new therapeutic approaches were developed based on these targets

(neoadjuvant chemotherapy targeting distant metastasis, antiangiogenesis therapy targeting VEGF). It is concluded that the research hypotheses of this thesis have been confirmed.

The result of this thesis has confirmed the clinical importance of hypoxia and angiogenesis in NPC and also supported these as potential therapeutic targets in NPC. As a follow up, we have further investigated the hypoxia targeting agent tirapazamine (Hong et al. 2009) and the HIF-1 inhibitor YC-1 (Hong et al. 2010) in NPC and reported promising preliminary results.

Although the multi-targeted receptor tyrosine kinase inhibitor sunitinib as an antiangiogenesis agent demonstrated modest clinical activity in heavily pretreated NPC patients, we have also encountered severe toxicity. On the other hand, axitinib is a highly selective receptor tyrosine kinase inhibitors directed at a single type of growth factor receptor (VEGFR). It has the potential to decrease toxicity and improve the therapeutic ratio. Selectively targeting a single growth factor receptor pathway provides the potential to rationally adjust dosages and combine drugs directed at specific parts of the pathway to minimize toxicity and achieve the optimum therapeutic benefit. A phase 2 clinical trial of axitinib will be initiated in NPC patients which will exclude those patients at high risk of bleeding as identified from study 7 (chapter 9).

Distant metastasis is now being recognized as the major cause of treatment failure and death in nasopharyngeal cancer. Recent experimental evidence suggests that osteopontin is the lead molecule involved in cancer progression and metastasis (Wai and Kuo 2007). Circulating osteopontin is recently discovered to be responsible for

the systemic endocrine instigation of indolent tumor growth at distant sites (McAllister et al. 2008). Our preliminary data suggested that elevated plasma osteopontin was associated with distant metastasis in nasopharyngeal cancer, and pre-treatment level was predictive of response to radiotherapy (study 4, chapter 6) (Hui et al. 2008).

We are currently proposing a prospective longitudinal cohort study recruiting 300 patients of newly diagnosed nasopharyngeal cancer, and who is planned for curative radiotherapy treatment. We hypothesize that plasma osteopontin level correlates with and predicts the development of distant metastasis, and that pre-treatment level is prognostic of clinical outcomes in nasopharyngeal cancer. We intend to establish the clinical role of plasma osteopontin as a prognostic factor in nasopharyngeal cancer. With the collection of paired pre-treatment tumor biopsy and plasma sample, and serial longitudinal measurements and clinical follow up after radiotherapy, we aim to provide new knowledge on the effect of radiotherapy on the serial changes in plasma osteopontin in nasopharyngeal cancer, and the time course of plasma osteopontin to subsequent clinical progression and metastasis. The outcome of this project will enhance our understanding on the clinical significance of osteopontin in the development of metastasis in nasopharyngeal cancer. This knowledge will lead to future therapeutic strategies to detect and prevent cancer metastasis at its earliest inception.

SECTION V

REFERENCES

Aaronson, N. K., Ahmedzai, S., Bergman, B., et al. 1993. The European Organization for Research and Treatment of Cancer QLQ-C30: a quality-of-life instrument for use in international clinical trials in oncology. *J Natl Cancer Inst* 85 (5):365-76.

Abrams, T. J., Lee, L. B., Murray, L. J., et al. 2003. SU11248 inhibits KIT and platelet-derived growth factor receptor beta in preclinical models of human small cell lung cancer. *Mol Cancer Ther* 2 (5):471-8.

Abrams, T. J., Murray, L. J., Pesenti, E., et al. 2003. Preclinical evaluation of the tyrosine kinase inhibitor SU11248 as a single agent and in combination with "standard of care" therapeutic agents for the treatment of breast cancer. *Mol Cancer Ther* 2 (10):1011-21.

Adelstein, D. J., and Leblanc, M. 2006. Does induction chemotherapy have a role in the management of locoregionally advanced squamous cell head and neck cancer? *J Clin Oncol* 24 (17):2624-8.

Aebersold, D. M., Burri, P., Beer, K. T., et al. 2001. Expression of hypoxia-inducible factor-1alpha: a novel predictive and prognostic parameter in the radiotherapy of oropharyngeal cancer. *Cancer Res* 61 (7):2911-6.

———. 2001. Expression of hypoxia-inducible factor-1alpha: a novel predictive and prognostic parameter in the radiotherapy of oropharyngeal cancer. *Cancer Res* 61 (7):2911-6.

Agulnik, M., and Siu, L. L. 2005. State-of-the-art management of nasopharyngeal carcinoma: current and future directions. *Br J Cancer* 92 (5):799-806.

Ahmad, A., and Stefani, S. 1986. Distant metastases of nasopharyngeal carcinoma: a study of 256 male patients. *J Surg Oncol* 33 (3):194-7.

Airoldi, M., Pedani, F., Marchionatti, S., et al. 2002. Carboplatin plus taxol is an effective third-line regimen in recurrent undifferentiated nasopharyngeal carcinoma. *Tumori* 88 (4):273-6.

Al-Sarraf, M., LeBlanc, M., Giri, P. G., et al. 1998. Chemoradiotherapy versus radiotherapy in patients with advanced nasopharyngeal cancer: phase III randomized Intergroup study 0099. *J Clin Oncol* 16 (4):1310-7.

———. 2001. Superiority of Five Year Survival with Chemo-Radiotherapy (CT-RT) vs Radiotherapy in Patients (Pts) with Locally Advanced Nasopharyngeal Cancer (NPC). Intergroup (0099) (SWOG 8892, RTOG 8817, ECOG 2388) Phase III Study: Final Report. *Proc Am Soc Clin Oncol* 20:(abstract 905).

Al-Shahrour, F., Diaz-Uriarte, R., and Dopazo, J. 2004. FatiGO: a web tool for finding significant associations of Gene Ontology terms with groups of genes. *Bioinformatics* 20 (4):578-80.

Ameri, K., Lewis, C. E., Raida, M., et al. 2004. Anoxic induction of ATF-4 through HIF-1-independent pathways of protein stabilization in human cancer cells. *Blood* 103 (5):1876-82.

Ang, C., Chambers, A. F., Tuck, A. B., et al. 2005. Plasma osteopontin levels are predictive of disease

stage in patients with transitional cell carcinoma of the bladder. *BJU Int* 96 (6):803-5.

Au, E., and Ang, P. T. 1994. A phase II trial of 5-fluorouracil and cisplatinum in recurrent or metastatic nasopharyngeal carcinoma. *Ann Oncol* 5 (1):87-9.

Au, E., Tan, E. H., and Ang, P. T. 1998. Activity of paclitaxel by three-hour infusion in Asian patients with metastatic undifferentiated nasopharyngeal cancer. *Ann Oncol* 9 (3):327-9.

Bachtiary, B., Schindl, M., Potter, R., et al. 2003. Overexpression of hypoxia-inducible factor 1alpha indicates diminished response to radiotherapy and unfavorable prognosis in patients receiving radical radiotherapy for cervical cancer. *Clin Cancer Res* 9 (6):2234-40.

Bar-Sela, G., Kuten, A., Ben-Eliezer, S., et al. 2003. Expression of HER2 and C-KIT in nasopharyngeal carcinoma: implications for a new therapeutic approach. *Mod Pathol* 16 (10):1035-40.

Baujat, B., Audry, H., Bourhis, J., et al. 2006. Chemotherapy as an adjunct to radiotherapy in locally advanced nasopharyngeal carcinoma. *Cochrane Database Syst Rev* (4):CD004329.

Beasley, N. J., Leek, R., Alam, M., et al. 2002. Hypoxia-inducible factors HIF-1alpha and HIF-2alpha in head and neck cancer: relationship to tumor biology and treatment outcome in surgically resected patients. *Cancer Res* 62 (9):2493-7.

Beasley, N. J., Wykoff, C. C., Watson, P. H., et al. 2001. Carbonic anhydrase IX, an endogenous hypoxia marker, expression in head and neck squamous cell carcinoma and its relationship to hypoxia, necrosis, and microvessel density. *Cancer Res* 61 (13):5262-7.

Benasso, M., Sanguineti, G., D'Amico, M., et al. 2000. Induction chemotherapy followed by alternating chemo-radiotherapy in stage IV undifferentiated nasopharyngeal carcinoma. *Br J Cancer* 83 (11):1437-42.

Bertout, J. A., Patel, S. A., and Simon, M. C. 2008. The impact of O2 availability on human cancer. *Nat Rev Cancer* 8 (12):967-75.

Bindra, R. S., Schaffer, P. J., Meng, A., et al. 2005. Alterations in DNA Repair Gene Expression under Hypoxia: Elucidating the Mechanisms of Hypoxia-Induced Genetic Instability. *Ann N Y Acad Sci* 1059:184-95.

Birner, P., Gatterbauer, B., Oberhuber, G., et al. 2001. Expression of hypoxia-inducible factor-1 alpha in oligodendrogliomas: its impact on prognosis and on neoangiogenesis. *Cancer* 92 (1):165-71.

Birner, P., Schindl, M., Obermair, A., et al. 2001. Expression of hypoxia-inducible factor 1alpha in epithelial ovarian tumors: its impact on prognosis and on response to chemotherapy. *Clin Cancer Res* 7 (6):1661-8.

———. 2000. Overexpression of hypoxia-inducible factor 1alpha is a marker for an unfavorable prognosis in early-stage invasive cervical cancer. *Cancer Res* 60 (17):4693-6.

Bjordal, K., Hammerlid, E., Ahlner-Elmqvist, M., et al. 1999. Quality of life in head and neck cancer

patients: validation of the European Organization for Research and Treatment of Cancer Quality of Life Questionnaire-H&N35. *J Clin Oncol* 17 (3):1008-19.

Blais, J. D., Filipenko, V., Bi, M., et al. 2004. Activating transcription factor 4 is translationally regulated by hypoxic stress. *Mol Cell Biol* 24 (17):7469-82.

Bos, R., van der Groep, P., Greijer, A. E., et al. 2003. Levels of hypoxia-inducible factor-1alpha independently predict prognosis in patients with lymph node negative breast carcinoma. *Cancer* 97 (6):1573-81.

Boussen, H., Cvitkovic, E., Wendling, J. L., et al. 1991. Chemotherapy of metastatic and/or recurrent undifferentiated nasopharyngeal carcinoma with cisplatin, bleomycin, and fluorouracil. *J Clin Oncol* 9 (9):1675-81.

Bramwell, V. H., Doig, G. S., Tuck, A. B., et al. 2006. Serial plasma osteopontin levels have prognostic value in metastatic breast cancer. *Clin Cancer Res* 12 (11 Pt 1):3337-43.

Brennan, D. J., Jirstrom, K., Kronblad, A., et al. 2006. CA IX is an independent prognostic marker in premenopausal breast cancer patients with one to three positive lymph nodes and a putative marker of radiation resistance. *Clin Cancer Res* 12 (21):6421-31.

Brizel, D. M., Scully, S. P., Harrelson, J. M., et al. 1996. Tumor oxygenation predicts for the likelihood of distant metastases in human soft tissue sarcoma. *Cancer Res* 56 (5):941-3.

Brizel, D. M., Sibley, G. S., Prosnitz, L. R., et al. 1997. Tumor hypoxia adversely affects the prognosis of carcinoma of the head and neck. *Int J Radiat Oncol Biol Phys* 38 (2):285-9.

Brown, J. M. 1999. The hypoxic cell: a target for selective cancer therapy--eighteenth Bruce F. Cain Memorial Award lecture. *Cancer Res* 59 (23):5863-70.

———. 2001. Therapeutic targets in radiotherapy. *Int J Radiat Oncol Biol Phys* 49 (2):319-26.

Brown, J. M., and Le, Q. T. 2002. Tumor hypoxia is important in radiotherapy, but how should we measure it? *Int J Radiat Oncol Biol Phys* 54 (5):1299-301.

Burri, P., Djonov, V., Aebersold, D. M., et al. 2003. Significant correlation of hypoxia-inducible factor-1alpha with treatment outcome in cervical cancer treated with radical radiotherapy. *Int J Radiat Oncol Biol Phys* 56 (2):494-501.

Chan, A. T., Gregoire, V., Lefebvre, J. L., et al. 2010. Nasopharyngeal cancer: EHNS-ESMO-ESTRO Clinical Practice Guidelines for diagnosis, treatment and follow-up. *Ann Oncol* 21 Suppl 5:v187-9.

Chan, A. T., Hsu, M. M., Goh, B. C., et al. 2005. Multicenter, phase II study of cetuximab in combination with carboplatin in patients with recurrent or metastatic nasopharyngeal carcinoma. *J Clin Oncol* 23 (15):3568-76.

Chan, A. T., Hui, E. P., and Leung, S. F. 2007. Nasopharyngeal cancer: ESMO clinical recommendations for diagnosis, treatment and follow-up. *Ann Oncol* 18 Suppl 2:ii67-8.

Chan, A. T., Leung, S. F., Ngan, R. K., et al. 2005. Overall survival after concurrent

cisplatin-radiotherapy compared with radiotherapy alone in locoregionally advanced nasopharyngeal carcinoma. *J Natl Cancer Inst* 97 (7):536-9.

Chan, A. T., Lo, Y. M., Zee, B., et al. 2002. Plasma Epstein-Barr virus DNA and residual disease after radiotherapy for undifferentiated nasopharyngeal carcinoma. *J Natl Cancer Inst* 94 (21):1614-9.

Chan, A. T., Ma, B. B., Lo, Y. M., et al. 2004. Phase II study of neoadjuvant carboplatin and paclitaxel followed by radiotherapy and concurrent cisplatin in patients with locoregionally advanced nasopharyngeal carcinoma: therapeutic monitoring with plasma Epstein-Barr virus DNA. *J Clin Oncol* 22 (15):3053-60.

Chan, A. T., Teo, P. M., and Huang, D. P. 2004. Pathogenesis and treatment of nasopharyngeal carcinoma. *Semin Oncol* 31 (6):794-801.

Chan, A. T., Teo, P. M., Leung, T. W., et al. 1998. The role of chemotherapy in the management of nasopharyngeal carcinoma. *Cancer* 82 (6):1003-12.

———. 1995. A prospective randomized study of chemotherapy adjunctive to definitive radiotherapy in advanced nasopharyngeal carcinoma. *Int J Radiat Oncol Biol Phys* 33 (3):569-77.

Chan, A. T., Teo, P. M., Ngan, R. K., et al. 2002. Concurrent chemotherapy-radiotherapy compared with radiotherapy alone in locoregionally advanced nasopharyngeal carcinoma: progression-free survival analysis of a phase III randomized trial. *J Clin Oncol* 20 (8):2038-44.

Chang, Y. S., Kim, H. J., Chang, J., et al. 2007. Elevated circulating level of osteopontin is associated with advanced disease state of non-small cell lung cancer. *Lung Cancer* 57 (3):373-80.

Cheng, S. H., Yen, K. L., Jian, J. J., et al. 2001. Examining prognostic factors and patterns of failure in nasopharyngeal carcinoma following concomitant radiotherapy and chemotherapy: impact on future clinical trials. *Int J Radiat Oncol Biol Phys* 50 (3):717-26.

Cheung, S. T., Huang, D. P., Hui, A. B., et al. 1999. Nasopharyngeal carcinoma cell line (C666-1) consistently harbouring Epstein-Barr virus. *Int J Cancer* 83 (1):121-6.

Chi, J. T., Wang, Z., Nuyten, D. S., et al. 2006. Gene Expression Programs in Response to Hypoxia: Cell Type Specificity and Prognostic Significance in Human Cancers. *PLoS Med* 3 (3):e47.

Chi, K. H., Chan, W. K., Cooper, D. L., et al. 1994. A phase II study of outpatient chemotherapy with cisplatin, 5-fluorouracil, and leucovorin in nasopharyngeal carcinoma. *Cancer* 73 (2):247-52.

Chi, K. H., Chang, Y. C., Chan, W. K., et al. 1997. A phase II study of carboplatin in nasopharyngeal carcinoma. *Oncology* 54 (3):203-7.

Chi, K. H., Chang, Y. C., Guo, W. Y., et al. 2002. A phase III study of adjuvant chemotherapy in advanced nasopharyngeal carcinoma patients. *Int J Radiat Oncol Biol Phys* 52 (5):1238-44.

Chia, S. K., Wykoff, C. C., Watson, P. H., et al. 2001. Prognostic significance of a novel hypoxia-regulated marker, carbonic anhydrase ix, in invasive breast carcinoma. *J Clin Oncol*

19 (16):3660-8.

Cho, M., Grabmaier, K., Kitahori, Y., et al. 2000. Activation of the MN/CA9 gene is associated with hypomethylation in human renal cell carcinoma cell lines. *Mol Carcinog* 27 (3):184-9.

Choo, R., and Tannock, I. 1991. Chemotherapy for recurrent or metastatic carcinoma of the nasopharynx. A review of the Princess Margaret Hospital experience. *Cancer* 68 (10):2120-4.

Choong, N. W., Kozloff, M., Taber, D., et al. 2009. Phase II study of sunitinib malate in head and neck squamous cell carcinoma. *Invest New Drugs* Epub 2009/08/04, DOI 10.1007/s10637-009-9296-7, .

Chow, L. Q., and Eckhardt, S. G. 2007. Sunitinib: from rational design to clinical efficacy. *J Clin Oncol* 25 (7):884-96.

Christensen, J. G. 2007. A preclinical review of sunitinib, a multitargeted receptor tyrosine kinase inhibitor with anti-angiogenic and antitumour activities. *Ann Oncol* 18 Suppl 10:x3-10.

Chua, D. T., Kwong, D. L., Sham, J. S., et al. 2000. A phase II study of ifosfamide, 5-fluorouracil and leucovorin in patients with recurrent nasopharyngeal carcinoma previously treated with platinum chemotherapy. *Eur J Cancer* 36 (6):736-41.

Chua, D. T., Ma, J., Sham, J. S., et al. 2005. Long-term survival after cisplatin-based induction chemotherapy and radiotherapy for nasopharyngeal carcinoma: a pooled data analysis of two phase III trials. *J Clin Oncol* 23 (6):1118-24.

Chua, D. T., Sham, J. S., and Au, G. K. 2003. A phase II study of capecitabine in patients with recurrent and metastatic nasopharyngeal carcinoma pretreated with platinum-based chemotherapy. *Oral Oncol* 39 (4):361-6.

———. 2005. A phase II study of docetaxel and cisplatin as first-line chemotherapy in patients with metastatic nasopharyngeal carcinoma. *Oral Oncol* 41 (6):589-95.

Chua, D. T., Sham, J. S., Choy, D., et al. 1998. Preliminary report of the Asian-Oceanian Clinical Oncology Association randomized trial comparing cisplatin and epirubicin followed by radiotherapy versus radiotherapy alone in the treatment of patients with locoregionally advanced nasopharyngeal carcinoma. Asian-Oceanian Clinical Oncology Association Nasopharynx Cancer Study Group. *Cancer* 83 (11):2270-83.

Chua, D. T., Sham, J. S., Kwong, D. L., et al. 2003. Treatment outcome after radiotherapy alone for patients with Stage I-II nasopharyngeal carcinoma. *Cancer* 98 (1):74-80.

Chua, D., Wei, W. I., Sham, J. S., et al. 2008. Capecitabine monotherapy for recurrent and metastatic nasopharyngeal cancer. *Jpn J Clin Oncol* 38 (4):244-9.

Ciuleanu, E., Irimie, A., Ciuleanu, T. E., et al. 2008. Capecitabine as salvage treatment in relapsed nasopharyngeal carcinoma: a phase II study. *J BUON* 13 (1):37-42.

Cox, J. D., Stetz, J., and Pajak, T. F. 1995. Toxicity criteria of the Radiation Therapy Oncology Group (RTOG) and the European Organization for Research and Treatment of Cancer (EORTC). *Int*

J Radiat Oncol Biol Phys 31 (5):1341-6.

Crane, C. H., Ellis, L. M., Abbruzzese, J. L., et al. 2006. Phase I trial evaluating the safety of bevacizumab with concurrent radiotherapy and capecitabine in locally advanced pancreatic cancer. *J Clin Oncol* 24 (7):1145-51.

Creating the gene ontology resource: design and implementation. 2001. *Genome Res* 11 (8):1425-33.

Cruz, J. J., Ocana, A., Navarro, M., et al. 2008. New options in the treatment of locally advanced head and neck cancer: role for induction chemotherapy. *Cancer Treat Rev* 34 (3):268-74.

Cumashi, A., Tinari, N., Rossi, C., et al. 2008. Sunitinib malate (SU-11248) alone or in combination with low-dose docetaxel inhibits the growth of DU-145 prostate cancer xenografts. *Cancer Lett* 270 (2):229-33.

Czabanka, M., Vinci, M., Heppner, F., et al. 2009. Effects of sunitinib on tumor hemodynamics and delivery of chemotherapy. *Int J Cancer* 124 (6):1293-300.

Dahlquist, K. D., Salomonis, N., Vranizan, K., et al. 2002. GenMAPP, a new tool for viewing and analyzing microarray data on biological pathways. *Nat Genet* 31 (1):19-20.

Dales, J. P., Garcia, S., Meunier-Carpentier, S., et al. 2005. Overexpression of hypoxia-inducible factor HIF-1alpha predicts early relapse in breast cancer: retrospective study in a series of 745 patients. *Int J Cancer* 116 (5):734-9.

Dayan, F., Roux, D., Brahimi-Horn, M. C., et al. 2006. The oxygen sensor factor-inhibiting hypoxia-inducible factor-1 controls expression of distinct genes through the bifunctional transcriptional character of hypoxia-inducible factor-1alpha. *Cancer Res* 66 (7):3688-98.

De Schutter, H., Landuyt, W., Verbeken, E., et al. 2005. The prognostic value of the hypoxia markers CA IX and GLUT 1 and the cytokines VEGF and IL 6 in head and neck squamous cell carcinoma treated by radiotherapy +/- chemotherapy. *BMC Cancer* 5:42.

Decker, D. A., Drelichman, A., Al-Sarraf, M., et al. 1983. Chemotherapy for nasopharyngeal carcinoma. A ten-year experience. *Cancer* 52 (4):602-5.

Denko, N. C., Fontana, L. A., Hudson, K. M., et al. 2003. Investigating hypoxic tumor physiology through gene expression patterns. *Oncogene* 22 (37):5907-14.

Dugan, M., Choy, D., Ngai, A., et al. 1993. Multicenter phase II trial of mitoxantrone in patients with advanced nasopharyngeal carcinoma in Southeast Asia: an Asian-Oceanian Clinical Oncology Association Group study. *J Clin Oncol* 11 (1):70-6.

Durand, R. E. 1989. Distribution and activity of antineoplastic drugs in a tumor model. *J Natl Cancer Inst* 81 (2):146-52.

Eckert, A. W., Schubert, J., and Taubert, H. 2010. Optimising the therapeutic ratio in head and neck cancer. *Lancet Oncol* 11 (6):511-2.

Elice, F., Jacoub, J., Rickles, F. R., et al. 2008. Hemostatic complications of angiogenesis inhibitors in cancer patients. *Am J Hematol* 83 (11):862-70.

Elser, C., Siu, L. L., Winquist, E., et al. 2007. Phase II trial of sorafenib in patients with recurrent or

metastatic squamous cell carcinoma of the head and neck or nasopharyngeal carcinoma. *J Clin Oncol* 25 (24):3766-73.

Erler, J. T., Bennewith, K. L., Cox, T. R., et al. 2009. Hypoxia-induced lysyl oxidase is a critical mediator of bone marrow cell recruitment to form the premetastatic niche. *Cancer Cell* 15 (1):35-44.

Erler, J. T., Bennewith, K. L., Nicolau, M., et al. 2006. Lysyl oxidase is essential for hypoxia-induced metastasis. *Nature* 440 (7088):1222-6.

Eskens, F. A., and Verweij, J. 2006. The clinical toxicity profile of vascular endothelial growth factor (VEGF) and vascular endothelial growth factor receptor (VEGFR) targeting angiogenesis inhibitors; a review. *Eur J Cancer* 42 (18):3127-39.

Faivre, S., Delbaldo, C., Vera, K., et al. 2006. Safety, pharmacokinetic, and antitumor activity of SU11248, a novel oral multitarget tyrosine kinase inhibitor, in patients with cancer. *J Clin Oncol* 24 (1):25-35.

Faivre, S., Demetri, G., Sargent, W., et al. 2007. Molecular basis for sunitinib efficacy and future clinical development. *Nat Rev Drug Discov* 6 (9):734-45.

Fandi, A., Bachouchi, M., Azli, N., et al. 2000. Long-term disease-free survivors in metastatic undifferentiated carcinoma of nasopharyngeal type. *J Clin Oncol* 18 (6):1324-30.

Fedarko, N. S., Jain, A., Karadag, A., et al. 2001. Elevated serum bone sialoprotein and osteopontin in colon, breast, prostate, and lung cancer. *Clin Cancer Res* 7 (12):4060-6.

Ferrara, N. 1999. Role of vascular endothelial growth factor in the regulation of angiogenesis. *Kidney Int* 56 (3):794-814.

Fleming, I.D., Cooper, J.S., Henson, D.E., et al. 1997. *American Joint Committee on Cancer: AJCC Cancer Staging Manual*. 5th ed. Philadelphia: Lippincott-Raven.

Foo, K. F., Tan, E. H., Leong, S. S., et al. 2002. Gemcitabine in metastatic nasopharyngeal carcinoma of the undifferentiated type. *Ann Oncol* 13 (1):150-6.

Foote, R. L., Weidner, N., Harris, J., et al. 2005. Evaluation of tumor angiogenesis measured with microvessel density (MVD) as a prognostic indicator in nasopharyngeal carcinoma: results of RTOG 9505. *Int J Radiat Oncol Biol Phys* 61 (3):745-53.

Fountzilas, G., Fragkoulidi, A., Kalogera-Fountzila, A., et al. 2010. A phase II study of sunitinib in patients with recurrent and/or metastatic non-nasopharyngeal head and neck cancer. *Cancer Chemother Pharmacol* 65 (4):649-60.

Geara, F. B., Sanguineti, G., Tucker, S. L., et al. 1997. Carcinoma of the nasopharynx treated by radiotherapy alone: determinants of distant metastasis and survival. *Radiother Oncol* 43 (1):53-61.

Generali, D., Berruti, A., Brizzi, M. P., et al. 2006. Hypoxia-inducible factor-1alpha expression predicts a poor response to primary chemoendocrine therapy and disease-free survival in primary human breast cancer. *Clin Cancer Res* 12 (15):4562-8.

Generali, D., Fox, S. B., Berruti, A., et al. 2006. Role of carbonic anhydrase IX expression in prediction of the efficacy and outcome of primary epirubicin/tamoxifen therapy for breast cancer. *Endocr Relat Cancer* 13 (3):921-30.

Giatromanolaki, A., Koukourakis, M. I., Sivridis, E., et al. 2001. Expression of Hypoxia-inducible Carbonic Anhydrase-9 Relates to Angiogenic Pathways and Independently to Poor Outcome in Non-Small Cell Lung Cancer. *Cancer Res* 61 (21):7992-7998.

———. 2001. Relation of hypoxia inducible factor 1 alpha and 2 alpha in operable non-small cell lung cancer to angiogenic/molecular profile of tumours and survival. *Br J Cancer* 85 (6):881-90.

Glaser, R., Zhang, H. Y., Yao, K. T., et al. 1989. Two epithelial tumor cell lines (HNE-1 and HONE-1) latently infected with Epstein-Barr virus that were derived from nasopharyngeal carcinomas. *Proc Natl Acad Sci U S A* 86 (23):9524-8.

Glynne-Jones, R., and Hoskin, P. 2007. Neoadjuvant cisplatin chemotherapy before chemoradiation: a flawed paradigm? *J Clin Oncol* 25 (33):5281-6.

Graeber, T. G., Osmanian, C., Jacks, T., et al. 1996. Hypoxia-mediated selection of cells with diminished apoptotic potential in solid tumours. *Nature* 379 (6560):88-91.

Gray, L. H., Conger, A. D., Ebert, M., et al. 1953. The concentration of oxygen dissolved in tissues at the time of irradiation as a factor in radiotherapy. *Br J Radiol* 26 (312):638-48.

Gray, L.H., Conger, A.D., Ebert, M., et al. 1953. The concentration of oxygen dissolved in tissue at the time of irradiation as a factor in radiotherapy. *Br J Radiol* 26:638-648.

Greijer, A. E., van der Groep, P., Kemming, D., et al. 2005. Up-regulation of gene expression by hypoxia is mediated predominantly by hypoxia-inducible factor 1 (HIF-1). *J Pathol* 206 (3):291-304.

Greijer, A. E., and van der Wall, E. 2004. The role of hypoxia inducible factor 1 (HIF-1) in hypoxia induced apoptosis. *J Clin Pathol* 57 (10):1009-14.

Griffiths, E. A., Pritchard, S. A., Valentine, H. R., et al. 2007. Hypoxia-inducible factor-1alpha expression in the gastric carcinogenesis sequence and its prognostic role in gastric and gastro-oesophageal adenocarcinomas. *Br J Cancer* 96 (1):95-103.

Griffiths, E. A., Pritchard, S. A., Welch, I. M., et al. 2005. Is the hypoxia-inducible factor pathway important in gastric cancer? *Eur J Cancer* 41 (18):2792-805.

Gruber, G., Greiner, R. H., Hlushchuk, R., et al. 2004. Hypoxia-inducible factor 1 alpha in high-risk breast cancer: an independent prognostic parameter? *Breast Cancer Res* 6 (3):R191-8.

Guang-Wu, H., Sunagawa, M., Jie-En, L., et al. 2000. The relationship between microvessel density, the expression of vascular endothelial growth factor (VEGF), and the extension of nasopharyngeal carcinoma. *Laryngoscope* 110 (12):2066-9.

Guerin, O., Formento, P., Lo Nigro, C., et al. 2008. Supra-additive antitumor effect of sunitinib malate

(SU11248, Sutent) combined with docetaxel. A new therapeutic perspective in hormone refractory prostate cancer. *J Cancer Res Clin Oncol* 134 (1):51-7.

Hall, P. S., Kancherla, K., Sastry, P. S., et al. 2008. Severe epistaxis with tyrosine kinase inhibitors. *Clin Oncol (R Coll Radiol)* 20 (4):318-9.

Hareyama, M., Sakata, K., Shirato, H., et al. 2002. A prospective, randomized trial comparing neoadjuvant chemotherapy with radiotherapy alone in patients with advanced nasopharyngeal carcinoma. *Cancer* 94 (8):2217-23.

Hasbini, A., Mahjoubi, R., Fandi, A., et al. 1999. Phase II trial combining mitomycin with 5-fluorouracil, epirubicin, and cisplatin in recurrent and metastatic undifferentiated carcinoma of nasopharyngeal type. *Ann Oncol* 10 (4):421-5.

Haugland, H. K., Vukovic, V., Pintilie, M., et al. 2002. Expression of hypoxia-inducible factor-1alpha in cervical carcinomas: correlation with tumor oxygenation. *Int J Radiat Oncol Biol Phys* 53 (4):854-61.

Hedley, D., Pintilie, M., Woo, J., et al. 2003. Carbonic anhydrase IX expression, hypoxia, and prognosis in patients with uterine cervical carcinomas. *Clin Cancer Res* 9 (15):5666-74.

Ho, J. H. 1978. An epidemiologic and clinical study of nasopharyngeal carcinoma. *Int J Radiat Oncol Biol Phys* 4 (3-4):182-98.

Hockel, M., Knoop, C., Schlenger, K., et al. 1993. Intratumoral pO2 predicts survival in advanced cancer of the uterine cervix. *Radiother Oncol* 26 (1):45-50.

Hockel, M., Schlenger, K., Aral, B., et al. 1996. Association between tumor hypoxia and malignant progression in advanced cancer of the uterine cervix. *Cancer Res* 56 (19):4509-15.

Hockel, M., and Vaupel, P. 2001. Tumor hypoxia: definitions and current clinical, biologic, and molecular aspects. *J Natl Cancer Inst* 93 (4):266-76.

Hong, B., Lui, V. W., Hui, E. P., et al. 2010. Reverse phase protein array identifies novel anti-invasion mechanisms of YC-1. *Biochem Pharmacol* 79 (6):842-52.

———. 2009. Hypoxia-targeting by tirapazamine (TPZ) induces preferential growth inhibition of nasopharyngeal carcinoma cells with Chk1/2 activation. *Invest New Drugs* Epub 2009/12/17, DOI: 10.1007/s10637-009-9356-z.

Hong, R. L., Lin, C. Y., Ting, L. L., et al. 2004. Comparison of clinical and molecular surveillance in patients with advanced nasopharyngeal carcinoma after primary therapy: the potential role of quantitative analysis of circulating Epstein-Barr virus DNA. *Cancer* 100 (7):1429-37.

Hoogsteen, I. J., Marres, H. A., Bussink, J., et al. 2007. Tumor microenvironment in head and neck squamous cell carcinomas: predictive value and clinical relevance of hypoxic markers. A review. *Head Neck* 29 (6):591-604.

Hoogsteen, I. J., Marres, H. A., van der Kogel, A. J., et al. 2007. The hypoxic tumour microenvironment, patient selection and hypoxia-modifying treatments. *Clin Oncol (R Coll*

Radiol) 19 (6):385-96.

Horsman, M. R. 1998. Measurement of tumor oxygenation. *Int J Radiat Oncol Biol Phys* 42 (4):701-4.

Hotte, S. J., Winquist, E. W., Stitt, L., et al. 2002. Plasma osteopontin: associations with survival and metastasis to bone in men with hormone-refractory prostate carcinoma. *Cancer* 95 (3):506-12.

Huang, D. P., Ho, J. H., Poon, Y. F., et al. 1980. Establishment of a cell line (NPC/HK1) from a differentiated squamous carcinoma of the nasopharynx. *Int J Cancer* 26 (2):127-32.

Hui, E. P., Leung, S. F., Au, J. S., et al. 2004. Lung metastasis alone in nasopharyngeal carcinoma: a relatively favorable prognostic group. A study by the Hong Kong Nasopharyngeal Carcinoma Study Group. *Cancer* 101 (2):300-6.

Hui, E. P., Sung, F. L., Yu, B. K., et al. 2008. Plasma osteopontin, hypoxia, and response to radiotherapy in nasopharyngeal cancer. *Clin Cancer Res* 14 (21):7080-7.

Hussain, S. A., Ganesan, R., Reynolds, G., et al. 2007. Hypoxia-regulated carbonic anhydrase IX expression is associated with poor survival in patients with invasive breast cancer. *Br J Cancer* 96 (1):104-9.

Hutchison, G. J., Valentine, H. R., Loncaster, J. A., et al. 2004. Hypoxia-inducible factor 1alpha expression as an intrinsic marker of hypoxia: correlation with tumor oxygen, pimonidazole measurements, and outcome in locally advanced carcinoma of the cervix. *Clin Cancer Res* 10 (24):8405-12.

Ikezoe, T., Nishioka, C., Tasaka, T., et al. 2006. The antitumor effects of sunitinib (formerly SU11248) against a variety of human hematologic malignancies: enhancement of growth inhibition via inhibition of mammalian target of rapamycin signaling. *Mol Cancer Ther* 5 (10):2522-30.

International histological classification of tumours No 19. 1978. In *Histological typing of upper respiratory tract tumours*: World Health Organisation.

Ishikawa, H., Sakurai, H., Hasegawa, M., et al. 2004. Expression of hypoxic-inducible factor 1alpha predicts metastasis-free survival after radiation therapy alone in stage IIIB cervical squamous cell carcinoma. *Int J Radiat Oncol Biol Phys* 60 (2):513-21.

Ivanov, S., Liao, S. Y., Ivanova, A., et al. 2001. Expression of hypoxia-inducible cell-surface transmembrane carbonic anhydrases in human cancer. *Am J Pathol* 158 (3):905-19.

Je, Y., Schutz, F. A., and Choueiri, T. K. 2009. Risk of bleeding with vascular endothelial growth factor receptor tyrosine-kinase inhibitors sunitinib and sorafenib: a systematic review and meta-analysis of clinical trials. *Lancet Oncol* 10 (10):967-74.

Jiang, Y., Wei, Y. Q., Luo, F., et al. 2005. Gemcitabine and cisplatin in advanced nasopharyngeal carcinoma: a pilot study. *Cancer Invest* 23 (2):123-8.

Johnson, D. H., Fehrenbacher, L., Novotny, W. F., et al. 2004. Randomized phase II trial comparing bevacizumab plus carboplatin and paclitaxel with carboplatin and paclitaxel alone in previously untreated locally advanced or metastatic non-small-cell lung cancer. *J Clin Oncol*

22 (11):2184-91.

Johnson, F. M., Garden, A., Palmer, J. L., et al. 2004. A Phase II study of docetaxel and carboplatin as neoadjuvant therapy for nasopharyngeal carcinoma with early T status and advanced N status. *Cancer* 100 (5):991-8.

Jonathan, R. A., Wijffels, K. I., Peeters, W., et al. 2006. The prognostic value of endogenous hypoxia-related markers for head and neck squamous cell carcinomas treated with ARCON. *Radiother Oncol* 79 (3):288-97.

Jones, A., Fujiyama, C., Blanche, C., et al. 2001. Relation of vascular endothelial growth factor production to expression and regulation of hypoxia-inducible factor-1 alpha and hypoxia-inducible factor-2 alpha in human bladder tumors and cell lines. *Clin Cancer Res* 7 (5):1263-72.

Kam, M. K., Teo, P. M., Chau, R. M., et al. 2004. Treatment of nasopharyngeal carcinoma with intensity-modulated radiotherapy: the Hong Kong experience. *Int J Radiat Oncol Biol Phys* 60 (5):1440-50.

Kim, J. H., Skates, S. J., Uede, T., et al. 2002. Osteopontin as a potential diagnostic biomarker for ovarian cancer. *JAMA* 287 (13):1671-9.

Kim, J., Ki, S. S., Lee, S. D., et al. 2006. Elevated plasma osteopontin levels in patients with hepatocellular carcinoma. *Am J Gastroenterol* 101 (9):2051-9.

Kim, S. J., Rabbani, Z. N., Vollmer, R. T., et al. 2004. Carbonic anhydrase IX in early-stage non-small cell lung cancer. *Clin Cancer Res* 10 (23):7925-33.

King, W. W., Teo, P. M., and Li, A. K. 1992. Patterns of failure after radical neck dissection for recurrent nasopharyngeal carcinoma. *Am J Surg* 164 (6):599-602.

Kon, S., Maeda, M., Segawa, T., et al. 2000. Antibodies to different peptides in osteopontin reveal complexities in the various secreted forms. *J Cell Biochem* 77 (3):487-98.

Koopmann, J., Fedarko, N. S., Jain, A., et al. 2004. Evaluation of osteopontin as biomarker for pancreatic adenocarcinoma. *Cancer Epidemiol Biomarkers Prev* 13 (3):487-91.

Koshiji, M., To, K. K., Hammer, S., et al. 2005. HIF-1alpha induces genetic instability by transcriptionally downregulating MutSalpha expression. *Mol Cell* 17 (6):793-803.

Koukourakis, M. I., Bentzen, S. M., Giatromanolaki, A., et al. 2006. Endogenous markers of two separate hypoxia response pathways (hypoxia inducible factor 2 alpha and carbonic anhydrase 9) are associated with radiotherapy failure in head and neck cancer patients recruited in the CHART randomized trial. *J Clin Oncol* 24 (5):727-35.

Koukourakis, M. I., Giatromanolaki, A., Sivridis, E., et al. 2002. Hypoxia-inducible factor (HIF1A and HIF2A), angiogenesis, and chemoradiotherapy outcome of squamous cell head-and-neck cancer. *Int J Radiat Oncol Biol Phys* 53 (5):1192-202.

———. 2001. Hypoxia-regulated Carbonic Anhydrase-9 (CA9) Relates to Poor Vascularization and

Resistance of Squamous Cell Head and Neck Cancer to Chemoradiotherapy. *Clin Cancer Res* 7 (11):3399-403.

Koukourakis, M. I., Giatromanolaki, A., Skarlatos, J., et al. 2001. Hypoxia inducible factor (HIF-1a and HIF-2a) expression in early esophageal cancer and response to photodynamic therapy and radiotherapy. *Cancer Res* 61 (5):1830-2.

Krishna, S. M., James, S., and Balaram, P. 2006. Expression of VEGF as prognosticator in primary nasopharyngeal cancer and its relation to EBV status. *Virus Res* 115 (1):85-90.

Kwan, W. H., Teo, P. M., Chow, L. T., et al. 1996. Nasopharyngeal carcinoma with metastatic disease to mediastinal and hilar lymph nodes: an indication for more aggressive treatment. *Clin Oncol (R Coll Radiol)* 8 (1):55-8.

Kwong, D. L., Sham, J. S., Au, G. K., et al. 2004. Concurrent and adjuvant chemotherapy for nasopharyngeal carcinoma: a factorial study. *J Clin Oncol* 22 (13):2643-53.

Kwong, D., Sham, J., and Choy, D. 1994. The effect of loco-regional control on distant metastatic dissemination in carcinoma of the nasopharynx: an analysis of 1301 patients. *Int J Radiat Oncol Biol Phys* 30 (5):1029-36.

Kyzas, P. A., Stefanou, D., Batistatou, A., et al. 2005. Hypoxia-induced tumor angiogenic pathway in head and neck cancer: an in vivo study. *Cancer Lett* 225 (2):297-304.

La Vine, D. B., Coleman, T. A., Davis, C. H., et al. 2009. Frequent Dose Interruptions are Required for Patients Receiving Oral Kinase Inhibitor Therapy for Advanced Renal Cell Carcinoma. *Am J Clin Oncol* Epub 2009/09/12, DOI 10.1097/COC.0b013e3181a650a6.

Le, Q. T., Sutphin, P. D., Raychaudhuri, S., et al. 2003. Identification of osteopontin as a prognostic plasma marker for head and neck squamous cell carcinomas. *Clin Cancer Res* 9 (1):59-67.

Lee, A. W., Lau, W. H., Tung, S. Y., et al. 2005. Preliminary results of a randomized study on therapeutic gain by concurrent chemotherapy for regionally-advanced nasopharyngeal carcinoma: NPC-9901 Trial by the Hong Kong Nasopharyngeal Cancer Study Group. *J Clin Oncol* 23 (28):6966-75.

Lee, A. W., Poon, Y. F., Foo, W., et al. 1992. Retrospective analysis of 5037 patients with nasopharyngeal carcinoma treated during 1976-1985: overall survival and patterns of failure. *Int J Radiat Oncol Biol Phys* 23 (2):261-70.

Lee, A. W., Tung, S. Y., Chua, D. T., et al. 2010. Randomized trial of radiotherapy plus concurrent-adjuvant chemotherapy vs radiotherapy alone for regionally advanced nasopharyngeal carcinoma. *J Natl Cancer Inst* 102 (15):1188-98.

Lee, A. W., Yau, T. K., Wong, D. H., et al. 2005. Treatment of stage IV(A-B) nasopharyngeal carcinoma by induction-concurrent chemoradiotherapy and accelerated fractionation. *Int J Radiat Oncol Biol Phys* 63 (5):1331-8.

Lee, N., Xia, P., Quivey, J. M., et al. 2002. Intensity-modulated radiotherapy in the treatment of nasopharyngeal carcinoma: an update of the UCSF experience. *Int J Radiat Oncol Biol Phys*

53 (1):12-22.

Leek, R. D., Lewis, C. E., Whitehouse, R., et al. 1996. Association of macrophage infiltration with angiogenesis and prognosis in invasive breast carcinoma. *Cancer Res* 56 (20):4625-9.

Leek, R. D., Talks, K. L., Pezzella, F., et al. 2002. Relation of hypoxia-inducible factor-2 alpha (HIF-2 alpha) expression in tumor-infiltrative macrophages to tumor angiogenesis and the oxidative thymidine phosphorylase pathway in Human breast cancer. *Cancer Res* 62 (5):1326-9.

Leibel, S. A., Scott, C. B., Mohiuddin, M., et al. 1991. The effect of local-regional control on distant metastatic dissemination in carcinoma of the head and neck: results of an analysis from the RTOG head and neck database. *Int J Radiat Oncol Biol Phys* 21 (3):549-56.

Leong, S. S., Wee, J., Tay, M. H., et al. 2005. Paclitaxel, carboplatin, and gemcitabine in metastatic nasopharyngeal carcinoma: a Phase II trial using a triplet combination. *Cancer* 103 (3):569-75.

Leung, S. F., Teo, P. M., Shiu, W. W., et al. 1991. Clinical features and management of distant metastases of nasopharyngeal carcinoma. *J Otolaryngol* 20 (1):27-9.

Leung, S. F., Zee, B., Ma, B. B., et al. 2006. Plasma Epstein-Barr viral deoxyribonucleic acid quantitation complements tumor-node-metastasis staging prognostication in nasopharyngeal carcinoma. *J Clin Oncol* 24 (34):5414-8.

Li, Y. H., Wang, F. H., Jiang, W. Q., et al. 2008. Phase II study of capecitabine and cisplatin combination as first-line chemotherapy in Chinese patients with metastatic nasopharyngeal carcinoma. *Cancer Chemother Pharmacol* 62 (3):539-44.

Lin, J. C., Jan, J. S., Hsu, C. Y., et al. 2003. Phase III study of concurrent chemoradiotherapy versus radiotherapy alone for advanced nasopharyngeal carcinoma: positive effect on overall and progression-free survival. *J Clin Oncol* 21 (4):631-7.

Lin, J. C., Wang, W. Y., Chen, K. Y., et al. 2004. Quantification of plasma Epstein-Barr virus DNA in patients with advanced nasopharyngeal carcinoma. *N Engl J Med* 350 (24):2461-70.

Liu, F. Y., Chang, J. T., Wang, H. M., et al. 2006. [18F]fluorodeoxyglucose positron emission tomography is more sensitive than skeletal scintigraphy for detecting bone metastasis in endemic nasopharyngeal carcinoma at initial staging. *J Clin Oncol* 24 (4):599-604.

Liu, F. Y., Lin, C. Y., Chang, J. T., et al. 2007. 18F-FDG PET can replace conventional work-up in primary M staging of nonkeratinizing nasopharyngeal carcinoma. *J Nucl Med* 48 (10):1614-9.

Liu, G., Loraine, A. E., Shigeta, R., et al. 2003. NetAffx: Affymetrix probesets and annotations. *Nucleic Acids Res* 31 (1):82-6.

Lo, K. W., To, K. F., and Huang, D. P. 2004. Focus on nasopharyngeal carcinoma. *Cancer Cell* 5 (5):423-8.

Lo, Y. M., Chan, A. T., Chan, L. Y., et al. 2000. Molecular prognostication of nasopharyngeal carcinoma by quantitative analysis of circulating Epstein-Barr virus DNA. *Cancer Res* 60 (24):6878-81.

Lo, Y. M., Chan, L. Y., Chan, A. T., et al. 1999. Quantitative and temporal correlation between circulating cell-free Epstein-Barr virus DNA and tumor recurrence in nasopharyngeal carcinoma. *Cancer Res* 59 (21):5452-5.

Lo, Y. M., Chan, L. Y., Lo, K. W., et al. 1999. Quantitative analysis of cell-free Epstein-Barr virus DNA in plasma of patients with nasopharyngeal carcinoma. *Cancer Res* 59 (6):1188-91.

Lo, Y. M., Leung, S. F., Chan, L. Y., et al. 2000. Kinetics of plasma Epstein-Barr virus DNA during radiation therapy for nasopharyngeal carcinoma. *Cancer Res* 60 (9):2351-5.

Loncaster, J. A., Harris, A. L., Davidson, S. E., et al. 2001. Carbonic anhydrase (CA IX) expression, a potential new intrinsic marker of hypoxia: correlations with tumor oxygen measurements and prognosis in locally advanced carcinoma of the cervix. *Cancer Res* 61 (17):6394-9.

Lordick, F., Geinitz, H., Theisen, J., et al. 2006. Increased risk of ischemic bowel complications during treatment with bevacizumab after pelvic irradiation: report of three cases. *Int J Radiat Oncol Biol Phys* 64 (5):1295-8.

Ludwig, J. A., and Weinstein, J. N. 2005. Biomarkers in cancer staging, prognosis and treatment selection. *Nat Rev Cancer* 5 (11):845-56.

Lui, V. W., Boehm, A. L., Koppikar, P., et al. 2007. Antiproliferative mechanisms of a transcription factor decoy targeting signal transducer and activator of transcription (STAT) 3: the role of STAT1. *Mol Pharmacol* 71 (5):1435-43.

Lukacova, S., Overgaard, J., Alsner, J., et al. 2006. Strain and tumour specific variations in the effect of hypoxia on osteopontin levels in experimental models. *Radiother Oncol* 80 (2):165-71.

Ma, B. B., and Chan, A. T. 2005. Recent perspectives in the role of chemotherapy in the management of advanced nasopharyngeal carcinoma. *Cancer* 103 (1):22-31.

Ma, B. B., Hui, E. P., Wong, S. C., et al. 2009. Multicenter phase II study of gemcitabine and oxaliplatin in advanced nasopharyngeal carcinoma--correlation with excision repair cross-complementing-1 polymorphisms. *Ann Oncol* 20 (11):1854-9.

Ma, B. B., King, A., Lo, Y. M., et al. 2006. Relationship between pretreatment level of plasma Epstein-Barr virus DNA, tumor burden, and metabolic activity in advanced nasopharyngeal carcinoma. *Int J Radiat Oncol Biol Phys* 66 (3):714-20.

Ma, B. B., Poon, T. C., To, K. F., et al. 2003. Prognostic significance of tumor angiogenesis, Ki 67, p53 oncoprotein, epidermal growth factor receptor and HER2 receptor protein expression in undifferentiated nasopharyngeal carcinoma--a prospective study. *Head Neck* 25 (10):864-72.

Ma, B. B., Tannock, I. F., Pond, G. R., et al. 2002. Chemotherapy with gemcitabine-containing regimens for locally recurrent or metastatic nasopharyngeal carcinoma. *Cancer* 95 (12):2516-23.

Ma, J., Mai, H. Q., Hong, M. H., et al. 2001. Results of a prospective randomized trial comparing neoadjuvant chemotherapy plus radiotherapy with radiotherapy alone in patients with locoregionally advanced nasopharyngeal carcinoma. *J Clin Oncol* 19 (5):1350-7.

Machiels, J. P., Henry, S., Zanetta, S., et al. 2010. Phase II study of sunitinib in recurrent or metastatic squamous cell carcinoma of the head and neck: GORTEC 2006-01. *J Clin Oncol* 28 (1):21-8.

Maris, J. M., Courtright, J., Houghton, P. J., et al. 2008. Initial testing (stage 1) of sunitinib by the pediatric preclinical testing program. *Pediatr Blood Cancer* 51 (1):42-8.

Matsuyama, T., Nakanishi, K., Hayashi, T., et al. 2005. Expression of hypoxia-inducible factor-1alpha in esophageal squamous cell carcinoma. *Cancer Sci* 96 (3):176-82.

Maxwell, P. H., Wiesener, M. S., Chang, G. W., et al. 1999. The tumour suppressor protein VHL targets hypoxia-inducible factors for oxygen-dependent proteolysis. *Nature* 399 (6733):271-5.

Mayer, A., Wree, A., Hockel, M., et al. 2004. Lack of correlation between expression of HIF-1alpha protein and oxygenation status in identical tissue areas of squamous cell carcinomas of the uterine cervix. *Cancer Res* 64 (16):5876-81.

Maynard, M. A., and Ohh, M. 2007. The role of hypoxia-inducible factors in cancer. *Cell Mol Life Sci* 64 (16):2170-80.

McAllister, S. S., Gifford, A. M., Greiner, A. L., et al. 2008. Systemic endocrine instigation of indolent tumor growth requires osteopontin. *Cell* 133 (6):994-1005.

McCarthy, J. S., Tannock, I. F., Degendorfer, P., et al. 2002. A Phase II trial of docetaxel and cisplatin in patients with recurrent or metastatic nasopharyngeal carcinoma. *Oral Oncol* 38 (7):686-90.

Mendel, D. B., Laird, A. D., Xin, X., et al. 2003. In vivo antitumor activity of SU11248, a novel tyrosine kinase inhibitor targeting vascular endothelial growth factor and platelet-derived growth factor receptors: determination of a pharmacokinetic/pharmacodynamic relationship. *Clin Cancer Res* 9 (1):327-37.

Miller, A. B., Hoogstraten, B., Staquet, M., et al. 1981. Reporting results of cancer treatment. *Cancer* 47 (1):207-14.

Mocanu, J. D., Yip, K. W., Alajez, N. M., et al. 2007. Imaging the modulation of adenoviral kinetics and biodistribution for cancer gene therapy. *Mol Ther* 15 (5):921-9.

Morris, M., Eifel, P. J., Lu, J., et al. 1999. Pelvic radiation with concurrent chemotherapy compared with pelvic and para-aortic radiation for high-risk cervical cancer. *N Engl J Med* 340 (15):1137-43.

Murono, S., Inoue, H., Tanabe, T., et al. 2001. Induction of cyclooxygenase-2 by Epstein-Barr virus latent membrane protein 1 is involved in vascular endothelial growth factor production in nasopharyngeal carcinoma cells. *Proc Natl Acad Sci U S A* 98 (12):6905-10.

Murray, L. J., Abrams, T. J., Long, K. R., et al. 2003. SU11248 inhibits tumor growth and CSF-1R-dependent osteolysis in an experimental breast cancer bone metastasis model. *Clin Exp Metastasis* 20 (8):757-66.

Ngan, R. K., Lau, W. H., Yip, T. T., et al. 2001. Remarkable application of serum EBV EBER-I in monitoring response of nasopharyngeal cancer patients to salvage chemotherapy. *Ann N Y Acad Sci* 945:73-9.

Ngan, R. K., Yiu, H. H., Lau, W. H., et al. 2002. Combination gemcitabine and cisplatin chemotherapy for metastatic or recurrent nasopharyngeal carcinoma: report of a phase II study. *Ann Oncol* 13 (8):1252-8.

Ngeow, J., Lim, W. T., Leong, S. S., et al. 2010. Docetaxel is effective in heavily pretreated patients with disseminated nasopharyngeal carcinoma. *Ann Oncol*.

Ning, W., Chu, T. J., Li, C. J., et al. 2004. Genome-wide analysis of the endothelial transcriptome under short-term chronic hypoxia. *Physiol Genomics* 18 (1):70-8.

Nordsmark, M., Bentzen, S. M., Rudat, V., et al. 2005. Prognostic value of tumor oxygenation in 397 head and neck tumors after primary radiation therapy. An international multi-center study. *Radiother Oncol* 77 (1):18-24.

Nordsmark, M., Eriksen, J. G., Gebski, V., et al. 2007. Differential risk assessments from five hypoxia specific assays: The basis for biologically adapted individualized radiotherapy in advanced head and neck cancer patients. *Radiother Oncol* 83 (3):389-97.

Nordsmark, M., Overgaard, M., and Overgaard, J. 1996. Pretreatment oxygenation predicts radiation response in advanced squamous cell carcinoma of the head and neck. *Radiother Oncol* 41 (1):31-9.

———. 1996. Pretreatment oxygenation predicts radiation response in advanced squamous cell carcinoma of the head and neck. *Radiother Oncol* 41 (1):31-9.

O'Farrell, A. M., Abrams, T. J., Yuen, H. A., et al. 2003. SU11248 is a novel FLT3 tyrosine kinase inhibitor with potent activity in vitro and in vivo. *Blood* 101 (9):3597-605.

Oh, J. L., Vokes, E. E., Kies, M. S., et al. 2003. Induction chemotherapy followed by concomitant chemoradiotherapy in the treatment of locoregionally advanced nasopharyngeal cancer. *Ann Oncol* 14 (4):564-9.

Olive, P. L., Aquino-Parsons, C., MacPhail, S. H., et al. 2001. Carbonic anhydrase 9 as an endogenous marker for hypoxic cells in cervical cancer. *Cancer Res* 61 (24):8924-9.

Ong, Y. K., Heng, D. M., Chung, B., et al. 2003. Design of a prognostic index score for metastatic nasopharyngeal carcinoma. *Eur J Cancer* 39 (11):1535-41.

Onita, T., Ji, P. G., Xuan, J. W., et al. 2002. Hypoxia-induced, perinecrotic expression of endothelial Per-ARNT-Sim domain protein-1/hypoxia-inducible factor-2alpha correlates with tumor progression, vascularization, and focal macrophage infiltration in bladder cancer. *Clin Cancer Res* 8 (2):471-80.

Opavsky, R., Pastorekova, S., Zelnik, V., et al. 1996. Human MN/CA9 gene, a novel member of the carbonic anhydrase family: structure and exon to protein domain relationships. *Genomics* 33 (3):480-7.

Osusky, K. L., Hallahan, D. E., Fu, A., et al. 2004. The receptor tyrosine kinase inhibitor SU11248 impedes endothelial cell migration, tubule formation, and blood vessel formation in vivo, but

has little effect on existing tumor vessels. *Angiogenesis* 7 (3):225-33.

Overgaard, J., Eriksen, J. G., Nordsmark, M., et al. 2005. Plasma osteopontin, hypoxia, and response to the hypoxia sensitiser nimorazole in radiotherapy of head and neck cancer: results from the DAHANCA 5 randomised double-blind placebo-controlled trial. *Lancet Oncol* 6 (10):757-64.

Ozturk, B., Buyukberber, S., Akmansu, M., et al. 2007. The results of three different treatment modalities in patients with locally advanced nasopharyngeal carcinoma. *Med Oncol.*

Pan, H.J., Lin, C.L. , Tsai, M.Y., et al. 2000. A Pilot Study of Vinorelbine on a Weekly Schedule in Metastatic Nasopharyngeal Carcinoma (NPC). *Proc Am Soc Clin Oncol* 19:(abstract 1689).

Pass, H. I., Lott, D., Lonardo, F., et al. 2005. Asbestos exposure, pleural mesothelioma, and serum osteopontin levels. *N Engl J Med* 353 (15):1564-73.

Pastorek, J., Pastorekova, S., Callebaut, I., et al. 1994. Cloning and characterization of MN, a human tumor-associated protein with a domain homologous to carbonic anhydrase and a putative helix-loop-helix DNA binding segment. *Oncogene* 9 (10):2877-88.

Pastorekova, S., Zavadova, Z., Kostal, M., et al. 1992. A novel quasi-viral agent, MaTu, is a two-component system. *Virology* 187 (2):620-6.

Peters, N. A., Richel, D. J., Verhoeff, J. J., et al. 2008. Bowel perforation after radiotherapy in a patient receiving sorafenib. *J Clin Oncol* 26 (14):2405-6.

Petrik, D., Lavori, P. W., Cao, H., et al. 2006. Plasma osteopontin is an independent prognostic marker for head and neck cancers. *J Clin Oncol* 24 (33):5291-7.

Poon, D., Chowbay, B., Cheung, Y. B., et al. 2005. Phase II study of irinotecan (CPT-11) as salvage therapy for advanced nasopharyngeal carcinoma. *Cancer* 103 (3):576-81.

Poon, R. T., Fan, S. T., and Wong, J. 2001. Clinical implications of circulating angiogenic factors in cancer patients. *J Clin Oncol* 19 (4):1207-25.

Posner, M. R., Hershock, D. M., Blajman, C. R., et al. 2007. Cisplatin and fluorouracil alone or with docetaxel in head and neck cancer. *N Engl J Med* 357 (17):1705-15.

Potapova, O., Laird, A. D., Nannini, M. A., et al. 2006. Contribution of individual targets to the antitumor efficacy of the multitargeted receptor tyrosine kinase inhibitor SU11248. *Mol Cancer Ther* 5 (5):1280-9.

Pouessel, D., and Culine, S. 2008. High frequency of intracerebral hemorrhage in metastatic renal carcinoma patients with brain metastases treated with tyrosine kinase inhibitors targeting the vascular endothelial growth factor receptor. *Eur Urol* 53 (2):376-81.

Pouyssegur, J., Dayan, F., and Mazure, N. M. 2006. Hypoxia signalling in cancer and approaches to enforce tumour regression. *Nature* 441 (7092):437-43.

Prestwich, R., Dyker, K., and Sen, M. 2010. Improving the therapeutic ratio in head and neck cancer. *Lancet Oncol* 11 (6):512-3.

Qian, C. N., Min, H. Q., Lin, H. L., et al. 1999. Anti-tumor effect of angiogenesis inhibitor TNP-470 on the human nasopharyngeal carcinoma cell line NPC/HK1. *Oncology* 57 (1):36-41.

———. 1998. Primary study in experimental antiangiogenic therapy of nasopharyngeal carcinoma with AGM-1470 (TNP-470). *J Laryngol Otol* 112 (9):849-53.

Qian, C. N., Zhang, C. Q., Guo, X., et al. 2000. Elevation of serum vascular endothelial growth factor in male patients with metastatic nasopharyngeal carcinoma. *Cancer* 88 (2):255-61.

Ramankulov, A., Lein, M., Kristiansen, G., et al. 2007. Plasma osteopontin in comparison with bone markers as indicator of bone metastasis and survival outcome in patients with prostate cancer. *Prostate* 67 (3):330-40.

———. 2007. Elevated plasma osteopontin as marker for distant metastases and poor survival in patients with renal cell carcinoma. *J Cancer Res Clin Oncol* 133 (9):643-52.

Reynolds, T. Y., Rockwell, S., and Glazer, P. M. 1996. Genetic instability induced by the tumor microenvironment. *Cancer Res* 56 (24):5754-7.

Rischin, D., Corry, J., Smith, J., et al. 2002. Excellent disease control and survival in patients with advanced nasopharyngeal cancer treated with chemoradiation. *J Clin Oncol* 20 (7):1845-52.

Rischin, D., Hicks, R. J., Fisher, R., et al. 2006. Prognostic significance of [18F]-misonidazole positron emission tomography-detected tumor hypoxia in patients with advanced head and neck cancer randomly assigned to chemoradiation with or without tirapazamine: a substudy of Trans-Tasman Radiation Oncology Group Study 98.02. *J Clin Oncol* 24 (13):2098-104.

Rossi, A., Molinari, R., Boracchi, P., et al. 1988. Adjuvant chemotherapy with vincristine, cyclophosphamide, and doxorubicin after radiotherapy in local-regional nasopharyngeal cancer: results of a 4-year multicenter randomized study. *J Clin Oncol* 6 (9):1401-10.

Rubio, L., Burgos, J. S., Lopez-Guerrero, J. A., et al. 2002. Expression of p53 protein and tumor angiogenesis as prognostic factors in nasopharyngeal carcinoma patients. *Pathol Res Pract* 198 (2):97-102.

Rubio, L., Burgos, J. S., Morera, C., et al. 2000. Morphometric study of tumor angiogenesis as a new prognostic factor in nasopharyngeal carcinoma patients. *Pathol Oncol Res* 6 (3):210-6.

Said, H. M., Katzer, A., Flentje, M., et al. 2005. Response of the plasma hypoxia marker osteopontin to in vitro hypoxia in human tumor cells. *Radiother Oncol* 76 (2):200-5.

Salomonis, N., Hanspers, K., Zambon, A. C., et al. 2007. GenMAPP 2: new features and resources for pathway analysis. *BMC Bioinformatics* 8:217.

Sanguineti, G., Bossi, P., Pou, A., et al. 2003. Timing of chemoradiotherapy and patient selection for locally advanced nasopharyngeal carcinoma. *Clin Oncol (R Coll Radiol)* 15 (8):451-60.

Sauter, E. R., Nesbit, M., Watson, J. C., et al. 1999. Vascular endothelial growth factor is a marker of tumor invasion and metastasis in squamous cell carcinomas of the head and neck. *Clin Cancer Res* 5 (4):775-82.

Schindl, M., Schoppmann, S. F., Samonigg, H., et al. 2002. Overexpression of hypoxia-inducible factor 1alpha is associated with an unfavorable prognosis in lymph node-positive breast

cancer. *Clin Cancer Res* 8 (6):1831-7.

Schoppmann, S. F., Fenzl, A., Schindl, M., et al. 2006. Hypoxia inducible factor-1alpha correlates with VEGF-C expression and lymphangiogenesis in breast cancer. *Breast Cancer Res Treat* 99 (2):135-41.

Schorge, J. O., Drake, R. D., Lee, H., et al. 2004. Osteopontin as an adjunct to CA125 in detecting recurrent ovarian cancer. *Clin Cancer Res* 10 (10):3474-8.

Semenza, G. L. 2000. HIF-1: mediator of physiological and pathophysiological responses to hypoxia. *J Appl Physiol* 88 (4):1474-80.

———. 2000. Hypoxia, clonal selection, and the role of HIF-1 in tumor progression. *Crit Rev Biochem Mol Biol* 35 (2):71-103.

———. 2010. Defining the role of hypoxia-inducible factor 1 in cancer biology and therapeutics. *Oncogene* 29 (5):625-34.

Sha, D., and He, Y. J. 2006. Expression and clinical significance of VEGF and its receptors Flt-1 and KDR in nasopharyngeal carcinoma. *Ai Zheng* 25 (2):229-34.

Sham, J. S., Choy, D., and Choi, P. H. 1990. Nasopharyngeal carcinoma: the significance of neck node involvement in relation to the pattern of distant failure. *Br J Radiol* 63 (746):108-13.

Sher, A.F., Chu, D., and Wu, S. 2009. Risk of bleeding in cancer patients treated with the angiogenesis inhibitor bevacizumab: A meta-analysis. *J Clin Oncol* 27:15s (suppl; abstr 9584).

Sheu, L. F., Lee, W. C., Lee, H. S., et al. 2005. Co-expression of c-kit and stem cell factor in primary and metastatic nasopharyngeal carcinomas and nasopharyngeal epithelium. *J Pathol* 207 (2):216-23.

Sheu, L. F., Young, Z. H., Lee, W. C., et al. 2007. STI571 sensitizes nasopharyngeal carcinoma cells to cisplatin: sustained activation of ERK with improved growth inhibition. *Int J Oncol* 30 (2):403-11.

Shimada, Y., Watanabe, G., Kawamura, J., et al. 2005. Clinical significance of osteopontin in esophageal squamous cell carcinoma: comparison with common tumor markers. *Oncology* 68 (2-3):285-92.

Simon, R. 1989. Optimal two-stage designs for phase II clinical trials. *Control Clin Trials* 10 (1):1-10.

Singhal, H., Bautista, D. S., Tonkin, K. S., et al. 1997. Elevated plasma osteopontin in metastatic breast cancer associated with increased tumor burden and decreased survival. *Clin Cancer Res* 3 (4):605-11.

Siu, L. L., Czaykowski, P. M., and Tannock, I. F. 1998. Phase I/II study of the CAPABLE regimen for patients with poorly differentiated carcinoma of the nasopharynx. *J Clin Oncol* 16 (7):2514-21.

Sivridis, E., Giatromanolaki, A., Gatter, K. C., et al. 2002. Association of hypoxia-inducible factors 1alpha and 2alpha with activated angiogenic pathways and prognosis in patients with

endometrial carcinoma. *Cancer* 95 (5):1055-63.

Sizhong, Z., Xiukung, G., and Yi, Z. 1983. Cytogenetic studies on an epithelial cell line derived from poorly differentiated nasopharyngeal carcinoma. *Int J Cancer* 31 (5):587-90.

Smith, B. D., Smith, G. L., Carter, D., et al. 2000. Prognostic significance of vascular endothelial growth factor protein levels in oral and oropharyngeal squamous cell carcinoma. *J Clin Oncol* 18 (10):2046-52.

Sohda, M., Ishikawa, H., Masuda, N., et al. 2004. Pretreatment evaluation of combined HIF-1alpha, p53 and p21 expression is a useful and sensitive indicator of response to radiation and chemotherapy in esophageal cancer. *Int J Cancer* 110 (6):838-44.

Sonna, L. A., Cullivan, M. L., Sheldon, H. K., et al. 2003. Effect of hypoxia on gene expression by human hepatocytes (HepG2). *Physiol Genomics* 12 (3):195-207.

Sonpavde, G., Jian, W., Liu, H., et al. 2008. Sunitinib malate is active against human urothelial carcinoma and enhances the activity of cisplatin in a preclinical model. *Urol Oncol.*

Sorensen, B. S., Alsner, J., Overgaard, J., et al. 2007. Hypoxia induced expression of endogenous markers in vitro is highly influenced by pH. *Radiother Oncol* 83 (3):362-6.

Specenier, P. M., and Vermorken, J. B. 2007. Neoadjuvant chemotherapy in head and neck cancer: should it be revisited? *Cancer Lett* 256 (2):166-77.

Stein, M. E., Ruff, P., Weaving, A., et al. 1996. A phase II study of cisplatin/ifosfamide in recurrent/metastatic undifferentiated nasopharyngeal carcinoma among young blacks in southern Africa. *Am J Clin Oncol* 19 (4):386-8.

Stratford, I. J., and Workman, P. 1998. Bioreductive drugs into the next millennium. *Anticancer Drug Des* 13 (6):519-28.

Su, W. C., Chen, T. Y., Kao, R. H., et al. 1993. Chemotherapy with cisplatin and continuous infusion of 5-fluorouracil and bleomycin for recurrent and metastatic nasopharyngeal carcinoma in Taiwan. *Oncology* 50 (4):205-8.

Subarsky, P., and Hill, R. P. 2003. The hypoxic tumour microenvironment and metastatic progression. *Clin Exp Metastasis* 20 (3):237-50.

Sun, Y., Hildesheim, A., Li, H., et al. 1995. The von Hippel-Lindau (VHL) disease tumor-suppressor gene is not mutated in nasopharyngeal carcinomas. *Int J Cancer* 61 (3):437-8.

Sung, F. L., Hui, E. P., Tao, Q., et al. 2007. Genome-wide expression analysis using microarray identified complex signaling pathways modulated by hypoxia in nasopharyngeal carcinoma. *Cancer Lett* 253 (1):74-88.

Sung, F. L., Poon, T. C., Hui, E. P., et al. 2005. Antitumor effect and enhancement of cytotoxic drug activity by cetuximab in nasopharyngeal carcinoma cells. *In Vivo* 19 (1):237-45.

Swinson, D. E., Jones, J. L., Cox, G., et al. 2004. Hypoxia-inducible factor-1 alpha in non small cell lung cancer: relation to growth factor, protease and apoptosis pathways. *Int J Cancer* 111 (1):43-50.

Swinson, D. E., Jones, J. L., Richardson, D., et al. 2003. Carbonic anhydrase IX expression, a novel surrogate marker of tumor hypoxia, is associated with a poor prognosis in non-small-cell lung cancer. *J Clin Oncol* 21 (3):473-82.

Taamma, A., Fandi, A., Azli, N., et al. 1999. Phase II trial of chemotherapy with 5-fluorouracil, bleomycin, epirubicin, and cisplatin for patients with locally advanced, metastatic, or recurrent undifferentiated carcinoma of the nasopharyngeal type. *Cancer* 86 (7):1101-8.

Talks, K. L., Turley, H., Gatter, K. C., et al. 2000. The expression and distribution of the hypoxia-inducible factors HIF-1alpha and HIF-2alpha in normal human tissues, cancers, and tumor-associated macrophages. *Am J Pathol* 157 (2):411-21.

Tan, E. H., Khoo, K. S., Wee, J., et al. 1999. Phase II trial of a paclitaxel and carboplatin combination in Asian patients with metastatic nasopharyngeal carcinoma. *Ann Oncol* 10 (2):235-7.

Tang, K. F., Tan, S. Y., Chan, S. H., et al. 2001. A distinct expression of CC chemokines by macrophages in nasopharyngeal carcinoma: implication for the intense tumor infiltration by T lymphocytes and macrophages. *Hum Pathol* 32 (1):42-9.

Tao, Q., and Chan, A. T. 2007. Nasopharyngeal carcinoma: molecular pathogenesis and therapeutic developments. *Expert Rev Mol Med* 9 (12):1-24.

Tao, Q., Huang, H., Geiman, T. M., et al. 2002. Defective de novo methylation of viral and cellular DNA sequences in ICF syndrome cells. *Hum Mol Genet* 11 (18):2091-102.

Teo, P., Lee, W. Y., and Yu, P. 1996. The prognostic significance of parapharyngeal tumour involvement in nasopharyngeal carcinoma. *Radiother Oncol* 39 (3):209-21.

Teo, P. M., Kwan, W. H., Lee, W. Y., et al. 1996. Prognosticators determining survival subsequent to distant metastasis from nasopharyngeal carcinoma. *Cancer* 77 (12):2423-31.

Teo, P. M., Kwan, W. H., Yu, P., et al. 1996. A retrospective study of the role of intracavitary brachytherapy and prognostic factors determining local tumour control after primary radical radiotherapy in 903 non-disseminated nasopharyngeal carcinoma patients. *Clin Oncol (R Coll Radiol)* 8 (3):160-6.

Teo, P., Yu, P., Lee, W. Y., et al. 1996. Significant prognosticators after primary radiotherapy in 903 nondisseminated nasopharyngeal carcinoma evaluated by computer tomography. *Int J Radiat Oncol Biol Phys* 36 (2):291-304.

Therasse, P., Arbuck, S. G., Eisenhauer, E. A., et al. 2000. New guidelines to evaluate the response to treatment in solid tumors. European Organization for Research and Treatment of Cancer, National Cancer Institute of the United States, National Cancer Institute of Canada. *J Natl Cancer Inst* 92 (3):205-16.

Trastour, C., Benizri, E., Ettore, F., et al. 2007. HIF-1alpha and CA IX staining in invasive breast carcinomas: prognosis and treatment outcome. *Int J Cancer* 120 (7):1451-8.

Tsui, N. B., Chim, S. S., Chiu, R. W., et al. 2004. Systematic micro-array based identification of placental mRNA in maternal plasma: towards non-invasive prenatal gene expression profiling.

J Med Genet 41 (6):461-7.

Turley, H., Scott, P. A., Watts, V. M., et al. 1998. Expression of VEGF in routinely fixed material using a new monoclonal antibody VG1. *J Pathol* 186 (3):313-8.

Turner, K. J., Crew, J. P., Wykoff, C. C., et al. 2002. The hypoxia-inducible genes VEGF and CA9 are differentially regulated in superficial vs invasive bladder cancer. *Br J Cancer* 86 (8):1276-82.

van der Veldt, A. A., Boven, E., Helgason, H. H., et al. 2008. Predictive factors for severe toxicity of sunitinib in unselected patients with advanced renal cell cancer. *Br J Cancer* 99 (2):259-65.

Vaupel, P., and Mayer, A. 2007. Hypoxia in cancer: significance and impact on clinical outcome. *Cancer Metastasis Rev* 26 (2):225-39.

Vengellur, A., Phillips, J. M., Hogenesch, J. B., et al. 2005. Gene expression profiling of hypoxia signaling in human hepatocellular carcinoma cells. *Physiol Genomics* 22 (3):308-18.

Verheul, H. M., and Pinedo, H. M. 2007. Possible molecular mechanisms involved in the toxicity of angiogenesis inhibition. *Nat Rev Cancer* 7 (6):475-85.

Vermorken, J. B., Remenar, E., van Herpen, C., et al. 2007. Cisplatin, fluorouracil, and docetaxel in unresectable head and neck cancer. *N Engl J Med* 357 (17):1695-704.

Vikram, B., Mishra, U. B., Strong, E. W., et al. 1986. Patterns of failure in carcinoma of the nasopharynx: failure at distant sites. *Head Neck Surg* 8 (4):276-9.

Vleugel, M. M., Greijer, A. E., Shvarts, A., et al. 2005. Differential prognostic impact of hypoxia induced and diffuse HIF-1alpha expression in invasive breast cancer. *J Clin Pathol* 58 (2):172-7.

Volm, M., and Koomagi, R. 2000. Hypoxia-inducible factor (HIF-1) and its relationship to apoptosis and proliferation in lung cancer. *Anticancer Res* 20 (3A):1527-33.

Vordermark, D., and Brown, J. M. 2003. Endogenous markers of tumor hypoxia predictors of clinical radiation resistance? *Strahlenther Onkol* 179 (12):801-11.

Vordermark, D., Said, H. M., Katzer, A., et al. 2006. Plasma osteopontin levels in patients with head and neck cancer and cervix cancer are critically dependent on the choice of ELISA system. *BMC Cancer* 6:207.

Vukovic, V., Haugland, H. K., Nicklee, T., et al. 2001. Hypoxia-inducible Factor-1alpha Is an Intrinsic Marker for Hypoxia in Cervical Cancer Xenografts. *Cancer Res* 61 (20):7394-8.

VUMCA-I. 1996. Preliminary results of a randomized trial comparing neoadjuvant chemotherapy (cisplatin, epirubicin, bleomycin) plus radiotherapy vs. radiotherapy alone in stage IV(> or = N2, M0) undifferentiated nasopharyngeal carcinoma: a positive effect on progression-free survival. International Nasopharynx Cancer Study Group. VUMCA I trial. *Int J Radiat Oncol Biol Phys* 35 (3):463-9.

Wachsberger, P., Burd, R., and Dicker, A. P. 2003. Tumor response to ionizing radiation combined with antiangiogenesis or vascular targeting agents: exploring mechanisms of interaction. *Clin Cancer Res* 9 (6):1957-71.

Wai, P. Y., and Kuo, P. C. 2007. Osteopontin: regulation in tumor metastasis. *Cancer Metastasis Rev.*

Wakisaka, N., Wen, Q. H., Yoshizaki, T., et al. 1999. Association of vascular endothelial growth factor expression with angiogenesis and lymph node metastasis in nasopharyngeal carcinoma. *Laryngoscope* 109 (5):810-4.

Wang, C. C., Chang, J. Y., Liu, T. W., et al. 2006. Phase II study of gemcitabine plus vinorelbine in the treatment of cisplatin-resistant nasopharyngeal carcinoma. *Head Neck* 28 (1):74-80.

Wang, T. L., and Tan, Y. O. 1991. Cisplatin and 5-fluorouracil continuous infusion for metastatic nasopharyngeal carcinoma. *Ann Acad Med Singapore* 20 (5):601-3.

Wee, J. 2008. 4th FY Khoo Memorial Lecture 2008: Nasopharyngeal Cancer Workgroup--the past, the present and the future. *Ann Acad Med Singapore* 37 (7):606-14.

Wee, J., Tan, E. H., Tai, B. C., et al. 2005. Randomized trial of radiotherapy versus concurrent chemoradiotherapy followed by adjuvant chemotherapy in patients with American Joint Committee on Cancer/International Union against cancer stage III and IV nasopharyngeal cancer of the endemic variety. *J Clin Oncol* 23 (27):6730-8.

Wei, W. I., and Sham, J. S. 2005. Nasopharyngeal carcinoma. *Lancet* 365 (9476):2041-54.

Weinmann, M., Belka, C., Guner, D., et al. 2005. Array-based comparative gene expression analysis of tumor cells with increased apoptosis resistance after hypoxic selection. *Oncogene* 24 (38):5914-22.

Wiesener, M. S., Turley, H., Allen, W. E., et al. 1998. Induction of endothelial PAS domain protein-1 by hypoxia: characterization and comparison with hypoxia-inducible factor-1alpha. *Blood* 92 (7):2260-8.

Winter, S. C., Shah, K. A., Han, C., et al. 2006. The relation between hypoxia-inducible factor (HIF)-1alpha and HIF-2alpha expression with anemia and outcome in surgically treated head and neck cancer. *Cancer* 107 (4):757-66.

Wong, J. H., Lui, V. W., Umezawa, K., et al. 2009. A small molecule inhibitor of NF-kappaB, dehydroxymethylepoxyquinomicin (DHMEQ), suppresses growth and invasion of nasopharyngeal carcinoma (NPC) cells. *Cancer Lett.*

Wong, T. S., Kwong, D. L., Sham, J., et al. 2005. Elevation of plasma osteopontin level in patients with undifferentiated nasopharyngeal carcinoma. *Eur J Surg Oncol* 31 (5):555-8.

Wong, T. S., Tang, K. C., Kwong, D. L., et al. 2003. Differential gene methylation in undifferentiated nasopharyngeal carcinoma. *Int J Oncol* 22 (4):869-74.

Wu, C. Y., Wu, M. S., Chiang, E. P., et al. 2007. Elevated plasma osteopontin associated with gastric cancer development, invasion and survival. *Gut* 56 (6):782-9.

Wykoff, C. C., Beasley, N. J., Watson, P. H., et al. 2000. Hypoxia-inducible expression of tumor-associated carbonic anhydrases. *Cancer Res* 60 (24):7075-83.

Wykoff, C. C., Beasley, N., Watson, P. H., et al. 2001. Expression of the hypoxia-inducible and tumor-associated carbonic anhydrases in ductal carcinoma in situ of the breast. *Am J Pathol*

158 (3):1011-9.

Xiao, X., Wu, J., Zhu, X., et al. 2007. Induction of cell cycle arrest and apoptosis in human nasopharyngeal carcinoma cells by ZD6474, an inhibitor of VEGFR tyrosine kinase with additional activity against EGFR tyrosine kinase. *Int J Cancer* 121 (9):2095-104.

Xie, F. Y., Qi, S. N., Hu, W. H., et al. 2007. [Comparison of efficacy of docetaxel combined cisplatin (TP regimen) and cisplatin combined 5-fluorouracil (PF regimen) on locally advanced nasopharyngeal carcinoma]. *Ai Zheng* 26 (8):880-4.

Yang, T. S., Ng, K. T., Wang, H. M., et al. 1996. Prognostic factors of locoregionally recurrent nasopharyngeal carcinoma--a retrospective review of 182 cases. *Am J Clin Oncol* 19 (4):337-43.

Yeh, S. H., Liu, R. S., Wu, L. C., et al. 1996. Fluorine-18 fluoromisonidazole tumour to muscle retention ratio for the detection of hypoxia in nasopharyngeal carcinoma. *Eur J Nucl Med* 23 (10):1378-83.

Yeo, W., Leung, T. W., Chan, A. T., et al. 1998. A phase II study of combination paclitaxel and carboplatin in advanced nasopharyngeal carcinoma. *Eur J Cancer* 34 (13):2027-31.

Yeo, W., Leung, T. W., Leung, S. F., et al. 1996. Phase II study of the combination of carboplatin and 5-fluorouracil in metastatic nasopharyngeal carcinoma. *Cancer Chemother Pharmacol* 38 (5):466-70.

Yu, K. H., Leung, S. F., Tung, S. Y., et al. 2005. Survival outcome of patients with nasopharyngeal carcinoma with first local failure: a study by the Hong Kong Nasopharyngeal Carcinoma Study Group. *Head Neck* 27 (5):397-405.

Zhang, H., Ye, Q. H., Ren, N., et al. 2006. The prognostic significance of preoperative plasma levels of osteopontin in patients with hepatocellular carcinoma. *J Cancer Res Clin Oncol* 132 (11):709-17.

Zhang, L., Zhang, Y., Huang, P. Y., et al. 2008. Phase II clinical study of gemcitabine in the treatment of patients with advanced nasopharyngeal carcinoma after the failure of platinum-based chemotherapy. *Cancer Chemother Pharmacol* 61 (1):33-8.

Zhang, L., Zhao, C., Peng, P. J., et al. 2005. Phase III study comparing standard radiotherapy with or without weekly oxaliplatin in treatment of locoregionally advanced nasopharyngeal carcinoma: preliminary results. *J Clin Oncol* 23 (33):8461-8.

Zhong, H., De Marzo, A. M., Laughner, E., et al. 1999. Overexpression of hypoxia-inducible factor 1alpha in common human cancers and their metastases. *Cancer Res* 59 (22):5830-5.

Zips, D., Eicheler, W., Geyer, P., et al. 2005. Enhanced susceptibility of irradiated tumor vessels to vascular endothelial growth factor receptor tyrosine kinase inhibition. *Cancer Res* 65 (12):5374-9.

SECTION VI

APPENDICES

A. Acknowledgements

This thesis is not possible without the joint efforts of many people. Firstly I would like to thank Prof Anthony TC Chan, Department of Clinical Oncology, who led me into the door of clinical research when I was a trainee in Medical Oncology. It was following his recommendation to join a clinical research fellowship program at University of Oxford in 2001, I embarked in this series of research work leading to this thesis. I would like to express my sincere gratitude for his constant mentorship and encouragement in my research work and the preparation of this thesis.

I would also like to thank Prof Adrian Harris and Dr Francesco Pezzella at Cancer Research UK, University of Oxford, who introduced me into the fascinating research area of hypoxia and angiogenesis. They gave me tremendous support for my laboratory work at the Weatherall Institute of Molecular Medicine, John Radcliffe Hospital, University of Oxford, UK.

From the Chinese University of Hong Kong, I would like to thank Prof KF To and the late Prof Dolly Huang, Department of Anatomical and Cellular Pathology, for their valuable advice and support in the pathological studies of NPC; Prof Terence Poon, Department of Medicine and Therapeutics, who taught my first laboratory session on immunohistochemistry; Dr Nancy Tsui and Prof Dennis Lo, Department of Chemical Pathology, for their excellent support in the microarray experiments.

I would also like to thank colleagues at the laboratories of Sir YK Pao Cancer Centre, Prof Cesar Wong, Prof Vivian Lui, Prof Qian Tao, Dr Fion Sung, Wai-lap Wong, Andrew Chan, Xiaorong Lin and the staff of the Cancer Drug Testing Unit (Cecilia Lau, Crystal Cheung and Kakiu Ho) for all the advice and technical support. I would also like to thank the research staff of the Comprehensive Cancer Trials Unit (CCTU) of Department of Clinical Oncology for the support of the clinical trials, and Dr Frankie Mo for his statistical advice and support. Finally, I would like to give compliments to my colleagues at Department of Clinical Oncology of Prince of Wales Hospital, Prof Brigette Ma, Dr SF Leung, Dr Brian Yu, Dr Michael Kam, Prof Winnie Yeo, Prof Tony Mok, and Prof Benny Zee for their constant support.

B. Publications and Presentations Resulting from the Work of the Thesis

Study 1:

Hui EP, Leung SF, Au JS, Zee B, Tung S, Chua D, Sze WM, Law CK, Leung TW, Chan AT. Lung metastasis alone in nasopharyngeal carcinoma: a relatively favorable prognostic group. A study by the Hong Kong Nasopharyngeal Carcinoma Study Group. *Cancer* 2004;101:300-6.

Study 2:

Sung FL*, **Hui EP***, Tao Q, Li H, Tsui NB, Dennis Lo YM, Ma BB, To KF, Harris AL, Chan AT. Genome-wide expression analysis using microarray identified complex signaling pathways modulated by hypoxia in nasopharyngeal carcinoma. *Cancer letters* 2007;253:74-88. (**co-first author*)

This work has been presented in part as poster at the 2005 annual meeting of the American Association for Cancer Research (AACR).

Study 3:

Hui EP, Chan AT, Pezzella F, Turley H, To KF, Poon TC, Zee B, Mo F, Teo PM, Huang DP, Gatter KC, Johnson PJ, Harris AL. Coexpression of hypoxia-inducible factors 1-alpha and 2-alpha, carbonic anhydrase IX, and vascular endothelial growth factor in nasopharyngeal carcinoma and relationship to survival. *Clin Cancer Res* 2002;8:2595-604.

This work has been presented as poster at the 2002 annual meeting of the American Association for Cancer Research (AACR) and won the Scholar-in-Training award.

Study 4:

Hui EP, Sung FL, Yu BK, Wong CS, Ma BB, Lin X, Chan A, Wong WL, Chan AT. Plasma osteopontin, hypoxia, and response to radiotherapy in nasopharyngeal cancer. *Clin Cancer Res* 2008;14:7080-7.

This work has been presented in part as poster at the 2006 annual meeting of the American Association for Cancer Research (AACR).

Study 5:

Hui EP, Ma BB, Leung SF, King AD, Mo F, Kam MK, Yu BK, Chiu SK, Kwan WH, Ho R, Chan I, Ahuja AT, Zee BC, Chan AT. Randomized phase II trial of concurrent cisplatin-radiotherapy with or without neoadjuvant docetaxel and cisplatin in advanced nasopharyngeal carcinoma. *J Clin Oncol* 2009;27:242-9.

This work has been presented in part at the 41st annual meeting of the American Society of Clinical Oncology, Orlando, Florida, May 13-17, 2005; at the 13th European Cancer Conference, Paris, France, Oct 30 to Nov 3, 2006; and at the 43rd annual meeting of the American Society of Clinical Oncology, Chicago, Illinois, June 2-5, 2007.

This work has been presented by the candidate as invited lectures:
(a) "A randomized phase II study of induction chemotherapy in NPC", at The Hong Kong Head and Neck Society Symposium, 30 Oct 2008, InterContinental Hotel, Hong Kong.
(b) "Neoadjuvant chemotherapy in NPC: a new perspective", at Hong Kong Sanatorium & Hospital Continuing Medical Education symposium, 10 June 2009, Hong Kong Sanatorium and Hospital, Hong Kong.

Study 6:

Hui EP, Lui VW, Wong CS, Ma BB, Lau CP, Cheung CS, Ho K, Cheng SH, Ng MH, Chan AT. Preclinical evaluation of sunitinib as single agent or in combination with chemotherapy in nasopharyngeal carcinoma. *Invest New Drugs* 2010 May 15. [Epub ahead of print].

This work has been presented as poster at the 7th Asia Pacific Oncology Summit (APOS), Taipei, Taiwan, 24-25 Oct 2009.

Study 7:

Hui EP, Ma BB, King AD, Mo F, Chan SL, Kam MK, Loong HH, Ahuja AT, Zee BC,

Chan AT. Hemorrhagic complications in a phase 2 study of sunitinib in patients of nasopharyngeal carcinoma who has previously received high dose radiation. *(Ann Oncol 2010, in press)*

This work has been presented as poster at the Multidisciplinary Head and Neck Cancer Symposium, Co-sponsored by the American Head and Neck Society (AHNS), American Society of Clinical Oncology (ASCO), American Society for Radiation Oncology (ASTRO). Chandler, Ariz, 25-27 Feb, 2010.

Book chapters:

Edwin P. Hui and Anthony T.C. Chan. The Evolving Role of Systemic Therapy in Nasopharyngeal Carcinoma: Current Strategies and Perspectives. *In: Nasopharyngeal Carcinomas*, edited by Pierre Busson. Landes Bioscience and Springer Science, 2008.

This work has been presented by the candidate as invited lecture, "Systemic Therapy in Nasopharyngeal Cancer: Current Strategies and Future Perspectives", at 2007 Asia-Pacific Conference of Tumor Biology and Medicine, China Anti-Cancer Association (CACA), 15-17 Sep 2007, PLA 301 Hospital, Beijing, China.

C. Supplementary Tables

(1) Table S1

Biological process of up-regulated genes by hypoxia in NPC

(2) Table S2

Biological process of down-regulated genes by hypoxia in NPC

(1) Table S1. Biological processes of up regulated genes by hypoxia in NPC

Gene Symbol	Gene Name	Genbank	Probe Set ID	Fold change CNE-2	Fold change HONE-1
	Apoptosis				
BIK	BCL2-interacting killer (apoptosis-inducing)	NM_001197	205780_at	2.8	2.0
BNIP3	BCL2/adenovirus E1B 19kDa interacting protein 3	U15174	201848_s_at	5.1	12.0
BNIP3	BCL2/adenovirus E1B 19kDa interacting protein 3	NM_004052	201849_at	3.6	17.8
BNIP3L	BCL2/adenovirus E1B 19kDa interacting protein 3-like	AL132665	221478_at	3.3	8.2
BNIP3L	BCL2/adenovirus E1B 19kDa interacting protein 3-like	AF060922	221479_s_at	4.8	4.5
BTG1	B-cell translocation gene 1, anti-proliferative	AL535380	200920_s_at	2.6	3.4
E2IG5	growth and transformation-dependent protein	NM_014367	220942_x_at	3.6	5.7
E2IG5	growth and transformation-dependent protein	AF201944	223193_x_at	3.3	6.9
E2IG5	growth and transformation-dependent protein	AF107495	224345_x_at	3.6	7.1
EGLN3	egl nine homolog 3 (C. elegans)	NM_022073	219232_s_at	11.5	56.8
EGLN3	egl nine homolog 3 (C. elegans)	AI378406	222847_s_at	5.3	28.2
GADD45B	growth arrest and DNA-damage-inducible, beta	NM_015675	207574_s_at	7.7	15.1
GADD45B	growth arrest and DNA-damage-inducible, beta	AF087853	209304_x_at	7.0	8.4
GADD45B	growth arrest and DNA-damage-inducible, beta	AF078077	209305_s_at	13.9	13.6
IER3	immediate early response 3	NM_003897	201631_s_at	5.5	10.7
IGFBP3	insulin-like growth factor binding protein 3	M31159	210095_s_at	4.7	11.3
MTP18	mitochondrial protein 18 kDa	AF060924	223172_s_at	1.8	2.2
NOL3	nucleolar protein 3 (apoptosis repressor with CARD domain)	AI912351	59625_at	3.0	3.7
PPP1R15A	protein phosphatase 1, regulatory (inhibitor) subunit 15A	U83981	37028_at	2.0	2.1
RHOB	ras homolog gene family, member B	AI263909	212099_at	2.8	2.4
SOCS3	suppressor of cytokine signaling 3	AI244908	227697_at	1.8	2.8
TGFB1	transforming growth factor, beta 1 (Camurati-Engelmann disease)	BC000125	203085_s_at	2.2	2.1
	Carbohydrate metabolism				
ALDOC	aldolase C, fructose-bisphosphate	NM_005165	202022_at	6.9	12.4
ENO2	enolase 2 (gamma, neuronal)	NM_001975	201313_at	30.1	53.5
GBE1	glucan (1,4-alpha-), branching enzyme 1 (glycogen branching enzyme, Andersen disease, glycogen storage disease type IV)	NM_000158	203282_at	2.2	4.1
GPI	glucose phosphate isomerase	NM_000175	208308_s_at	2.0	1.9
HK2	hexokinase 2	AI761561	202934_at	6.9	12.6
IRS2	insulin receptor substrate 2	AF073310	209185_s_at	1.9	2.2
PDK1	pyruvate dehydrogenase kinase, isoenzyme 1	NM_002610	206686_at	3.0	7.0
PDK1	pyruvate dehydrogenase kinase, isoenzyme 1	AU146532	226452_at	3.5	6.5
PFKFB3	6-phosphofructo-2-kinase/fructose-2,6-biphosphatase 3	NM_004566	202464_s_at	10.1	27.8

(1) Table S1. Biological processes of up regulated genes by hypoxia in NPC

Gene Symbol	Gene Name	Genbank	Probe Set ID	Fold change CNE-2	Fold change HONE-1
PFKFB4	6-phosphofructo-2-kinase/fructose-2,6-biphosphatase 4	AL038787	228499_at	11.9	9.2
PFKP	phosphofructokinase, platelet	NM_002627	201037_at	2.2	2.0
PGK1	phosphoglycerate kinase 1	NM_000291	200737_at	2.4	2.9
PGK1	phosphoglycerate kinase 1	AA069778	227068_at	2.8	2.1
PGK1	Phosphoglycerate kinase 1	BE856250	228483_s_at	10.1	9.0
SLC2A3	solute carrier family 2 (facilitated glucose transporter), member 3	AI631159	202497_x_at	7.3	32.9
SLC2A3	solute carrier family 2 (facilitated glucose transporter), member 3	BE550486	202498_s_at	8.2	22.2
SLC2A3	solute carrier family 2 (facilitated glucose transporter), member 3	NM_006931	202499_s_at	8.5	33.2
SLC2A3 /// SLC2A14	solute carrier family 2 (facilitated glucose transporter), member 3 /// solute carrier family 2 (facilitated glucose transporter), member 14	AL110298	216236_s_at	8.0	15.0
SLC2A3 /// SLC2A14	solute carrier family 2 (facilitated glucose transporter), member 3 /// solute carrier family 2 (facilitated glucose transporter), member 14	AA778684	222088_s_at	9.0	31.2
	Cell cycle, communication and differentiation				
ADM	adrenomedullin	NM_001124	202912_at	19.7	27.4
CCNG2	Cyclin G2	AW134535	202769_at	3.0	6.6
CCNG2	cyclin G2	NM_004354	202770_s_at	4.1	9.9
CCNG2	cyclin G2	L49506	211559_s_at	6.2	7.8
CDKN1C	cyclin-dependent kinase inhibitor 1C (p57, Kip2)	R78668	213182_x_at	3.7	3.1
CDKN1C	Cyclin-dependent kinase inhibitor 1C (p57, Kip2)	N33167	213348_at	2.3	3.5
CDKN1C	cyclin-dependent kinase inhibitor 1C (p57, Kip2)	D64137	216894_x_at	3.1	2.8
CDKN1C	cyclin-dependent kinase inhibitor 1C (p57, Kip2)	NM_000076	219534_x_at	2.6	3.0
CLK1	CDC-like kinase 1	AI251890	214683_s_at	2.9	5.0
CSRP2	cysteine and glycine-rich protein 2	NM_001321	207030_s_at	2.3	2.0
CUL4B	cullin 4B	AV694732	215997_s_at	1.8	1.8
EDN2	endothelin 2	NM_001956	206758_at	6.6	33.4
EFNA1	ephrin-A1	NM_004428	202023_at	6.8	14.6
EFNA3	ephrin-A3	AW189015	210132_at	3.7	2.9
FN1	fibronectin 1	AF130095	210495_x_at	2.0	1.9
GPCR5A	G protein-coupled receptor, family C, group 5, member A	AA156240	212444_at	2.9	3.5
GPRC5C	G protein-coupled receptor, family C, group 5, member C	NM_022036	219327_s_at	2.1	2.3
IGFBP3	insulin-like growth factor binding protein 3	M31159	210095_s_at	4.7	11.3
INSIG1	insulin induced gene 1	BE300521	201625_s_at	3.0	4.0
INSIG1	insulin induced gene 1	BG292233	201626_at	5.4	5.6
INSIG1	insulin induced gene 1	NM_005542	201627_s_at	6.0	5.2
ITGA5	integrin, alpha 5 (fibronectin receptor, alpha polypeptide)	NM_002205	201389_at	3.2	5.1

(1) Table S1. Biological processes of up regulated genes by hypoxia in NPC

Gene Symbol	Gene Name	Genbank	Probe Set ID	Fold change CNE-2	Fold change HONE-1
KRT17	keratin 17	NM_000422	205157_s_at	1.9	2.3
KRT17	keratin 17	Z19574	212236_x_at	2.0	2.2
LOX	lysyl oxidase	NM_002317	204298_s_at	8.6	22.7
LOX	lysyl oxidase	L16895	215446_s_at	9.0	33.1
LOXL2	lysyl oxidase-like 2	BE251211	202997_s_at	2.8	2.6
LOXL2	lysyl oxidase-like 2	NM_002318	202998_s_at	3.0	3.2
MARCKS	myristoylated alanine-rich protein kinase C substrate	M68956	201670_s_at	2.0	1.9
NCKIPSD	NCK interacting protein with SH3 domain	NM_016453	218697_at	2.0	2.3
NDRG1	N-myc downstream regulated gene 1	NM_006096	200632_s_at	9.1	64.3
OSMR	Oncostatin M receptor	AI133452	226621_at	2.0	2.2
PAG1	phosphoprotein associated with glycosphingolipid microdomains 1	AK000680	225626_at	9.7	17.5
PBEF1	Pre-B-cell colony enhancing factor 1	AA873350	243296_at	5.8	5.1
PTDSR	phosphatidylserine receptor	AK021780	212723_at	2.1	2.6
RAB40C	RAB40C, member RAS oncogene family	AW007215	227698_s_at	6.6	7.9
RALGDS	ral guanine nucleotide dissociation stimulator	AI421559	209050_s_at	2.5	2.6
SEMA4B	sema domain, immunoglobulin domain (Ig), transmembrane domain (TM) and short cytoplasmic domain, (semaphorin) 4B	AK026133	234725_s_at	3.2	3.8
SH3PX3	SH3 and PX domain containing 3	BE464841	227151_at	2.5	2.9
SNF1LK	SNF1-like kinase	NM_030751	208078_s_at	1.9	14.7
STC2	stanniocalcin 2	AI435828	203438_at	2.1	6.2
STC2	stanniocalcin 2	BC000658	203439_s_at	4.7	5.9
TPBG	trophoblast glycoprotein	NM_006670	203476_at	3.7	2.9
VEGF	vascular endothelial growth factor	AF022375	210512_s_at	2.3	3.3
VEGF	vascular endothelial growth factor	H95344	212171_x_at	2.0	2.0
WASF2	WAS protein family, member 2	AI962978	221725_at	1.9	1.9
WASF2	WAS protein family, member 2	AK025566	224562_at	1.9	2.3
WSB1	WD repeat and SOCS box-containing 1	NM_015626	201296_s_at	2.4	4.4
WSB1	WD repeat and SOCS box-containing 1	AL110243	210561_s_at	2.2	3.6
WSB1	WD repeat and SOCS box-containing 1	AI377135	227501_at	6.7	4.4
	Defense and Immune Response				
CLEC2B	C-type lectin domain family 2, member B	BC005254	209732_at	2.6	2.6
F3	coagulation factor III (thromboplastin, tissue factor)	NM_001993	204363_at	2.0	2.0
FN1	fibronectin 1	AF130095	210495_x_at	2.0	1.9
FOS	v-fos FBJ murine osteosarcoma viral oncogene homolog	BC004490	209189_at	7.6	23.9
GPI	glucose phosphate isomerase	NM_000175	208308_s_at	2.0	1.9

(1) Table S1. Biological processes of up regulated genes by hypoxia in NPC

Gene Symbol	Gene Name	Genbank	Probe Set ID	Fold change CNE-2	Fold change HONE-1
IRF2	interferon regulatory factor 2	NM_002199	203275_at	2.3	2.5
KLF6	Kruppel-like factor 6	BG250721	224606_at	2.5	2.1
NFIL3	nuclear factor, interleukin 3 regulated	NM_005384	203574_at	3.3	7.9
PAG1	phosphoprotein associated with glycosphingolipid microdomains 1	AK000680	225626_at	9.7	17.5
TNIP1	TNFAIP3 interacting protein 1	NM_006058	207196_s_at	1.9	2.1
	Metabolism of macromolecues				
AK3L1	adenylate kinase 3-like 1	NM_013410	204348_s_at	2.6	2.4
AK3L1	adenylate kinase 3-like 1	AK026966	225342_at	3.0	4.0
CA9	carbonic anhydrase IX	NM_001216	205199_at	3.8	7.7
CLK3	CDC-like kinase 3	NM_003992	202140_s_at	2.8	2.9
DHRS3	dehydrogenase/reductase (SDR family) member 3	NM_004753	202481_at	2.7	2.5
DUSP9	dual specificity phosphatase 9	NM_001395	205777_at	2.0	4.1
EGLN1	egl nine homolog 1 (C. elegans)	BC005369	221497_x_at	2.0	4.3
EGLN1	egl nine homolog 1 (C. elegans)	AL117352	223046_at	1.9	2.8
FUT11	fucosyltransferase 11 (alpha (1,3) fucosyltransferase)	BF541967	238551_at	5.9	10.7
HMGCL	3-hydroxymethyl-3-methylglutaryl-Coenzyme A lyase (hydroxymethylglutaricaciduria)	NM_000191	202772_at	2.1	2.3
IL1RAP	interleukin 1 receptor accessory protein	AF167343	210233_at	2.4	3.4
NPEPPS	aminopeptidase puromycin sensitive	AJ132583	201455_s_at	2.0	2.0
P4HA1	procollagen-proline, 2-oxoglutarate 4-dioxygenase (proline 4-hydroxylase), alpha polypeptide I	NM_000917	207543_s_at	2.2	3.4
P4HA2	procollagen-proline, 2-oxoglutarate 4-dioxygenase (proline 4-hydroxylase), alpha polypeptide II	NM_004199	202733_at	2.6	3.7
PLOD2	procollagen-lysine, 2-oxoglutarate 5-dioxygenase 2	AI754404	202619_s_at	3.8	9.5
PLOD2	procollagen-lysine, 2-oxoglutarate 5-dioxygenase 2	NM_000935	202620_s_at	2.6	10.2
RIOK3	RIO kinase 3 (yeast)	AA725102	202130_at	2.1	2.6
RIPK4	receptor-interacting serine-threonine kinase 4	NM_020639	221215_s_at	1.9	2.9
TIPARP	TCDD-inducible poly(ADP-ribose) polymerase	AL556438	212665_at	3.7	4.3
TMPRSS3	transmembrane protease, serine 3	AB038160	223949_at	1.9	2.0
TNIP1	TNFAIP3 interacting protein 1	NM_006058	207196_s_at	1.9	2.1
TRA1	Tumor rejection antigen (gp96) 1	AI684643	239451_at	3.0	2.7
TRPT1	tRNA phosphotransferase 1	BC005133	223436_s_at	2.0	2.0
	Regulation of transcription				
BCL3	B-cell CLL/lymphoma 3	NM_005178	204908_s_at	2.2	3.4

(1) Table S1. Biological processes of up regulated genes by hypoxia in NPC

Gene Symbol	Gene Name	Genbank	Probe Set ID	Fold change CNE-2	Fold change HONE-1
BHLHB2	basic helix-loop-helix domain containing, class B, 2	BG326045	201169_s_at	9.7	24.9
BHLHB2	basic helix-loop-helix domain containing, class B, 2	NM_003670	201170_s_at	3.4	14.3
CITED2	Cbp/p300-interacting transactivator, with Glu/Asp-rich carboxy-terminal domain, 2	NM_006079	207980_s_at	2.3	3.1
CNOT8	CCR4-NOT transcription complex, subunit 8	AI769416	202162_s_at	3.7	2.1
CNOT8	CCR4-NOT transcription complex, subunit 8	NM_004779	202163_s_at	2.8	2.7
CNOT8	CCR4-NOT transcription complex, subunit 8	AF180476	202164_s_at	4.5	2.9
ELF3	E74-like factor 3 (ets domain transcription factor, epithelial-specific)	U73844	210827_s_at	4.9	7.2
FOS	v-fos FBJ murine osteosarcoma viral oncogene homolog	BC004490	209189_at	7.6	23.9
FOSL2	FOS-like antigen 2	NM_005253	205409_at	2.8	5.1
FOSL2	FOS-like antigen 2	N36408	218880_at	6.3	22.7
FOSL2	FOS-like antigen 2	AI860150	228188_at	1.9	8.2
FOXD1	forkhead box D1	NM_004472	206307_s_at	3.2	3.5
FOXO3A	forkhead box O3A	N25732	204131_s_at	2.7	2.0
FOXO3A	forkhead box O3A	NM_001455	204132_s_at	1.9	2.6
HES1	hairy and enhancer of split 1, (Drosophila)	BE973687	203394_s_at	5.3	20.3
HES1	hairy and enhancer of split 1, (Drosophila)	NM_005524	203395_s_at	2.7	10.3
HEY1	hairy/enhancer-of-split related with YRPW motif 1	NM_012258	218839_at	4.1	13.8
HEY1	hairy/enhancer-of-split related with YRPW motif 1	R61374	44783_s_at	3.3	13.7
IRF2	interferon regulatory factor 2	NM_002199	203275_at	2.3	2.5
JMJD2B	jumonji domain containing 2B	BE256900	212496_s_at	2.9	3.6
KLF6	Kruppel-like factor 6	BG250721	224606_at	2.5	2.1
MAFF	v-maf musculoaponeurotic fibrosarcoma oncogene homolog F (avian)	AL021977	36711_at	2.6	4.2
MAFK	v-maf musculoaponeurotic fibrosarcoma oncogene homolog K (avian)	BG231691	226206_at	2.9	2.1
MXI1	MAX interactor 1	NM_005962	202364_at	9.3	12.0
NFIL3	nuclear factor, interleukin 3 regulated	NM_005384	203574_at	3.3	7.9
PHF21A	PHD finger protein 21A	NM_016621	203278_s_at	2.5	2.2
PRKCBP1	protein kinase C binding protein 1	AB032951	209048_s_at	1.8	2.2
RAI17	retinoic acid induced 17	AF070622	212124_at	2.0	2.2
RARA	retinoic acid receptor, alpha	AI806984	203749_s_at	3.1	5.0
RBPSUH	recombining binding protein suppressor of hairless (Drosophila)	AL513759	211974_x_at	2.3	1.9
SAP30	sin3-associated polypeptide, 30kDa	NM_003864	204900_x_at	2.1	2.0
SERTAD2	SERTA domain containing 2	BG107456	202656_s_at	2.4	3.0
SERTAD2	SERTA domain containing 2	NM_014755	202657_s_at	2.1	2.4
TSC22D3	TSC22 domain family, member 3	AL110191	208763_s_at	3.0	3.2
YEATS2	YEATS domain containing 2	NM_018023	221203_s_at	2.4	3.5

(1) Table S1. Biological processes of up regulated genes by hypoxia in NPC

Gene Symbol	Gene Name	Genbank	Probe Set ID	Fold change CNE-2	Fold change HONE-1
ZNF292	zinc finger protein 292	AA972711	212368_at	3.5	5.2
ZNF395	zinc finger protein 395	NM_017606	218149_s_at	4.6	3.6
	Response to stress/stimulus				
CLEC2B	C-type lectin domain family 2, member B	BC005254	209732_at	2.6	2.6
DUSP1	dual specificity phosphatase 1	NM_004417	201041_s_at	3.2	4.3
ERRFI1	ERBB receptor feedback inhibitor 1	AL034417	224657_at	5.8	4.8
F3	coagulation factor III (thromboplastin, tissue factor)	NM_001993	204363_at	2.0	2.0
HIG2	hypoxia-inducible protein 2	NM_013332	218507_at	23.4	34.2
MT1X	metallothionein 1X	NM_002450	204326_x_at	2.4	2.9
SERPINE1	serpin peptidase inhibitor, clade E (nexin, plasminogen activator inhibitor type 1), member 1	AL574210	202627_s_at	3.0	4.8
STC1	Stanniocalcin 1	AW003173	230746_s_at	2.7	46.1
	Transport				
COL5A1	collagen, type V, alpha 1	N30339	212488_at	2.5	1.9
COL5A1	collagen, type V, alpha 1	AI983428	212489_at	2.3	1.9
ERO1L	ERO1-like (S. cerevisiae)	NM_014584	218498_s_at	2.6	3.7
ERO1L	ERO1-like (S. cerevisiae)	BE966748	225750_at	3.6	4.7
RAB20	RAB20, member RAS oncogene family	NM_017817	219622_at	2.6	6.2
SFXN3	sideroflexin 3	NM_030971	220974_x_at	2.4	2.3
SLC16A3	solute carrier family 16 (monocarboxylic acid transporters), member 3	AL513917	202855_s_at	1.9	2.4
SLC2A1	solute carrier family 2 (facilitated glucose transporter), member 1	NM_006516	201250_s_at	4.8	9.2
SLC6A6	solute carrier family 6 (neurotransmitter transporter, taurine), member 6	BG150485	228754_at	2.3	2.8
SLC6A8	solute carrier family 6 (neurotransmitter transporter, creatine), member 8	NM_005629	202219_at	7.6	6.4
SLC6A8	solute carrier family 6 (neurotransmitter transporter, creatine), member 8	U17986	210854_x_at	5.5	3.4
SLC6A8	solute carrier family 6 (neurotransmitter transporter, creatine), member 8	AW276522	213843_x_at	5.0	3.7
SLC6A8 /// FLJ43855	solute carrier family 6 (neurotransmitter transporter, creatine), member 8 /// similar to sodium- and chloride-dependent creatine transporter	U41163	215812_s_at	4.5	3.4
SLCO4A1	solute carrier organic anion transporter family, member 4A1	NM_016354	219911_s_at	1.8	2.0

(2) Table S2. Biological processes of down regulated genes by hypoxia in NPC

Gene Symbol	Gene Name	Genbank	Probe Set ID	Fold change CNE-2	Fold change HONE-1
	Apoptosis				
BAG2	BCL2-associated athanogene 2	AF095192	209406_at	0.4	0.3
BIRC4	baculoviral IAP repeat-containing 4	BF109251	228363_at	0.5	0.4
CUL3	cullin 3	AF062537	201371_s_at	0.5	0.4
CUL5	cullin 5	BF435809	203531_at	0.5	0.4
FAIM	Fas apoptotic inhibitory molecule	NM_018147	220643_s_at	0.6	0.5
MGC5297	hypothetical protein MGC5297	NM_024091	219200_at	0.4	0.4
PSEN1	presenilin 1 (Alzheimer disease 3)	NM_007318	203460_s_at	0.5	0.5
UTP11L	UTP11-like, U3 small nucleolar ribonucleoprotein, (yeast)	NM_016037	218235_s_at	0.5	0.5
	Biosynthesis and metabolism of macromolecules				
ALG2	asparagine-linked glycosylation 2 homolog (yeast, alpha-1,3-mannosyltransferase)	BE967331	225621_at	0.5	0.5
AMD1	adenosylmethionine decarboxylase 1	M21154	201196_s_at	0.4	0.3
AMD1	adenosylmethionine decarboxylase 1	NM_001634	201197_at	0.3	0.4
CGI-37	comparative gene identification transcript 37	NM_016101	219031_s_at	0.4	0.3
CTPS	CTP synthase	NM_001905	202613_at	0.5	0.3
DNAJA5	DnaJ homology subfamily A member 5	BG112118	235032_at	0.5	0.3
DNAJB1	DnaJ (Hsp40) homolog, subfamily B, member 1	NM_006145	200666_s_at	0.5	0.4
FLAD1	Fad1, flavin adenine dinucleotide synthetase, homolog (yeast)	NM_025207	205661_s_at	0.5	0.4
GCH1	GTP cyclohydrolase 1 (dopa-responsive dystonia)	NM_000161	204224_s_at	0.5	0.6
GTPBP4	GTP binding protein 4	NM_012341	218238_at	0.6	0.4
GTPBP4	GTP binding protein 4	NM_012341	218239_s_at	0.5	0.5
MAT2A	methionine adenosyltransferase II, alpha	NM_005911	200769_s_at	0.4	0.1
NBLA00058	putative protein product of Nbla00058	NM_019048	217987_at	0.4	0.4
ODC1	ornithine decarboxylase 1	NM_002539	200790_at	0.5	0.2
PPM2C	protein phosphatase 2C, magnesium-dependent, catalytic subunit	BG542521	222572_at	0.5	0.3
RCHY1	ring finger and CHY zinc finger domain containing 1	AI096477	212749_s_at	0.5	0.4
RRS1	RRS1 ribosome biogenesis regulator homolog (S. cerevisiae)	BC001811	209567_at	0.3	0.1
TGFBR2	transforming growth factor, beta receptor II (70/80kDa)	D50683	208944_at	0.5	0.4
TP53RK	TP53 regulating kinase	BG339450	225402_at	0.4	0.4
UMPS	uridine monophosphate synthetase (orotate phosphoribosyl transferase and orotidine-5'-decarboxylase)	D86227	202706_s_at	0.5	0.3

(2) Table S2. Biological processes of down regulated genes by hypoxia in NPC

Gene Symbol	Gene Name	Genbank	Probe Set ID	Fold change CNE-2	Fold change HONE-1
UTP14A	UTP14, U3 small nucleolar ribonucleoprotein, homolog A (yeast)	BC001149	221514_at	0.5	0.4
ZCSL2	zinc finger, CSL-type containing 2	AI825858	225195_at	0.5	0.4
	Cell growth and differentiation				
BYSL	bystin-like	NM_004053	203612_at	0.5	0.5
CUL3	cullin 3	AF062537	201371_s_at	0.5	0.4
CUL5	cullin 5	BF435809	203531_at	0.5	0.4
E2F3	E2F transcription factor 3	NM_001949	203693_s_at	0.6	0.5
FLJ40432	Hypothetical protein FLJ40432	AK026922	227280_s_at	0.4	0.4
IFRD1	interferon-related developmental regulator 1	AA747426	202146_at	0.4	0.2
IFRD1	interferon-related developmental regulator 1	NM_001550	202147_s_at	0.3	0.2
PAFAH1B1	platelet-activating factor acetylhydrolase, isoform Ib, alpha subunit 45kDa	NM_000430	200816_s_at	0.4	0.5
PAK1IP1	PAK1 interacting protein 1	NM_017906	218886_at	0.5	0.3
PALM2-AKAP2	PALM2-AKAP2 protein	BG540494	226694_at	0.4	0.4
RBBP7	Retinoblastoma binding protein 7	AI885312	227520_at	0.4	0.3
RFP	ret finger protein	AF230394	210541_s_at	0.4	0.2
RFP	ret finger protein	NM_006510	212116_at	0.4	0.2
SOCS4	suppressor of cytokine signaling 4	BF446961	226178_at	0.4	0.3
TGFBR2	transforming growth factor, beta receptor II (70/80kDa)	D50683	208944_at	0.5	0.4
	DNA repair				
ASF1A	ASF1 anti-silencing function 1 homolog A (S. cerevisiae)	NM_014034	203427_at	0.5	0.4
ASF1A	ASF1 anti-silencing function 1 homolog A (S. cerevisiae)	AB028628	203428_s_at	0.5	0.3
GTF2H2	general transcription factor IIH, polypeptide 2, 44kDa	BC005345	223758_s_at	0.5	0.3
POLE2	polymerase (DNA directed), epsilon 2 (p59 subunit)	NM_002692	205909_at	0.4	0.5
RFC3	replication factor C (activator 1) 3, 38kDa	NM_002915	204128_s_at	0.5	0.5
TSN	translin	AI435302	201504_s_at	0.4	0.4
	Immune Response				
XBP1	X-box binding protein 1	NM_005080	200670_at	0.5	0.3
	Regulation of translation				
EIF3S1	eukaryotic translation initiation factor 3, subunit 1 alpha, 35kDa	NM_003758	208264_s_at	0.5	0.5
EIF5	eukaryotic translation initiation factor 5	NM_001969	208290_s_at	0.4	0.1

(2) Table S2. Biological processes of down regulated genes by hypoxia in NPC

Gene Symbol	Gene Name	Genbank	Probe Set ID	Fold change CNE-2	Fold change HONE-1
EIF5	eukaryotic translation initiation factor 5	BG481972	208705_s_at	0.5	0.2
EIF5	eukaryotic translation initiation factor 5	AK026933	208706_s_at	0.4	0.2
EIF5	eukaryotic translation initiation factor 5	AL080102	208708_x_at	0.4	0.1
ETF1	eukaryotic translation termination factor 1	NM_004730	201574_at	0.5	0.5
GFM1	G elongation factor, mitochondrial 1	AI814295	225153_at	0.5	0.5
GFM1	G elongation factor, mitochondrial 1	BF978647	225158_at	0.5	0.5
GFM1	G elongation factor, mitochondrial 1	AI659020	225161_at	0.5	0.4
PRKRIR	protein-kinase, interferon-inducible double stranded RNA dependent inhibitor, repressor of (P58 repressor)	AF081567	209323_at	0.5	0.4
	Regulation of transcription				
E2F3	E2F transcription factor 3	NM_001949	203693_s_at	0.6	0.5
E2F3	E2F transcription factor 3	NM_001949	203693_s_at	0.6	0.5
HIRA	HIR histone cell cycle regulation defective homolog A (S. cerevisiae)	X75296	217427_s_at	0.5	0.4
PAWR	PRKC, apoptosis, WT1, regulator	AI091432	226223_at	0.4	0.4
POLR1B	polymerase (RNA) I polypeptide B, 128kDa	BC004882	223403_s_at	0.3	0.2
RFP	ret finger protein	AF230394	210541_s_at	0.4	0.2
RFP	ret finger protein	NM_006510	212116_at	0.4	0.2
SIX1	Sine oculis homeobox homolog 1 (Drosophila)	N79004	228347_at	0.5	0.5
XBP1	X-box binding protein 1	NM_005080	200670_at	0.5	0.3
ZNF281	Zinc finger protein 281	AA121673	228785_at	0.5	0.4
ZNF639	zinc finger protein 639	BF001614	222623_s_at	0.5	0.5
	RNA processing				
CPSF2	cleavage and polyadenylation specific factor 2, 100kDa	AK023583	225994_at	0.4	0.5
CPSF2	cleavage and polyadenylation specific factor 2, 100kDa	AA583986	233208_x_at	0.5	0.5
DBR1	debranching enzyme homolog 1 (S. cerevisiae)	AK000116	234295_at	0.3	0.4
EXOSC4	exosome component 4	NM_019037	218695_at	0.5	0.3
EXOSC4	exosome component 4	AL039469	58696_at	0.6	0.4
HEAB	ATP/GTP-binding protein	NM_006831	204370_at	0.4	0.4
HNRPA0	heterogeneous nuclear ribonucleoprotein A0	BE966599	201054_at	0.4	0.5
MPHOSPH10	M-phase phosphoprotein 10 (U3 small nucleolar ribonucleoprotein)	AL545921	212885_at	0.5	0.4
NOL5A	nucleolar protein 5A (56kDa with KKE/D repeat)	NM_006392	200875_s_at	0.5	0.3

(2) Table S2. Biological processes of down regulated genes by hypoxia in NPC

Gene Symbol	Gene Name	Genbank	Probe Set ID	Fold change CNE-2	Fold change HONE-1
NOLA1	nucleolar protein family A, member 1 (H/ACA small nucleolar RNPs)	NM_018983	219110_at	0.5	0.4
NOLC1	nucleolar and coiled-body phosphoprotein 1	NM_004741	205895_s_at	0.5	0.4
PSPC1	paraspeckle component 1	AI872384	226574_at	0.5	0.4
SFRS6	splicing factor, arginine/serine-rich 6	AL031681	208804_s_at	0.5	0.5
TFB2M	transcription factor B2, mitochondrial	NM_022366	218605_at	0.5	0.5
TRNT1	tRNA nucleotidyl transferase, CCA-adding, 1	BE552215	222754_at	0.4	0.5
UTP11L	UTP11-like, U3 small nucleolar ribonucleoprotein, (yeast)	NM_016037	218235_s_at	0.5	0.5
	Transport				
Dlc2	Dynein light chain 2	BG478726	225494_at	0.5	0.5
KIAA2010	KIAA2010	NM_017936	220368_s_at	0.4	0.5
MGC4399	mitochondrial carrier protein	BC004991	223296_at	0.3	0.4
SLC25A32	solute carrier family 25, member 32	NM_030780	221020_s_at	0.4	0.4
SLC7A11	solute carrier family 7, (cationic amino acid transporter, y+ system) member 11	AA488687	217678_at	0.4	0.4
SLC7A11	solute carrier family 7, (cationic amino acid transporter, y+ system) member 11	AB040875	209921_at	0.4	0.5
TFRC	transferrin receptor (p90, CD71)	N76327	237215_s_at	0.4	0.1